

GEOMETRIC INTEGRATORS FOR COUPLED NONLINEAR SCHRÖDINGER
EQUATION

A THESIS SUBMITTED TO
THE GRADUATE SCHOOL OF NATURAL AND APPLIED SCIENCES
OF
MIDDLE EAST TECHNICAL UNIVERSITY

BY

AYHAN AYDIN

IN PARTIAL FULFILLMENT OF THE REQUIREMENTS
FOR
THE DEGREE OF DOCTOR OF PHILOSOPHY
IN
MATHEMATICS

JANUARY 2005

Approval of the Graduate School of Natural and Applied Sciences.

Prof. Dr. Canan Özgen
Director

I certify that this thesis satisfies all the requirements as a thesis for the degree of Doctor of Philosophy.

Prof.Dr. Şafak Alpay
Head of Department

This is to certify that we have read this thesis and that in our opinion it is fully adequate, in scope and quality, as a thesis for the degree of Doctor of Philosophy.

Prof.Dr. Bülent Karasözen
Supervisor

Examining Committee Members

Prof.Dr. Ali Yazıcı (TOBB - ETU) _____

Prof. Dr. Bülent Karasözen (METU) _____

Prof.Dr. Marat Akhmet (METU) _____

Prof.Dr. Gerhard Wilhelm Weber (METU) _____

Assoc.Prof.Dr. Tanıl Ergenç (METU) _____

I hereby declare that all information in this document has been obtained and presented in accordance with academic rules and ethical conduct. I also declare that, as required by these rules and conduct, I have fully cited and referenced all material and results that are not original to this work.

Name, Last Name: AYHAN AYDIN

Signature :

ABSTRACT

GEOMETRIC INTEGRATORS FOR COUPLED NONLINEAR SCHRÖDINGER EQUATION

AYDIN, AYHAN

Ph.D., Department of Mathematics

Supervisor : Prof.Dr. Bülent Karasözen

January 2005, 153 pages

Multisymplectic integrators like Preissman and six-point schemes and a semi-explicit symplectic method are applied to the coupled nonlinear Schrödinger equations (CNLSE). Energy, momentum and additional conserved quantities are preserved by the multisymplectic integrators, which are shown using modified equations. The multisymplectic schemes are backward stable and non-dissipative. A semi-explicit method which is symplectic in the space variable and based on linear-nonlinear, even-odd splitting in time is derived. These methods are applied to the CNLSE with plane wave and soliton solutions for various combinations of the parameters of the equation. The numerical results confirm the excellent long time behavior of the conserved quantities and preservation of the shape of the soliton solutions in space and time.

Keywords: nonlinear Schrödinger equation, coupled nonlinear Schrödinger equation, symplectic integrators, multisymplectic integrators, dispersion analysis, backward error analysis, modified equations, plane wave solution, soliton solution

ÖZ

DOĞRUSAL OLMAYAN İKİLİ SCHRÖDINGER DENKLEMİ İÇİN GEOMETRİK ENTEGRASYON YÖNTEMLER

AYDIN, AYHAN

Doktora, Matematik Bölümü

Tez Yöneticisi : Prof. Dr. Bülent KARASÖZEN

Ocak 2005, 153 sayfa

Preissman ve altı-nokta olarak adlandırılan çoklu simplektik yöntemler ve yarı-açık simplektik yöntem doğrusal olmayan ikili Schrödinger denkleminin (CNLSE) uygulanmıştır. Enerji, momentum ve ilave korunum özelliklerinin çoklu simplektik yöntemler tarafından korunması geriye dönük hata analizi ile açıklanmıştır. Çoklu simplektik yöntemler geriye dönük kararlı olup, dalga dağılımı özelliği göstermezler. Uzak değişkenine göre simplektik, doğrusal-doğrusal olmayan, tek-çift ayrışımına dayalı yarı-açık yeni bir yöntem geliştirilmiştir. Yöntemler CNLS'in çeşitli parametrelerine uygulanmıştır. Elde edilen sayısal sonuçlar korunum kurallarının, soliton çözümlerinin uzak ve uzun zaman aralığında çok iyi korunmakta olduğunu doğrulamaktadır.

Anahtar Kelimeler: tek ve ikili doğrusal olmayan Schrödinger denklemi, simplektik ve çoklu simplektik entegrasyon yöntemleri, geriye dönük hata analizi, düzeltilmiş denklemler, düzlem dalga ve soliton şeklinde çözümler.

To my grandfather

ACKNOWLEDGMENTS

I would like to thank my supervisor Prof.Dr. Bülent Karasözen for his help, suggestions and encouragement through the discussion of this thesis.

I am also thankful to Prof.Dr. Huseyin Huseyinov, Atılım University Department of Mathematics, and Assist.Prof.Dr. Ahmet Yaşar Özban, Atılım University Department of Mathematics, for their helps whenever I needed.

TABLE OF CONTENTS

PLAGIARISM	iii
ABSTRACT	iv
ÖZ	v
DEDICATON	vi
ACKNOWLEDGMENTS	vii
TABLE OF CONTENTS	viii
LIST OF TABLES	x
LIST OF FIGURES	xi
 CHAPTER	
0 INTRODUCTION	1
1 HAMILTONIAN and SYMPLECTIC STRUCTURES	7
1.1 Hamiltonian ODE's	7
1.2 Symplectic Methods for Hamiltonian ODE's	11
1.3 Hamiltonian PDE's	13
1.4 Multisymplectic PDE's	14
1.4.1 Symplecticity	16
1.4.2 Energy and Momentum Conservation	17
2 NONLINEAR SCHRÖDINGER EQUATION	21
2.1 The Nonlinear Schrödinger Equation	21
2.1.1 Hamiltonian Formulation	22
2.1.2 Multisymplectic Formulation	23
2.1.3 Conserved Quantities	26
2.2 Coupled Nonlinear Schrödinger Equation	27
2.2.1 Hamiltonian Formulation	28
2.2.2 Multisymplectic Formulation	30
2.2.2.1 Conserved Quantities	33
2.3 N-Coupled Nonlinear Schrödinger Equation	34

3	NUMERICAL METHODS	36
3.1	The Ablowitz-Ladik Discrete NLS System	37
3.2	Symplectic Integrators for CNLSE	39
3.3	Multisymplectic Integrators	41
3.3.1	The Preissman Box Scheme	42
3.4	Multisymplectic Integration of NLSE	47
3.5	Multisymplectic Integration of CNLSE	49
3.6	Six-point scheme for CNLSE	51
3.7	A Semi-Explicit Symplectic Integrator for CNLSE	58
3.7.1	Linear-Nonlinear Splitting	58
3.7.2	Even-Odd Splitting	60
3.7.3	Composition method	63
4	LINEARIZED EQUATIONS AND DISPERSION RELATIONS	65
4.1	Dispersion Relation	66
4.1.1	The Preissman Box Scheme	69
4.2	Linearized NLS	71
4.3	Linearized CNLSE	74
4.3.1	The Preissman Box Scheme	77
4.3.2	Coupled Six-Point Scheme	78
4.4	Linear Stability Analysis for Six-Point Scheme	81
5	BACKWARD ERROR ANALYSIS	89
6	NUMERICAL RESULTS	99
6.1	The plane wave solutions of CNLSE	100
6.1.1	Numerical Simulation I: Elliptical Polarization ($e = 1$)	103
6.1.2	Numerical Simulation II: Linear Polarization ($e = 2/3$)	105
6.1.3	Numerical Simulation III: Circular polarization ($e = 2$)	107
6.2	Soliton Solutions of CNLSE	109
6.2.1	Numerical Simulation I: Evolution of Single Soliton .	112
6.2.2	Numerical Simulation II : Evolution of Colliding Soliton	113
6.3	CONCLUSION and FUTURE WORK	115
	VITA	117
	REFERENCES	148

LIST OF TABLES

TABLES

Table 6.1 Values of parameter for the initial condition (6.13) of the CNLS equation (6.11).	103
Table 6.2 Elliptic polarization ($e = 1$): The absolute maximum error in the local and global conservation laws for the CNLS equation (6.11).	105
Table 6.3 Elliptic polarization ($e = 1$): Exact and approximate values of the conserved quantities (6.12) for various time for the CNLS equation (6.11).	106
Table 6.4 Linear polarization ($e = 2/3$): The absolute maximum error in the local and global conservation laws for the CNLS equation (6.11)	108
Table 6.5 Various values for the conserved quantities (6.12) for the CNLS equation (6.14) with initial data (6.16) with $\alpha = 0.5, v = 1.0, e = 2/3, \delta = 0.5$ over the spatial interval $[-40, 40]$ and time interval $[0, 40]$ using MS and MS6 integrators with $N = 400, \Delta t = 0.1$	112
Table 6.6 Accuracy of the MS integrator using L_∞ error norm 6.17 for the CNLS equation (6.14) with initial data (6.16) with $\alpha = 0.5, v = 1.0, e = 2/3, \delta = 0.5$ over the spatial interval $[-40, 40]$ and time interval $[0, 40]$ using MS integrator with $N = 400, \Delta t = 0.1$	113
Table 6.7 Various values for the conserved quantities (6.12) for the CNLS equation (6.14) with initial data (6.18) with $e = 2/3$ over the spatial interval $[-40, 40]$ and time interval $[0, 40]$ using MS and MS6 integrators with $N = 400, \Delta t = 0.1$	114

LIST OF FIGURES

FIGURES

Figure 3.1 Schematic of the Preissman scheme (3.22) and six-point difference scheme (3.61)-(3.62) for the CNLSE (2.26)-(2.27).	55
Figure 4.1 The effect of discretization in space ($\Delta t \rightarrow 0$) for linearized NLSE (4.19). Solid line: exact dispersion relation (4.24); crossed: numerical dispersion relation with continuous time (4.28). The left plot: with $\Delta x = 0.5$. The right plot : with $\Delta x = 0.1$. The top plot : $\mathbf{a} = -1 < 0$, The middle plot : $\mathbf{a} = 0$. The bottom plot : $\mathbf{a} = 1 > 0$	83
Figure 4.2 The effect of discretization for linearized NLSE (4.19). Solid line: exact dispersion relation (4.24); crossed: numerical dispersion relation (4.27). The left plot: with $\Delta x = 0.1, \Delta t = 0.1$. The right plot : with $\Delta x = 0.1, \Delta t = 0.01$. The top plot : $\mathbf{a} = -1 < 0$, The middle plot : $\mathbf{a} = 0$. The bottom plot : $\mathbf{a} = 1 > 0$	84
Figure 4.3 For $\Delta x = \Delta t = 0.1, \delta_1 = \delta_2 = 1, d_1 = d_2 = 1, c_1 = c_2 = 1$, exact (solid) and numerical (crossed) dispersion relation for linearized CNLSE (4.35)-(4.36).	85
Figure 4.4 For $\Delta x = \Delta t = 0.1, \delta_1 = \delta_2 = 1, d_1 = d_2 = 1, c_1 = c_2 = 0$, exact (solid) and numerical (crossed) dispersion relation for linearized CNLSE (4.35)-(4.36).	85
Figure 4.5 For $\Delta x = \Delta t = 0.1, \delta_1 = \delta_2 = 1, d_1 = d_2 = 1, c_1 = c_2 = -10$, exact (solid) and numerical (crossed) dispersion relation for linearized CNLSE (4.35)-(4.36).	86
Figure 4.6 For $\Delta x = 0.05, \Delta t = 0.02, \delta_1 = \delta_2 = 1, d_1 = d_2 = 1, c_1 = c_2 = -10$, exact (solid) and numerical (crossed) dispersion relation for linearized CNLSE (4.35)-(4.36).	86
Figure 4.7 For $c_1 = 0.01 < \Delta x = \Delta t = 0.1 < c_2 = 1, \delta_1 = \delta_2 = 1, d_1 = d_2 = 1$, exact (solid) and numerical (crossed) dispersion relation for linearized CNLSE (4.35)-(4.36).	87
Figure 4.8 For $c_2 = 0.01 < \Delta x = \Delta t = 0.1 < c_1 = 1, \delta_1 = \delta_2 = 1, d_1 = d_2 = 1$, exact (solid) and numerical (crossed) dispersion relation for linearized CNLSE (4.35)-(4.36).	87
Figure 4.9 Dispersion curves of the integrable case: $\delta_1 = 5, \delta_2 = -5, d_1 = d_2 = 1/2$, with $c_1 = c_2 = 1, \Delta x = \Delta t = 0.1$. Exact (solid) and numerical (crossed) dispersion relation for linearized CNLSE (4.35)-(4.36).	88
Figure 4.10 Dispersion curves of the non-integrable case: $\delta_1 = 5, \delta_2 = -5, 1/2 = d_1 \neq d_2 = -1/2$, with $c_1 = c_2 = 1, \Delta x = \Delta t = 0.1$. Exact (solid) and numerical (crossed) dispersion relation for linearized CNLSE (4.35)-(4.36).	88

Figure 6.1 Long-time evolution of the destabilized wave solutions for CNLSE with $e = 1$, $a_0 = 0.5$, $b_0 = 0.5$, $\varepsilon = 0.1$, $\theta = 0$, $N = 256$, $T = 100$. Left plots : surface of $ \psi_1 $. Right plots : surface of $ \psi_2 $. (a-b) The multisymplectic scheme MS (c-d) the multisymplectic six point scheme MS6 (e-f) the semi-explicit scheme SE	119
Figure 6.2 Errors in local energy and momentum conservation laws of the destabilized wave solutions for CNLSE with $e = 1$, $a_0 = 0.5$, $b_0 = 0.5$, $\varepsilon = 0.1$, $\theta = 0$, $N = 256$, $T = 100$. Left plots : error in local energy. Right plots : error in local momentum. (a-b) The multisymplectic scheme MS (c-d) the multisymplectic six point scheme MS6 (e-f) the semi-explicit scheme SE	120
Figure 6.3 Errors in local additional conservation laws of the destabilized wave solutions for CNLSE with $e = 1$, $a_0 = 0.5$, $b_0 = 0.5$, $\varepsilon = 0.1$, $\theta = 0$, $N = 256$, $T = 100$. Left plots : error in local energy. Right plots : error in local momentum. (a-b) The multisymplectic scheme MS (c-d) the multisymplectic six point scheme MS6 (e-f) the semi-explicit scheme SE	121
Figure 6.4 Errors in global energy and momentum conservation laws of the destabilized wave solutions for CNLSE with $e = 1$, $a_0 = 0.5$, $b_0 = 0.5$, $\varepsilon = 0.1$, $\theta = 0$, $N = 256$, $T = 100$. Left plots : error in local energy. Right plots: error in local momentum. (a-b) The multisymplectic scheme MS (c-d) the multisymplectic six point scheme MS6 (e-f) the semi-explicit scheme SE	122
Figure 6.5 Conservation property of the MS6 scheme for the destabilized wave solutions of the CNLSE with $e = 1$, $a_0 = 0.5$, $b_0 = 0.5$, $\varepsilon = 0.1$, $\theta = 0$, $N = 256$, $T = 100$. (a) The conserved quantity (3.71) (b) The conserved quantity (3.73)	123
Figure 6.6 Long-time evolution of the destabilized wave solutions for CNLSE with $e = 1$, $a_0 = 0.5$, $b_0 = 0.5$, $\varepsilon = 0.1$, $\theta = 3\pi/2$, $N = 256$, $T = 100$. Surfaces of $ \psi_1 $ and $ \psi_2 $.(a) The multisymplectic scheme MS6 (b) the semi-explicit scheme SE (c) Local energy errors; left plot: MS6, right plot: SE	124
Figure 6.7 Long-time evolution of the destabilized wave solutions for CNLSE with $e = 1$, $a_0 = 0.68$, $b_0 = 0.2$, $\varepsilon = 0.1$, $\theta = 3\pi/2$, $N = 256$, $T = 100$. Surfaces of $ \psi_1 $ and $ \psi_2 $. (a) The multisymplectic scheme MS6 (b) the semi-explicit scheme SE (c) Local energy errors; left plot: MS6, right plot: SE	125
Figure 6.8 Long-time evolution of the destabilized wave solutions for CNLSE with $e = 2/3$, $a_0 = 0.5$, $b_0 = 0.5$, $\varepsilon = 0.1$, $\theta = 0$, $N = 256$, $T = 100$. Surfaces of $ \psi_1 $ and $ \psi_2 $: (a) The multisymplectic scheme MS6 (b) the semi-explicit scheme SE (c)Local energy errors; left plot: MS6; right plot :SE	126
Figure 6.9 Long-time evolution of the destabilized wave solutions for CNLSE with $e = 2/3$, $a_0 = 0.5$, $b_0 = 0.5$, $\varepsilon = 0.1$, $\theta = 3\pi/2$, $N = 256$, $T = 100$. Surfaces of $ \psi_1 $ and $ \psi_2 $: (a) The multisymplectic scheme MS6 (b) the semi-explicit scheme SE (c) Local energy errors; left plot: MS6; right plot :SE	127

Figure 6.10 Long-time evolution of the destabilized wave solutions for CNLSE with $e = 2/3$, $a_0 = 0.63$, $b_0 = 0.2$, $\varepsilon = 0.1$, $\theta = 0$, $N = 256$, $T = 100$. Surfaces of $ \psi_1 $ and $ \psi_2 $: (a) The multisymplectic scheme MS6 (b) the semi-explicit scheme SE (c) Local energy errors; left plot: MS6; right plot :SE	128
Figure 6.11 Long-time evolution of the destabilized wave solutions for CNLSE with $e = 2$, $a_0 = 0.5$, $b_0 = 0.5$, $\varepsilon = 0.1$, $\theta = 0$, $N = 256$, $T = 100$. Left plots :Contour plot of $ \psi_1 $. Right plots : surface of $ \psi_1 $. (a) The multisymplectic scheme MS (b) the multisymplectic six point scheme MS6 (c) the semi-explicit scheme SE	129
Figure 6.12 Errors in local energy conservation laws of the destabilized wave solutions for CNLSE with $e = 2$, $a_0 = 0.5$, $b_0 = 0.5$, $\varepsilon = 0.1$, $\theta = 0$, $N = 256$, $T = 100$. (a) The multisymplectic scheme MS (b) the multisymplectic six point scheme MS6 (c) the semi-explicit scheme SE	130
Figure 6.13 Long-time evolution of the destabilized wave solutions for CNLSE with $e = 2$, $a_0 = 0.5$, $b_0 = 0.5$, $\varepsilon = 0.1$, $\theta = 3\pi/2$, $N = 256$, $T = 100$. Left plots: Contour plots of $ \psi_1 $. Right plots: Local energy error. (a) The multi-symplectic scheme MS (b) the multi-symplectic six point scheme MS6 (c) the semi-explicit scheme SE	131
Figure 6.14 Long-time evolution of the destabilized wave solutions for CNLSE with $e = 2$, $a_0 = 0.78$, $b_0 = 0.2$, $\varepsilon = 0.1$, $\theta = 0$, $N = 256$, $T = 100$. Left plots : Contour plots of $ \psi_1 $. Right plots: Local energy error (a) The multi-symplectic scheme MS (b) the multi-symplectic six point scheme MS6 (c) the semi-explicit scheme SE	132
Figure 6.15 Wave forms : One soliton solution of CNLSE with $e = 2/3$, $\delta_1 = \delta_2 = 0.5$, $d_1 = d_2 = 0.5$, $a_1 = a_2 = 1$, $N = 400$, $\Delta t = 0.1$. (a) MS integrator, (b) MS6 integrator	133
Figure 6.16 Evolution of the wave $ \psi_1 $: One soliton solution of CNLSE with $e = 2/3$ obtained using MS6 integrator	134
Figure 6.17 Local and global conservation of energy : One soliton solution of CNLSE with $e = 2/3$. Left plots: MS integrator; right plots: MS6 integrator	135
Figure 6.18 Elastic collision of two solitons with $e = 1$ obtained using (a) MS integrator (b) MS6 integrator	136
Figure 6.19 Evolution of the wave $ \psi_1 $: Two soliton solution of CNLSE with $e = 1$ obtained using MS integrator.	137
Figure 6.20 Errors in local and global energy and additional conservation lows : Two soliton solution of CNLSE with $e = 1$. Left plots: MS integrator; right plots: MS6 integrator.	138
Figure 6.21 Contour plots: Two soliton solution of CNLSE with $e = 1$ obtained using (a) MS integrator (b) MS6 integrator.	139
Figure 6.22 Inelastic collision of two solitons with : $e = 2/3$ obtained using (a) MS integrator (b) MS6 integrator	140
Figure 6.23 Evolution of the wave $ \psi_1 $: Two soliton solution of CNLSE with $e = 2/3$, $\delta_1 = \delta_2 = 0.5$ obtained using MS integrator	141
Figure 6.24 Local and global conservation of energy and additional conservation : Two soliton solution of CNLSE with $e = 2/3$, $\delta_1 = \delta_2 = 0.5$. Left plots: MS integrator; right plots: MS6 integrator.	142
Figure 6.25 Contour plots: Two soliton solution of CNLSE with $e = 2/3$, $\delta_1 = \delta_2 = 0.5$, obtained using (a) MS integrator (b) MS6 integrator.	143

Figure 6.26 Inelastic collision of two solitons of CNLSE with $e = 2/3, \delta_1 = \delta_2 = 0.2$, obtained using (a) MS integrator (b) MS6 integrator.	144
Figure 6.27 Evolution of the wave $ \psi_1 $: Two soliton solution of CNLSE with $e = 2/3, \delta_1 = \delta_2 = 0.2$, obtained using MS6 integrator.	145
Figure 6.28 Local and global conservation of energy and momentum conservation : Two soliton solution of CNLSE with $e = 2/3, \delta_1 = \delta_2 = 0.2$. Left plots: MS integrator; right plots: MS6 integrator	146
Figure 6.29 Contour plots: Two soliton solution of CNLSE with $e = 2/3, \delta_1 = \delta_2 = 0.2, d_1 = d_2 = 0.5, a_1 = a_2 = 1, N = 400, \Delta t = 0.1$ obtained using (a) MS integrator (b) MS6 integrator	147

CHAPTER 0

INTRODUCTION

There has been a great activity in the field of geometric integration of differential equations in recent years. A numerical method that preserves the geometric features of a differential equation such as energy, momentum, symplecticity is known as geometric integrator. In particular, if the differential equation is a Hamiltonian system with a symplectic structure, symplectic integrators give excellent results in long time integration which can be explained by backward error analysis. Preserving the symplectic structure, symmetries and the reversibility of certain ordinary differential equations (ODE's) by numerical methods became almost a routine in recent years (see the monographs [33, 69]). Geometric integrators are now commonly used in many applications including celestial mechanics and molecular dynamics.

In this thesis we are concerned with the numerical integration of the coupled nonlinear Schrödinger equation (CNLSE) which is a Hamiltonian partial differential equation (PDE). The two CNLSE were first derived in 1967 by Benney and Newell [14] for two nonlinear interacting wave packets in a dispersive and conservative system. Since the CNLSE is used in optical-soliton based telecommunication systems there was a need for a through study of the solution behavior of the these equations. This is why the CNLSE has attracted a great deal of attention Hamiltonian PDE's are essential in the theory of wave phenomena. Numerical computations of solutions for these problems are very important to get insight into the behavior of a particular dynamics of the system. Most of the nonlinear PDE's like CNLSE can be solved analytically only for a few number of parameters; for a wide range of physically interesting phenomena, solutions must be obtained by numerical methods.

In recent years several approaches were carried out for solving nonlinear PDE's using geometric integrators. Among these there are two main approaches: either a

semi-discretization in space to obtain a system of Hamiltonian ODE's, or simultaneous symplectic discretization in space and time to obtain multisymplectic systems.

In the first approach, discretizing the PDE in the space variable is done using finite differences or spectral methods to obtain a Hamiltonian system of ODE's or an integrable system, and applying the known symplectic geometric integrators developed for ODE's. If the resulting system of ODE's is in canonical Hamiltonian form, then the application of symplectic methods is straightforward. For Hamiltonian system in non-canonical form, or so called Poisson structure, symplectic methods can not be directly applied (for a recent review of Poisson integrators see [33] Chapter VII and [44]).

For low dimensional Hamiltonian systems the phase structure is accurately preserved by symplectic schemes. However, for higher dimensional systems arising from semi-discretization of Hamiltonian PDE's this is not well established [5]. The reason for the failure is that the symplectic integrator preserves, in this form, only the global invariants of the underlying system. A more satisfactory approach is to develop a local concept of symplecticity for Hamiltonian PDE's since symplecticity may vary from point to point in space and time. Hence local conservation is more important than global conservation for symplectic integration of PDEs. To overcome these disadvantages, Bridges and Reich introduced the concept of multisymplectic integrators based on the multisymplectic structure of some conservative PDEs [18, 21] which leads to the second approach mentioned above.

Various discretization methods such as Fourier spectral, Gauss-Legendre collocation, finite volume have been shown to be multisymplectic (see [21, 22, 64, 65] and reference therein). However, a through analysis of the local and global properties of multisymplectic integrators has yet to be carried out.

Let \mathbf{M} and \mathbf{K} be any skew-symmetric matrices on \mathbf{R}^n ($n \geq 3$) and let $S : \mathbf{R} \rightarrow \mathbf{R}$ be any smooth function. Then, a system of the following form

$$\mathbf{M}z_t + \mathbf{K}z_x = \nabla_z S(z), \quad z \in \mathbf{R}^n \quad (0.1)$$

is called a Hamiltonian system with a multisymplectic structure, or a multisymplectic PDE [18, 21] where ∇_z denotes the gradient operator in \mathbf{R}^n . The system (0.1) is multisymplectic with skew-symmetric matrices \mathbf{M} and \mathbf{K}

$$\omega(U, V) = \langle \mathbf{M}U, V \rangle, \quad \kappa(U, V) = \langle \mathbf{K}U, V \rangle$$

which define a space-time symplectic structure where $U, V \in \mathbf{R}^n$ are solutions of the variational equation

$$\mathbf{M}dz_t + \mathbf{K}dz_x = D_{zz}S(z)dz$$

associated with (0.1).

Any system of the form (0.1) satisfies the conservation of symplecticity equation

$$\partial_t \omega + \partial_x \kappa = 0$$

with $\partial_t = \partial/\partial t$ and $\partial_x = \partial/\partial x$. When the Hamiltonian S is independent of x and t , then the system (0.1) has local energy and momentum conservation laws

$$\partial_t E + \partial_x F = 0, \quad \partial_t I + \partial_x G = 0$$

where

$$\begin{aligned} E(z) &= S(z) - \frac{1}{2}\kappa(z_x, z), & F(z) &= \frac{1}{2}\kappa(z_t, z), \\ G(z) &= S(z) - \frac{1}{2}\omega(z_t, z), & I(z) &= \frac{1}{2}\omega(z_x, z). \end{aligned} \quad (0.2)$$

Usually the Hamiltonian S itself is not a conserved quantity. There are some additional conservation laws which follows from Noether theory due to certain symmetries of the underlying PDE. Under periodic boundary conditions, global conservations can be obtained by integrating the local conservations in space [40]. Many PDE's can be formulated in a multisymplectic form such as the KdV, nonlinear Schrödinger models, Boussinesq models, geostrophic flow, water waves, Sine-Gordon, Klein-Gordon equation and Kadomtsev-Petviashvili (KP) equation [13, 19, 22, 17, 37, 40, 47, 83, 93]. The nonlinear Schrödinger equation with the generalized power nonlinearity [70]

$$iu_t + u_{xx} + a|u|^{l-1}u = 0, \quad l \geq 3$$

where $i = \sqrt{-1}$, $u = u(x, t)$ is complex-valued, $x \in \mathbf{R}^n$, and $a \in \mathbf{R}$ has also a multisymplectic structure. Several multisymplectic methods have been derived in recent years for solving the nonlinear Schrödinger equation (NLSE) with cubic nonlinearity $l = 3$ (see [23, 24, 25, 39] and reference therein).

The main subject of this thesis is the development and investigation of numerical methods for CNLSE

$$i \left(\frac{\partial \psi_1}{\partial t} + \delta_1 \frac{\partial \psi_1}{\partial x} \right) + d_1 \frac{\partial^2 \psi_1}{\partial x^2} + (a_1 |\psi_1|^2 + e |\psi_2|^2) \psi_1 = 0 \quad (0.3)$$

$$i \left(\frac{\partial \psi_2}{\partial t} + \delta_2 \frac{\partial \psi_2}{\partial x} \right) + d_2 \frac{\partial^2 \psi_2}{\partial x^2} + (e |\psi_1|^2 + a_2 |\psi_2|^2) \psi_2 = 0 \quad (0.4)$$

where $\delta_1, \delta_2, d_1, d_2, a_1, a_2$ and e are all real constants, and $\psi_1(x, t)$ and $\psi_2(x, t)$ are complex valued functions of $(x, t) \in \mathbf{R}^2$. CNLSE has many applications such as nonlinear optics, plasma physics, water waves and geophysical fluids [19, 20, 42, 48, 53, 82]. The parameters and their values vary from one application to another. In this work the parameters are taken from nonlinear optics in which d_1, d_2 are dispersion coefficients, a_1, a_2 are Landau constants which describes the self-modulation of the wave packets, and e is the wave-wave interaction coefficient which describe the cross-modulations of the wave packets. There are few integrable cases for some parameter values; among the most known is the Manakov system with $d_1 = d_2$ and $a_1 = a_2 = e$ [48]; others are given for the parameter values $d_1 = -d_2$ and $a_1 = a_2 = -e$ [91]. Integrable forms of CNLSE can be solved exactly using inverse scattering theory.

The most known multisymplectic integrator is the Preissman or box scheme which corresponds to concatenating the midpoint scheme in space and time. This method was successfully applied to many Hamiltonian PDE's like Korteweg-de Vries (KdV) equation [13, 93], nonlinear Klein-Gordon equation [83], wave equation [37], KP equation [47], and to the nonlinear Schrödinger equation (NLSE) [24, 25, 23, 71].

The behavior of the solution of the NLSE integrated by the Preissman scheme preservation of the phase invariant structure was investigated in [39, 40] and a backward error analysis was carried out in [55] in order to show the conserved quantities such as energy and momentum are almost conserved.

In this thesis, in addition to the Preissman scheme we have formulated and applied the so called six-point scheme to CNLSE. The Preissman and six-point schemes are fully implicit. At each time step a large nonlinear system of equations is to be solved. Since this requires a huge amount of computation to obtain accurate results over a long time interval, we have developed a semi-explicit symplectic integrator based on linear-nonlinear, even-odd splitting.

In Chapter 1, Hamiltonian systems of ODE's and PDE's are introduced. Multi-symplectic PDE's including their conservation properties such as symplecticity, energy, momentum and additional conservation laws are given. In Chapter 2, NLSE and CNLSE are formulated as a Hamiltonian and multisymplectic PDE with the corresponding conservation laws. Also in this chapter the N coupled NLSE is formulated in a multisymplectic form. Derivation of multisymplectic methods like Preissman and the six-point scheme, and a semi-explicit method, and an investigation of their

conservation properties are given in Chapter 3. In Chapter 4, dispersion relations of the CNLSE for both continuous and discrete equations are discussed for linearized multisymplectic PDE's, in particular for CNLSE. The multisymplectic integrators like Preissman and six-point scheme are non-dissipative due to their multisymplectic nature, but the semi-explicit method is not. The nondissipative character of a numerical method is the most preferable property for nonlinear wave equations. Dispersion analysis of the linearized CNLSE shows that both the Preissman and six-point schemes follow the exact dispersion properties for most of the mesh sizes in space and time variables. The semi-explicit method has less desirable dispersion properties than the Preissman and six-point schemes.

Since the conserved quantities are only exactly preserved by multisymplectic methods for linearized PDE's, we have analyzed the conservation of the energy, momentum over long time intervals using modified equations and backward error analysis in Chapter 5. In this chapter we have also applied the backward error analysis which was developed for multisymplectic method for PDE's in [55, 56] to CNLSE. The modified equations for the solution and conserved quantities of CNLSE for Preissman and six-point schemes are presented, which show that the modified conserved quantities are preserved at higher order and over long time intervals.

In Chapter 6 numerical results have been presented. We have considered two types of CNLSE; one with travelling wave solutions and the other with solitary waves. The travelling wave solutions for periodic boundary conditions were investigated for three types of polarizations of CNLSE, namely elliptic, linear and circular. All of these correspond to different combinations of the parameters of CNLSE. In the literature, usually, the CNLSE is integrated in the space variable either using finite differences or spectral methods and integrated in time using higher order Runge-Kutta methods [75], or Hopscotch method [81]; or it is integrated using a symplectic discretization in space variable and applying the implicit midpoint rule in the time variable [42]. In all these works only the global quadratic conserved quantities of CNLSE which corresponds to the preservation of the norm square of the solutions are conserved. The preservation of these quantities were shown analytically and numerically. In this work we have shown that, due to their multisymplectic nature, the Preissman and six-point schemes preserves the local energy, momentum and additional conserved quantity of the CNLSE. The numerical results obtained in these schemes are presented

in form of the solutions of CNLSE, propagation of conserved quantities over time and space variables are compared with those found in the literature. It turns out that the Preissman and six-point schemes give the wave propagation of the CNLSE very accurately due to their non-dissipative character and preservation properties of the local conserved quantities for long time steps. As expected, the semi-explicit method does not have such a good behavior, but the numerical results obtained for small time steps are almost identical with those in the literature obtained by other methods. It has to be mentioned that the number of variables by the six-point scheme is half of that in the Preissman scheme and therefore requires less computational time. The semi-explicit method does not require solutions of large implicit equations but it requires smaller time steps in order to resolve the desired accuracy of the solutions.

The solitary wave solutions of CNLSE was investigated in the literature using finite difference semi-discretization in space variable and integrated the resulting differential equation by using implicit midpoint rule in [42] and by Runge-Kutta method in [41] and by Preissman scheme in [72]. In this work soliton solutions for several combination of the parameters of the CNLSE are computed; one soliton , elastic (which corresponds to the integrable CNLSE) collision and inelastic collision are obtained by the Preissman and six-point schemes. All numerical results show excellent preservation of the conservation quantities in time and the shape of the solitons over long time interval are as expected and the results are similar to the results obtained in the literature by other numerical methods. The computation times are by far less for the six-point scheme than for the Preissman. The semi-explicit method does not work satisfactorily especially for collision of solitons.

CHAPTER 1

HAMILTONIAN and SYMPLECTIC STRUCTURES

The Hamiltonian formalism was first introduced by Hamilton in 1834 for the problems in optic. Later, it has been applied to different fields by many authors because most of the problems in physics and engineering sciences can be described by Hamilton's formalism such as classical and celestial mechanics, molecular dynamics, optics, non-linear waves and soliton propagation, plasma physics, rigid body, robotics, and so on. Detailed description of Hamiltonian systems can be found in [33, 50, 60, 69].

In this chapter, we summarize the known results about the Hamiltonian systems and their properties. This chapter is organized as follows: In Section (1.1), we present the Hamiltonian ordinary differential equations (ODE's), including its conservation properties such as symplecticity and energy conservation. In Section (1.2), we present some symplectic methods for integrating Hamiltonian systems. In Section (1.3), we provide generalization of Hamiltonian ODE's to Hamiltonian partial differential equations (PDE's). In Section (1.4), we present the multisymplectic PDE's and also provide the conservation laws of multisymplectic PDE's such as multisymplecticity, energy and momentum conservation. In that section, we also provide an additional conservation law which arises from the symmetry of multisymplectic PDE's.

1.1 Hamiltonian ODE's

We will start by giving the formulation of Hamiltonian systems for ODE's as described in [33, 69]. Let \mathcal{M} be an even dimensional smooth manifold of points $(\mathbf{q}, \mathbf{p}) = (q_1, \dots, q_d, p_1, \dots, p_d)$. Let T be an open interval of the real line R of the time variable t . If $H = H(\mathbf{q}, \mathbf{p}, t)$ is a sufficiently smooth real function defined on $\mathcal{M} \times T$, then the

Hamiltonian system of differential equations is given by

$$\frac{d\mathbf{q}_i}{dt} = \frac{\partial H}{\partial \mathbf{p}_i}, \quad \frac{d\mathbf{p}_i}{dt} = -\frac{\partial H}{\partial \mathbf{q}_i} \quad i = 1, \dots, d \quad (1.1)$$

with the Hamiltonian H . If H is independent of time i.e. $H = H(\mathbf{q}, \mathbf{p})$ then (1.1) is called an autonomous Hamiltonian equation, otherwise it is called non-autonomous. The system (1.1) is a system of $2d$ differential equation. The integer d is called the degrees of freedom which identifies how many coordinates we need to describe the motion. The state space \mathcal{M} is called the phase space and the product $\mathcal{M} \times T$ is the extended phase space. The axis of the phase space gives the values of the \mathbf{q} 's and \mathbf{p} 's. Hence, if we have d degrees of freedom, we have d pairs of \mathbf{q} 's and \mathbf{p} 's, and the phase space will have a $2d$ dimensions. Therefore, for a Hamiltonian system (with no explicit time dependence in H), the phase space will have $2d$ dimension. We assume that H is at least C^2 continuous, hence the right-hand side of the system (1.1) is C^1 , so that the standard existence and uniqueness theorems can be applied to the corresponding initial value problem. The variables \mathbf{q} and \mathbf{p} are called the canonical variables and the set of equations (1.1) construct a canonical Hamiltonian system. In applications to mechanics, the variables \mathbf{q} denote the generalized coordinates, the variables \mathbf{p} denote the generalized momenta and the Hamiltonian H usually corresponds to the total energy of the system (1.1). All generalized coordinates together form the configuration space.

For autonomous Hamiltonian systems, it is sometimes useful to combine the dependent variables in (1.1) in a $2d$ -dimensional vector $z = (\mathbf{q}(t), \mathbf{p}(t))^T$. Then (1.1) takes the form

$$\frac{dz}{dt} = J^{-1} \nabla H \quad (1.2)$$

where ∇H is the gradient of the real valued Hamiltonian function $H(z)$ and J is the $2d \times 2d$ constant skew-symmetric structure matrix

$$J = \begin{pmatrix} \mathbf{0}_d & -\mathbf{I}_d \\ \mathbf{I}_d & \mathbf{0}_d \end{pmatrix} \quad (1.3)$$

Here \mathbf{I}_d and $\mathbf{0}_d$ represent $d \times d$ identity and zero matrices, respectively. The matrix (1.3) has the following properties:

- J is skew-symmetric : $J^T = -J$;
- J is orthogonal : $J^T J = I_{2d} = J J^T$; and

- $\det J = 1$.

The flow $\varphi_t : \mathcal{M} \rightarrow \mathbf{R}^{2d}$ of the Hamiltonian system (1.1) is the mapping that advances the solution by time t , i.e. $\varphi_t(\mathbf{q}_0, \mathbf{p}_0) = (\mathbf{q}(\mathbf{q}_0, \mathbf{p}_0, t), \mathbf{p}(\mathbf{q}_0, \mathbf{p}_0, t))$ where $(\mathbf{q}(\mathbf{q}_0, \mathbf{p}_0, t), \mathbf{p}(\mathbf{q}_0, \mathbf{p}_0, t))$ is the solution of the system (1.1) corresponding to initial values $\mathbf{q}(0) = \mathbf{q}_0$, and $\mathbf{p}(0) = \mathbf{p}_0$ [33].

If we consider the total derivative of the Hamiltonian $H(\mathbf{q}, \mathbf{p}, t)$ using (1.1) we get

$$\frac{d}{dt}H(\mathbf{q}, \mathbf{p}, t) = \sum_{i=1}^d \frac{\partial H}{\partial q_i} \frac{dq_i}{dt} + \sum_{i=1}^d \frac{\partial H}{\partial p_i} \frac{dp_i}{dt} + \frac{\partial H}{\partial t} = \frac{\partial H}{\partial t}. \quad (1.4)$$

If the Hamiltonian function H is independent of time (i.e. autonomous Hamiltonian systems), then

$$\frac{\partial H(\mathbf{q}, \mathbf{p}, t)}{\partial t} = 0, \quad (1.5)$$

from which (1.4) becomes

$$\frac{d}{dt}H(\mathbf{q}, \mathbf{p}) = 0. \quad (1.6)$$

This shows that the Hamiltonian H or the total energy of the system remains constant along all the solutions of (1.1). i.e. H is conserved. Conservation of energy tells us that energy is neither created nor destroyed throughout the solution of (1.1).

Besides the conservation of the total energy, an autonomous Hamiltonian systems preserves exactly the symplectic form which is defined by

$$\omega = d\mathbf{p} \wedge d\mathbf{q} = d\mathbf{p}^T d\mathbf{q} - d\mathbf{q}^T d\mathbf{p}, \quad (1.7)$$

that is

$$\frac{d\omega}{dt} = d\mathbf{p}_t \wedge d\mathbf{q} + d\mathbf{p} \wedge d\mathbf{q}_t = 0 \quad (1.8)$$

where $d\mathbf{p}, d\mathbf{q} \in \mathbf{R}^{2d \times 2d}$ are solutions of the variational equation

$$d\mathbf{q}_t = D_{\mathbf{p}\mathbf{p}}H(\mathbf{q}, \mathbf{p})d\mathbf{p} + D_{\mathbf{q}\mathbf{p}}H(\mathbf{q}, \mathbf{p})d\mathbf{q} \quad (1.9)$$

$$d\mathbf{p}_t = -D_{\mathbf{p}\mathbf{q}}H(\mathbf{q}, \mathbf{p})d\mathbf{p} - D_{\mathbf{q}\mathbf{q}}H(\mathbf{q}, \mathbf{p})d\mathbf{q}. \quad (1.10)$$

Here \wedge denotes the wedge or exterior product. To understand the geometric meaning of the symplecticity, we summarize the results given in [33]. We consider a two-dimensional parallelogram lying in \mathbf{R}^{2d} . Let P be the parallelogram spanned by two vectors

$$\xi = \begin{pmatrix} \xi^{\mathbf{p}} \\ \xi^{\mathbf{q}} \end{pmatrix}, \quad \eta = \begin{pmatrix} \eta^{\mathbf{p}} \\ \eta^{\mathbf{q}} \end{pmatrix} \quad (1.11)$$

in the (\mathbf{q}, \mathbf{p}) space where $\xi^{\mathbf{p}}, \xi^{\mathbf{q}}, \eta^{\mathbf{p}}, \eta^{\mathbf{q}}$ are in \mathbf{R}^d . If $d = 1$, then the oriented area of the parallelogram P is given by [33] as

$$\text{area}(P) = \det \begin{pmatrix} \xi^{\mathbf{p}} & \eta^{\mathbf{p}} \\ \xi^{\mathbf{q}} & \eta^{\mathbf{q}} \end{pmatrix} = \xi^{\mathbf{p}}\eta^{\mathbf{q}} - \xi^{\mathbf{q}}\eta^{\mathbf{p}}. \quad (1.12)$$

Therefore, in one dimension symplecticity is the conservation of area. In higher dimensions, we replace this by the sum of the oriented areas of the projections of P onto the coordinate planes $(\mathbf{q}_i, \mathbf{p}_i)$ (see [33] for details).

A linear mapping $A : \mathbf{R}^{2d} \rightarrow \mathbf{R}^{2d}$ is called symplectic if

$$A^T J A = J \quad (1.13)$$

or equivalently if $\omega(A\xi, A\eta) = \omega(\xi, \eta)$ for all $\xi, \eta \in \mathbf{R}^{2d}$ where J is given in (1.3).

The flow φ_t of the (autonomous) Hamiltonian system (1.1) is a symplectic map. Therefore the area in (1.12) is conserved throughout the evolution. In fact, all symplectic mappings are area preserving.

If we take the determinant of (1.13) we obtain

$$\det(A^T J A) = \det(J) = 1. \quad (1.14)$$

Since $\det(A) = \det(A^T)$, the equality (1.14) implies

$$(\det(A))^2 = 1. \quad (1.15)$$

A function F is said to be a first integral for the Hamiltonian system (1.1) if and only if

$$\{F, H\} = 0 \quad (1.16)$$

where the bracket $\{\cdot, \cdot\}$ is defined in [60] as

$$\{F, H\} = \sum_{i=1}^d \frac{\partial F}{\partial q_i} \frac{\partial H}{\partial p_i} - \frac{\partial F}{\partial p_i} \frac{\partial H}{\partial q_i} \quad (1.17)$$

and satisfies the following properties for arbitrary smooth real-valued function F_1, F_2 and F_3 on \mathcal{M} :

i) Bilinearity:

$$\begin{aligned} \{cF_1 + c'F_2, F_3\} &= c\{F_1, F_3\} + c'\{F_2, F_3\}, \\ \{F_1, cF_2 + c'F_3\} &= c\{F_1, F_2\} + c'\{F_1, F_3\} \end{aligned}$$

for constants $c, c' \in \mathbf{R}$

ii) Skew-symmetry: $\{F_1, F_2\} = -\{F_2, F_1\}$,

iii) The Jacobi identity: $\{\{F_1, F_2\}, F_3\} + \{\{F_3, F_1\}, F_2\} + \{\{F_2, F_3\}, F_1\} = 0$.

The bracket in (1.17) is called the canonical Poisson bracket. We notice from the skew-symmetry property that $\{H, H\} = 0$ and therefore the Hamiltonian itself is a first integral. In particular, if the Hamiltonian system (1.1) has d first integrals F_1, \dots, F_d satisfying

$$\{F_i, F_j\} = 0,$$

for all i, j then it is said to be completely integrable.

In some Hamiltonian systems there are additional quantities whose values also remain constant as the trajectory evolves. For example, consider the following case. Suppose one of the \mathbf{p} 's, say \mathbf{p}_k does not change in time. That is,

$$\frac{d\mathbf{p}_k}{dt} = -\frac{\partial H}{\partial \mathbf{q}_k}. \quad (1.18)$$

Then, (1.18) can be 0 for all $(\mathbf{q}(t), \mathbf{p}(t))$ values along the trajectory if and only if $H(\mathbf{q}, \mathbf{p})$ does not depend on \mathbf{q}_k . Thus, we say that the momentum \mathbf{p}_k is a constant of motion if and only if the Hamiltonian $H(\mathbf{q}, \mathbf{p})$ does not depend on the corresponding \mathbf{q}_k explicitly.

1.2 Symplectic Methods for Hamiltonian ODE's

Most of the phenomena in classical physics, chemistry, biology and other sciences are often modelled by Hamiltonian systems of differential equations. The name symplectic integrator is usually attached to a numerical scheme that intends to solve such a hamiltonian system approximately, while preserving its underlying symplectic structure. Astrophysics is one of the most interesting sources of numerical experiments employing symplectic integrators. Other experiments of symplectic integrators can be found in molecular dynamics, where some results have been achieved in the long-time integration of some complicated collisions or long-lived trajectories (see, [33] CH.VII, and [69] and reference therein)

A numerical approximation

$$z_{n+1} = \Phi_{\Delta t}(z_n) \quad z_n = (q_n, p_n), \quad t_{n+1} = t_n + \Delta t \quad (1.19)$$

for autonomous Hamiltonian system corresponding to (1.2) is said to be symplectic if it satisfies the symplecticity condition (1.13) or if it is a discrete approximation for (1.8):

$$\frac{\omega_{n+1} - \omega_n}{\Delta t} = \frac{d\mathbf{p}_{n+1} \wedge d\mathbf{q}_{n+1} - d\mathbf{p}_n \wedge d\mathbf{q}_n}{\Delta t} = 0 \quad (1.20)$$

that is

$$d\mathbf{p}_{n+1} \wedge d\mathbf{q}_{n+1} = d\mathbf{p}_n \wedge d\mathbf{q}_n \quad (1.21)$$

For example a one-step method applied to (1.2)

$$\mathbf{q}_{n+1} = \mathbf{q}_n + \Delta t \frac{\partial H}{\partial \mathbf{q}}(\mathbf{q}_{n+1}, \mathbf{p}_n), \quad (1.22)$$

$$\mathbf{p}_{n+1} = \mathbf{p}_n - \Delta t \frac{\partial H}{\partial \mathbf{p}}(\mathbf{q}_{n+1}, \mathbf{p}_n) \quad (1.23)$$

is called the symplectic Euler scheme of order 1 and the implicit mid-point rule

$$\mathbf{q}_{n+1} = \mathbf{q}_n + \Delta t \frac{\partial H}{\partial \mathbf{p}}((\mathbf{q}_{n+1} + \mathbf{q}_n)/2, (\mathbf{p}_{n+1} + \mathbf{p}_n)/2), \quad (1.24)$$

$$\mathbf{p}_{n+1} = \mathbf{p}_n - \Delta t \frac{\partial H}{\partial \mathbf{p}}((\mathbf{q}_{n+1} + \mathbf{q}_n)/2, (\mathbf{p}_{n+1} + \mathbf{p}_n)/2), \quad (1.25)$$

is a symplectic method of order 2.

A Störmer/Verlet method applied to the first order system $\dot{q} = v$, $\dot{v} = f(q)$

$$v_{n+1/2} = v_n + \frac{\Delta t}{2} f(q_n)$$

$$q_{n+1} = q_n + \Delta t v_{n+1/2} \quad (1.26)$$

$$v_{n+1} = v_{n+1/2} + \frac{\Delta t}{2} f(q_{n+1}) \quad (1.27)$$

is an explicit method which is also symplectic of order 2.

An s -stage Runge–Kutta method

$$k_i = f\left(y_0 + \Delta t \sum_{j=1}^s a_{ij} k_j\right), \quad i = 1, \dots, s$$

$$y_1 = y_0 + \Delta t \sum_{i=1}^s b_i k_i \quad (1.28)$$

applied to the problem $\dot{y} = f(y)$ is symplectic if it satisfies

$$b_i a_{ij} + b_j a_{ji} - b_i b_j = 0$$

for all $i, j = 1, \dots, s$ where b_j, a_{ij} ($i, j = 1, \dots, s$) are real numbers and $c_j = \sum_{i=1}^s a_{ij}$.

One of the most important property of symplectic integrators is that they preserve quadratic invariants. For example, all symplectic Runge-Kutta methods preserves quadratic invariant (see [33] for details). They have excellent long-time behavior which can be explained by backward error analysis [63].

1.3 Hamiltonian PDE's

Partial differential equations with a Hamiltonian structure are important in the study of solitons such as the Korteweg-de Vries (KdV) and NLSE. Many PDE's can be put into a Hamiltonian formulation and admitted symmetries of this formulation can lead, via Noether's theorem, to conservation laws [50, 60]. There are several approaches aimed at exploiting this structure in discretization of the PDE's, all of which can be labelled geometrical. One is based upon using the Hamiltonian formulation of the PDE's on multisymplectic structures, generalizing the classical Hamiltonian structure by assigning a distinct symplectic operator for each space direction and time [18, 21, 65]. In this section we will summarize some of the ideas presented in the monograph [60].

Many differential equations of the form

$$u_t = F(x, u, u_x, u_{xx}, \dots)$$

can be represented in the Hamiltonian form

$$u_t = \mathcal{D} \left(\frac{\delta \mathcal{H}}{\delta u} \right), \quad \mathcal{H}[u] = \int H(x, u, u_x, u_{xx}, \dots) dx.$$

Typically the domain of integration is the real line or the circle (corresponding to periodic boundary conditions for the PDE). Here \mathcal{H} is a functional map from the function space in which u is defined to the real line. The variational derivative $\delta \mathcal{H} / \delta u$ is the function defined via the Gateaux derivative [60]

$$\left(\frac{d}{d\varepsilon} \mathcal{H}[u + \varepsilon v] \right) \Big|_{\varepsilon=0} = \int \frac{\delta \mathcal{H}}{\delta u} v dx.$$

If, for example, u is a scalar function and $H = H(u, u_x)$ then the variational derivative is given by

$$\frac{\delta \mathcal{H}}{\delta u} = \frac{\partial H}{\partial u} - \frac{\partial}{\partial x} \left(\frac{\partial H}{\partial u_x} \right). \quad (1.29)$$

The operator \mathcal{D} is called Hamiltonian if the functionals $\mathcal{A}[u]$ and $\mathcal{B}[u]$ it generates a Poisson bracket $\{\cdot, \cdot\}$ given as

$$\{\mathcal{A}, \mathcal{B}\} = \int \frac{\delta \mathcal{A}}{\delta u} \mathcal{D} \frac{\delta \mathcal{B}}{\delta u} dx.$$

The Poisson bracket must satisfy the skew-symmetry condition

$$\{\mathcal{A}, \mathcal{B}\} = - \{\mathcal{B}, \mathcal{A}\}$$

and the Jacobi identity

$$\{\{\mathcal{A}, \mathcal{B}\}, \mathcal{C}\} + \{\{\mathcal{B}, \mathcal{C}\}, \mathcal{A}\} + \{\{\mathcal{C}, \mathcal{A}\}, \mathcal{B}\} = 0,$$

for all functional $\mathcal{A}, \mathcal{B}, \mathcal{C}$. The Hamiltonian PDE for time evolution of the system is then given by

$$u_t = \{u, \mathcal{H}\}.$$

If the Hamiltonian functional \mathcal{H} is not explicitly dependent on time then it is conserved.

In many PDE's in the past, when approximating the solution of the differential equations using a numerical integrator, properties of the differential equation were neglected and they were discretized in space and time simultaneously. However, it worths to preserve as many properties of the exact evolution equation as possible. For this purpose, they are discretized in space first and then discretized in time by symplectic methods when the symplectic structure was considered. Symplectic methods are accurate and efficient in the long-time integration of Hamiltonian ODE's [69]. In addition, symplectic integrators lead to a useful interpretation of backward error analysis, in which a modified equation, the equation solved by a numerical scheme to higher order than the original equation, is used to understand the discretization error induced by the numerical scheme [63]. Recently, the idea of the symplectic integration was extended to Hamiltonian PDE, by studying multisymplectic structure of the PDE's [18, 19, 20, 21, 22, 64, 65].

1.4 Multisymplectic PDE's

In this section we summarize some of the ideas for multisymplectic PDE's and the conservation laws which are discussed in [18, 21, 49, 57]. If a variational description of a Lagrangian formulation for a continuous dynamical system with the Lagrangian $\mathcal{L}(u, u_t, u_x)$ is available

$$\delta \int \int \mathcal{L}(u, u_t, u_x) dt dx = 0, \quad (1.30)$$

then the equation of motion is formally given by

$$-\partial_t \frac{\partial \mathcal{L}}{\partial u_t} - \partial_x \frac{\partial \mathcal{L}}{\partial u_x} + \frac{\partial \mathcal{L}}{\partial u} = 0. \quad (1.31)$$

By introducing a conjugate variable v related to the temporal derivative u_t

$$v \equiv \frac{\partial \mathcal{L}}{\partial u_t}, \quad (1.32)$$

and assuming that the transformation above is invertible, i.e. $u_t = u_t(v)$, then the Hamiltonian is defined by a Legendre transformation [50]

$$\mathcal{H}(u, v) = \int v u_t(v) - \mathcal{L}(u, u_t(v), u_x) dx. \quad (1.33)$$

By having the variational derivatives (1.29) of \mathcal{H} required to satisfy the original equation of motion (1.31) and by the definition of the conjugate variable v (1.32), we get

$$\frac{\delta \mathcal{H}}{\delta u} = \partial_x \frac{\partial \mathcal{L}}{\partial u_x} - \frac{\partial \mathcal{L}}{\partial u} = -\partial_t v \quad (1.34)$$

$$\frac{\delta \mathcal{H}}{\delta v} = u_t(v) + v u'_t(v) - \frac{\partial \mathcal{L}}{\partial u_t} u'_t(v) = \partial_t u \quad (1.35)$$

or, with $y = (u, v)^T$

$$\mathbf{y}_t = J^{-1} \frac{\delta \mathcal{H}}{\delta \mathbf{y}} \quad (1.36)$$

with J as the skew-symmetric structure matrix (1.3) with $d = 1$. The equation (1.36) is the formulation of (1.31) as an infinite-dimensional Hamiltonian system. If y is a solution of the variational equation associated with (1.36), then the symplectic two-form defined as

$$\partial_t \frac{1}{2} \int dy \wedge J dy dx = 0 \quad (1.37)$$

is globally conserved. Here \wedge denotes the external product (1.7).

There are two disadvantages of the infinite-dimensional Hamiltonian formulation (1.36); the symplectic structure (1.37) is infinite dimensional, and a function space is required for the x -dependence. For example, to define the integral of the Hamiltonian function (1.33), the domain of integration over the spatial variable x must be specified. On the other hand, a multisymplectic formulation is defined on a phase space of finite-dimension, and no integration is required.

Introducing a second conjugate variable, this time with respect to the spatial variable u_x ,

$$\omega \equiv \frac{\partial \mathcal{L}}{\partial u_x}, \quad (1.38)$$

yields a multisymplectic structure [18]. Again we assume that this is an invertible relation $u_x = u_x(\omega)$, and a new Hamiltonian defined by a Legendre transformation

with respect to both v and ω is

$$S(u, v, \omega) = vu_t + \omega u_x - \mathcal{L}(u, u_t(v), u_x(\omega)). \quad (1.39)$$

The partial derivatives of S with respect to (u, v, ω) are required to satisfy the equation (1.31) as well as the definitions of v (1.32) and ω (1.38):

$$\frac{\partial S}{\partial u} = -\frac{\partial \mathcal{L}}{\partial u} = -\partial_t v - \partial_x \omega, \quad (1.40)$$

$$\frac{\partial S}{\partial v} = u_t(v) + vu'_t(v) - \frac{\partial \mathcal{L}}{\partial u_t} u'_t(v) = \partial_t u, \quad (1.41)$$

$$\frac{\partial S}{\partial \omega} = u_t(\omega) + \omega u'_x(v) - \frac{\partial \mathcal{L}}{\partial u_x} u'_x(v) = \partial_x u. \quad (1.42)$$

The multisymplectic formulation can be written in a compact form as

$$\mathbf{M}z_t + \mathbf{K}z_x = \nabla_z S(z), \quad z \in R^3, \quad (1.43)$$

where

$$\mathbf{M} = \begin{pmatrix} 0 & -1 & 0 \\ 1 & 0 & 0 \\ 0 & 0 & 0 \end{pmatrix}, \quad \mathbf{K} = \begin{pmatrix} 0 & 0 & -1 \\ 0 & 0 & 0 \\ 1 & 0 & 0 \end{pmatrix}, \quad (1.44)$$

and $z = (u, v, \omega)^T$. In this definition ∇_z is the gradient operator given by $\nabla_z = (\partial/\partial u, \partial/\partial v, \partial/\partial \omega)$.

The multisymplectic formalism can be extended for higher dimensional systems with $n \geq 3$, skew-symmetric matrices \mathbf{M} and \mathbf{K} , and a smooth function $S : \mathbf{R}^n \rightarrow \mathbf{R}$ [21, 18].

1.4.1 Symplecticity

The system (1.43) is multisymplectic in the following sense: associated with \mathbf{M} and \mathbf{K} are pre-symplectic forms

$$\omega(U, V) = \langle \mathbf{M}U, V \rangle \quad \text{and} \quad \kappa(U, V) = \langle \mathbf{K}U, V \rangle,$$

where $U, V \in R^n$, ω defines a symplectic structure on R^m , ($m = \text{rank } \mathbf{M} \leq n$) which is associated with the time variable t , and κ defines a symplectic structure on R^k ($k = \text{rank } \mathbf{K} \leq n$) which is associated with the space variable x . Any system of the form (1.43) conserves the symplectic structure

$$\partial_t \omega + \partial_x \kappa = 0. \quad (1.45)$$

To show this, we assume that $U, V \in R^n$ are any two solution of the variational equation associate with (1.43),

$$\mathbf{M}dz_t + \mathbf{K}dx_x = \mathbf{D}_{zz}S(z) dz. \quad (1.46)$$

Then

$$\begin{aligned} \partial_t \omega &= \langle \mathbf{M}U_t, V \rangle + \langle \mathbf{M}U, V_t \rangle \\ \partial_x \kappa &= \langle \mathbf{K}U_x, V \rangle + \langle \mathbf{K}U, V_x \rangle \end{aligned}$$

and since the Hessian matrix \mathbf{D}_{zz} is symmetric, we obtain the multisymplectic conservation law

$$\begin{aligned} \partial_t \omega + \partial_x \kappa &= \langle \mathbf{M}U_t + \mathbf{K}U_x, V \rangle - \langle U, \mathbf{M}V_t + \mathbf{K}V_x \rangle \\ &= \langle \mathbf{D}_{zz}S(z)U, V \rangle - \langle U, \mathbf{D}_{zz}S(z)V \rangle \\ &= 0. \end{aligned} \quad (1.47)$$

Using the wedge product notation the multisymplectic conservation law (1.45) can be written as

$$\partial_t(dz \wedge \mathbf{M}dz) + \partial_x(dz \wedge \mathbf{K}dz) = 0. \quad (1.48)$$

1.4.2 Energy and Momentum Conservation

In addition to the multisymplectic conservation law (1.45), multisymplectic PDE's possesses two additional conservation laws [21]. When the Hamiltonian function $S(z)$ is independent of t and x , the PDE's in multisymplectic form (1.43) has local energy and local momentum conservation laws. Conservation of energy and momentum are associated with translation invariance in time and space respectively. Using the time invariance of (1.43) an energy conservation law can be derived by multiplying (1.43) with z_t^T from the left

$$z_t^T \mathbf{K}z_x = z_t^T \nabla_z S(z) = \partial_t S(z) \quad (1.49)$$

because of the skew-symmetry of \mathbf{M} , $z_t^T \mathbf{M}z_t = 0$. Noting that

$$z_t^T \mathbf{K}z_x = \frac{1}{2} \partial_t (z^T \mathbf{K}z_x) - \frac{1}{2} \partial_x (z^T \mathbf{K}z_t) \quad (1.50)$$

we obtain the energy conservation law

$$\partial_t E(z) + \partial_x F(z) = 0 \quad (1.51)$$

where

$$E(z) = S(z) - \frac{1}{2} \kappa(z_x, z), \quad F(z) = \frac{1}{2} \kappa(z_t, z), \quad (1.52)$$

are known as energy density and energy flux respectively. Similarly, the spatial invariance of (1.43) can be used by multiplying (1.43) with z_x^T from the left, which gives

$$z_x^T \mathbf{M} z_t = z_x^T \nabla_z S(z) = \partial_x S(z) \quad (1.53)$$

because the skew-symmetry of \mathbf{M} implies $z_x^T \mathbf{K} z_x = 0$. Using the identity

$$z_x^T \mathbf{M} z_t = \frac{1}{2} \partial_x (z^T \mathbf{M} z_t) - \frac{1}{2} \partial_t (z^T \mathbf{M} z_x) \quad (1.54)$$

we obtain the momentum conservation law

$$\partial_t I(z) + \partial_x G(z) = 0 \quad (1.55)$$

where

$$G(z) = S(z) - \frac{1}{2} w(z_t, z), \quad I(z) = \frac{1}{2} \omega(z_x, z) \quad (1.56)$$

are known as momentum density and momentum flux respectively.

However, the Hamiltonian function $S(z)$ associated with the multisymplectic structure (1.43) is not preserved. This can be shown by

$$\begin{aligned} \frac{\partial S(z)}{\partial t} &= \langle \nabla_z S(z), z_t \rangle = \langle \mathbf{K} z_x, z_t \rangle = \kappa(z_x, z_t), \\ \frac{\partial S(z)}{\partial x} &= \langle \nabla_z S(z), z_x \rangle = \langle \mathbf{M} z_t, z_x \rangle = \kappa(z_t, z_x). \end{aligned} \quad (1.57)$$

There are also some additional conservation laws for multisymplectic PDE's [57]. This follows from Noether theory and the derivation of the multisymplectic formulation from a Lagrangian functional

$$\mathcal{L} = \int L dt dx \quad \text{for } L = \frac{1}{2} z^T (\mathbf{M} z_t + \mathbf{K} z_x) - S(z). \quad (1.58)$$

Taking a linear one-parameter family of linear coordinate transformation given by

$$\mathcal{G}_\varepsilon = e^{\varepsilon \mathbf{A}} z \quad (1.59)$$

which is chosen in such a way that it is symplectic with respect to both ω and κ we obtain

$$A^T \mathbf{M} + \mathbf{M} A = 0 \quad A^T \mathbf{K} + \mathbf{K} A = 0.$$

Because the Lagrangian is invariant under such a transformation

$$0 = \left. \frac{\partial \mathcal{L}}{\partial \varepsilon} \right|_{\varepsilon=0} = \int S'(z) \mathbf{A} z dt dx$$

and we obtain the invariance condition

$$S'(z)\mathbf{A}z = 0. \quad (1.60)$$

Direct application of $S'(z)\mathbf{A}z = 0$ to the multisymplectic formulation yields

$$(\mathbf{A}z)^T \mathbf{M}z_t + (\mathbf{A}z)^T \mathbf{K}z_x = (\mathbf{A}z)^T \nabla_z S(z) = 0$$

which can be written as a conservation law

$$\partial_t T + \partial_x V = 0 \quad (1.61)$$

with $T = (z^T \mathbf{M} \mathbf{A} z)$ and $V = (z^T \mathbf{K} \mathbf{A} z)$, which is called an additional conservation law.

We note that all these conservation laws are of local nature. The local conservation property is stronger than the global conservation since for Hamiltonian PDE's symplecticity may vary from point to point in space and from time to time. However local conservation may lead to global conservation. Boundary conditions play an important role here. In order to show this we consider the multisymplectic PDE (1.43) with periodic boundary conditions and the multisymplectic conservation law (1.45). To obtain the global conservation, we take the integral of (1.45) over the spatial domain and obtain

$$\int_0^L \left(\frac{\partial}{\partial x} \kappa \right) dx = \kappa(L, t) - \kappa(0, t) = 0, \quad (1.62)$$

and

$$\int_0^L \left(\frac{\partial}{\partial x} \omega \right) dx = \frac{\partial}{\partial x} \left(\int_0^L \omega dx \right) = \frac{d}{dt} \hat{\omega} = 0, \quad (1.63)$$

where we used the periodicity of the boundary conditions in (1.62). We notice that (1.63) corresponds to the conservation of symplecticity of Hamiltonian ODE's.

Integrating $E(z)$, $I(z)$ and $T(z)$ over the spatial domain with periodic boundary conditions lead to global conservation of energy

$$\frac{d}{dt} \mathcal{E}(z) = 0 \quad \text{with} \quad \mathcal{E}(z) = \int_0^L E(z) dx, \quad (1.64)$$

the global conservation of momentum

$$\frac{d}{dt} \mathcal{I}(z) = 0 \quad \text{with} \quad \mathcal{I}(z) = \int_0^L I(z) dx, \quad (1.65)$$

and the global conservation of additional conservation law

$$\frac{d}{dt} \mathcal{T}(z) = 0 \quad \text{with} \quad \mathcal{T}(z) = \int_0^L T(z) dx. \quad (1.66)$$

where L is the length of the spatial domain.

It is possible to simplify the multisymplectic conservation law (1.48) by taking a non-unique splitting of matrices \mathbf{M} and \mathbf{K} such that

$$\mathbf{M} = \mathbf{M}_+ + \mathbf{M}_- \quad \text{and} \quad \mathbf{K} = \mathbf{K}_+ + \mathbf{K}_-, \quad (1.67)$$

with

$$\mathbf{M}_+^T = -\mathbf{M}_- \quad \text{and} \quad \mathbf{K}_+^T = -\mathbf{K}_-. \quad (1.68)$$

Noting that

$$dz \wedge \mathbf{M}_+ dz = dz \wedge \mathbf{M}_- dz \quad \text{and} \quad dz \wedge \mathbf{K}_+ dz = dz \wedge \mathbf{K}_- dz, \quad (1.69)$$

the multisymplectic conservation law (1.48) holds with

$$\omega = dz \wedge \mathbf{M}_+ dz \quad \text{and} \quad \kappa = dz \wedge \mathbf{K}_+ dz. \quad (1.70)$$

This splitting can be used in the multisymplectic discretization of (1.43).

CHAPTER 2

NONLINEAR SCHRÖDINGER EQUATION

The subject of integrable models is very fascinating largely because of their innumerable symmetries and a special class of solutions known as soliton solutions. However, only a few systems are integrable. The NLSE is an example of an integrable equation. In contrast to many PDE's like KdV and Sine-Gordon, the dependent variable in NLSE is complex rather than real, so the evolutions of two quantities are governed by the equation. It plays an important role in nonlinear physics [34, 46]. It is a completely integrable system, having infinite number of conservation law, and admits stable solitary wave solutions [59]. Various types of numerical schemes have been proposed to simulate the NLSE (see, for example [4, 45, 66] and reference therein). The CNLSE's and N-CNLSE's are often used to describe the more general physical situations. They are also model PDE's in such as plasma physics, optics, biophysics and water waves (see [19, 20, 42, 48, 53, 82, 43] and reference therein). But in many situation, they are not integrable.

This Chapter is organized as follows: In Section 2.1 the Hamiltonian and multisymplectic structure of the NLSE and its conserved quantities are discussed. The Hamiltonian and multisymplectic structure of the CNLSE and its conserved quantities are given in Section 2.2. We present the multisymplectic structure of the N-CNLSE in Section 2.3.

2.1 The Nonlinear Schrödinger Equation

The cubic NLSE can be written as

$$i u_t + u_{xx} + a|u|^2 u = 0 \tag{2.1}$$

where $x \in R$, a is a constant, $i = \sqrt{-1}$, $|\cdot|$ denotes the modulus, and $u(x, t)$ is complex function. It is a completely integrable system, possesses an infinite number of conservation laws, and admits stable solitary-waves called solitons [46, 59]. Equations with higher-order nonlinearities are also useful for numerical experiments, since they can provide more severe tests for approximation schemes. The Schrödinger equation with power nonlinearity (GPNLSE) [66]

$$i u_t + u_{xx} + a|u|^{l-1}u = 0 \quad (2.2)$$

where $i = \sqrt{-1}$, $u = u(\mathbf{x}, t)$ is complex-valued, $\mathbf{x} \in \mathbf{R}^n$, a is a real constant, and $l > 1$ has been used to model nonlinear dispersive waves. We will consider the case $\mathbf{x} \in \mathbf{R}$ with the initial condition $u(x, 0) = u_0(x)$ decays exponentially to zero as $|x| \rightarrow \infty$. For $l = 3$, (2.2) reduces to the cubic NLSE (2.1). While the cubic NLSE (2.1) has been examined in various numerical studied, less attention has been paid to the more general Schrödinger equation (2.2) of which the cubic NLSE is a special case. The GPNLSE (2.2) has been studied using the orthogonal spline collocation method for spatial discretization (see [66] and reference therein)

In this thesis, we shown that the GPNLSE has Hamiltonian structure. Because of the Hamiltonian structure one can use symplectic methods to simulate it. We also show that GPNLSE has a multisymplectic formulation. Because of the multisymplectic structure one can use multisymplectic methods to simulate it.

2.1.1 Hamiltonian Formulation

The Schrödinger equation with power nonlinearity (2.2) can be written as an infinite Hamiltonian system

$$u_t = \frac{\delta H}{\delta u^*} \quad (2.3)$$

with the Hamiltonian

$$H(u, u^*) = i \int \left(\frac{2a}{l+1} |u|^{l+1} - |u_x|^2 \right) dx \quad (2.4)$$

where u^* denotes the complex conjugates of u . If p and q are real valued functions then substituting $u = p - iq$ into (2.3) we get

$$\begin{aligned} q_t + p_{xx} + a(p^2 + q^2)^{\frac{l-1}{2}} p &= 0, \\ -p_t + q_{xx} + a(p^2 + q^2)^{\frac{l-1}{2}} q &= 0, \end{aligned} \quad (2.5)$$

or equivalently

$$z_t = J^{-1} \frac{\delta \mathcal{H}}{\delta z}, \quad (2.6)$$

where $z = (p, q)^T$, J is defined in (1.3), and the Hamiltonian or energy is

$$\mathcal{H}(z) = \int H(z) dx, \quad \text{for } H(z) = \int \frac{1}{2} \left[\frac{2a}{l+1} (p^2 + q^2)^{\frac{l+1}{2}} - p_x^2 - q_x^2 \right] dx. \quad (2.7)$$

The main idea is to discretize the space appropriately so that the resulting semi-discrete system can be written as a finite dimensional Hamiltonian system in the time direction. The resulting system of ODE's can be integrated by a symplectic method. The Hamiltonian formulation of the NLSE allows us to identify the symplectic structure, and the conserved quantities and therefore allows the application of a symplectic integrator for its solution.

A symplectic and non-symplectic integration of (2.1) with periodic initial data and boundary conditions was made in [35]. In [78], the properties of a symplectic method were tested using different initial data: one-soliton and three-soliton solutions.

2.1.2 Multisymplectic Formulation

The GPNLSE (2.2) can be cast into a multisymplectic Hamiltonian system (1.43).

Using $u = p - iq$ the GPNLSE can be rewritten as a pair of real-valued equations

$$\begin{aligned} q_t + p_{xx} + a(p^2 + q^2)^{\frac{l-1}{2}} p &= 0, \\ p_t - q_{xx} - a(p^2 + q^2)^{\frac{l-1}{2}} q &= 0. \end{aligned} \quad (2.8)$$

Introducing the pair of conjugate momenta $v = p_x$, $\omega = q_x$, we obtain the multisymplectic PDE

$$\begin{aligned} -q_t - v_x &= a(p^2 + q^2)^{\frac{l-1}{2}} p \\ p_t - \omega_x &= a(p^2 + q^2)^{\frac{l-1}{2}} q \\ p_x &= v \\ q_x &= \omega \end{aligned} \quad (2.9)$$

with the state variable $z = (p, q, v, \omega)^T$ and the Hamiltonian

$$S(z) = \frac{1}{2} \left(\frac{2a}{l+1} (p^2 + q^2)^{\frac{l+1}{2}} + v^2 + \omega^2 \right). \quad (2.10)$$

In this case,

$$M = \begin{pmatrix} 0 & -1 & 0 & 0 \\ 1 & 0 & 0 & 0 \\ 0 & 0 & 0 & 0 \\ 0 & 0 & 0 & 0 \end{pmatrix}, \quad K = \begin{pmatrix} 0 & 0 & -1 & 0 \\ 0 & 0 & 0 & -1 \\ 1 & 0 & 0 & 0 \\ 0 & 1 & 0 & 0 \end{pmatrix}. \quad (2.11)$$

The corresponding multisymplectic conservation law is

$$\frac{\partial}{\partial t}(dp \wedge dq) + \frac{\partial}{\partial x}(dp \wedge dv + dq \wedge d\omega) = 0. \quad (2.12)$$

The time invariance leads to the corresponding energy conservation law (1.51) as

$$\frac{\partial}{\partial t}(S(z) - v^2 - \omega^2) + \frac{\partial}{\partial x}(vp_t + \omega q_t) = 0 \quad (2.13)$$

and space invariance leads to the momentum conservation law (1.55) as

$$\frac{\partial}{\partial t}(qv - pw) + \frac{\partial}{\partial x}(S(z) - \frac{1}{2}(qp_t - pq_t)) = 0. \quad (2.14)$$

When we integrate these three equations with respect to x , we obtain the global conservation of energy (Hamiltonian), momentum, and norm.

The multisymplectic form of NLSE (2.9) is invariant under the action of the one-parameter group of rotations $SO(2)$, given by $\mathcal{G}_\theta(z) = \mathbf{R}_\theta z$, with

$$\mathbf{R}_\theta = \begin{bmatrix} \cos \theta & -\sin \theta & 0 & 0 \\ \sin \theta & \cos \theta & 0 & 0 \\ 0 & 0 & \cos \theta & -\sin \theta \\ 0 & 0 & \sin \theta & \cos \theta \end{bmatrix}$$

We define the matrix \mathbf{A} such that

$$\mathbf{A}z = \frac{d}{d\theta}\mathcal{G}_\theta(z)|_{\theta=0} = [-p, q, -\omega, v]^T.$$

Then, we have

$$z^T \mathbf{M} \mathbf{A} z = p^2 + q^2, \quad z^T \mathbf{K} \mathbf{A} z = 2(p\omega - qv) \quad (2.15)$$

which shows that the additional conservation law (1.61) is satisfied in the form

$$\frac{\partial}{\partial t} \left[\frac{1}{2}(p^2 + q^2) \right] - \frac{\partial}{\partial x}(p\omega - qv) = 0 \quad (2.16)$$

which is called the norm or additional conservation law for NLSE.

All these conservation laws are local ones. For global conservation, boundary conditions play an important role. In order to show, how boundary conditions are crucial for global conservation we consider the NLSE (2.5) with cubic nonlinearity $l = 3$ on $x \in [0, L]$ where $L \in \mathbf{r}$ is length of space. If we take the derivative of H with respect to t using the energy functional (2.7), we get

$$\begin{aligned}\frac{\partial H}{\partial t} &= \frac{1}{2} \frac{\partial}{\partial t} \left[\frac{a}{2} (p^2 + q^2)^2 - p_x^2 - q_x^2 \right] \\ &= a(p^2 + q^2)(pp_t + qq_t) - p_x p_{xt} - q_x q_{xt} \\ &= a(p^2 + q^2)(pp_t + qq_t) + p_t p_{xx} + q_t q_{xx} - \frac{\partial}{\partial x} (p_x p_t + q_x q_t)\end{aligned}\quad (2.17)$$

To simplify this expression, we multiply the first equation of (2.5) by p_t and the second equation of (2.5) by q_t and obtain

$$\begin{aligned}p_t q_t + p_t q_{xx} + a(p^2 + q^2) p_t p &= 0, \\ -q_t p_t + q_t p_{xx} + a(p^2 + q^2) q_t q &= 0,\end{aligned}\quad (2.18)$$

If we add these equalities we get

$$p_t p_{xx} + q_t q_{xx} + a(p^2 + q^2)(pp_t + qq_t) = 0. \quad (2.19)$$

Substituting this into (2.17) yields

$$\frac{\partial H}{\partial t} = -\frac{\partial}{\partial x} (p_x p_t + q_x q_t). \quad (2.20)$$

Let $\zeta \in [0, L]$ be any point. Evaluating (2.20) at $x = \zeta$ gives

$$\frac{\partial}{\partial t} H(\zeta, t) = -\frac{\partial}{\partial x} (p_x(\zeta, t) p_t(\zeta, t) + q_x(\zeta, t) q_t(\zeta, t)) = 0.$$

Therefore, energy is conserved locally inside the integration domain. This shows that the boundary conditions does not effect the local conservation. However, for global conservation of energy, boundary conditions are crucial. To see the effect of boundary condition for the global conservation we take the derivative of \mathcal{H} with respect to time and we get

$$\begin{aligned}\frac{d}{dt} \mathcal{H} &= \int_0^L \frac{d}{dt} H dx \\ &= (p_x p_t + q_x q_t) \Big|_0^L \\ &= [p_x(0, t) p_t(0, t) + q_x(0, t) q_t(0, t)] - [p_x(L, t) p_t(L, t) + q_x(L, t) q_t(L, t)].\end{aligned}$$

Notice that, for the periodic boundary condition

$$p(0, t) = p(L, t), \quad q(0, t) = q(L, t), \quad p_x(0, t) = p_x(L, t), \quad q_x(0, t) = q_x(L, t),$$

$$\frac{d}{dt}\mathcal{H} = 0,$$

i.e. energy is conserved globally. This example shows the difference between local and global conservation, as well as how the boundary conditions effect the conservation.

2.1.3 Conserved Quantities

Although the general case of the GPNLSE is non-integrable, rapidly decaying solutions to (2.2) at the boundaries do satisfies three conservation laws. The first conservation law can be derived by multiplying (2.2) by u^* , then taking the imaginary part and integrating over the real line. Then, we get the squared L^2 norm of the solution

$$C_1(u) = \int_{-\infty}^{\infty} |u|^2 dx, \quad (2.21)$$

which is conserved in time. The second conservation law

$$C_2(u) = \int_{-\infty}^{\infty} \left(|u_x|^2 - \frac{2a}{l+1} |u|^{l+1} \right) dx, \quad (2.22)$$

is obtained by multiplying (2.2) by u_t^* , taking the real part, and integrating over the real line. Also,

$$C_3(u) = \int_{-\infty}^{\infty} 2\text{Im}(uu_x^*) dx, \quad (2.23)$$

is conserved in time, which can be found by multiplying (2.2) by u_x^* , taking the real part and integrating over the real line.

In the focusing ($a > 0$) and refocusing ($a < 0$) cases the situations that arise are quite different. In particular, we have the following cases [70].

- a) If $a < 0$ and $l < \infty$, solutions exist for all t .
- b) If $a > 0$ and $l < 5$, solutions exist for all t with some regularity properties.
- c) If $a > 0, l \geq 5$, and $C_2(u_0) < 0$, the no smooth solution can exist for all positive t .

If $a > 0$ and $l \geq 5$, even if $C_2(u_0) > 0$, it is possible that blow-up may occur under some conditions. Also, solitary-wave solutions of the GPNLSE are known to be unstable if $l \geq 5$ (see [84] and reference therein).

2.2 Coupled Nonlinear Schrödinger Equation

Optical fiber communications are advancing very rapidly. One of the major transmission formats is to use optical solitons as information bits. For optical soliton, the pulse can transmit without change of shape. In physical applications, pulse-pulse interactions have been studied in the past 20 years. Most of these studies used the NLSE model, which is appropriate when fiber birefringence is neglected. In an ideal fiber, optical solitons can be modelled approximately by the NLSE, whose solution behaviors are completely known [6, 92]. But in reality, optical fibers are birefringent. When fiber birefringence is taken into consideration, pulse propagation is actually governed by two CNLSE. Pulses travel at slightly different speeds along the two orthogonal polarization axes. This effect has been analyzed in [52], where two CNLSE's were derived for the pulse propagation along the two polarization axes. Such a pulse is called a vector soliton in the optics literature. We note that a "vector soliton" here is just a solitary wave solution. In a linear birefringent fiber, the cross-phase modulation coefficient e is $3/2$. But it may take other values if the birefringence is elliptic [54]. Birefringent fibers also support optical solitons [53, 88]. The collision of vector solitons is critical in many optical switching devices and nonlinear telecommunication networks. In all the above situations, collision of vector solitons is an important issue. Collision of vector solitons in the CNLSE's has been studied before. In the integrable Manakov model, the soliton collision is elastic, and the outcome has been explicitly specified.

A wide range of the CNLSE model can be written in the general form

$$i \left(\frac{\partial \psi_1}{\partial t} + \delta_1 \frac{\partial \psi_1}{\partial x} \right) + d_1 \frac{\partial^2 \psi_1}{\partial x^2} = \frac{\delta \mathcal{H}}{\delta \bar{\psi}_1} \quad (2.24)$$

$$i \left(\frac{\partial \psi_2}{\partial t} + \delta_2 \frac{\partial \psi_2}{\partial x} \right) + d_2 \frac{\partial^2 \psi_2}{\partial x^2} = \frac{\delta \mathcal{H}}{\delta \bar{\psi}_2} \quad (2.25)$$

where $\delta_1, \delta_2, d_1, d_2$ are real parameters and $\psi_1(x, t), \psi_2(x, t)$ are complex valued functions of $(x, t) \in R$ and $\mathcal{H}(\psi_1, \bar{\psi}_1, \psi_2, \bar{\psi}_2)$ is a real valued function called as the Hamiltonian. For the classical CNLSE with cubic coupling \mathcal{H} takes the form

$$\mathcal{H}(\psi_1, \bar{\psi}_1, \psi_2, \bar{\psi}_2) = b_1 |\psi_1|^4 + b_2 |\psi_2|^4 + b_3 |\psi_1|^2 |\psi_2|^2,$$

with real parameters b_1, b_2, b_3 . Thus the system (2.24)-(2.25) becomes

$$i \left(\frac{\partial \psi_1}{\partial t} + \delta_1 \frac{\partial \psi_1}{\partial x} \right) + d_1 \frac{\partial^2 \psi_1}{\partial x^2} + (a_1 |\psi_1|^2 + e |\psi_2|^2) \psi_1 = 0 \quad (2.26)$$

$$i \left(\frac{\partial \psi_2}{\partial t} + \delta_2 \frac{\partial \psi_2}{\partial x} \right) + d_2 \frac{\partial^2 \psi_2}{\partial x^2} + (e |\psi_1|^2 + a_2 |\psi_2|^2) \psi_2 = 0 \quad (2.27)$$

where $\delta_1, \delta_2, d_1, d_2, a_1, a_2$ and e are all real constants. In applications the real parameters d_1, d_2 are the dispersion coefficients, a_1, a_2, e are the Landau constants which describe the self-modulation of the wave packets, and e is the wave-wave interaction coefficient which describes the cross-modulations of the wave packets. When $e = 0$, the system decouples into two NLSEs. The coefficients in (2.26)-(2.27) are variable parameters for the geophysical fluid dynamics. For nonlinear optics, the coefficients are some fixed constants (see [48, 75, 81] and reference therein). In this work the coefficients are taken from nonlinear optics.

In general the system (2.26)-(2.27) is a non-integrable system, that is, we can not find infinitely many conservation laws [82]. The conservation laws can be written as

$$\frac{\partial D_j}{\partial t} + \frac{\partial F_j}{\partial x} = 0$$

where the D_j are called the conserved density and the F_j are called the conserved flux. In [82] four conserved quantities of CNLSE are listed among which two are

$$\begin{aligned} D_1 &= \psi_1^* \psi_1, & F_1 &= \delta_1 \psi_1^* \psi_1 + i d_1 (\psi_{1x} \psi_1 - \psi_1^* \psi_{1x}), \\ D_2 &= \psi_2^* \psi_2, & F_2 &= \delta_2 \psi_2^* \psi_2 + i d_2 (\psi_{2x} \psi_2 - \psi_2^* \psi_{2x}). \end{aligned} \quad (2.28)$$

However, for some parameters the system (2.26)-(2.27) is integrable. For example, in [48] the integrability of the CNLSE (2.26)-(2.27) is shown in the case $d_1 = d_2 = 1$, $a_1 = a_2 = e$. Later, in [91] it was shown that the CNLSE (2.26)-(2.27) is integrable only for the following two cases:

- a) The Manakov case : $d_1 = d_2$, $a_1 = a_2 = e$,

and

- b) $d_1 = -d_2$ $a_1 = a_2 = -e$.

In a recent study [53] on optical fibers with a linear birefringence, (2.26)-(2.27) with $\delta_1 = -\delta_2 = \delta$, $d_1 = d_2, a_1 = a_2 = 1$, and $e = 2/3$ has been proposed.

2.2.1 Hamiltonian Formulation

If a PDE is an infinite-dimensional Hamiltonian system, then semi-discretization leads to a system of ODE's with symplectic form which is then solved by a symplectic method. In this section we will review the Hamiltonian formulation of CNLSE.

It is well known that the system (2.26)-(2.27) can be written as an infinite-dimensional Hamiltonian system [16, 19, 91]. The Lagrangian density for (2.26)-(2.27) is given in [82] as

$$\begin{aligned} \mathcal{L} = & \frac{i}{2} \sum_{k=1}^2 (\psi_k^* \psi_{kt} - \psi_{kt}^* \psi_k) + \frac{i}{2} \sum_{k=1}^2 \delta_k (\psi_k^* \psi_{kx} - \psi_{kx}^* \psi_k) \\ & - \sum_{k=1}^2 d_k \psi_{kx}^* \psi_{kx} + \frac{a_1}{2} |\psi_1|^4 + e |\psi_1|^2 |\psi_2|^2 + \frac{a_2}{2} |\psi_2|^4. \end{aligned} \quad (2.29)$$

Here ψ^* denotes the complex conjugate of ψ , and the subscripts t and x denote partial differentiations with respect to time and space. Then the Euler-Lagrange equations

$$\begin{aligned} \frac{\partial}{\partial t} \left(\frac{\partial \mathcal{L}}{\partial \psi_{kt}} \right) + \frac{\partial}{\partial x} \left(\frac{\partial \mathcal{L}}{\partial \psi_{kx}} \right) - \frac{\partial \mathcal{L}}{\partial \psi_k} &= 0, \\ \frac{\partial}{\partial t} \left(\frac{\partial \mathcal{L}}{\partial \psi_{kt}^*} \right) + \frac{\partial}{\partial x} \left(\frac{\partial \mathcal{L}}{\partial \psi_{kx}^*} \right) - \frac{\partial \mathcal{L}}{\partial \psi_k^*} &= 0, \end{aligned} \quad (2.30)$$

yield the CNLSE system (2.26)-(2.27) and its complex conjugates. Introducing so called conjugate momenta

$$\Upsilon_k = \frac{\partial \mathcal{L}}{\partial \psi_{kt}} = \frac{i}{2} \psi_k^*, \quad \Upsilon_k^* = \frac{\partial \mathcal{L}}{\partial \psi_{kt}^*} = -\frac{i}{2} \psi_k \quad (2.31)$$

the Hamiltonian density is defined by

$$\begin{aligned} \mathcal{H} &= \sum_{k=1}^2 (\Upsilon_k \psi_{kt} + \Upsilon_k^* \psi_{kt}^*) - \mathcal{L} \\ &= \sum_{k=1}^2 \left(d_k \psi_{kx}^* \psi_{kx} - \frac{i \delta_k}{2} (\psi_k^* \psi_{kx} - \psi_{kx}^* \psi_k) \right) - \frac{a_1}{2} |\psi_1|^4 - e |\psi_1|^2 |\psi_2|^2 - \frac{a_2}{2} |\psi_2|^4. \end{aligned}$$

The Poisson bracket is given in [82] as

$$[A, B] = -i \int dx \left(\frac{\delta A}{\delta \psi_k} \frac{\delta B}{\delta \psi_k^*} - \frac{\delta A}{\delta \psi_k^*} \frac{\delta B}{\delta \psi_k} \right), \quad k = 1, 2, \quad (2.32)$$

where the variational derivative is defined in (1.29). Hence, the CNLSE can be written as a non-canonical Hamiltonian, or Poisson system

$$\begin{aligned} \frac{\partial \psi_1}{\partial t} &= [\psi_1, H] = id_1 \frac{\partial^2 \psi_1}{\partial x^2} - \delta_1 \frac{\partial \psi_1}{\partial x} + ia_1 |\psi_1|^2 \psi_1 + ie |\psi_2|^2 \psi_1, \\ \frac{\partial \psi_2}{\partial t} &= [\psi_2, H] = id_2 \frac{\partial^2 \psi_2}{\partial x^2} - \delta_2 \frac{\partial \psi_2}{\partial x} + ie |\psi_1|^2 \psi_2 + ia_2 |\psi_2|^2 \psi_2. \end{aligned} \quad (2.33)$$

We will now write the real form of CNLSE as an infinite-dimensional Hamiltonian system by decomposing the complex functions ψ_1, ψ_2 into real and imaginary parts as

$$\psi_1(x, t) = q_1(x, t) + iq_2(x, t), \quad \psi_2(x, t) = q_3(x, t) + iq_4(x, t) \quad (2.34)$$

where q_i 's $i = 1 \cdots, 4$ are real functions. By substituting (2.34) into (2.26)-(2.27), we obtain a system of real-valued equations

$$\begin{aligned}
\frac{\partial q_1}{\partial t} + \delta_1 \frac{\partial q_1}{\partial x} + d_1 \frac{\partial^2 q_2}{\partial x^2} + z_1(q)q_2 &= 0, \\
\frac{\partial q_2}{\partial t} + \delta_1 \frac{\partial q_2}{\partial x} - d_1 \frac{\partial^2 q_1}{\partial x^2} - z_1(q)q_1 &= 0, \\
\frac{\partial q_3}{\partial t} + \delta_2 \frac{\partial q_3}{\partial x} + d_2 \frac{\partial^2 q_4}{\partial x^2} + z_2(q)q_4 &= 0, \\
\frac{\partial q_4}{\partial t} + \delta_2 \frac{\partial q_4}{\partial x} - d_2 \frac{\partial^2 q_3}{\partial x^2} - z_2(q)q_3 &= 0
\end{aligned} \tag{2.35}$$

where

$$z_1(q) = a_1(q_1^2 + q_2^2) + e(q_3^2 + q_4^2) \quad \text{and} \quad z_2(q) = e(q_1^2 + q_2^2) + a_2(q_3^2 + q_4^2) \tag{2.36}$$

with $q = (q_1, q_2, q_3, q_4)^T$. Then the CNLSE can be expressed in the canonical Hamiltonian form

$$\frac{\partial u_j}{\partial t} = -\frac{\delta \mathcal{H}}{\delta v_j}, \quad \frac{\partial v_j}{\partial t} = \frac{\delta \mathcal{H}}{\delta u_j}, \quad j = 1, 2 \tag{2.37}$$

where $u = (q_1, q_3)^T$, $v = (q_2, q_4)^T$ and

$$\begin{aligned}
\mathcal{H}(z) = \int \left\{ \mathcal{W} - \frac{d_1}{2} \left(\left(\frac{\partial q_1}{\partial x} \right)^2 + \left(\frac{\partial q_2}{\partial x} \right)^2 \right) - \frac{d_2}{2} \left(\left(\frac{\partial q_3}{\partial x} \right)^2 + \left(\frac{\partial q_4}{\partial x} \right)^2 \right) \right. \\
\left. - \delta_1 \left(q_1 \frac{\partial q_2}{\partial x} \right) - \delta_2 \left(q_3 \frac{\partial q_4}{\partial x} \right) \right\} dx.
\end{aligned} \tag{2.38}$$

with

$$\mathcal{W} = \frac{1}{4} \left[a_1 (q_1^2 + q_2^2)^2 + a_2 (q_3^2 + q_4^2)^2 \right] + \frac{e}{2} (q_1^2 + q_2^2)(q_3^2 + q_4^2).$$

Using (2.37) the CNLSE can be written as the canonical Hamiltonian system (1.36) in variables $q = (q_1, q_2, q_3, q_4)^T$

$$q_t = \mathbf{J}^{-1} \frac{\delta H}{\delta q} \tag{2.39}$$

where

$$\mathbf{J} = \begin{pmatrix} J^{-1} & 0 \\ 0 & J^{-1} \end{pmatrix} \tag{2.40}$$

with J defined in (1.3) with $d = 1$

2.2.2 Multisymplectic Formulation

In this section we will give the multisymplectic formulation of the CNLSE (2.26)-(2.27) [19]. Following the derivations in Sec. 1.4, we will obtain the energy, momentum

and the additional conservation laws of the CNLSE based on the multisymplectic formulation.

Introducing the real functions $p_i, i = 1, \dots, 4$

$$p_1 + ip_2 = d_1 \frac{\partial \psi_1}{\partial x} + \frac{1}{2} i \delta_1 \psi_1, \quad (2.41)$$

$$p_3 + ip_4 = d_2 \frac{\partial \psi_2}{\partial x} + \frac{1}{2} i \delta_2 \psi_2, \quad (2.42)$$

the coupled system (2.26)-(2.27) is equivalent to the following first-order system of equations

$$\begin{aligned} \frac{\partial q_2}{\partial t} - \frac{\partial p_1}{\partial x} &= z_1(q) q_1 - \frac{\delta_1}{2d_1} \left(p_2 - \frac{\delta_1}{2} q_1 \right) \\ -\frac{\partial q_1}{\partial t} - \frac{\partial p_2}{\partial x} &= z_1(q) q_2 + \frac{\delta_1}{2d_1} \left(p_1 + \frac{\delta_1}{2} q_2 \right) \\ \frac{\partial q_4}{\partial t} - \frac{\partial p_3}{\partial x} &= z_2(q) q_3 - \frac{\delta_2}{2d_2} \left(p_4 - \frac{\delta_2}{2} q_3 \right) \\ -\frac{\partial q_3}{\partial t} - \frac{\partial p_4}{\partial x} &= z_2(q) q_4 + \frac{\delta_2}{2d_2} \left(p_3 + \frac{\delta_2}{2} q_4 \right) \\ \frac{\partial q_1}{\partial x} &= \frac{1}{d_1} \left(p_1 + \frac{\delta_1}{2} q_2 \right) \\ \frac{\partial q_2}{\partial x} &= \frac{1}{d_1} \left(p_2 - \frac{\delta_1}{2} q_1 \right) \\ \frac{\partial q_3}{\partial x} &= \frac{1}{d_2} \left(p_3 + \frac{\delta_2}{2} q_4 \right) \\ \frac{\partial q_4}{\partial x} &= \frac{1}{d_2} \left(p_4 - \frac{\delta_2}{2} q_3 \right). \end{aligned} \quad (2.43)$$

The system (2.43) can be rewritten in the multisymplectic Hamiltonian system (1.43) in coordinates $z = (q_1, q_2, q_3, q_4, p_1, p_2, p_3, p_4)^T$ with

$$\mathbf{M} = \begin{pmatrix} -J & 0_2 & 0_2 & 0_2 \\ 0_2 & -J & 0_2 & 0_2 \\ 0_2 & 0_2 & 0_2 & 0_2 \\ 0_2 & 0_2 & 0_2 & 0_2 \end{pmatrix}, \quad \mathbf{K} = \begin{pmatrix} 0_2 & 0_2 & -I_2 & 0_2 \\ 0_2 & 0_2 & 0_2 & -I_2 \\ I_2 & 0_2 & 0_2 & 0_2 \\ 0_2 & I_2 & 0_2 & 0_2 \end{pmatrix} \quad (2.44)$$

where J is defined in (1.3) with $d = 1$ and $0_2, I_2$ are 2×2 zero and identity matrices respectively, and

$$\begin{aligned} S(z) &= \mathcal{W} + \frac{1}{2d_1} (p_1^2 + p_2^2) + \frac{1}{2d_2} (p_3^2 + p_4^2) + \frac{\delta_1}{2d_1} (p_1 q_2 - p_2 q_1) \\ &+ \frac{\delta_2}{2d_2} (p_3 q_4 - p_4 q_3) + \frac{\delta_1^2}{8d_1} (q_1^2 + q_2^2) + \frac{\delta_2^2}{8d_2} (q_3^2 + q_4^2) \end{aligned} \quad (2.45)$$

with

$$\mathcal{W} = \frac{a_1}{4} (q_1^2 + q_1^2)^2 + \frac{a_2}{4} (q_3^2 + q_4^2)^2 + \frac{e}{2} (q_1^2 + q_1^2) (q_3^2 + q_4^2).$$

By direct computation we can prove that (2.26)-(2.27) has the multisymplectic conservation law

$$\partial_t \omega + \partial_x \kappa = 0$$

where ω and κ are the two-forms associated with the skew-symmetric matrices \mathbf{M} and \mathbf{K} given in (2.44). The local energy conservation law (1.51) can be obtained with the energy density

$$E(z) = S(z) + \frac{1}{2} \left(\sum_{j=1}^4 q_j \frac{\partial p_j}{\partial x} - \sum_{j=1}^4 p_j \frac{\partial q_j}{\partial x} \right) \quad (2.46)$$

and energy flux

$$F(z) = \frac{1}{2} \left(\sum_{j=1}^4 p_j \frac{\partial q_j}{\partial t} - \sum_{j=1}^4 q_j \frac{\partial p_j}{\partial t} \right) \quad (2.47)$$

and the local momentum conservation law (1.55) can be obtained with the momentum density

$$I(z) = \frac{1}{2} \left[q_1 \frac{\partial q_2}{\partial x} - p_2 \frac{\partial q_1}{\partial x} + q_3 \frac{\partial q_4}{\partial x} - p_4 \frac{\partial q_3}{\partial x} \right] \quad (2.48)$$

and the momentum flux

$$G(z) = S(z) - \frac{1}{2} \left[q_1 \frac{\partial q_2}{\partial t} - q_2 \frac{\partial q_1}{\partial t} + q_3 \frac{\partial q_4}{\partial t} - q_4 \frac{\partial q_3}{\partial t} \right]. \quad (2.49)$$

The CNLSE (2.26)-(2.27) has a phase invariance [20], where $(e^{i\theta_1} \psi_1, e^{i\theta_2} \psi_2)$ is a solution of CNLSE whenever (ψ_1, ψ_2) is a solution, for any $(\theta_1, \theta_2) \in R^2$. If we define [20]

$$\mathbf{R}_\theta = \begin{pmatrix} \cos \theta & -\sin \theta \\ \sin \theta & \cos \theta \end{pmatrix},$$

then

$$\mathbf{G}(\theta_1, \theta_2) = \mathbf{R}_{\theta_1} \oplus \mathbf{R}_{\theta_2} \oplus \mathbf{R}_{\theta_1} \oplus \mathbf{R}_{\theta_2} \in R^{8 \times 8}$$

is a action on $R^{8 \times 8}$ and the equalities

$$\mathbf{G}(\theta_1, \theta_2) \mathbf{M} = \mathbf{M} \mathbf{G}(\theta_1, \theta_2), \quad \mathbf{G}(\theta_1, \theta_2) \mathbf{K} = \mathbf{K} \mathbf{G}(\theta_1, \theta_2) \quad \text{and} \quad \mathbf{S}(\mathbf{G}(\theta_1, \theta_2) \mathbf{z}) = \mathbf{S}(\mathbf{z})$$

hold for all $(\theta_1, \theta_2) \in R^2$. If we define [20]

$$g_j = \frac{\partial}{\partial \theta_j} \mathbf{G}(\theta_1, \theta_2) |_{\theta_j=0}, \quad j = 1, 2, \quad \text{and} \quad \mathbf{A} = g_1 + g_2, \quad (2.50)$$

then it can be shown that

$$\partial_t(z^T \mathbf{M} \mathbf{A} z) + \partial_x(z^T \mathbf{K} \mathbf{A} z) = 0. \quad (2.51)$$

Thus the additional conservation law (1.61) is given by

$$T = z^T \mathbf{M} \mathbf{A} z = q_1^2 + q_2^2 + q_3^2 + q_4^2, \quad (2.52)$$

$$V = z^T \mathbf{K} \mathbf{A} z = 2(q_1 p_2 - q_2 p_1 + q_3 p_4 - q_4 p_3). \quad (2.53)$$

2.2.2.1 Conserved Quantities

In this section we will show that how the CNLSE (2.26)-(2.27) satisfies the energy densities

$$C_1 = \int_{-\infty}^{\infty} |\psi_1|^2 dx, \quad C_2 = \int_{-\infty}^{\infty} |\psi_2|^2 dx \quad (2.54)$$

where ψ_1 and ψ_2 are given in (2.28). In [42] it was shown that the CNLSE (2.26)-(2.27) satisfies the energy densities (2.54) under homogenous Neumann type boundary conditions. Here we will show that the densities (2.54) are satisfied by the CNLSE under periodic boundary condition. To show that system (2.35) satisfies (2.54), we will write system (2.35) as

$$\frac{\partial \mathbf{w}}{\partial t} + \delta_1 \frac{\partial \mathbf{w}}{\partial x} + \frac{1}{2} \frac{\partial^2 \mathbf{w}}{\partial x^2} + z_1 J \mathbf{w} = 0, \quad (2.55)$$

$$\frac{\partial \mathbf{v}}{\partial t} + \delta_2 \frac{\partial \mathbf{v}}{\partial x} + \frac{1}{2} \frac{\partial^2 \mathbf{v}}{\partial x^2} + z_2 J \mathbf{v} = 0, \quad (2.56)$$

where J is the skew-symmetric matrix (1.3) with $d = 1$, $\mathbf{w} = (q_1, q_2)^T$ and $\mathbf{v} = (q_3, q_4)^T$. Now, multiplying (2.55) and (2.56) by \mathbf{w}^T and \mathbf{v}^T respectively and integrating with respect to x yields

$$\frac{d}{dt} \int_{x_L}^{x_R} \mathbf{w}^t \mathbf{w} dx = 0, \quad \frac{d}{dt} \int_{x_L}^{x_R} \mathbf{v}^t \mathbf{v} dx = 0. \quad (2.57)$$

Here the integrals above vanish due to the skew-symmetry property of the matrix J and the imposing of the periodic boundary conditions at x_L and x_R

$$\begin{aligned} z_1 \mathbf{w}^T J \mathbf{w} &= 0, & \mathbf{w}^T J \mathbf{w}_{xx} &= (\mathbf{w}^T J \mathbf{w}_x), \\ z_2 \mathbf{v}^T J \mathbf{v} &= 0, & \mathbf{v}^T J \mathbf{v}_{xx} &= (\mathbf{v}^T J \mathbf{v}_x) \end{aligned} \quad (2.58)$$

Thus, from (2.57), we have

$$C_1 = \int_{x_L}^{x_R} \mathbf{w}^t \mathbf{w} dx = \int_{x_L}^{x_R} |\psi_1|^2 dx = \text{const}, \quad (2.59)$$

and

$$C_2 = \int_{x_L}^{x_R} \mathbf{v}^t \mathbf{v} \, dx = \int_{x_L}^{x_R} |\psi_2|^2 \, dx = \text{const.} \quad (2.60)$$

Conservation of the energies (2.59) and (2.60) imply L^2 boundedness of the solution and no blow up is expected.

2.3 N-Coupled Nonlinear Schrödinger Equation

In recent years the concept of soliton has been treated in optical communications. It has been found that soliton propagation through optical fiber arrays is governed by a set of equations related to the CNLSEs [8, 10],

$$i \frac{\partial \psi_j}{\partial t} + \varepsilon_j \frac{\partial^2 \psi_j}{\partial x^2} + 2\mu \sum_{k=1}^N |\psi_k|^2 \psi_j = 0, \quad j = 1, 2, \dots, N, \quad (2.61)$$

where ψ_j is the j -th component of the beam, 2μ is the strength of nonlinearity, x is the transverse coordinate and t is the coordinate along the direction of propagation. For $N = 1$, $\varepsilon = 1$, and $\mu > 0$ equation (2.61) reduces to the standard envelope soliton possessing integrable Schrödinger equation (2.1). For $N = 2$, equation (2.61) governs the integrable Manakov system. Recently the exact two-soliton solution has been obtained and novel shape changing inelastic collision property has been brought out [48, 62]. However, the results are rare for $N \geq 3$, even though the underlying systems are of considerable physical interest. For instance, in addition to optical communication, in the context of biophysics the case $N = 3$ can be used to study the launching and propagation of solitons along the three spines of an alpha-helix in protein. Similarly, the CNLSE (2.61) and its generalization for $N \geq 3$ are of physical interest in the theory of soliton (see [43] and reference therein).

For $\varepsilon = 1/2$ and $\mu = 1/2$, the set of equations (2.61) is a generalized Manakov set which has been shown to be integrable. This means that all solutions, in principle, can be written in analytical form. Periodic waves for the single-component regime, or the $N = 1$ case of equation (2.61) have been studied earlier. [9]. Periodic waves for N -coupled system (2.61) with three and four component are established in [27]. Analytical solutions of equation (2.61) have been derived for both the regimes of anomalous and normal dispersion $\varepsilon = +1$ or -1 , respectively, and all interaction coefficients 2μ being $+1$ from two to six components [26]. Recently, the case of μ

being allowed to be both positive and negative has been considered (see [36] and reference therein).

The N-coupled nonlinear Schrödinger equation (N-CNLS) (2.61) has a multisymplectic structure (1.43). Using $\psi_k = q_{2k-1} + iq_{2k}$ $k = 1, 2, \dots, N$, we can rewrite (2.61) as a pair of real-valued equations

$$\begin{aligned}
-\frac{\partial q_2}{\partial t} + \varepsilon_1 \frac{\partial^2 q_1}{\partial x^2} + 2\mu (q_1^2 + q_2^2 + \dots + q_{2N}^2) q_1 &= 0 \\
\frac{\partial q_1}{\partial t} + \varepsilon_1 \frac{\partial^2 q_2}{\partial x^2} + 2\mu (q_1^2 + q_2^2 + \dots + q_{2N}^2) q_2 &= 0 \\
\vdots & \\
-\frac{\partial q_{2N}}{\partial t} + \varepsilon_N \frac{\partial^2 q_{2N-1}}{\partial x^2} + 2\mu (q_1^2 + q_2^2 + \dots + q_{2N}^2) q_{2N-1} &= 0 \\
\frac{\partial q_{2N-1}}{\partial t} + \varepsilon_N \frac{\partial^2 q_{2N}}{\partial x^2} + 2\mu (q_1^2 + q_2^2 + \dots + q_{2N}^2) q_{2N} &= 0
\end{aligned} \tag{2.62}$$

Introducing $p_k(x, t) = \partial q_k(x, t) / \partial x$ $k = 1, 2, \dots, 2N$, the N-CNLS (2.61) can be reformulated to multisymplectic form (1.43)

$$\mathbf{M}z_t + \mathbf{K}z_x = \nabla_z S(\mathbf{z}), \tag{2.63}$$

in which $\mathbf{z} = (\mathbf{q}, \mathbf{p})^T$ with $\mathbf{q} = (q_1, \dots, q_{2N})$, $\mathbf{p} = (p_1, \dots, p_{2N})$,

$$\mathbf{M} = \begin{pmatrix} \mathbf{A} & \mathbf{0} \\ \mathbf{0} & \mathbf{0} \end{pmatrix}, \quad \mathbf{K} = \begin{pmatrix} \mathbf{0} & \mathbf{B} \\ -\mathbf{B} & \mathbf{0} \end{pmatrix},$$

where $\mathbf{A} = \text{diag}(J)$, with J defined in (1.3) ($d = 1$), $\mathbf{0}$ is a $2N \times 2N$ zero matrix, $\mathbf{B} = \text{diag}(E_k)$ with

$$E_k = \begin{pmatrix} \varepsilon_k & 0 \\ 0 & \varepsilon_k \end{pmatrix}, \quad k = 1, \dots, N,$$

and

$$S(\mathbf{z}) = -\frac{\mu}{2} \left(\sum_{k=1}^{2N} q_k^2 \right)^2 - \frac{1}{2} \sum_{k=1}^N \varepsilon_k (p_{2k-1}^2 + p_{2k}^2)$$

By direct computation, it can be shown that (2.63) has the multisymplectic conservation law

$$\frac{\partial}{\partial t} \left(- \sum_{k=1}^N dq_{2k-1} \wedge dq_{2k} \right) + \frac{\partial}{\partial x} \left(\sum_{k=1}^N \varepsilon_k (dq_{2k-1} \wedge dp_{2k-1} + dq_{2k} \wedge dp_{2k}) \right) = 0. \tag{2.64}$$

CHAPTER 3

NUMERICAL METHODS

For conservative systems, many properties of the system are lost in discretization. A basic idea behind the design of numerical schemes is preserving the properties such as integrability, symplecticity and energy of the original problems as much as possible. From the symplectic viewpoint, there are two approaches for developing symplectic methods for ODE's. In the first approach, if the system is a Hamiltonian ODE one can define a symplectic method which preserves the underlying symplectic structure. The second approach considers the Lagrangian viewpoint and uses a discrete variational principle (see for example [33] CH.6). The idea of the symplectic integration of ODE's is then extended to that of PDE's. The main idea in defining symplectic methods for PDE's is to discretize the space appropriately so that the resulting semi-discrete system can be cast into a finite dimensional Hamiltonian system in time; then the resulting system of ODE's are integrated in time by a symplectic method. Recently, multisymplectic integrators were developed for PDE's in the multisymplectic form. Multisymplectic methods were first introduced in [49] based on the variational approach. Later, Bridges and Reich [21] introduced a different approach that defined a multisymplectic integrator as a numerical method that satisfies a discrete multisymplectic conservation law. This approach was later applied to many PDE's such as KdV, NLS, and Klein-Gordon equations (see [13, 24, 25, 39, 64, 65, 83, 93] and reference therein). In this thesis we use the second approach. Multisymplectic PDE's have a symplectic structure associated with each of the temporal and spatial variables. Therefore it is natural to preserve this structure under discretization.

The outline of this chapter is as follows. In Sec. 3.1 we review the integrable Ablowitz-Ladik discrete NLS system. In Sec. 3.2 symplectic integrators for CNLSE are constructed. In Sec. 3.3 multisymplectic integrators and Preissman scheme are discussed. Multisymplectic integrators for NLSE and CNLSE are presented in Sec. 3.4

and Sec. 3.5 respectively. In Sec. 3.6 a multisymplectic six-point scheme is derived for the CNLSE. In Sec. 3.7 a semi-explicit scheme based on the linear-nonlinear, even-odd splitting is constructed for the CNLSE.

Here and throughout the remainder of the thesis, we use uniform grid points $(x_m, t_n) \in \mathbf{R}^2$ with mesh-length $\Delta x = x_m - x_{m-1}$, $m = 1, 2, \dots, M$ in the x -direction and the time-step $\Delta t = t_n - t_{n-1}$, $n = 1, 2, \dots, N$ in the t -direction where M is the number of grid points and N is the number of time steps. The space-time domain of our problem will then be approximated by points $(x_m, t_n) = (m\Delta x, n\Delta t)$. The value of a variable $z(x, t)$ at the mesh points (x_m, t_n) will be denoted by z_m^n . The first order derivatives z_x and z_t are approximated as follow.

$$\delta_x^+ z_m^n := \frac{z_{m+1}^n - z_m^n}{\Delta x} \quad \text{and} \quad \delta_t^+ z_m^n := \frac{z_m^{n+1} - z_m^n}{\Delta t}, \quad (3.1)$$

$$\delta_x^- z_m^n := \frac{z_m^n - z_{m-1}^n}{\Delta x} \quad \text{and} \quad \delta_t^- z_m^n := \frac{z_m^n - z_m^{n-1}}{\Delta t}, \quad (3.2)$$

$$\delta_x^1 z_m^n := \frac{z_{m+1}^n - z_{m-1}^n}{2\Delta x} \quad (3.3)$$

where δ^+ and δ^- are the forward and backward and δ^0 the central difference operators, respectively. Using these difference operators the approximation for the second derivatives z_{xx} is defined by

$$\delta_x^2 z_m^n := \frac{z_{m+1}^n - 2z_m^n + z_{m-1}^n}{\Delta x} = \delta_x^+ \delta_x^- z_m^n. \quad (3.4)$$

Using the average operators

$$\delta_x z_m^n := \frac{z_{m+1}^n + z_m^n}{2} \quad \text{and} \quad \delta_t z_m^n := \frac{z_m^{n+1} + z_m^n}{2}, \quad (3.5)$$

$$(3.6)$$

the values of $z(x, t)$ at the midpoints $(m + \frac{1}{2}, n)$ and $(m, n + \frac{1}{2})$ are defined as

$$z_{m+\frac{1}{2}}^n = \delta_x z_m^n \quad z_m^{n+\frac{1}{2}} = \delta_t z_m^n.$$

3.1 The Ablowitz-Ladik Discrete NLS System

The NLSE (2.1) is integrable, i.e. has infinite number of conservation laws. This implies that solutions of the NLSE are well behaved and, in particular, one does not expect to find any chaotic behavior. However in the discrete case this phenomenon is not always true. Many numerical schemes have been proposed to simulate the NLSE

(2.1), including a number of conservative schemes (see [35, 68, 77, 78] and reference therein). Application of the standard difference scheme to the NLSE (2.1) gives the discrete NLS (DNLS) [1]

$$i \frac{d}{dt} u_n + \frac{u_{n+1} - 2u_n + u_{n-1}}{h^2} + a|u_n|^2 u_n = 0 \quad (3.7)$$

which has the canonical Hamiltonian structure with the Hamiltonian

$$H = -i \sum_{j=0}^{N-1} \left(\frac{|u_{j+1} - u_j|^2}{h^2} - \frac{a}{2} |u_j|^4 \right) \quad (3.8)$$

where $h = L/N$ denote the grid spacing. The DNLS system (3.7) has only two integrals: the Hamiltonian (3.8) and the energy $I = \sum_{j=1}^{N-1} |u_j|^2$. Therefore it is not integrable.

One of the most important discrete models of NLSE (2.1) is the integrable Ablowitz-Ladik (AL) model

$$i \frac{d}{dt} u_n + \frac{u_{n+1} - 2u_n + u_{n-1}}{\Delta x^2} + \frac{a}{2} |u_n|^2 (u_{n+1} - u_{n-1}) = 0, \quad n = \dots, -1, 0, 1, \dots \quad (3.9)$$

It is completely integrable, i.e. has an infinite number of conserved quantities [2, 77]. The solution of (3.9) converges to the that of (2.1) for $\Delta x \rightarrow 0$ [77]. On the other hand, the Hamiltonian structure of the AL model (3.9) is noncanonical. When we split u_n into real and imaginary parts via $u_n = v_n + iw_n$, (3.9) can be rewritten as

$$\begin{aligned} \frac{d}{dt} v_n + \frac{w_{n+1} - 2w_n + w_{n-1}}{\Delta x^2} + \frac{a}{2} (v_n^2 + w_n^2) (w_{n+1} - w_{n-1}) &= 0 \\ \frac{d}{dt} w_n - \frac{v_{n+1} - 2v_n + v_{n-1}}{\Delta x^2} - \frac{a}{2} (v_n^2 + w_n^2) (v_{n+1} - v_{n-1}) &= 0. \end{aligned} \quad (3.10)$$

Introducing the notation $z = (v_1, \dots, v_N, w_1, \dots, w_N)$, (3.10) can be transformed to an $2N \times 2N$ non-canonical Hamiltonian or Poisson system

$$\frac{d}{dt} z = P(z) \nabla H(z) \quad (3.11)$$

where the skew-symmetric structure matrix is given by

$$P(z) = \begin{pmatrix} \mathbf{0} & -D \\ D & \mathbf{0} \end{pmatrix}, \quad D = \text{diag}(d_1, \dots, d_N), \quad \text{with} \quad d_k = 1 + \frac{a}{2} \Delta x^2 (v_k^2 + w_k^2)$$

with the Hamiltonian

$$H = \frac{1}{\Delta x^2} \sum_{k=1}^N (v_k v_{k-1} + w_k w_{k-1}) - \frac{2}{a \Delta x^4} \sum_{k=1}^N \ln \left(1 + \frac{a}{2} \Delta x^2 (v_k^2 + w_k^2) \right).$$

The nonintegrable DNLS (3.7) was integrated in [78] by symplectic Runge-Kutta methods which preserve the Hamiltonian and the energy. Since the phase space structure of the integrable AL system (3.9) has a non-canonical structure (3.11), the standard symplectic integrators can not be applied. The system (3.11) is a Poisson system. Therefore, Poisson integrators can be used to integrate (3.11). However, in the context of the Darboux theorem [7, 12], (3.11) can be transformed into canonical form using a suitable local transformation; then symplectic integrators can be used to integrate (3.9). In [77], two symplectic schemes were considered to simulate the AL (3.9) system and a comparison between symplectic and non-symplectic methods was made. Symplectic methods based on generating functions for integrating AL system under periodic boundary conditions have been developed and have been generalized to generate symplectic integrators of arbitrary order for general non-canonical system having a symplectic structure of the AL type (see [39] and reference therein).

3.2 Symplectic Integrators for CNLSE

In Sec. 2.2.1 we have shown that the CNLSE system (2.26)-(2.27) has a canonical Hamiltonian structure. Therefore it can be integrated by a symplectic scheme. In this section we construct a symplectic scheme to integrate the Hamiltonian system (2.39). We notice that equation (2.39) can be rewritten as

$$q_t = JAq \quad (3.12)$$

where

$$A = \begin{pmatrix} d_1 D_2 + z_1(q) & -\delta_1 D_1 & 0 & 0 \\ \delta_1 D_1 & d_1 D_2 + z_1(q) & 0 & 0 \\ 0 & 0 & d_2 D_2 + z_2(q) & -\delta_2 D_1 \\ 0 & 0 & \delta_2 D_1 & d_2 D_2 + z_2(q) \end{pmatrix}, \quad (3.13)$$

$D_1 = \frac{\partial}{\partial x}$, $D_2 = \frac{\partial^2}{\partial x^2}$ are differential operators and $z_1(q), z_2(q)$ are nonlinear terms defined in (2.36). Equation (3.12) is semi-discretized in the space variables using the central differences $\delta_x^1 z_m^n$ and $\delta_x^2 z_m^n$ to obtain a semi-discrete system

$$\frac{d}{dt} z = J^{-1} A z \quad (3.14)$$

where $z = (q_{11}, \dots, q_{1M}, q_{21}, \dots, q_{2M}, q_{31}, \dots, q_{3M}, q_{41}, \dots, q_{4M})^T$, J is defined in (1.3) with $d = M$,

$$A = \begin{pmatrix} d_1 B_2 + \mathcal{Z}_1(q) & -\delta_1 B_1 & 0 & 0 \\ \delta_1 B_1 & d_1 B_2 + \mathcal{Z}_1(q) & 0 & 0 \\ 0 & 0 & d_2 B_2 + \mathcal{Z}_2(q) & -\delta_2 B_1 \\ 0 & 0 & \delta_2 B_1 & d_2 B_2 + \mathcal{Z}_2(q) \end{pmatrix}$$

with $\mathcal{Z}_i = \text{diag}\{(z_i)_1, \dots, (z_i)_M\}$, $i = 1, 2$, I is $M \times M$ identity matrix, and

$$B_1 = \frac{1}{2\Delta x} \begin{pmatrix} 0 & 1 & 0 & \dots & -1 \\ -1 & 0 & 1 & \dots & 0 \\ & \ddots & \ddots & & \\ 0 & 0 & \dots & 0 & 1 \\ 1 & 0 & \dots & -1 & 0 \end{pmatrix}, \quad B_2 = \frac{1}{\Delta x^2} \begin{pmatrix} -2 & 1 & 0 & \dots & 1 \\ 1 & -2 & 1 & \dots & 0 \\ & \ddots & \ddots & & \\ 0 & 0 & \dots & -2 & 1 \\ 1 & 0 & \dots & 1 & -2 \end{pmatrix},$$

which correspond to the central difference approximation of the differential operators D_1 and D_2 .

Equation (3.14) can be formulated as a finite dimensional Hamiltonian system as

$$\frac{dz}{dt} = J^{-1} \nabla_z H(z), \quad (3.15)$$

with $z = (q_{11}, \dots, q_{1M}, q_{21}, \dots, q_{2M}, q_{31}, \dots, q_{3M}, q_{41}, \dots, q_{4M})^T$, and the Hamiltonian

$$\begin{aligned} H(z) &= \frac{d_1}{2} [\mathbf{q}_1^T M_1 \mathbf{q}_1 + \mathbf{q}_2^T M_1 \mathbf{q}_2] + \frac{d_2}{2} [\mathbf{q}_3^T M_1 \mathbf{q}_3 + \mathbf{q}_4^T M_1 \mathbf{q}_4] \\ &\quad - \delta_1 \mathbf{q}_1^T M_2 \mathbf{q}_2 + \delta_2 \mathbf{q}_3^T M_2 \mathbf{q}_4 \\ &\quad + \sum_{m=1}^N \frac{1}{4} \left[a_1 \left((\mathbf{q}_1)_m^2 + (\mathbf{q}_2)_m^2 \right)^2 + a_2 \left((\mathbf{q}_3)_m^2 + (\mathbf{q}_4)_m^2 \right)^2 \right] \\ &\quad + \sum_{m=1}^N \frac{e}{2} \left((\mathbf{q}_1)_m^2 + (\mathbf{q}_2)_m^2 \right) \left((\mathbf{q}_3)_m^2 + (\mathbf{q}_4)_m^2 \right) \end{aligned}$$

where $\mathbf{q}_j = (q_{j1}, \dots, q_{jM})^T$, $j = 1, 2, 3, 4$. One can then apply a symplectic method to construct a symplectic integrator of (3.15) such as the implicit mid-point rule

$$z_{n+1} - z_n = \Delta t J \nabla_z H \left(\frac{z_{n+1} + z_n}{2} \right), \quad (3.16)$$

which is second order in time.

3.3 Multisymplectic Integrators

Multisymplectic integrators exhibit a new approach for solving the infinite-dimensional Hamiltonian systems. The basic idea in the multisymplectic integrators is applying a suitable discretization to each independent variables to preserve the discrete version of the multisymplectic conservation laws. For discretization in space usually finite difference, finite volume or pseudo-spectral methods were used (see [21, 22, 64, 24, 23] and references therein). The multisymplectic methods differ from the usual semi-discretization by the fact that they are constructed to preserve the local conserved quantities. Because of the local conservation properties, the global conserved quantities are also well preserved in long term integration.

In [56] it was shown that applying the symplectic Euler and explicit midpoint discretization both in space and time variables yields a multisymplectic integrator. In [83] the multisymplectic structure of the nonlinear Klein-Gordon equation was derived from the variational principle and a series of multisymplectic schemes were constructed for the nonlinear Klein-Gordon equation. In [37] Hamiltonian PDE's with $m \geq 2$ space dimensions were considered and it was shown that discretizing each independent variable by the implicit midpoint rule yields a multisymplectic integrator. Further multisymplectic discretization for the generalized KP equation and the wave equation with 2 space dimensions were given. A nine-point variational integrator from the discrete variational principle and a six-point multisymplectic integrator from the Preissman scheme for NLSE were derived in [24]. It was also shown there that the two integrators are essentially equivalent. In [64] a finite volume cell-vertex method was developed for multisymplectic PDE's. Usually the multisymplectic finite difference and finite volume methods are of second order in space. Higher order methods can be constructed by compositions method [90]. Spectral methods usually provide higher order accuracy with smooth solutions. The local and global properties of multisymplectic discretization based on finite differences and Fourier spectral approximations were discussed in [40]. Further it was shown that the benefits of multisymplectic integrators include improved resolution of the local conservation laws, dynamical invariants and complicated phase space structure. In [71] a new six-point scheme of the CNLSE was derived from the symplectic scheme and collision behavior of soliton waves were studied. Numerical experiment show that the new six-point scheme has

excellent long-time numerical behavior. From the numerical experiment results the collisions of the soliton waves in the CNLSE was shown to be sensitive to the collision velocity and the cross-modulation coefficient. Symplectic and multisymplectic methods for the KdV equation were studied in [13]. It was pointed out there that it was possible to design a very stable, conservative difference scheme for the nonlinear conservative KdV equation. It was also shown that the symplectic or multisymplectic schemes were the best of all such schemes. The multisymplectic structure of the KdV equation was presented directly from the variational principle. A multisymplectic 12-points scheme which is equivalent to the multisymplectic Preissman scheme was tested on the solitary waves over long time intervals.

In this work we present the difference scheme known as the Preissman box scheme and then show that the Preissman box scheme is a multisymplectic integrator [21]. After then, we will show that the Preissman box scheme preserves the semi-discrete energy and momentum conservation laws.

A numerical discretization of system (1.43) can be written schematically as

$$\mathbf{M}\partial_t^{m,n}z_m^n + \mathbf{K}\partial_x^{m,n}z_m^n = (\nabla_z S(z_m^n))_m^n, \quad (3.17)$$

where ∂_t^{mn} and ∂_x^{mn} denote the discretization of the derivatives $\partial_t = \partial/\partial t$ and $\partial_x = \partial/\partial x$. Using the same discretization as in (3.17), a discrete conservation of the multisymplectic conservation law (1.45) can be written as

$$\partial_t^{m,n}\omega_m^n + \partial_x^{m,n}\kappa_m^n = 0 \quad (3.18)$$

where

$$\omega_m^n = \langle \mathbf{M}U_m^n, V_m^n \rangle, \quad \kappa_m^n = \langle \mathbf{K}U_m^n, V_m^n \rangle, \quad (3.19)$$

and $\{U_m^n\}$ and $\{V_m^n\}$ satisfy the discrete variational equations

$$\mathbf{M}\partial_t^{m,n}dz_m^n + \mathbf{K}\partial_x^{m,n}dz_m^n = D_{zz}^{m,n}S(z_m^n)dz_m^n. \quad (3.20)$$

The numerical scheme (3.17) is said to be multisymplectic if (3.18) is a discrete conservation law for (3.17).

3.3.1 The Preissman Box Scheme

A standard method for constructing multisymplectic schemes is to apply a known symplectic discretization to each independent variable. One possibility is concatenating a pair of implicit midpoint discretization, one in the t -direction and one in the

x -direction [21, 65]. Discretizing the multisymplectic PDE (1.43) in time and space by the implicit midpoint rule yields

$$\mathbf{M}\delta_t^+ z_{m+\frac{1}{2}}^n + \mathbf{K}\delta_x^+ z_m^{n+\frac{1}{2}} = \nabla_z S \left(z_{m+\frac{1}{2}}^{n+\frac{1}{2}} \right) \quad (3.21)$$

or

$$\mathbf{M} \left(\frac{z_{m+\frac{1}{2}}^{n+1} - z_{m+\frac{1}{2}}^n}{\Delta t} \right) + \mathbf{K} \left(\frac{z_{m+1}^{n+\frac{1}{2}} - z_m^{n+\frac{1}{2}}}{\Delta x} \right) = \nabla_z S \left(z_{m+\frac{1}{2}}^{n+\frac{1}{2}} \right), \quad (3.22)$$

where

$$z_{m+\frac{1}{2}}^{n+\frac{1}{2}} = \frac{1}{4} \left(z_m^n + z_{m+1}^n + z_m^{n+1} + z_{m+1}^{n+1} \right),$$

which is called centered cell discretization or the Preissman box scheme [61].

Proposition 3.1 [21] *The centered cell discretization (3.22) is multisymplectic. That is, the discretization satisfies the discrete version of the multisymplectic conservation law*

$$\frac{\omega_{m+\frac{1}{2}}^{n+1} - \omega_{m+\frac{1}{2}}^n}{\Delta t} + \frac{\kappa_{m+1}^{n+\frac{1}{2}} - \kappa_m^{n+\frac{1}{2}}}{\Delta x} = 0 \quad (3.23)$$

where

$$\omega_m^n = \langle \mathbf{M}U_m^n, V_m^n \rangle \quad \text{and} \quad \kappa_m^n = \langle \mathbf{K}U_m^n, V_m^n \rangle \quad (3.24)$$

and $\{U_m^n\}, \{V_m^n\}$ are any two solutions of the discrete variational equation corresponding to (3.22).

Proof: We introduce the discrete variational equation associated with (3.22)

$$\mathbf{M} \left(\frac{\mathbf{d}z_{m+\frac{1}{2}}^{n+1} - \mathbf{d}z_{m+\frac{1}{2}}^n}{\Delta t} \right) + \mathbf{K} \left(\frac{\mathbf{d}z_{m+1}^{n+\frac{1}{2}} - \mathbf{d}z_m^{n+\frac{1}{2}}}{\Delta x} \right) = \mathbf{S}_{m+\frac{1}{2}}^{n+\frac{1}{2}} \mathbf{d}z_{m+\frac{1}{2}}^{n+\frac{1}{2}}, \quad (3.25)$$

with

$$\mathbf{S}_{m+\frac{1}{2}}^{n+\frac{1}{2}} := \mathbf{D}_{zz} S \left(z_{m+\frac{1}{2}}^{n+\frac{1}{2}} \right).$$

Let U_m^n and V_m^n be any two solutions of (3.25). Taking the inner product of (3.25) with $V_{m+\frac{1}{2}}^{n+\frac{1}{2}}$ and using the fact that

$$z_{m+\frac{1}{2}}^{n+\frac{1}{2}} = \frac{1}{2} \left(z_{m+\frac{1}{2}}^{n+1} + z_{m+\frac{1}{2}}^n \right) = \frac{1}{2} \left(z_{m+1}^{n+\frac{1}{2}} + z_m^{n+\frac{1}{2}} \right).$$

we obtain

$$\begin{aligned} \langle \mathbf{S}U_{m+\frac{1}{2}}^{n+\frac{1}{2}}, V_{m+\frac{1}{2}}^{n+\frac{1}{2}} \rangle &= \frac{1}{\Delta t} \langle \mathbf{M}(U_{m+\frac{1}{2}}^{n+1} - U_{m+\frac{1}{2}}^n), V_{m+\frac{1}{2}}^{n+\frac{1}{2}} \rangle \\ &\quad + \frac{1}{\Delta x} \langle \mathbf{K}(U_{m+1}^{n+\frac{1}{2}} - U_m^{n+\frac{1}{2}}), V_{m+\frac{1}{2}}^{n+\frac{1}{2}} \rangle. \end{aligned} \quad (3.26)$$

Then equality (3.26) can be rewritten as

$$\begin{aligned} \langle \mathbf{S}U_{m+\frac{1}{2}}^{n+\frac{1}{2}}, V_{m+\frac{1}{2}}^{n+\frac{1}{2}} \rangle &= \frac{1}{\Delta t} \langle \mathbf{M}(U_{m+\frac{1}{2}}^{n+1} - U_{m+\frac{1}{2}}^n), \frac{1}{2}(V_{m+\frac{1}{2}}^{n+1} + V_{m+\frac{1}{2}}^n) \rangle \\ &+ \frac{1}{\Delta x} \langle \mathbf{K}(U_{m+1}^{n+\frac{1}{2}} - U_m^{n+\frac{1}{2}}), \frac{1}{2}(V_{m+1}^{n+\frac{1}{2}} + V_m^{n+\frac{1}{2}}) \rangle. \end{aligned} \quad (3.27)$$

We obtain similarly

$$\begin{aligned} \langle \mathbf{S}V_{m+\frac{1}{2}}^{n+\frac{1}{2}}, U_{m+\frac{1}{2}}^{n+\frac{1}{2}} \rangle &= \frac{1}{\Delta t} \langle \mathbf{M}(V_{m+\frac{1}{2}}^{n+1} - V_{m+\frac{1}{2}}^n), \frac{1}{2}(U_{m+\frac{1}{2}}^{n+1} + U_{m+\frac{1}{2}}^n) \rangle \\ &+ \frac{1}{\Delta x} \langle \mathbf{K}(V_{m+1}^{n+\frac{1}{2}} - V_m^{n+\frac{1}{2}}), \frac{1}{2}(U_{m+1}^{n+\frac{1}{2}} + U_m^{n+\frac{1}{2}}) \rangle \end{aligned} \quad (3.28)$$

Subtracting (3.28) from (3.27) and using (3.24) we obtain

$$\langle \mathbf{S}U_{m+\frac{1}{2}}^{n+\frac{1}{2}}, V_{m+\frac{1}{2}}^{n+\frac{1}{2}} \rangle - \langle \mathbf{S}V_{m+\frac{1}{2}}^{n+\frac{1}{2}}, U_{m+\frac{1}{2}}^{n+\frac{1}{2}} \rangle = \frac{\omega_{m+\frac{1}{2}}^{n+1} - \omega_{m+\frac{1}{2}}^n}{\Delta t} + \frac{\kappa_{m+1}^{n+\frac{1}{2}} - \kappa_m^{n+\frac{1}{2}}}{\Delta x}. \quad (3.29)$$

Since \mathbf{S} is symmetric, a straightforward calculation using the inner product leads to

$$\langle \mathbf{S}U, V \rangle - \langle \mathbf{S}V, U \rangle = \langle \mathbf{S}U, V \rangle - \langle U, \mathbf{S}V \rangle = \langle (\mathbf{S} - \mathbf{S}^T)U, V \rangle = 0.$$

where $U = U_{m+\frac{1}{2}}^{n+\frac{1}{2}}$, $V = V_{m+\frac{1}{2}}^{n+\frac{1}{2}}$. Therefore the left-hand side of (3.29) vanishes and (3.23) holds.

Besides the multisymplectic conservation law, the Preissman scheme preserves other properties. First we will discuss the semi-discrete conservation laws.

Proposition 3.2 [57] *Spatial discretization of (1.51) using the implicit midpoint rule yield the semi-discrete energy conservation law*

$$\partial_t E^{m+\frac{1}{2}} + \frac{F^{m+1} - F^m}{\Delta x} = 0 \quad (3.30)$$

with

$$E^{m+\frac{1}{2}} = \partial_t \left[S(z^{m+\frac{1}{2}}) - \frac{1}{2}(z^{\frac{1}{2}})^T \mathbf{K} \frac{z^{m+1} - z^m}{\Delta x} \right], \quad F^m = \frac{1}{2}(z^m)^T \mathbf{K} z_t^m$$

Proof: In order to prove (3.30), we discretize (1.43) spatially using the implicit midpoint rule. Then the spatial discrete equation becomes

$$\mathbf{M}z_t^{m+\frac{1}{2}} + \mathbf{K}\delta_x^+ z^m = \nabla S(z^{m+\frac{1}{2}}).$$

Taking the product with $(z_t^{m+\frac{1}{2}})^T$ from the left yields

$$\partial_t S(z^{m+\frac{1}{2}}) - (z_t^{m+\frac{1}{2}})^T \mathbf{K}\delta_x^+ z^m = 0, \quad (3.31)$$

where we have used the fact that $(z_t^{m+\frac{1}{2}})^T \mathbf{M} z_t^{m+\frac{1}{2}} = 0$ by the skew-symmetry of \mathbf{M} . Notice that

$$(z_t^{m+\frac{1}{2}})^T \mathbf{K} \delta_x^+ z^m = \frac{1}{2} \partial_t \left((z^{m+\frac{1}{2}})^T \mathbf{K} \delta_x^+ z^m \right) + \frac{1}{2} \delta_x^+ \left((z_t^{m+\frac{1}{2}})^T \mathbf{K} z^{m+\frac{1}{2}} \right)$$

which corresponds to the spatial discretization of the identity (1.50). Putting this identity into (3.31) we get the semi-discrete conservation law (3.30).

The semi-discrete momentum conservation law can be derived in a similar way by changing the role of spatial and temporal variables which we will show in the following proposition.

Proposition 3.3 [57] *Temporal discretization of (1.43) using the implicit midpoint rule exactly preserves the semi-discrete momentum conservation law*

$$\frac{I^{n+1} - I^n}{\Delta t} + \partial_x G^{m+\frac{1}{2}} = 0, \quad (3.32)$$

where

$$I^n = \frac{1}{2} (z^n)^T \mathbf{M} z_x^n$$

and

$$G^{m+\frac{1}{2}} = S(z^{n+\frac{1}{2}}) - \frac{1}{2} (z^{n+\frac{1}{2}})^T \mathbf{M} \delta_t^+ z^n.$$

Proof: To prove (3.32), we consider the temporal discretization of (1.43) using the implicit midpoint rule, which yields

$$\mathbf{M} \delta_t^+ z^n + \mathbf{K} z_x^{n+\frac{1}{2}} = \nabla_z S(z^{n+\frac{1}{2}}).$$

Multiplying this identity by $(z_x^{n+\frac{1}{2}})^T$ from the left we get

$$(z_x^{n+\frac{1}{2}})^T \mathbf{M} \delta_t^+ z^n - \partial_x S(z^{n+\frac{1}{2}}) = 0 \quad (3.33)$$

where we have used the fact that $(z_x^{m+\frac{1}{2}})^T \mathbf{K} z_x^{m+\frac{1}{2}} = 0$ by the skew-symmetry of \mathbf{K} .

We note that the identity

$$(z_x^{n+\frac{1}{2}})^T \mathbf{M} \delta_t^+ z^n = \frac{1}{2} \partial_x \left((z^{n+\frac{1}{2}})^T \mathbf{M} \delta_t^+ z^n \right) - \delta_t^4 \left((z^{n+\frac{1}{2}})^T \mathbf{M} z_x^{n+\frac{1}{2}} \right)$$

is the temporal discretization of (1.54). Substituting this identity into (3.33) we obtain the semi-discrete momentum conservation law (3.32).

Applying the implicit midpoint rule to both space and time yields the discrete version of the energy conservation law (1.51), the momentum conservation law (1.55)

and the additional conservation law (1.61). The residuals in the energy and momentum conservation law are of the form

$$RE_{m+\frac{1}{2}}^{n+\frac{1}{2}} = \frac{E_{m+\frac{1}{2}}^{n+1} - E_{m+\frac{1}{2}}^n}{\Delta t} + \frac{F_{m+1}^{n+\frac{1}{2}} - F_m^{n+\frac{1}{2}}}{\Delta x} \quad (3.34)$$

$$RM_{m+\frac{1}{2}}^{n+\frac{1}{2}} = \frac{I_{m+\frac{1}{2}}^{n+1} - I_{m+\frac{1}{2}}^n}{\Delta t} + \frac{G_{m+1}^{n+\frac{1}{2}} - G_m^{n+\frac{1}{2}}}{\Delta x} \quad (3.35)$$

and the residual in the additional conservation law is of the form

$$RA_{m+\frac{1}{2}}^{n+\frac{1}{2}} = \frac{T_{m+\frac{1}{2}}^{n+1} - T_{m+\frac{1}{2}}^n}{\Delta t} + \frac{V_{m+1}^{n+\frac{1}{2}} - V_m^{n+\frac{1}{2}}}{\Delta x}. \quad (3.36)$$

If $S(z)$ is quadratic in z , namely $S(z) = \frac{1}{2}z^T \mathbf{A}z$ (*symmetric*), and the z_m^n is the solution of the Preissman box scheme (3.22), then the local conservation laws are conserved exactly [21] and the residuals become zero. For other nonlinear forms of $S(z)$ rather than quadratic, residuals are not zero, i.e. the conserved quantities are not exactly preserved. We notice that while the energy density (2.46) and the momentum flux (2.49) of the CNLSE are quartic, the energy flux (2.47), the momentum density (2.48) and the additional conservation (2.51) are quadratic. In order to show that they don't grow over long time interval, we have resort to backward error analysis in Chapter 5.

Discrete conservation of symplecticity, energy, momentum and other additional invariants are all local properties of a numerical scheme. However, for periodic boundary conditions, the discrete local conservation implies discrete global conservation. To show how the boundary conditions are crucial in discrete global conservation we consider the Preissman box scheme (3.22) with periodic boundary condition. Summing (3.22) over all the grid points in the spatial direction we obtain

$$\frac{1}{\Delta t} \sum_{m=1}^N \left(\omega_{m+\frac{1}{2}}^{n+1} - \omega_{m+\frac{1}{2}}^n \right) \Delta x = 0, \quad (3.37)$$

where the sum

$$\sum_{m=1}^N \left(\kappa_{m+\frac{1}{2}}^{n+\frac{1}{2}} - \kappa_m^{n+\frac{1}{2}} \right) = \kappa_{N+\frac{1}{2}}^{n+\frac{1}{2}} - \kappa_{\frac{1}{2}}^{n+\frac{1}{2}} \quad (3.38)$$

vanishes because the periodicity implies $\kappa_{\frac{1}{2}}^{n+\frac{1}{2}} = \kappa_{N+\frac{1}{2}}^{n+\frac{1}{2}}$ for all n . Introducing

$$\hat{\omega} = \sum_{m=1}^N \omega_{m+\frac{1}{2}}^n \Delta x \quad (3.39)$$

yields

$$\hat{\omega}_{n+1} = \hat{\omega}_n \quad (3.40)$$

which is the conservation of symplecticity in the time direction. Notice that (3.37) is the discretization of (1.63) and (3.38) is the discretization of (1.62).

Proposition 3.4 [57] *If the multisymplectic PDE (1.43) satisfies the conservation law (1.61), the Preissman box scheme satisfies the discrete conservation law*

$$\delta_t^+ \left((z_{m+\frac{1}{2}}^n)^T \mathbf{MA} z_{m+\frac{1}{2}}^n \right) + \delta_x^+ \left((z_m^{n+\frac{1}{2}})^T \mathbf{KA} z_m^{n+\frac{1}{2}} \right) = 0. \quad (3.41)$$

Proof: In order to derive this conservation law, we multiply (3.22) by $\left(\mathbf{A} z_{m+\frac{1}{2}}^{n+\frac{1}{2}} \right)^T$ and we get

$$\left(z_{m+\frac{1}{2}}^{n+\frac{1}{2}} \right)^T \mathbf{MA} \delta_t^+ z_{m+\frac{1}{2}}^n + \left(z_{m+\frac{1}{2}}^{n+\frac{1}{2}} \right)^T \mathbf{KA} \delta_x^+ z_m^{n+\frac{1}{2}} = 0. \quad (3.42)$$

Using the identity

$$\begin{aligned} \left(z_{m+\frac{1}{2}}^n \right)^T \mathbf{MA} z_{m+\frac{1}{2}}^{n+1} &= \left(\mathbf{A} z_{m+\frac{1}{2}}^{n+1} \right)^T \mathbf{M}^T z_{m+\frac{1}{2}}^n \\ &= \left(z_{m+\frac{1}{2}}^{n+1} \right)^T \mathbf{A}^T \mathbf{M}^T z_{m+\frac{1}{2}}^n \\ &= \left(z_{m+\frac{1}{2}}^{n+1} \right)^T \mathbf{MA} z_{m+\frac{1}{2}}^n \end{aligned}$$

the first term in (3.42) can be rewritten as

$$\begin{aligned} \left(z_{m+\frac{1}{2}}^{n+\frac{1}{2}} \right)^T \mathbf{MA} \delta_t^+ z_{m+\frac{1}{2}}^n &= \frac{1}{2} \left[\left(z_{m+\frac{1}{2}}^{n+1} \right)^T \mathbf{MA} + \left(z_{m+\frac{1}{2}}^n \right)^T \mathbf{MA} \right] \delta_t^+ z_{m+\frac{1}{2}}^n \\ &= \frac{1}{2\Delta t} \left[\left(z_{m+\frac{1}{2}}^{n+1} \right)^T \mathbf{MA} z_{m+\frac{1}{2}}^{n+1} - \left(z_{m+\frac{1}{2}}^n \right)^T \mathbf{MA} z_{m+\frac{1}{2}}^n \right] \\ &= \frac{1}{2} \delta_t^+ \left((z_{m+\frac{1}{2}}^n)^T \mathbf{MA} z_{m+\frac{1}{2}}^n \right). \end{aligned} \quad (3.43)$$

Similarly, the second term in (3.42) can be rewritten as

$$\begin{aligned} \left(z_{m+\frac{1}{2}}^{n+\frac{1}{2}} \right)^T \mathbf{KA} \delta_x^+ z_m^{n+\frac{1}{2}} &= \frac{1}{2\Delta x} \left[\left(z_{m+1}^{n+\frac{1}{2}} \right)^T \mathbf{KA} z_{m+1}^{n+\frac{1}{2}} - \left(z_m^{n+\frac{1}{2}} \right)^T \mathbf{KA} z_m^{n+\frac{1}{2}} \right] \\ &= \frac{1}{2} \delta_x^+ \left((z_m^{n+\frac{1}{2}})^T \mathbf{KA} z_m^{n+\frac{1}{2}} \right). \end{aligned} \quad (3.44)$$

Substituting the identities (3.43) and (3.44) into (3.42) we get the discrete conservation law (3.41). Thus, (1.61) is conserved exactly under the Preissman box discretization.

3.4 Multisymplectic Integration of NLSE

In Section 2.1 we reviewed the Hamiltonian and multisymplectic structure of the NLSE (2.2). Therefore, it is natural to require a discretization or a semi-discretization to reflect these properties. Various type of numerical schemes have been proposed to

simulate the NLSE [35, 68, 78]. In [35] and [78] a space discretization of NLSE was considered generating a set of coupled ordinary differential equations that can be cast into a Hamiltonian structure. The resulting systems of ODE's are then integrated by a symplectic integrator. In [35] the NLSE is simulated with periodic initial data and boundary conditions. In [78] one soliton, two soliton and three soliton solutions were studied. Symplectic and non-symplectic schemes were compared to simulate the soliton solutions of the Ablowitz-Ladik model associated for homogenous boundary conditions in [77]. Symplectic and multisymplectic integrators for NLSE were considered first in [39] for periodic boundary conditions. It was shown that the multisymplectic Preissman box scheme preserves the local conservation laws extremely well over long times for different mesh sizes and time steps. Also the global invariants such as momentum and norm conservations are preserved within roundoff. For the multisymplectic formulation, a new six point scheme equivalent to the multisymplectic Preissman integrator is derived in [25] and its' performance is discussed for the soliton solutions.

In this Section we will review the multisymplectic integration of the NLSE and derive the local energy, momentum and additional conservation laws based on the Preissman box scheme. When we apply the multisymplectic Preissman box scheme to the NLS (2.9) we obtain

$$\begin{aligned}
-\frac{q_{m+\frac{1}{2}}^{n+1} - q_{m+\frac{1}{2}}^n}{\Delta t} - \frac{v_{m+\frac{1}{2}}^{n+\frac{1}{2}} - v_m^{n+\frac{1}{2}}}{\Delta x} &= a \left((p_{m+\frac{1}{2}}^{n+\frac{1}{2}})^2 \right)^{\frac{l-1}{2}} p_{m+\frac{1}{2}}^{n+\frac{1}{2}} \\
\frac{p_{m+\frac{1}{2}}^{n+1} - p_{m+\frac{1}{2}}^n}{\Delta t} - \frac{w_{m+\frac{1}{2}}^{n+\frac{1}{2}} - w_m^{n+\frac{1}{2}}}{\Delta x} &= a \left((p_{m+\frac{1}{2}}^{n+\frac{1}{2}})^2 \right)^{\frac{l-1}{2}} p_{m+\frac{1}{2}}^{n+\frac{1}{2}} \\
\frac{p_{m+\frac{1}{2}}^{n+\frac{1}{2}} - p_m^{n+\frac{1}{2}}}{\Delta x} &= v_{m+\frac{1}{2}}^{n+\frac{1}{2}} \\
\frac{q_{m+\frac{1}{2}}^{n+\frac{1}{2}} - q_m^{n+\frac{1}{2}}}{\Delta x} &= w_{m+\frac{1}{2}}^{n+\frac{1}{2}}.
\end{aligned} \tag{3.45}$$

The residual (3.34) in the discrete energy conservation law takes the form

$$\begin{aligned}
E_{m+\frac{1}{2}}^n &= S(z_{m+\frac{1}{2}}^n) - \left(v_{m+\frac{1}{2}}^n \right)^2 - \left(w_{m+\frac{1}{2}}^n \right)^2 \\
F_m^{n+\frac{1}{2}} &= v_m^{n+\frac{1}{2}} \left(\frac{p_m^{n+1} - p_m^n}{\Delta t} \right) + w_m^{n+\frac{1}{2}} \left(\frac{q_m^{n+1} - q_m^n}{\Delta t} \right)
\end{aligned} \tag{3.46}$$

and the residual (3.35) in the discrete momentum conservation law can be obtained

from

$$\begin{aligned} I_{m+\frac{1}{2}}^n &= \frac{1}{2} \left(q_{m+\frac{1}{2}}^n v_{m+\frac{1}{2}}^n - p_{m+\frac{1}{2}}^n w_{m+\frac{1}{2}}^n \right) \\ G_m^{n+\frac{1}{2}} &= S(z_m^{n+\frac{1}{2}}) - \frac{1}{2} \left(q_m^{n+\frac{1}{2}} \left(\frac{p_m^{n+1} - p_m^n}{\Delta t} \right) - p_m^{n+\frac{1}{2}} \left(\frac{q_m^{n+1} - q_m^n}{\Delta t} \right) \right) \end{aligned} \quad (3.47)$$

where

$$S(z_m^n) = \frac{1}{2} \left(\frac{2a}{l+1} \left((p_m^n)^2 + (q_m^n)^2 \right)^{\frac{l+1}{2}} + (v_m^n)^2 + (w_m^n)^2 \right). \quad (3.48)$$

The residual (3.36) in the discrete additional conservation can be easily obtained

$$\begin{aligned} N_{m+\frac{1}{2}}^n &= \frac{1}{2} \left(\left(p_{m+\frac{1}{2}}^n \right)^2 + \left(q_{m+\frac{1}{2}}^n \right)^2 \right) \\ Z_m^{n+\frac{1}{2}} &= q_m^{n+\frac{1}{2}} v_m^{n+\frac{1}{2}} - p_m^{n+\frac{1}{2}} w_m^{n+\frac{1}{2}}. \end{aligned} \quad (3.49)$$

3.5 Multisymplectic Integration of CNLSE

In Sec. 2.2 we have shown that the CNLSE (2.26)-(2.27) has a multisymplectic structure. Therefore, it is natural to preserve this structure under the discretization in space and time. In [81] the Hopscotch method was applied to the CNLSE (2.26)-(2.27) with $\delta_1 = \delta_2 = 0$ and effect of phase difference was studied numerically. In [75], the stability of solutions are studied analytically and criteria for the stability were derived using pseudospectral discretization in space and Runge-Kutta method of fourth order in time. The long term behavior of periodic solutions were studied for the parameter values $\delta_1 = \delta_2 = 0$ under periodic boundary conditions. The CNLSE was recently integrated using Preissman scheme with parameter values $\delta_1 = \delta_2 = 0$ for solitary wave solutions in [72]. Based on the multisymplectic structure, a new six point scheme, which is equivalent to the multisymplectic Preissman box scheme was derived. The numerical results show that the multisymplectic scheme has excellent long-time energy conservation property. Here we will apply the Preissman box discretization to the CNLSE (2.26)-(2.27) with nonzero δ_1 and δ_2 and obtain a multisymplectic integrator with the residuals in the energy, momentum and additional conservation laws.

Applying the centered cell discretization to system (2.26)-(2.27), we obtain the

multisymplectic Preissman scheme for CNLSE

$$\begin{aligned}
\frac{q_2^{n+1} - q_2^n}{\Delta t} + \frac{p_{1m+1}^{n+\frac{1}{2}} - p_{1m}^{n+\frac{1}{2}}}{\Delta x} &= \left(z_1 q_1 - \frac{\delta_1}{2d_1} \left(p_2 - \frac{\delta_1}{2} q_1 \right) \right)_{m+\frac{1}{2}}^{n+\frac{1}{2}} \\
-\frac{q_1^{n+1} - q_1^n}{\Delta t} - \frac{p_{2m+1}^{n+\frac{1}{2}} - p_{2m}^{n+\frac{1}{2}}}{\Delta x} &= \left(z_1 q_2 + \frac{\delta_1}{2d_1} \left(p_1 + \frac{\delta_1}{2} q_2 \right) \right)_{m+\frac{1}{2}}^{n+\frac{1}{2}} \\
\frac{q_4^{n+1} - q_4^n}{\Delta t} + \frac{p_{3m+1}^{n+\frac{1}{2}} - p_{3m}^{n+\frac{1}{2}}}{\Delta x} &= \left(z_2 q_3 - \frac{\delta_2}{2d_2} \left(p_4 - \frac{\delta_2}{2} q_3 \right) \right)_{m+\frac{1}{2}}^{n+\frac{1}{2}} \\
-\frac{q_3^{n+1} - q_3^n}{\Delta t} - \frac{p_{4m+1}^{n+\frac{1}{2}} - p_{4m}^{n+\frac{1}{2}}}{\Delta x} &= \left(z_2 q_4 + \frac{\delta_2}{2d_2} \left(p_3 + \frac{\delta_2}{2} q_4 \right) \right)_{m+\frac{1}{2}}^{n+\frac{1}{2}} \\
\frac{q_{1m+\frac{1}{2}}^{n+\frac{1}{2}} - q_{1m}^{n+\frac{1}{2}}}{\Delta x} &= \frac{1}{d_1} \left(p_1 + \frac{\delta_1}{2} q_2 \right)_{m+\frac{1}{2}}^{n+\frac{1}{2}} \\
\frac{q_{2m+\frac{1}{2}}^{n+\frac{1}{2}} - q_{2m}^{n+\frac{1}{2}}}{\Delta x} &= \frac{1}{d_1} \left(p_2 - \frac{\delta_1}{2} q_1 \right)_{m+\frac{1}{2}}^{n+\frac{1}{2}} \\
\frac{q_{3m+\frac{1}{2}}^{n+\frac{1}{2}} - q_{3m}^{n+\frac{1}{2}}}{\Delta x} &= \frac{1}{d_2} \left(p_3 + \frac{\delta_2}{2} q_4 \right)_{m+\frac{1}{2}}^{n+\frac{1}{2}} \\
\frac{q_{4m+\frac{1}{2}}^{n+\frac{1}{2}} - q_{4m}^{n+\frac{1}{2}}}{\Delta x} &= \frac{1}{d_2} \left(p_4 - \frac{\delta_2}{2} q_3 \right)_{m+\frac{1}{2}}^{n+\frac{1}{2}}
\end{aligned} \tag{3.50}$$

which is second order in space and time.

The corresponding residual in the discrete energy conservation law (3.34) can be computed using the the energy density (2.46)

$$\begin{aligned}
E_{m+\frac{1}{2}}^n &= S(z_{m+\frac{1}{2}}^n) - \frac{1}{2} \left[q_{1m+\frac{1}{2}}^n \left(\frac{p_{1m+1}^n - p_{1m}^n}{\Delta x} \right) + q_{2m+\frac{1}{2}}^n \left(\frac{p_{2m+1}^n - p_{2m}^n}{\Delta x} \right) \right. \\
&\quad + q_{3m+\frac{1}{2}}^n \left(\frac{p_{3m+1}^n - p_{3m}^n}{\Delta x} \right) + q_{4m+\frac{1}{2}}^n \left(\frac{p_{4m+1}^n - p_{4m}^n}{\Delta x} \right) \\
&\quad - p_{1m+\frac{1}{2}}^n \left(\frac{q_{1m+1}^n - q_{1m}^n}{\Delta x} \right) - p_{2m+\frac{1}{2}}^n \left(\frac{q_{2m+1}^n - q_{2m}^n}{\Delta x} \right) \\
&\quad \left. - p_{3m+\frac{1}{2}}^n \left(\frac{q_{3m+1}^n - q_{3m}^n}{\Delta x} \right) - p_{4m+\frac{1}{2}}^n \left(\frac{q_{4m+1}^n - q_{4m}^n}{\Delta x} \right) \right]
\end{aligned} \tag{3.51}$$

and using the energy flux (2.47)

$$\begin{aligned}
F_m^{n+\frac{1}{2}} &= \frac{1}{2} \left[-q_{1m}^{n+\frac{1}{2}} \left(\frac{p_{1m}^{n+1} - p_{1m}^n}{\Delta t} \right) - q_{2m}^{n+\frac{1}{2}} \left(\frac{p_{2m}^{n+1} - p_{2m}^n}{\Delta t} \right) \right. \\
&\quad - q_{3m}^{n+\frac{1}{2}} \left(\frac{p_{3m}^{n+1} - p_{3m}^n}{\Delta t} \right) - q_{4m}^{n+\frac{1}{2}} \left(\frac{p_{4m}^{n+1} - p_{4m}^n}{\Delta t} \right) \\
&\quad + p_{1m}^{n+\frac{1}{2}} \left(\frac{q_{1m}^{n+1} - q_{1m}^n}{\Delta t} \right) + p_{2m}^{n+\frac{1}{2}} \left(\frac{q_{2m}^{n+1} - q_{2m}^n}{\Delta t} \right) \\
&\quad \left. + p_{3m}^{n+\frac{1}{2}} \left(\frac{q_{3m}^{n+1} - q_{3m}^n}{\Delta t} \right) + p_{4m}^{n+\frac{1}{2}} \left(\frac{q_{4m}^{n+1} - q_{4m}^n}{\Delta t} \right) \right].
\end{aligned} \tag{3.52}$$

The residual in the discrete momentum conservation law (3.35) can be computed using the momentum density (2.48)

$$\begin{aligned}
I_{m+\frac{1}{2}}^n &= \frac{1}{2} \left[q_{1m+\frac{1}{2}}^n \left(\frac{q_{2m+1}^n - q_{2m}^n}{\Delta x} \right) - q_{2m+\frac{1}{2}}^n \left(\frac{q_{1m+1}^n - q_{1m}^n}{\Delta x} \right) \right. \\
&\quad \left. + q_{3m+\frac{1}{2}}^n \left(\frac{q_{4m+1}^n - q_{4m}^n}{\Delta x} \right) - q_{4m+\frac{1}{2}}^n \left(\frac{q_{3m+1}^n - q_{3m}^n}{\Delta x} \right) \right]
\end{aligned} \tag{3.53}$$

and using the momentum flux (2.49)

$$\begin{aligned}
G_i^{n+\frac{1}{2}} &= S(z_m^{n+\frac{1}{2}}) - \frac{1}{2} \left[q_{1m}^{n+\frac{1}{2}} \left(\frac{q_{2m}^{n+1} - q_{2m}^n}{\Delta t} \right) - q_{2m}^{n+\frac{1}{2}} \left(\frac{q_{1m}^{n+1} - q_{1m}^n}{\Delta t} \right) \right. \\
&\quad \left. + q_{3m}^{n+\frac{1}{2}} \left(\frac{q_{4m}^{n+1} - q_{4m}^n}{\Delta t} \right) - q_{4m}^{n+\frac{1}{2}} \left(\frac{q_{3m}^{n+1} - q_{3m}^n}{\Delta t} \right) \right].
\end{aligned} \tag{3.54}$$

The discrete additional conservation law (3.36) is written as

$$\begin{aligned}
T_{m+\frac{1}{2}}^n &= (q_{1m+\frac{1}{2}}^n)^2 + (q_{2m+\frac{1}{2}}^n)^2 + (q_{3m+\frac{1}{2}}^n)^2 + (q_{4m+\frac{1}{2}}^n)^2 \\
V_m^{n+\frac{1}{2}} &= 2 \left(q_{1m}^{n+\frac{1}{2}} p_{2m}^{n+\frac{1}{2}} - q_{2m}^{n+\frac{1}{2}} p_{1m}^{n+\frac{1}{2}} + q_{3m}^{n+\frac{1}{2}} p_{4m}^{n+\frac{1}{2}} - q_{4m}^{n+\frac{1}{2}} p_{3m}^{n+\frac{1}{2}} \right).
\end{aligned} \tag{3.55}$$

3.6 Six-point scheme for CNLSE

In Sec. 2.2 in order to show that the CNLSE (2.26)-(2.27) has a multisymplectic structure, we have introduced auxiliary variables p_1, p_2, p_3, p_4 . In Sec. 3.5 we applied the Preissman discretization and obtained a multisymplectic integrator for the CNLSE. However, in practice, we need to know the values of the functions ψ_1 and ψ_2 only.

Therefore we can eliminate the auxiliary variables p_1, p_2, p_3, p_4 in the discretization (3.50) and obtain a new scheme for the CNLSE (2.26)-(2.27). This idea was first introduced in [25] for NLSE (2.1). For the multisymplectic formulation, a new six-point difference scheme which is equivalent to the multisymplectic Preissman integrator was derived, and the linear stability of the new scheme was investigated. The performance of the six-point scheme was investigated by comparing with a symplectic scheme for the one soliton, two soliton and three soliton solution of the NLSE in [25]. In [24] a nine-point variational integrator from the discrete variational principle was derived for NLSE and it was shown that this new scheme is equivalent to the six-point integrator obtained from the Preissman box scheme. In [40] the six-point scheme for NLSE was considered by discussing the preservation of the local conservation laws. Some new difference schemes were derived for nonlinear Klein-Gordon equation in [83] and some numerical results were reported to show the effectiveness of the schemes. A multisymplectic 12-points scheme which is equivalent to the multisymplectic Preissman box scheme for KdV equation was developed and tested in [93] for solitary waves of the KdV equation and was shown that the new scheme well simulates the solitary waves very well. Then the 12-points scheme was simplified to an 8-points scheme in [13]. In [47] the multisymplectic Preissman box scheme was simplified to the 45-points scheme for KP equation. The new scheme was tested on solitary wave solutions of the KP equation over long time interval. It was reported that the 45-points scheme for KP equation well simulates the solitary solution of the KP equation.

In the literature there are two types of six-point integrators for the CNLSE system (2.26)-(2.27). One is based on the symplectic structure and the other is based on the multisymplectic structure of the CNLSE.

The symplectic six-point scheme based on the symplectic structure of the CNLSE system (2.26)-(2.27) with $\delta_1 = \delta_2 = 0$, $d_1 = d_2 = -1$, $a_1 = a_2 = 1$ and homogenous boundary conditions was investigated in [71]. The symplectic six-point scheme was tested for the integrable and non-integrable CNLSE on the evolution of the colliding solitary waves. But the numerical results shows that the symplectic six-point scheme is not efficient in the long time integration.

A multisymplectic six-point integrator for CNLSE system (2.26)-(2.27) with $\delta_1 = \delta_2 = 0$, $d_1 = d_2 = 1$, $a_1 = a_2 = 1$ under periodic boundary conditions was first derived in [72]. It was shown that the new multisymplectic scheme well simulates the evolution

of the solitons and preserves energy conservation well. But only the global energy was considered. In this section we will consider the CNLSE system (2.26)-(2.27) with nonzero parameter values δ_1, δ_2 and the corresponding multisymplectic discretization (3.50) and obtained a new scheme by eliminating the auxiliary variables p_1, p_2, p_3, p_4 in (3.50). Using the finite difference operators (3.1) the difference equation (3.50) takes the form

$$\begin{aligned}
\delta_t^+ \delta_x(q_2) + \frac{\delta_1}{2} \delta_x^+ \delta_t(q_2) - \delta_x^+ \delta_t(p_1) &= \delta_t \delta_x(z_1) \delta_t \delta_x(q_1), \\
-\delta_t^+ \delta_x(q_1) - \frac{\delta_1}{2} \delta_x^+ \delta_t(q_1) - \delta_x^+ \delta_t(p_2) &= \delta_t \delta_x(z_1) \delta_t \delta_x(q_2), \\
\delta_t^+ \delta_x(q_4) + \frac{\delta_2}{2} \delta_x^+ \delta_t(q_4) - \delta_x^+ \delta_t(p_3) &= \delta_t \delta_x(z_2) \delta_t \delta_x(q_3), \\
-\delta_t^+ \delta_x(q_3) - \frac{\delta_2}{2} \delta_x^+ \delta_t(q_3) - \delta_x^+ \delta_t(p_4) &= \delta_t \delta_x(z_2) \delta_t \delta_x(q_4), \\
\delta_x^+(q_1) &= \frac{1}{d_1} \delta_x \left(p_1 + \frac{\delta_1}{2} q_2 \right), \\
\delta_x^+(q_2) &= \frac{1}{d_1} \delta_x \left(p_2 - \frac{\delta_1}{2} q_1 \right), \\
\delta_x^+(q_3) &= \frac{1}{d_2} \delta_x \left(p_3 + \frac{\delta_2}{2} q_4 \right), \\
\delta_x^+(q_4) &= \frac{1}{d_2} \delta_x \left(p_4 + \frac{\delta_2}{2} q_3 \right).
\end{aligned} \tag{3.56}$$

Applying δ_x to the first and $\delta_x^+ \delta_t$ to the fifth equations and using the fact that the four operators mutually commutes, we can eliminate p_1 from the first and the fifth equations. Similarly, eliminating p_2, p_3 and p_4 yields

$$\begin{aligned}
\delta_t^+ \delta_x^2(q_2) + \delta_1 \delta_x^+ \delta_t \delta_x(q_2) - d_1 \delta_x^{+2} \delta_t(q_1) - \delta_x \mathbf{A}(\delta_t \delta_x q) &= 0, \\
\delta_t^+ \delta_x^2(q_1) + \delta_1 \delta_x^+ \delta_t \delta_x(q_1) + d_1 \delta_x^{+2} \delta_t(q_2) + \delta_x \mathbf{B}(\delta_t \delta_x q) &= 0,
\end{aligned} \tag{3.57}$$

$$\begin{aligned}
\delta_t^+ \delta_x^2(q_4) + \delta_2 \delta_x^+ \delta_t \delta_x(q_4) - d_2 \delta_x^{+2} \delta_t(q_3) - \delta_x \mathbf{C}(\delta_t \delta_x q) &= 0, \\
\delta_t^+ \delta_x^2(q_3) + \delta_2 \delta_x^+ \delta_t \delta_x(q_3) + d_2 \delta_x^{+2} \delta_t(q_4) + \delta_x \mathbf{D}(\delta_t \delta_x q) &= 0,
\end{aligned} \tag{3.58}$$

where $q = (q_1, q_2, q_3, q_4)$,

$$\begin{aligned}
\mathbf{A}(\delta_t \delta_x q) &= \delta_t \delta_x z_1 \delta_t \delta_x q_1, & \mathbf{B}(\delta_t \delta_x q) &= \delta_t \delta_x z_1 \delta_t \delta_x q_2, \\
\mathbf{C}(\delta_t \delta_x q) &= \delta_t \delta_x z_2 \delta_t \delta_x q_3, & \mathbf{D}(\delta_t \delta_x q) &= \delta_t \delta_x z_2 \delta_t \delta_x q_4.
\end{aligned}$$

Here z_1, z_2 are defined in (2.36).

Using the fact that $\psi_1 = q_1 + iq_2$ and $\psi_2 = q_3 + iq_4$, we get a six-point difference scheme

$$i \left[\delta_t^+ \delta_x^2(\psi_1) + \delta_1 \delta_x^+ \delta_t \delta_x(\psi_1) \right] + d_1 \delta_x^{+2} \delta_t(\psi_1) + \delta_x \left[a_1 |\delta_t \delta_x \psi_1|^2 + e |\delta_t \delta_x \psi_2|^2 \right] \delta_t \delta_x \psi_1 = 0, \quad (3.59)$$

$$i \left[\delta_t^+ \delta_x^2(\psi_2) + \delta_2 \delta_x^+ \delta_t \delta_x(\psi_2) \right] + d_2 \delta_x^{+2} \delta_t(\psi_2) + \delta_x \left[e |\delta_t \delta_x \psi_1|^2 + a_2 |\delta_t \delta_x \psi_2|^2 \right] \delta_t \delta_x \psi_2 = 0, \quad (3.60)$$

for ψ_1 and ψ_2 . Using the definitions (3.1), the six point scheme (3.59)-(3.60) for the CNLSE can be written explicitly as

$$i \left[\frac{(\psi_{1m-1}^{n+1} + 2\psi_{1m}^{n+1} + \psi_{1m+1}^{n+1}) - (\psi_{1m-1}^n + 2\psi_{1m}^n + \psi_{1m+1}^n)}{4\Delta t} - \delta_1 \frac{(\psi_{1m-1}^{n+1} - \psi_{1m+1}^{n+1}) + (\psi_{1m-1}^n - \psi_{1m+1}^n)}{4\Delta x} \right] + d_1 \frac{(\psi_{1m-1}^{n+1} - 2\psi_{1m+1}^{n+1} + \psi_{1m+1}^{n+1}) + (\psi_{1m-1}^n - 2\psi_{1m+1}^n + \psi_{1m+1}^n)}{2\Delta x^2} + \left(a_1 |\psi_{1m-1/2}^{n+1/2}|^2 + e |\psi_{2m-1/2}^{n+1/2}|^2 \right) \psi_{1m-1/2}^{n+1/2} + \left(a_1 |\psi_{1m+1/2}^{n+1/2}|^2 + e |\psi_{2m+1/2}^{n+1/2}|^2 \right) \psi_{1m+1/2}^{n+1/2} = 0, \quad (3.61)$$

$$i \left[\frac{(\psi_{2m-1}^{n+1} + 2\psi_{2m}^{n+1} + \psi_{2m+1}^{n+1}) - (\psi_{2m-1}^n + 2\psi_{2m}^n + \psi_{2m+1}^n)}{4\Delta t} - \delta_2 \frac{(\psi_{2m-1}^{n+1} - \psi_{2m+1}^{n+1}) + (\psi_{2m-1}^n - \psi_{2m+1}^n)}{4\Delta x} \right] + d_2 \frac{(\psi_{2m-1}^{n+1} - 2\psi_{2m+1}^{n+1} + \psi_{2m+1}^{n+1}) + (\psi_{2m-1}^n - 2\psi_{2m+1}^n + \psi_{2m+1}^n)}{2\Delta x^2} + \left(e |\psi_{1m-1/2}^{n+1/2}|^2 + a_2 |\psi_{2m-1/2}^{n+1/2}|^2 \right) \psi_{2m-1/2}^{n+1/2} + \left(e |\psi_{1m+1/2}^{n+1/2}|^2 + a_2 |\psi_{2m+1/2}^{n+1/2}|^2 \right) \psi_{2m+1/2}^{n+1/2} = 0, \quad (3.62)$$

The scheme (3.61)-(3.62) is a new six-point difference schemes for the CNLSE (2.26)-(2.27) (see Fig. 3.1). This new scheme is a multisymplectic integrator, because it is derived from a multisymplectic Preissman scheme (3.50). Note that the scheme couples two time levels in contrast to Preissman scheme, which involves three time levels. It has a three-point space average in the approximation of ψ_{1t} and ψ_{2t} , and two point time average in the approximation of ψ_{1x} and ψ_{2x} . Now we investigate the conservation property of the multisymplectic six point scheme (3.61)-(3.62) for

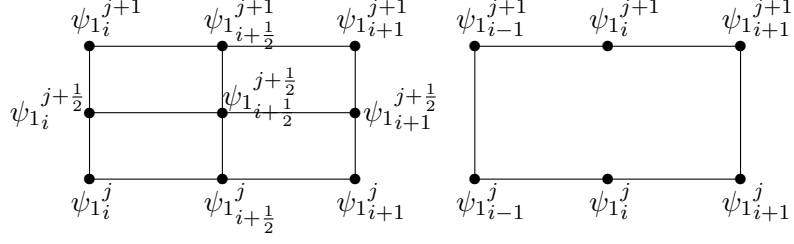


Figure 3.1: Schematic of the Preissman scheme (3.22) and six-point difference scheme (3.61)-(3.62) for the CNLSE (2.26)-(2.27). Left picture: Preissman scheme, right picture: six-point scheme.

the CNLSE. To do this, first we consider the multisymplectic integrator (3.61) in the following form

$$\begin{aligned}
& \frac{i}{2\Delta t} \left[(\psi_{1_{m-1/2}}^{n+1} - \psi_{1_{m-1/2}}^n) + (\psi_{1_{m+1/2}}^{n+1} - \psi_{1_{m+1/2}}^n) \right. \\
& \quad \left. - \frac{\delta_1}{2\Delta x} \left((\psi_{1_{m-1/2}}^{n+1} - \psi_{1_{m+1/2}}^{n+1}) + (\psi_{1_{m-1}}^n - \psi_{1_{m+1}}^n) \right) \right] \\
& \quad + \frac{d_1}{\Delta x^2} \left(\psi_{1_{m-1}}^{n+1/2} - 2\psi_{1_m}^{n+1/2} + \psi_{1_{m+1}}^{n+1/2} \right) \\
& \quad + \left(a_1 |\psi_{1_{m-1/2}}^{n+1/2}|^2 + e |\psi_{2_{m-1/2}}^{n+1/2}|^2 \right) \psi_{1_{m-1/2}}^{n+1/2} \\
& \quad + \left(a_1 |\psi_{1_{m+1/2}}^{n+1/2}|^2 + e |\psi_{2_{m+1/2}}^{n+1/2}|^2 \right) \psi_{1_{m+1/2}}^{n+1/2} = 0,
\end{aligned} \tag{3.63}$$

where

$$\psi_{1_{m+1/2}}^n = \frac{\psi_{1_{m+1}}^n + \psi_{1_m}^n}{2}, \quad \psi_{1_{m-1/2}}^n = \frac{\psi_{1_{m-1}}^n + \psi_{1_m}^n}{2}.$$

Multiplying the equation (3.63) by $\psi_{1_m}^{*n+1/2}$ and summing over m , we get

$$\begin{aligned}
& \frac{i}{2\Delta t} \left[\sum_{m=1}^M \left((\psi_{1_{m-1/2}}^{n+1} - \psi_{1_{m-1/2}}^n) \psi_{1_m}^{*n+1/2} + (\psi_{1_{m+1/2}}^{n+1} - \psi_{1_{m+1/2}}^n) \psi_{1_m}^{*n+1/2} \right) \right. \\
& \quad \left. - \frac{\delta_1}{2\Delta x} \sum_{m=1}^M \left((\psi_{1_{m-1/2}}^{n+1} - \psi_{1_{m+1/2}}^{n+1}) \psi_{1_m}^{*n+1/2} + (\psi_{1_{m-1}}^n - \psi_{1_{m+1}}^n) \psi_{1_m}^{*n+1/2} \right) \right] \\
& \quad + \frac{d_1}{\Delta x^2} \sum_{m=1}^M \left(\psi_{1_{m-1}}^{n+1/2} - 2\psi_{1_m}^{n+1/2} + \psi_{1_{m+1}}^{n+1/2} \right) \psi_{1_m}^{*n+1/2} \\
& \quad + \sum_{m=1}^M \left(a_1 |\psi_{1_{m-1/2}}^{n+1/2}|^2 + e |\psi_{2_{m-1/2}}^{n+1/2}|^2 \right) \psi_{1_{m-1/2}}^{n+1/2} \psi_{1_m}^{*n+1/2} \\
& \quad + \sum_{m=1}^M \left(a_1 |\psi_{1_{m+1/2}}^{n+1/2}|^2 + e |\psi_{2_{m+1/2}}^{n+1/2}|^2 \right) \psi_{1_{m+1/2}}^{n+1/2} \psi_{1_m}^{*n+1/2} = 0.
\end{aligned} \tag{3.64}$$

In (3.64) we note the followings:

$$\begin{aligned}
\sum_{m=1}^M (\psi_{1_{m-1/2}}^{n+1} - \psi_{1_{m-1/2}}^n) \psi_{1_m}^{*n+1/2} &= \sum_{m=1}^M (\psi_{1_{m+1/2}}^{n+1} - \psi_{1_{m+1/2}}^n) \psi_{1_{m+1}}^{*n+1/2} \\
&+ \frac{1}{2} (\psi_{1_0}^{n+1} + \psi_{1_1}^{n+1} - \psi_{1_0}^n - \psi_{1_1}^n) \psi_{1_1}^{*n+1/2} \\
&- \frac{1}{2} (\psi_{1_M}^{n+1} + \psi_{1_{M+1}}^{n+1} - \psi_{1_M}^n - \psi_{1_{M+1}}^n) \psi_{1_{M+1}}^{*n+1/2}
\end{aligned}$$

where we shift the index m to $m+1$ and then add and subtract the term corresponding to $m = M$. Thus, the last term vanishes by the periodic boundary conditions

$$\psi_{1_0} = \psi_{1_M}, \quad \psi_{1_1} = \psi_{1_{M+1}} \quad (3.65)$$

and only

$$\sum_{m=1}^M (\psi_{1_{m-1/2}}^{n+1} - \psi_{1_{m-1/2}}^n) \psi_{1_m}^{*n+1/2} = \sum_{m=1}^M (\psi_{1_{m+1/2}}^{n+1} - \psi_{1_{m+1/2}}^n) \psi_{1_{m+1}}^{*n+1/2} \quad (3.66)$$

remains. We note that in (3.64)

$$\begin{aligned}
&\sum_{m=1}^M \left(a_1 |\psi_{1_{m-1/2}}^{n+1/2}|^2 + e |\psi_{2_{m-1/2}}^{n+1/2}|^2 \right) \psi_{1_{m-1/2}}^{n+1/2} \psi_{1_m}^{*n+1/2} \\
&= \sum_{m=1}^M \left(a_1 |\psi_{1_{m+1/2}}^{n+1/2}|^2 + e |\psi_{2_{m+1/2}}^{n+1/2}|^2 \right) \psi_{1_{m+1/2}}^{n+1/2} \psi_{1_{m+1}}^{*n+1/2} \\
&+ \left(a_1 |\psi_{1_0}^{n+1/2} + \psi_{1_1}^{n+1/2}|^2 + e |\psi_{2_0}^{n+1/2} + \psi_{2_1}^{n+1/2}|^2 \right) (\psi_{1_0}^{n+1/2} + \psi_{1_1}^{n+1/2}) \psi_{1_1}^{*n+1/2} \\
&- \left(a_1 |\psi_{1_M}^{n+1/2} + \psi_{1_{M+1}}^{n+1/2}|^2 + e |\psi_{2_M}^{n+1/2} + \psi_{2_{M+1}}^{n+1/2}|^2 \right) (\psi_{1_M}^{n+1/2} + \psi_{1_{M+1}}^{n+1/2}) \psi_{1_{M+1}}^{*n+1/2}
\end{aligned}$$

where we shift the index m to $m+1$, expand the term corresponding to $m = 0$ and then add and subtract the term corresponding to $m = M$. The last term in the preceding identity vanishes by the periodic boundary conditions (3.65) and

$$\begin{aligned}
&\sum_{m=1}^M \left(a_1 |\psi_{1_{m-1/2}}^{n+1/2}|^2 + e |\psi_{2_{m-1/2}}^{n+1/2}|^2 \right) \psi_{1_{m-1/2}}^{n+1/2} \psi_{1_m}^{*n+1/2} \\
&= \sum_{m=1}^M \left(a_1 |\psi_{1_{m+1/2}}^{n+1/2}|^2 + e |\psi_{2_{m+1/2}}^{n+1/2}|^2 \right) \psi_{1_{m+1/2}}^{n+1/2} \psi_{1_{m+1}}^{*n+1/2}
\end{aligned} \quad (3.67)$$

remains. Substituting the identities (3.66) and (3.67) into (3.64) we obtain

$$\begin{aligned}
&\frac{i}{2\Delta t} \left[\sum_{m=1}^M (\psi_{1_{m+1/2}}^{n+1} - \psi_{1_{m+1/2}}^n) (\psi_{1_m}^{*n+1/2} + \psi_{1_{m+1}}^{*n+1/2}) \right. \\
&\quad \left. + \frac{\delta_1}{2\Delta x} \sum_{m=1}^M (\psi_{1_{m+1/2}}^{n+1} + \psi_{1_{m+1/2}}^n) (\psi_{1_{m+1}}^{*n+1/2} - \psi_{1_m}^{*n+1/2}) \right] \\
&- \frac{2d_1}{\Delta x^2} \sum_{m=1}^M \psi_{1_m}^{n+1/2} \psi_{1_m}^{*n+1/2} + \sum_{m=1}^M (\psi_{1_{m+1}}^{n+1/2} + \psi_{1_{m-1}}^{n+1/2}) \psi_{1_m}^{*n+1/2} \\
&+ \sum_{m=1}^M \left(a_1 |\psi_{1_{m+1/2}}^{n+1/2}|^2 + e |\psi_{2_{m+1/2}}^{n+1/2}|^2 \right) \psi_{1_{m+1/2}}^{n+1/2} (\psi_{1_m}^{*n+1/2} + \psi_{1_{m+1}}^{*n+1/2}) = 0.
\end{aligned} \quad (3.68)$$

Now conjugating (3.63), multiplying by $\psi_{1m}^{n+1/2}$ and summing over m we shall write

$$\begin{aligned}
& \frac{i}{2\Delta t} \left[\sum_{m=1}^M \left((\psi_{1m-1/2}^{*n+1} - \psi_{1m-1/2}^{*n}) \psi_{1m}^{n+1/2} + (\psi_{1m+1/2}^{*n+1} - \psi_{1m+1/2}^{*n}) \psi_{1m}^{n+1/2} \right) \right. \\
& \left. + \frac{\delta_1}{2\Delta x} \sum_{m=1}^M \left((\psi_{1m-1/2}^{*n+1} + \psi_{1m-1/2}^{*n}) \psi_{1m}^{n+1/2} - (\psi_{1m+1/2}^{*n+1} + \psi_{1m+1/2}^{*n}) \psi_{1m}^{n+1/2} \right) \right] \\
& \quad + \frac{d_1}{\Delta x^2} \sum_{m=1}^M \left(\psi_{1m-1}^{*n+1/2} - 2\psi_{1m}^{*n+1/2} + \psi_{1m+1}^{*n+1/2} \right) \psi_{1m}^{n+1/2} \\
& \quad + \sum_{m=1}^M \left(a_1 \left| \psi_{1m-1/2}^{n+1/2} \right|^2 + e \left| \psi_{2m-1/2}^{n+1/2} \right|^2 \right) \psi_{1m-1/2}^{*n+1/2} \psi_{1m}^{n+1/2} \\
& \quad + \sum_{m=1}^M \left(a_1 \left| \psi_{1m+1/2}^{n+1/2} \right|^2 + e \left| \psi_{2m+1/2}^{n+1/2} \right|^2 \right) \psi_{1m+1/2}^{*n+1/2} \psi_{1m}^{n+1/2} = 0.
\end{aligned} \tag{3.69}$$

In the same way, changing the index m to $m+1$, applying the periodic boundary conditions etc., we can write

$$\begin{aligned}
& \frac{i}{2\Delta t} \left[\sum_{m=1}^M \left(\psi_{1m+1/2}^{*n+1} - \psi_{1m+1/2}^{*n} \right) \left(\psi_{1m}^{n+1/2} + \psi_{1m+1}^{n+1/2} \right) \right. \\
& \quad \left. + \frac{\delta_1}{2\Delta x} \sum_{m=1}^M \left(\psi_{1m+1/2}^{*n+1} + \psi_{1m+1/2}^{*n} \right) \left(\psi_{1m+1}^{n+1/2} - \psi_{1m}^{n+1/2} \right) \right] \\
& \quad - \frac{2d_1}{\Delta x^2} \sum_{m=1}^M \psi_{1m}^{*n+1/2} \psi_{1m}^{n+1/2} + \sum_{m=1}^M \left(\psi_{1m+1}^{*n+1/2} + \psi_{1m-1}^{*n+1/2} \right) \psi_{1m}^{n+1/2} \\
& \quad + \sum_{m=1}^M \left(a_1 \left| \psi_{1m+1/2}^{n+1/2} \right|^2 + e \left| \psi_{2m+1/2}^{n+1/2} \right|^2 \right) \psi_{1m+1/2}^{*n+1/2} \left(\psi_{1m}^{n+1/2} + \psi_{1m+1}^{n+1/2} \right) = 0.
\end{aligned} \tag{3.70}$$

Comparing (3.68) and (3.70), we get the conservation laws for the six-point multisymplectic integrators (3.61)-(3.62)

$$\sum_{m=1}^M \left| \psi_{1m}^n + \psi_{1m+1}^n \right|^2 = \sum_{m=1}^M \left| \psi_{1m}^{n+1} + \psi_{1m+1}^{n+1} \right|^2 \tag{3.71}$$

$$\sum_{m=1}^M \left| \psi_{1m+1}^{n+1} + \psi_{1m+1}^n \right|^2 = \sum_{m=1}^M \left| \psi_{1m}^{n+1} + \psi_{1m}^n \right|^2 \tag{3.72}$$

Similarly, using (3.62) the conserved quantities

$$\sum_{m=1}^M \left| \psi_{2m}^n + \psi_{2m+1}^n \right|^2 = \sum_{m=1}^M \left| \psi_{2m}^{n+1} + \psi_{2m+1}^{n+1} \right|^2 \tag{3.73}$$

$$\sum_{m=1}^M \left| \psi_{2m+1}^{n+1} + \psi_{2m+1}^n \right|^2 = \sum_{m=1}^M \left| \psi_{2m}^{n+1} + \psi_{2m}^n \right|^2 \tag{3.74}$$

can be found. Here we notice that the conserved quantities (3.72) and (3.74) are related to the parameters δ_1 and δ_2 respectively because these conservation laws come

from the coefficients of δ_1 and δ_2 . Therefore, if δ_1 and δ_2 are chosen as zero these quantities will disappear. A final note about the conserved quantities (3.71)-(3.74) is that (3.71) and (3.73) have been investigated in [72] for the CNLSE (2.26)-(2.27) with the parameters $\delta_1 = \delta_2 = 0, d_1 = d_2 = 1, a_1 = a_2 = 1$.

3.7 A Semi-Explicit Symplectic Integrator for CNLSE

An efficient way of time discretization of semi-discretized PDE's in symplectic form is by splitting. Splitting can be performed either on the Hamiltonian or the vector field. Splitting techniques which are originally developed for multidimensional PDE's have been successfully applied to the ODE's on geometric integrators (for review see [51] and [33] Chapter II). If each vector field resulting from the splitting happens to be integrable, then a numerical integration scheme is obtained as the concatenation of the flows of the individual subsystems.

In this section a semi-explicit symplectic scheme for the CNLSE (2.26)-(2.27) will be derived by splitting the vector field of the CNLSE into linear and nonlinear parts. Then linear part will be solved exactly using the even-odd splitting. The even-odd splitting method was proposed in [67]. The nonlinear part in Hamiltonian form will be solved by the symplectic midpoint rule.

3.7.1 Linear-Nonlinear Splitting

We split the evolution equation of CNLSE (2.35) into linear and nonlinear parts as

$$q_t = \mathcal{L}q + \mathcal{N}q, \quad (3.75)$$

where $q = (q_1, q_2, q_3, q_4)^T$, and

$$\mathcal{L} = \begin{pmatrix} -\delta_1 \frac{\partial}{\partial x} & -d_1 \frac{\partial^2}{\partial x^2} & 0 & 0 \\ d_1 \frac{\partial^2}{\partial x^2} & -\delta_1 \frac{\partial}{\partial x} & 0 & 0 \\ 0 & 0 & -\delta_2 \frac{\partial}{\partial x} & -d_2 \frac{\partial^2}{\partial x^2} \\ 0 & 0 & d_2 \frac{\partial^2}{\partial x^2} & -\delta_2 \frac{\partial}{\partial x} \end{pmatrix}, \quad \mathcal{N} = \begin{pmatrix} -z_1(q) \\ z_1(q) \\ -z_2(q) \\ z_2(q) \end{pmatrix}.$$

If \mathcal{L} and \mathcal{N} are t independent, a formal solution of (3.75) can be given by

$$q(x, t + \Delta t) = \exp[\Delta t(\mathcal{L} + \mathcal{N})]q(x, t). \quad (3.76)$$

We split the equation (3.75) into linear

$$\begin{aligned}
\frac{\partial q_1}{\partial t} &= -\delta_1 \frac{\partial q_1}{\partial x} - d_1 \frac{\partial^2 q_2}{\partial x^2}, \\
\frac{\partial q_2}{\partial t} &= -\delta_1 \frac{\partial q_2}{\partial x} + d_1 \frac{\partial^2 q_1}{\partial x^2}, \\
\frac{\partial q_3}{\partial t} &= -\delta_2 \frac{\partial q_3}{\partial x} - d_2 \frac{\partial^2 q_4}{\partial x^2}, \\
\frac{\partial q_4}{\partial t} &= -\delta_2 \frac{\partial q_4}{\partial x} + d_2 \frac{\partial^2 q_3}{\partial x^2},
\end{aligned} \tag{3.77}$$

and the nonlinear subsystems

$$\begin{aligned}
\frac{\partial q_1}{\partial t} &= - [a_1 (q_1^2 + q_2^2) + e (q_3^2 + q_4^2)] q_2, \\
\frac{\partial q_2}{\partial t} &= [a_1 (q_1^2 + q_2^2) + e (q_3^2 + q_4^2)] q_1, \\
\frac{\partial q_3}{\partial t} &= - [e (q_1^2 + q_2^2) + a_2 (q_3^2 + q_4^2)] q_4, \\
\frac{\partial q_4}{\partial t} &= [e (q_1^2 + q_2^2) + a_2 (q_3^2 + q_4^2)] q_3.
\end{aligned} \tag{3.78}$$

The linear subproblem (3.77) can be written as an infinite dimensional Hamiltonian system (1.36) with

$$\begin{aligned}
H(z) = - \int \left[\frac{d_1}{2} \left(\left(\frac{\partial q_1}{\partial x} \right)^2 + \left(\frac{\partial q_2}{\partial x} \right)^2 \right) + \frac{d_2}{2} \left(\left(\frac{\partial q_3}{\partial x} \right)^2 + \left(\frac{\partial q_4}{\partial x} \right)^2 \right) \right. \\
\left. + \delta_1 q_1 \frac{\partial q_2}{\partial x} + \delta_2 q_3 \frac{\partial q_4}{\partial x} \right] dx.
\end{aligned} \tag{3.79}$$

and J as defined in (2.40). Next, introducing the variables in (2.41)-(2.42), the linear subproblem (3.77) can also be written in the multisymplectic form (1.43) with \mathbf{M} and \mathbf{K} as defined in (2.44) and

$$\begin{aligned}
S(z) &= \frac{1}{2d_1} (p_1^2 + p_2^2) + \frac{1}{2d_2} (p_3^2 + p_4^2) + \frac{\delta_1}{2d_1} (p_1 q_2 - p_2 q_1) + \frac{\delta_2}{2d_2} (p_3 q_4 - p_4 q_3) \\
&\quad + \frac{\delta_1^2}{8d_1} (q_1^2 + q_2^2) + \frac{\delta_2^2}{8d_2} (q_3^2 + q_4^2).
\end{aligned} \tag{3.80}$$

The nonlinear subproblem (3.78) has Hamiltonian structure (1.36) with the J defined in (2.40) and the Hamiltonian

$$H = \frac{1}{4} \left[a_1 (q_1^2 + q_2^2)^2 + a_2 (q_3^2 + q_4^2)^2 \right] + \frac{e}{2} (q_1^2 + q_2^2)(q_3^2 + q_4^2). \tag{3.81}$$

3.7.2 Even-Odd Splitting

We consider the infinite dimensional Hamiltonian formulation of the CNLSE (1.36). We discretize the Hamiltonian (2.38) by approximating the integral by a Riemann sum and use the central differences to approximate the space derivatives. We will apply periodic boundary conditions, with period L . For simplicity, we will use the notation $q_{1m} = q_1(m\Delta x, t)$, etc. Then, the discretized Hamiltonian is

$$\begin{aligned}
H = & \sum_{m=1}^N \left[\frac{\Delta x}{4} \left(a_1 (q_{1m}^2 + q_{2m}^2)^2 + a_2 (q_{3m}^2 + q_{4m}^2)^2 \right) \right. \\
& \left. + \frac{\Delta x}{2} e (q_{1m}^2 + q_{2m}^2)(q_{3m}^2 + q_{4m}^2) \right] \\
& - \frac{\Delta x}{2} d_1 \sum_{m=1}^N \left[\left(\frac{q_{1m+2} - q_{1m-2}}{4\Delta x} \right)^2 + \left(\frac{q_{2m+1} - q_{2m-1}}{2\Delta x} \right)^2 \right] \\
& - \frac{\Delta x}{2} d_2 \sum_{m=1}^N \left[\left(\frac{q_{3m+2} - q_{3m-2}}{4\Delta x} \right)^2 + \left(\frac{q_{4m+1} - q_{4m-1}}{2\Delta x} \right)^2 \right] \\
& - \Delta x \delta_1 \sum_{m=1}^N q_{1m} \left(\frac{q_{2m+1} - q_{2m-1}}{2\Delta x} \right) - \Delta x \delta_2 \sum_{m=1}^N q_{3m} \left(\frac{q_{4m+1} - q_{4m-1}}{2\Delta x} \right)
\end{aligned} \tag{3.82}$$

First, we split the discrete Hamiltonian (3.82) into linear and nonlinear parts as

$$H = H_{lin} + H_{non}$$

where

$$\begin{aligned}
H_{lin} = & - \frac{\Delta x}{2} d_1 \sum_{m=1}^N \left[\left(\frac{q_{1m+2} - q_{1m-2}}{4\Delta x} \right)^2 + \left(\frac{q_{2m+1} - q_{2m-1}}{2\Delta x} \right)^2 \right] \\
& - \frac{\Delta x}{2} d_2 \sum_{m=1}^N \left[\left(\frac{q_{3m+2} - q_{3m-2}}{4\Delta x} \right)^2 + \left(\frac{q_{4m+1} - q_{4m-1}}{2\Delta x} \right)^2 \right] \\
& - \Delta x \delta_1 \sum_{m=1}^N q_{1m} \left(\frac{q_{2m+1} - q_{2m-1}}{2\Delta x} \right) \\
& - \Delta x \delta_2 \sum_{m=1}^N q_{3m} \left(\frac{q_{4m+1} - q_{4m-1}}{2\Delta x} \right)
\end{aligned} \tag{3.83}$$

and

$$\begin{aligned}
H_{non} = & \sum_{m=1}^N \left[\frac{\Delta x}{4} \left(a_1 (q_{1m}^2 + q_{2m}^2)^2 + a_2 (q_{3m}^2 + q_{4m}^2)^2 \right) \right. \\
& \left. + \frac{\Delta x}{2} e (q_{1m}^2 + q_{2m}^2)(q_{3m}^2 + q_{4m}^2) \right]
\end{aligned} \tag{3.84}$$

Note that H_{non} corresponds to the discretization of (3.81) and H_{lin} corresponds to the discretization of (3.79). We notice in (3.83) that if m is even then the index of q_{1m}

and q_{3m} are even, while the index of q_{2m} and q_{4m} are odd and vice versa. Therefore we can apply even-odd splitting for the discrete Hamiltonian (3.83). Hence we can write

$$H_{lin} = H_{even} + H_{odd} \quad (3.85)$$

where

$$\begin{aligned} H_{even} = & -\frac{\Delta x}{2} d_1 \sum_{even}^N \left[\left(\frac{q_{1m+2} - q_{1m-2}}{4\Delta x} \right)^2 + \left(\frac{q_{2m+1} - q_{2m-1}}{2\Delta x} \right)^2 \right] \\ & -\frac{\Delta x}{2} d_2 \sum_{even}^N \left[\left(\frac{q_{3m+2} - q_{3m-2}}{4\Delta x} \right)^2 + \left(\frac{q_{4m+1} - q_{5m-1}}{2\Delta x} \right)^2 \right] \\ & -\Delta x \delta_1 \sum_{even}^N q_{1m} \left(\frac{q_{2m+1} - q_{2m-1}}{2\Delta x} \right) \\ & -\Delta x \delta_2 \sum_{even}^N q_{3m} \left(\frac{q_{4m+1} - q_{4m-1}}{2\Delta x} \right) \end{aligned} \quad (3.86)$$

and

$$\begin{aligned} H_{odd} = & -\frac{\Delta x}{2} d_1 \sum_{odd}^N \left[\left(\frac{q_{1m+2} - q_{1m-2}}{4\Delta x} \right)^2 + \left(\frac{q_{2m+1} - q_{2m-1}}{2\Delta x} \right)^2 \right] \\ & -\frac{\Delta x}{2} d_2 \sum_{odd}^N \left[\left(\frac{q_{3m+2} - q_{3m-2}}{4\Delta x} \right)^2 + \left(\frac{q_{4m+1} - q_{5m-1}}{2\Delta x} \right)^2 \right] \\ & -\Delta x \delta_1 \sum_{odd}^N q_{1m} \left(\frac{q_{2m+1} - q_{2m-1}}{2\Delta x} \right) \\ & -\Delta x \delta_2 \sum_{odd}^N q_{3m} \left(\frac{q_{4m+1} - q_{4m-1}}{2\Delta x} \right) \end{aligned} \quad (3.87)$$

Consequently, we split the Hamiltonian (3.82) into three parts

$$\begin{aligned} H &= H_{lin} + H_{non} \\ &= H_{even} + H_{odd} + H_{non} \end{aligned} \quad (3.88)$$

where H_{even} , H_{odd} and H_{non} are defined in (3.86), (3.87) and (3.84) respectively. Then the time evolution generated by H_{even} is

$$\begin{aligned} \frac{dq_{1m}}{dt} &= -\frac{1}{\Delta x} \frac{\partial H_{even}}{\partial q_{2m}}, & \frac{dq_{2m}}{dt} &= \frac{1}{\Delta x} \frac{\partial H_{even}}{\partial q_{1m}}, \\ \frac{dq_{3m}}{dt} &= -\frac{1}{\Delta x} \frac{\partial H_{even}}{\partial q_{4m}}, & \frac{dq_{4m}}{dt} &= \frac{1}{\Delta x} \frac{\partial H_{even}}{\partial q_{3m}}. \end{aligned} \quad (3.89)$$

This evolution is given by

$$\left. \begin{aligned} \frac{dq_{1m}}{dt} &= 0 \\ \frac{dq_{2m}}{dt} &= \frac{d_1(q_{1m-2} - 2q_{1m} + q_{1m+2})}{4\Delta x^2} + \frac{\delta_1(q_{2m-1} - q_{2m+1})}{2\Delta x} \\ \frac{dq_{3m}}{dt} &= 0 \\ \frac{dq_{4m}}{dt} &= \frac{d_2(q_{3m-2} - 2q_{3m} + q_{3m+2})}{4\Delta x^2} + \frac{\delta_2(q_{4m-1} - q_{4m+1})}{2\Delta x} \end{aligned} \right\} \text{for } m \text{ even} \quad (3.90)$$

and

$$\left. \begin{aligned} \frac{q_{1m}}{dt} &= -\frac{d_1(q_{2m-2} - 2q_{2m} + q_{1m+2})}{4\Delta x^2} + \frac{\delta_1(q_{1m-1} - q_{1m+1})}{2\Delta x} \\ \frac{q_{2m}}{dt} &= 0 \\ \frac{q_{3m}}{dt} &= -\frac{d_2(q_{4m-2} - 2q_{4m} + q_{4m+2})}{4\Delta x^2} + \frac{\delta_2(q_{3m-1} - q_{3m+1})}{2\Delta x} \\ \frac{q_{4m}}{dt} &= 0 \end{aligned} \right\} \text{for } m \text{ odd} \quad (3.91)$$

This system of equations can be solved exactly, since only even indexes q_{1m} , q_{3m} and odd indexes q_{2m} , q_{4m} occur on the right hand sides, and these are constant in time.

When we use H_{odd} for time evolution, the situation is reversed and H_{odd} generates solvable dynamics again by the following evolution equations:

$$\left. \begin{aligned} \frac{q_{1m}}{dt} &= -\frac{d_1(q_{2m-2} - 2q_{2m} + q_{1m+2})}{4\Delta x^2} + \frac{\delta_1(q_{1m-1} - q_{1m+1})}{2\Delta x} \\ \frac{q_{2m}}{dt} &= 0 \\ \frac{q_{3m}}{dt} &= -\frac{d_2(q_{4m-2} - 2q_{4m} + q_{4m+2})}{4\Delta x^2} + \frac{\delta_2(q_{3m-1} - q_{3m+1})}{2\Delta x} \\ \frac{q_{4m}}{dt} &= 0 \end{aligned} \right\} \text{for } m \text{ even} \quad (3.92)$$

and

$$\left. \begin{aligned} \frac{q_{1m}}{dt} &= 0 \\ \frac{q_{2m}}{dt} &= \frac{d_1(q_{1m-2} - 2q_{1m} + q_{1m+2})}{4\Delta x^2} + \frac{\delta_1(q_{2m-1} - q_{2m+1})}{2\Delta x} \\ \frac{q_{3m}}{dt} &= 0 \\ \frac{q_{4m}}{dt} &= \frac{d_2(q_{3m-2} - 2q_{3m} + q_{3m+2})}{4\Delta x^2} + \frac{\delta_2(q_{4m-1} - q_{4m+1})}{2\Delta x} \end{aligned} \right\} \text{for } m \text{ odd} \quad (3.93)$$

Similarly, the time evolution generated by H_{Non} is

$$\begin{aligned} \frac{dq_{1m}}{dt} &= -\frac{1}{\Delta x} \frac{\partial H_{Non}}{\partial q_{2m}}, & \frac{dq_{2m}}{dt} &= \frac{1}{\Delta x} \frac{\partial H_{Non}}{\partial q_{1m}}, \\ \frac{dq_{3m}}{dt} &= -\frac{1}{\Delta x} \frac{\partial H_{Non}}{\partial q_{4m}}, & \frac{dq_{4m}}{dt} &= \frac{1}{\Delta x} \frac{\partial H_{Non}}{\partial q_{3m}}. \end{aligned} \quad (3.94)$$

and the dynamics is evolved according to

$$\begin{aligned}
\frac{\partial q_{1m}}{\partial t} &= - [a_1 (q_{1m}^2 + q_{2m}^2) + e (q_{3m}^2 + q_{4m}^2)] q_{2m} \\
\frac{\partial q_{2m}}{\partial t} &= [a_1 (q_{1m}^2 + q_{2m}^2) + e (q_{3m}^2 + q_{4m}^2)] q_{1m} \\
\frac{\partial q_{3m}}{\partial t} &= - [e (q_{1m}^2 + q_{2m}^2) + a_2 (q_{3m}^2 + q_{4m}^2)] q_{4m} \\
\frac{\partial q_{4m}}{\partial t} &= [e (q_{1m}^2 + q_{2m}^2) + a_2 (q_{3m}^2 + q_{4m}^2)] q_{3m}.
\end{aligned} \tag{3.95}$$

which can be solved by a symplectic method. In this section we will use the implicit mid-point rule.

3.7.3 Composition method

The idea of the composition methods is to split the right hand side of a first-order system of differential equations into two or more pieces, so that each of which can be solved exactly or more conveniently than the original equation. The individual solutions are then combined in such a way as to approximate the evolution of the original equation for a time step.

Suppose that the linear and the nonlinear subsystems (3.77) and (3.78) have known exact solutions

$$q(x, t + \Delta t) = \exp[\Delta t(\mathcal{L})]q(x, t), \tag{3.96}$$

$$q(x, t + \Delta t) = \exp[\Delta t(\mathcal{N})]q(x, t). \tag{3.97}$$

respectively. Replacing the exponential operator in (3.76) by an appropriate combination of products of the exponential operators $\exp(\Delta t\mathcal{L})$ and $\exp(\Delta t\mathcal{N})$, we can approximate the exact solution of equation (3.75). But since \mathcal{L} and \mathcal{N} are noncommutative operators, this composition produces an error. The error of the noncommutative operators are analyzed by the Baker-Campbell-Hausdorff (BCH) formula [69, 90]. The BCH formula for two noncommutative operators X and Y can be formulated as

$$\exp(X) \exp(Y) = \exp \left\{ X + Y + \frac{1}{2}[X, Y] + \frac{1}{12}[X - Y, [X, Y]] + \dots \right\}, \tag{3.98}$$

where the commutator $[,]$ is defined by $[X, Y] = XY - YX$. A first-order approximation of the exponential operator in (3.76) is then

$$\varphi_1(\Delta t) = \exp(\Delta t\mathcal{L}) \exp(\Delta t\mathcal{N}).$$

The second-order approximation is given by

$$\varphi_2(\Delta t) = \exp\left(\frac{1}{2}\Delta t\mathcal{N}\right) \exp(\Delta t\mathcal{L}) \exp\left(\frac{1}{2}\Delta t\mathcal{N}\right)$$

which satisfies the reversibility relation $\varphi_2(-\Delta t) = \varphi_2^{-1}(\Delta t)$. Higher order composition techniques can be found in [51, 73, 90] and [33] (Chapter II).

Here we consider the second order semi-explicit symplectic integrator for the CNLSE (3.75) which is provided by the composition

$$\begin{aligned} \varphi_2(\Delta t) = \exp\left(\frac{1}{2}\Delta t H_{odd}\right) \circ \exp\left(\frac{1}{2}\Delta t H_{even}\right) \circ \exp(\Delta t H_{non}) \circ \\ \exp\left(\frac{1}{2}\Delta t H_{even}\right) \circ \exp\left(\frac{1}{2}\Delta t H_{odd}\right) \end{aligned} \quad (3.99)$$

where $\exp(tH)$ denotes the time- t flow of the vector field H .

The corresponding residuals in the energy and momentum conservation law are of the form

$$RE_m^n = \frac{E_m^{n+1} - E_m^n}{\Delta t} + \frac{F_{m+1}^{n+\frac{1}{2}} - F_{m-1}^{n+\frac{1}{2}}}{2\Delta x}, \quad (3.100)$$

$$RM_m^n = \frac{I_m^{n+1} - I_m^n}{\Delta t} + \frac{G_{m+1}^{n+\frac{1}{2}} - G_{m-1}^{n+\frac{1}{2}}}{2\Delta x}, \quad (3.101)$$

and the residual in the additional conservation law is of the form

$$RA_m^n = \frac{T_m^{n+1} - T_m^n}{\Delta t} + \frac{V_{m+1}^{n+\frac{1}{2}} - V_{m-1}^{n+\frac{1}{2}}}{2\Delta x}. \quad (3.102)$$

CHAPTER 4

LINEARIZED EQUATIONS AND DISPERSION RELATIONS

The difficult part of doing any analysis of numerical dispersion and dissipation properties of the numerical schemes of the NLSE's is that they are nonlinear. However, for linear problems the exact solution of the PDE can be found so that it is straightforward to make comparison with the exact solution and the numerical solution.

So far, we have discussed NLSE's and CNLSE's with some properties, expressed as conservation laws, which have a significant role in determining the dynamics of the system. We have also discussed three numerical schemes and have shown how some of these conservation laws are preserved by these schemes. However, these conservation laws do not give enough information about the solution of these schemes. For example, in every case, the energy and momentum conservation laws could not be preserved exactly for general nonlinear problems using these schemes [21]. To understand the solution behavior of these schemes, in this chapter we will consider the linearized equations. That is, we will consider (1.43) such that

$$S(z) = \frac{1}{2} \langle z, \mathbf{A}z \rangle$$

where \mathbf{A} is symmetric. This gives the linear multisymplectic PDE

$$\mathbf{M}z_t + \mathbf{K}z_x = \mathbf{A}z. \tag{4.1}$$

In [56] the Euler box scheme, the Preissman box scheme, the explicit midpoint scheme and a mixed discretization (explicit midpoint in space, implicit midpoint in time and vice versa) were applied to the linear multisymplectic PDE (4.1) and both continuous and discrete dispersion relations were discussed for two model problems: the linearized KdV and Boussinesq equations where the nonlinear wave equation is just a special case

for the latter equation. Now we give a short summary of [56] for linearized equations: In [56] it was shown that the dispersion relations for the Euler and Preissman schemes were close to the exact relation for the linearized Boussinesq equation. On the other hand, the explicit midpoint scheme produced computational modes. Computational modes are produced when the discretization yields different branches in the dispersion relation. In other words, there are modes where the numerical scheme produces good approximation and there are modes where the scheme yields poor approximations. Thus one must ensure that these modes are not stimulated during numerical applications for nonlinear problems (see [58]). For the linearized KdV equation it was shown that while the Euler and the explicit midpoint schemes produce computational modes, the Preissman scheme does not. Using the continuous and numerical dispersion relations, it was shown that the absence of numerically induced diffusion and the nonexistence of computational modes are two main characteristics expected of a multisymplectic integrator. For this reason the explicit midpoint scheme could not be a multisymplectic integrator and in some cases the Euler box scheme could not be a multisymplectic integrator either. Moreover in [13] numerical dispersion relations were presented for some symplectic and multisymplectic schemes for the linearized KdV equation. For detailed analysis of the numerical and continuous dispersion relations see also [58, 80].

In this chapter we will discuss the dispersion relation for both continuous and discrete equations to understand the solution behavior of our multisymplectic Preissman and coupled six point schemes for linearized problems. The Preissman scheme was first proposed by Preissman [61] and developed by Zhao and Qin [93]. A simpler version of this method was developed in [13]. Both the Preissman and the coupled six point schemes are non-dissipative. Thus these methods give qualitatively correct results for long times. Then using these results we will discuss the exact and the numerical dispersion relations for the linearized NLSE and CNLSE.

4.1 Dispersion Relation

Any time-dependent scalar, linear partial differential equation with constant coefficients on an unbounded space domain admits plane wave solutions [38, 80, 85],

$$u(x, t) = \mathbf{u}e^{i(\xi x + \omega t)}, \quad \xi \in \mathbf{R}, \quad i = \sqrt{-1} \quad (4.2)$$

where $\mathbf{u} = \mathbf{u}(\xi)$, and ξ is the wave number, ω is the frequency and $\lambda = 2\pi/\xi$ is the wave length. Note that we use the standard notation for the frequency which should not be confused with the auxiliary variable ω in the previous sections. If the initial data $u(x, 0) = e^{i\xi x}$ are supplied to an equation of this kind, then there is a solution for $t > 0$ consisting of $u(x, 0)$ multiplied by an oscillation factor $e^{i\xi x}$. The partial differential equation gives a relationship between ξ and ω , and this relationship

$$\omega = \omega(\xi) \quad (4.3)$$

is known as the dispersion relation. It must be noted that for every ξ there may be several different frequencies $\omega_j(\xi)$ corresponding to different modes. In many cases, the solution admits two modes such that $\omega_1 = -\omega_2$, corresponding to right and left travelling waves.

If ω is real, then the wave (4.2) is propagated with the speed $-\omega/\xi$. For complex $\omega = a + ib$, the plane wave solutions (4.2) takes the form

$$u(x, t) = e^{i(\xi x + at)} e^{-bt}. \quad (4.4)$$

The wave (4.4) decays as $t \rightarrow \infty$ if $Im(\omega) > 0$, it grows if $Im(\omega) < 0$ and neither grows nor decays if $Im(\omega) = 0$. Also, if $Re(\omega) = 0$ there will be no wave propagation. Substituting the plane wave solution (4.2) into the linear PDE (4.1) gives the linear system

$$(i\omega\mathbf{M} + i\xi\mathbf{K} - \mathbf{A})\mathbf{u} = 0. \quad (4.5)$$

If the determinant of the matrix derived from this equation is non-zero, then the only solution is $\mathbf{u} = 0$. This means that we have no wave solution. Therefore, the determinant must be zero. This gives the continuous dispersion relation [18]

$$\mathcal{D}_{\mathbf{A}}(\omega, \xi) = \det(i\omega\mathbf{M} + i\xi\mathbf{K} - \mathbf{A}) = 0, \quad (4.6)$$

which will be compared with the numeric dispersion relations. Notice that the matrix used in (4.6) is self-adjoint. This implies a real dispersion relation, meaning there is no diffusion ([85], Chapter 11).

The discrete approximations to differential equations also have plane wave solutions, at least if the grid is uniform, and so they have dispersion relations, too. Consider the discrete analog of the plane wave solutions (4.2)

$$u_m^n = \hat{\mathbf{u}} e^{i(\Xi x_m + \Omega t_n)} = \hat{\mathbf{u}} e^{i(\Xi m \Delta x + \Omega n \Delta t)}, \quad (4.7)$$

where $i = \sqrt{-1}$, $\Xi \in \mathbf{R}$ is the numerical wave number and Ω is the numerical frequency such that

$$\Xi \in [-\pi/\Delta x, \pi/\Delta x] \quad \text{and} \quad \Omega \in [-\pi/\Delta t, \pi/\Delta t]$$

because $x_m = m\Delta x$ and $t_n = n\Delta t$ ([15], Chapter 11). As in the continuous case, we consider $\Omega = \Omega(\Xi)$ so that the solution (4.7) will satisfy our difference equation. Note that while the numerical wave number will remain the same for each solution, the numerical wave frequency is different for each solution because of their dependency on the wave number changes according to the discretization, which will be clear in the following subsections. The function $\Omega(\Xi)$ will be called the discrete dispersion relation. Notice that at all spatial grid points x_m , the exponential $e^{i(2\pi N x_m/\Delta x)} = e^{i(2\pi N m)}$ is exactly 1 for any integer N . More generally, any numerical wave number Ξ is indistinguishable on the spatial grid from all other numerical wave numbers $\Xi + 2\pi N/\Delta x$. This means that (4.7) is $2\pi/\Delta x$ periodic on \mathbf{R} . To make sense of the idea of analyzing the plane wave solution, we shall normally restrict our attention to one period of u_m^n by looking only at wave numbers in the range $[-\pi/\Delta x, \pi/\Delta x]$. Similarly, we shall consider the numerical frequency $\Omega \in \mathbf{R}$ in the range $[-\pi/\Delta t, \pi/\Delta t]$. If $\Omega = a + ib$, the discrete plane wave solution (4.7) has the form

$$u_m^n = \hat{\mathbf{u}} e^{i(\Xi m \Delta x + a n \Delta t)} e^{-b n \Delta t}. \quad (4.8)$$

Thus, we see that the wave (4.8) decays as $n \rightarrow \infty$ if $Im(\Omega) > 0$, grows without bound (and the scheme will be unstable) if $Im(\Omega) < 0$ and neither grows nor decays if Ω real. Also, if $Re(\Omega) = 0$ there will be no wave propagation.

The numerical solution (4.7) can be used to derive a numerical dispersion relation for each of the schemes.

A strong method to determine the accuracy of a scheme is to compare the numerical solution to an analytical solution. The equations we are considering are wave equations and so we will compare the properties of waves. Dispersion relation gives information about the wave so that we will compare the continuous dispersion relation with the corresponding numeric relation. In the numerical discretization both the time step and the space step affect the accuracy. To investigate the effect of the space and time steps, we consider the numerical dispersion relation assuming $\Delta t \rightarrow 0$ and $\Delta x \rightarrow 0$ respectively.

4.1.1 The Preissman Box Scheme

Applying the Preissman box scheme (3.22) to the linear PDE (4.1) yields

$$\mathbf{M} \left(\frac{z_{m+\frac{1}{2}}^{n+1} - z_{m+\frac{1}{2}}^n}{\Delta t} \right) + \mathbf{K} \left(\frac{z_{m+1}^{n+\frac{1}{2}} - z_m^{n+\frac{1}{2}}}{\Delta x} \right) = \mathbf{A} z_{m+\frac{1}{2}}^{n+\frac{1}{2}}, \quad (4.9)$$

Using (4.7) we obtain the solution at $x = (m + 1/2)\Delta x$, $t = n\Delta t$ as

$$\begin{aligned} z_{m+\frac{1}{2}}^n &= \frac{1}{2}(z_{m+1}^n + z_m^n) \\ &= \frac{1}{2} \hat{\mathbf{u}} \left(e^{i(\Xi(m+1)\Delta x + \Omega n \Delta t)} + e^{i(\Xi m \Delta x + \Omega n \Delta t)} \right) \\ &= \frac{1}{2} \hat{\mathbf{u}} e^{i(\Xi(m+\frac{1}{2})\Delta x + \Omega(n+\frac{1}{2})\Delta t)} \left(e^{i(\frac{\Xi \Delta x}{2} - \frac{\Omega \Delta t}{2})} + e^{i(-\frac{\Xi \Delta x}{2} - \frac{\Omega \Delta t}{2})} \right) \\ &= \hat{z} e^{-i\frac{\Omega \Delta t}{2}} \left(e^{i\frac{\Xi \Delta x}{2}} + e^{-i\frac{\Xi \Delta x}{2}} \right) \end{aligned}$$

where

$$\hat{z} := \frac{1}{2} \hat{\mathbf{u}} \left(e^{i(\Xi(m+\frac{1}{2})\Delta x + \Omega(n+\frac{1}{2})\Delta t)} \right).$$

Similarly

$$\begin{aligned} z_{m+\frac{1}{2}}^{n+1} &= \hat{z} e^{i\frac{\Omega \Delta t}{2}} \left(e^{i\frac{\Xi \Delta x}{2}} + e^{-i\frac{\Xi \Delta x}{2}} \right) \\ z_{m+1}^{n+\frac{1}{2}} &= \hat{z} e^{i\frac{\Xi \Delta x}{2}} \left(e^{i\frac{\Omega \Delta t}{2}} + e^{-i\frac{\Omega \Delta t}{2}} \right) \\ z_m^{n+\frac{1}{2}} &= \hat{z} e^{-i\frac{\Xi \Delta x}{2}} \left(e^{i\frac{\Omega \Delta t}{2}} + e^{-i\frac{\Omega \Delta t}{2}} \right) \\ z_{m+\frac{1}{2}}^{n+\frac{1}{2}} &= \frac{1}{2} \hat{z} \left(e^{i\frac{\Xi \Delta x}{2}} + e^{-i\frac{\Xi \Delta x}{2}} \right) \left(e^{i\frac{\Omega \Delta t}{2}} + e^{-i\frac{\Omega \Delta t}{2}} \right) \end{aligned}$$

Thus we get

$$\begin{aligned} z_{m+\frac{1}{2}}^{n+1} - z_{m+\frac{1}{2}}^n &= \hat{z} \left(e^{i\frac{\Xi \Delta x}{2}} + e^{-i\frac{\Xi \Delta x}{2}} \right) \left(e^{i\frac{\Omega \Delta t}{2}} - e^{-i\frac{\Omega \Delta t}{2}} \right) \\ z_{m+1}^{n+\frac{1}{2}} - z_m^{n+\frac{1}{2}} &= \hat{z} \left(e^{i\frac{\Xi \Delta x}{2}} - e^{-i\frac{\Xi \Delta x}{2}} \right) \left(e^{i\frac{\Omega \Delta t}{2}} + e^{-i\frac{\Omega \Delta t}{2}} \right) \end{aligned}$$

Using the identities

$$e^{i\theta} + e^{-i\theta} = 2 \cos(\theta) \quad \text{and} \quad e^{i\theta} - e^{-i\theta} = 2i \sin(\theta)$$

we get

$$\begin{aligned} z_{m+\frac{1}{2}}^{n+1} - z_{m+\frac{1}{2}}^n &= 4i \cos\left(\frac{\Xi \Delta x}{2}\right) \sin\left(\frac{\Omega \Delta t}{2}\right) \hat{z}, \\ z_{m+1}^{n+\frac{1}{2}} - z_m^{n+\frac{1}{2}} &= 4i \cos\left(\frac{\Omega \Delta t}{2}\right) \sin\left(\frac{\Xi \Delta x}{2}\right) \hat{z}, \\ z_{m+\frac{1}{2}}^{n+\frac{1}{2}} &= 2i \cos\left(\frac{\Xi \Delta x}{2}\right) \sin\left(\frac{\Omega \Delta t}{2}\right) \hat{z}. \end{aligned}$$

After substituting these equalities into (4.9) we get a linear system

$$\left(i\mathbf{M} \frac{2 \tan\left(\frac{\Omega\Delta t}{2}\right)}{\Delta t} + i\mathbf{K} \frac{2 \tan\left(\frac{\Xi\Delta x}{2}\right)}{\Delta x} - \mathbf{A} \right) \hat{\mathbf{u}} = 0. \quad (4.10)$$

If we define the pseudo wave number and the pseudo frequency for the Preissman box scheme by

$$\Xi_P := \frac{2 \tan\left(\frac{\Xi\Delta x}{2}\right)}{\Delta x} \quad \text{and} \quad \Omega_P := \frac{2 \tan\left(\frac{\Omega\Delta t}{2}\right)}{\Delta t} \quad (4.11)$$

the linear system (4.10) can be written as

$$(i\Omega_P\mathbf{M} + i\Xi_P\mathbf{K} - \mathbf{A})\hat{\mathbf{u}} = 0, \quad (4.12)$$

which is the numerical dispersion relation for the Preissman box scheme [56]. We notice that the numerical dispersion relation (4.12) is the exact dispersion relation evaluated at the pseudo wave number and the pseudo frequency, that is

$$\mathcal{D}_{\mathbf{A}}(\Omega_P, \Xi_P) = 0, \quad (4.13)$$

where $\mathcal{D}_{\mathbf{A}}$ is defined in (4.6). Notice that the numerical dispersion relation (4.13) is found by taking the determinant of a self-adjoint matrix, meaning there is no diffusion induced by the numerical scheme.

Numerical dispersion relations for the Preissman scheme have also been presented and discussed for linearized Boussinesq and KdV equations in [56]. In [13] the exact and the numerical dispersion relation were compared for the linearized KdV equation based on the two box schemes (4×3 and 4×2 narrow box) and a 5×2 symplectic scheme. The results show that while the multisymplectic 12-point box scheme preserves the shape of the exact dispersion relation for all cases the 8-point narrow box scheme preserves the shape of the true dispersion relation under some conditions. On the other hand, it was shown that the symplectic midpoint scheme has parasitic waves. Parasites in space or time can both be harmful! However only the box scheme avoids this problem in both space following the proposition in [13].

Proposition 4.1 [13]. *The Preissman scheme qualitatively preserves the dispersion relation of any system of linear first-order pdes $\mathbf{M}z_x + \mathbf{K}z_t = \mathbf{A}z$. Specifically, there are diffeomorphisms Ψ_1 and Ψ_2 which conjugate the exact and numerical dispersion relations such that to each pair (ξ, ω) satisfying the numerical dispersion relation there corresponds a pair $(\Psi_1(\xi), \Psi_2(\omega))$ satisfying the exact dispersion relation.*

Proof. We set $z_m^n = \mathbf{a}e^{i(\xi m + \omega n)} = e^{i(\frac{\xi}{\Delta x}(m\Delta x) + \frac{\omega}{\Delta t}(n\Delta t))}$ where \mathbf{a} is a constant vector. The exact dispersion relation is obtained by letting $x = m\Delta x$ and $t = n\Delta t$ vary continuously, giving the generalized eigenvalue problem

$$\left(i\frac{\omega}{\Delta t}\mathbf{M} + i\frac{\xi}{\Delta x}\mathbf{K} - \mathbf{A} \right) \mathbf{a} = 0. \quad (4.14)$$

The dispersion relation is a nontrivial solution of the above system; that is it is a polynomial

$$\det \left(i\frac{\omega}{\Delta t}\mathbf{M} + i\frac{\xi}{\Delta x}\mathbf{K} - \mathbf{A} \right) = 0. \quad (4.15)$$

For the numerical scheme we get the numerical dispersion relation (as in (4.10)),

$$\det \left(i\frac{2}{\Delta t}\tan(\omega/2)\mathbf{M} + i\frac{\xi}{\Delta x}\tan(\xi/2)\mathbf{K} - \mathbf{A} \right) = 0. \quad (4.16)$$

Thus, the required diffeomorphisms are

$$\Psi_1 : (-\pi, \pi) \rightarrow \mathbf{R}, \quad \Psi_1(\xi) = 2\tan(\omega/2), \quad (4.17)$$

$$\Psi_2 : (-\pi, \pi) \rightarrow \mathbf{R}, \quad \Psi_2(\xi) = 2\tan(\xi/2). \quad (4.18)$$

This completes the proof.

Notice that the multisymplectic property (namely that \mathbf{M} and \mathbf{K} are antisymmetric and \mathbf{A} is symmetric) is not used. For large systems of PDEs the dispersion relation can be more complex. For example the relation may contain many branches. It is remarkable that the Preissman scheme can capture all of this with a shift in frequencies, unconditionally, for all Δt and Δx . Proposition 4.1 also holds for PDEs with any number of space dimensions [13].

Next we discuss the continuous and numerical dispersion relation for linearized NLS and linearized CNLSEs.

4.2 Linearized NLS

In this section we will consider the linearized Nonlinear Schrödinger equation

$$iu_t + u_{xx} + \mathbf{a}u = 0, \quad (4.19)$$

where $\mathbf{a} \in \mathbf{R}$ and u is a complex-valued function. Using $u = p + iq$ we can write (4.19) as a pair of real-valued equations

$$\begin{aligned} p_t + q_{xx} + \mathbf{a}q &= 0, \\ q_t - p_{xx} - \mathbf{a}p &= 0. \end{aligned} \quad (4.20)$$

The linearized NLSE (4.19) can be written as an infinite dimensional Hamiltonian system.

$$\frac{dz}{dt} = J^{-1} \frac{\delta \mathcal{H}}{\delta z}$$

where $z = (p, q)^T$, J as defined in (1.3) with $d = 1$ and the Hamiltonian

$$\mathcal{H} = \int \frac{1}{2} [p_x^2 + q_x^2 - \mathbf{a}(p^2 + q^2)] dx.$$

Introducing $v = p_x$ and $w = q_x$, the above system of equations can be written as a first-order system

$$\begin{aligned} q_t - v_x &= \mathbf{a}p \\ -p_t - w_x &= \mathbf{a}q \\ p_x &= v \\ q_x &= w \end{aligned} \tag{4.21}$$

which leads to the linearized multisymplectic Hamiltonian system (4.1) with M and K defined in (2.11) and

$$\mathbf{A} = \begin{pmatrix} \mathbf{a} & 0 & 0 & 0 \\ 0 & \mathbf{a} & 0 & 0 \\ 0 & 0 & 1 & 0 \\ 0 & 0 & 0 & 1 \end{pmatrix}$$

and we obtain

$$i\omega \mathbf{M} + i\xi \mathbf{K} - \mathbf{A} = \begin{pmatrix} -\mathbf{a} & i\omega & -i\xi & 0 \\ -i\omega & -\mathbf{a} & 0 & -i\xi \\ i\xi & 0 & -1 & 0 \\ 0 & i\xi & 0 & -1 \end{pmatrix} \tag{4.22}$$

Then the continuous dispersion relation of the linearized NLSE based on the multisymplectic structure can be found by taking the determinant of this matrix, which yields

$$\mathcal{D}(\omega, \xi) = \omega^2 - \xi^4 + 2\mathbf{a}\xi^2 - \mathbf{a}^2 = 0 \tag{4.23}$$

or equivalently

$$\omega^2 = (\mathbf{a} - \xi^2)^2. \tag{4.24}$$

Notice that for every wave number ξ , the solution admits two modes $\omega_1 = -\omega_2$ which corresponds to two equivalent waves travelling in opposite directions.

Using (4.13), the numeric dispersion relation of the linearized NLSE corresponding to the Preissman box scheme can be written as

$$\mathcal{D}_\Delta(\Omega_P, \Xi_P) = \Omega_P^2 - \Xi_P^4 + 2\mathbf{a}\Xi_P^2 - \mathbf{a}^2 = 0, \quad (4.25)$$

or, equivalently

$$\frac{4 \tan^2\left(\frac{\Omega\Delta t}{2}\right)}{\Delta t^2} = \left(\mathbf{a} - \frac{4 \tan^2\left(\frac{\Xi\Delta x}{2}\right)}{\Delta x^2}\right)^2. \quad (4.26)$$

Solving for Ω we find the numeric dispersion relation for the Preissman box scheme

$$\Omega = \pm \frac{2}{\Delta t} \tan^{-1} \left[\frac{\Delta t}{2} \left(\mathbf{a} - \frac{4 \tan^2\left(\frac{\Xi\Delta x}{2}\right)}{\Delta x^2} \right) \right], \quad \Omega \in [-\pi/\Delta t, \pi/\Delta t], \quad (4.27)$$

since $\tan(\Omega\Delta t/2)$ is invertible for $-\pi/2 < \Omega\Delta t/2 < \pi/2$. The numeric dispersion relation (4.27) can be compared to the continuous dispersion relation (4.24). First we notice that for every numerical wave number Ξ there correspond two numerical frequencies Ω as in the case of exact dispersion relation (4.24). In particular, if we decrease both the time step $\Delta t \rightarrow 0$ and the space step $\Delta x \rightarrow 0$, the numerical dispersion relation (4.26) approaches the continuous dispersion relation (4.24). Next, we will first investigate the effect of space step. For this, we consider the numeric dispersion relation (4.26) assuming $\Delta t \rightarrow 0$, which yields

$$\Omega^2 = \left(\mathbf{a} - \frac{4 \tan^2\left(\frac{\Xi\Delta x}{2}\right)}{\Delta x^2} \right)^2. \quad (4.28)$$

It is important to note that both in the exact and numeric dispersion relations (4.24) and (4.28), ω^2 and Ω^2 are positive and therefore they are real, implying that there is no diffusion.

We plot the numeric dispersion relation with continuous time (4.28) over the exact dispersion relation (4.24) in Fig. 4.1 for spatial step size $\Delta x = 0.5$ and $\Delta x = 0.1$. Notice that for every wave number the exact and the numerical dispersion relation gives two frequencies as expected. The direction of these frequencies are opposite meaning that two waves travelling in opposite direction as expected. We see that while the numerical dispersion relation is close to the exact dispersion relation for the spatial step size $\Delta x = 0.1$, it is not close for step size $\Delta x = 0.5$. However, in either cases there are no temporal or spatial parasitic waves.

Notice that the accuracy is good for small wave number which corresponds to long waves since the wave length is $\lambda = 2\pi/\xi$. Because the phase speed is ω/ξ , the

phase speed is large. Also we find that the group speed $\partial\omega/\partial\xi$ increasing because the tangent line drawn to the graph approaches the vertical as the wave number go far away from the origin.

Finally let us compare the numeric dispersion relation (4.27) to the exact dispersion relation (4.24). The dispersion curves are shown in Fig. 4.2. We see that the results are almost same with the previous case. The exact dispersion relation gives two frequencies for every wave number as expected. The plot shows the the numerical dispersion relation is close to the exact dispersion relation for small step size which corresponds to many grid points in discretization. Also we notice that neither temporal nor spatial parasitic waves are observed.

4.3 Linearized CNLSE

In this section we discuss the exact and numerical dispersion relation for the linearized CNLSE based on the multisymplectic structure and check the robustness of our multisymplectic schemes for plane wave solution. In [29] the CNLSE (2.26)-(2.27) was considered with $\delta_1 = \delta_2 = 0, d_1 = d_2 = 1$ and $a_1 = a_2 = e = \sigma/2$, where $\sigma \in \mathbf{R}$. Using the plane wave solutions

$$\psi_1 = ae^{i(\xi x - \omega t)}, \quad \psi_2 = be^{i(-\xi x - \omega t)} \quad (4.29)$$

an amplitude-dependent dispersion relation

$$\omega = \xi^2 - \frac{\sigma}{2}(|a|^2 + |b|^2), \quad a, b \in \mathbf{R}$$

was obtained. Then the linearized stability analysis is presented by perturbing the plane wave solutions. In [75] it was shown that the CNLSE (2.26)-(2.27) with $\delta_1 = \delta_2 = 0$ has the exact periodic solutions

$$\psi_1 = \nu_1 e^{i(\xi_1 x - \omega_1 t)}, \quad \psi_2 = \nu_2 e^{i(\xi_2 x - \omega_2 t)} \quad (4.30)$$

with the dispersion relations

$$\omega_1 = d_1 \xi_1^2 - (a_1 \nu_1^2 + e \nu_2^2), \quad \omega_2 = d_2 \xi_2^2 - (a_2 \nu_2^2 + e \nu_1^2), \quad (4.31)$$

where $\nu_1, \nu_2 \in \mathbf{R}$. In this section we consider the linearized CNLSE based on the multisymplectic structure and obtain the exact and numerical dispersion relation using the plane wave solutions of the form

$$\psi_1 = \mathbf{u}_1 e^{i(\xi x + \omega t)}, \quad \psi_2 = \mathbf{u}_2 e^{i(\xi x + \omega t)} \quad (4.32)$$

where \mathbf{u}_1 and \mathbf{u}_2 are the amplitudes of the wave which are assumed to be real without loss of generality, ξ is the wave number and ω is the frequency of the wave. In the CNLSE (2.26)-(2.27) the nonlinear terms are replaced by real constants c_1 and c_2 as

$$c_1 = a_1 |\psi_1|^2 + e |\psi_2|^2, \quad (4.33)$$

$$c_2 = e |\psi_1|^2 + a_2 |\psi_2|^2. \quad (4.34)$$

Thus the linearized CNLSE can be written as

$$i \left(\frac{\partial \psi_1}{\partial t} + \delta_1 \frac{\partial \psi_1}{\partial x} \right) + d_1 \frac{\partial^2 \psi_1}{\partial x^2} + c_1 \psi_1 = 0 \quad (4.35)$$

$$i \left(\frac{\partial \psi_2}{\partial t} + \delta_2 \frac{\partial \psi_2}{\partial x} \right) + d_2 \frac{\partial^2 \psi_2}{\partial x^2} + c_2 \psi_2 = 0 \quad (4.36)$$

The linearized CNLSE (4.35)-(4.36) admits a plane wave solutions

$$\psi_1 = \mathbf{u}_1 e^{i(\xi x + \omega t)}, \quad \psi_2 = \mathbf{u}_2 e^{i(\xi x + \omega t)}. \quad (4.37)$$

Substituting (4.37) into (4.35)-(4.36) and cancelling the exponential terms gives two homogenous equations

$$(\omega + \delta_1 \xi + d_1 \xi^2 - c_1) \mathbf{u}_1 = 0$$

$$(\omega + \delta_2 \xi + d_2 \xi^2 - c_2) \mathbf{u}_2 = 0$$

for \mathbf{u}_1 and \mathbf{u}_2 . If the determinant of the matrix derived from these two equations is non-zero, the only solution is $\mathbf{u}_1 = \mathbf{u}_2 = 0$. This means that we have no wave. Therefore the determinant must be zero. This gives

$$(\omega + \delta_1 \xi + d_1 \xi^2)(\omega + \delta_2 \xi + d_2 \xi^2) = 0.$$

Note that the coefficients of the first and the second factors are the coefficients of ψ_1 and ψ_2 , respectively. Thus, the dispersion relations for the linearized CNLSE (4.35)-(4.36) are given by

$$\omega_{1,\psi_1} = c_1 - \delta_1 \xi - d_1 \xi^2, \quad \omega_{2,\psi_2} = c_2 - \delta_2 \xi - d_2 \xi^2 \quad (4.38)$$

Now, we will derive the dispersion relation based on the multisymplectic structure. The system (4.35)-(4.36) can also be written as a linear multisymplectic PDE (4.1) for $z = (q_1, q_2, q_3, q_4, p_1, p_2, p_3, p_4)^T$

$$\mathbf{A} = \begin{pmatrix} J_1 & J_2 \\ -J_2 & J_3 \end{pmatrix}$$

where

$$J_1 = \begin{pmatrix} 2\tilde{c}_1 & 0 & 0 & 0 \\ 0 & 2\tilde{c}_1 & 0 & 0 \\ 0 & 0 & 2\tilde{c}_2 & 0 \\ 0 & 0 & 0 & 2\tilde{c}_2 \end{pmatrix} \quad J_2 = \begin{pmatrix} 0 & -\delta_1/2d_1 & 0 & 0 \\ \delta_1/2d_1 & 0 & 0 & 0 \\ 0 & 0 & 0 & -\delta_2/2d_2 \\ 0 & 0 & \delta_2/2d_2 & 0 \end{pmatrix}$$

$$J_3 = \begin{pmatrix} 1/d_1 & 0 & 0 & 0 \\ 0 & 1/d_1 & 0 & 0 \\ 0 & 0 & 1/d_2 & 0 \\ 0 & 0 & 0 & 1/d_2 \end{pmatrix}$$

$\tilde{c}_1 = c_1/2 + \delta_1^2/8d_1$, $\tilde{c}_2 = c_2/2 + \delta_2^2/8d_2$ and \mathbf{M} and \mathbf{K} defined in (2.44). Thus, finding the determinant of the matrix

$$(i\omega\mathbf{M} + i\xi\mathbf{K} - \mathbf{A}) = \begin{pmatrix} -2\tilde{c}_1 & i\omega & 0 & 0 & -i\xi & \delta_1/2d_1 & 0 & 0 \\ -i\omega & -2\tilde{c}_1 & 0 & 0 & -\delta_1/2d_1 & -i\xi & 0 & 0 \\ 0 & 0 & -2\tilde{c}_2 & i\omega & 0 & 0 & -i\xi & \delta_2/2d_2 \\ 0 & 0 & -i\omega & -2\tilde{c}_2 & 0 & 0 & -\delta_2/2d_2 & -i\xi \\ i\xi & -\delta_1/2d_1 & 0 & 0 & -1/d_1 & 0 & 0 & 0 \\ \delta_1/2d_1 & i\xi & 0 & 0 & 0 & -1/d_1 & 0 & 0 \\ 0 & 0 & i\xi & -\delta_2/2d_2 & 0 & 0 & -1/d_2 & 0 \\ 0 & 0 & \delta_2/2d_2 & i\xi & 0 & 0 & 0 & -1/d_2 \end{pmatrix}$$

gives the continuous dispersion relation for the multisymplectic linearized CNLSE (4.35)-(4.36)

$$\mathcal{D}(\omega, \xi) = \frac{1}{d_1^2 d_2^2} (c_1^2 - 2c_1 d_1 \xi^2 - \delta_1^2 \xi^2 + d_1^2 \xi^4 - 2\delta_1 \xi \omega - \omega^2)$$

$$(c_2^2 - 2c_2 d_2 \xi^2 - \delta_2^2 \xi^2 + d_2^2 \xi^4 - 2\delta_2 \xi \omega - \omega^2) = 0.$$

Note that the coefficients of the first factor are the coefficients of ψ_1 and the coefficients of the second factor are the coefficients of ψ_2 . Therefore, the first factor gives the continuous dispersion relation for ψ_1 and the second factor gives the continuous dispersion relation for ψ_2 , that is

$$\mathcal{D}_{\psi_1}(\omega, \xi) = c_1^2 - 2c_1 d_1 \xi^2 - \delta_1^2 \xi^2 + d_1^2 \xi^4 - 2\delta_1 \xi \omega - \omega^2 = 0, \quad (4.39)$$

$$\mathcal{D}_{\psi_2}(\omega, \xi) = c_2^2 - 2c_2 d_2 \xi^2 - \delta_2^2 \xi^2 + d_2^2 \xi^4 - 2\delta_2 \xi \omega - \omega^2 = 0, \quad (4.40)$$

Solving (4.39)-(4.40) for ω we get

$$\omega_{1,\psi_1} = c_1 - \delta_1\xi - d_1\xi^2, \quad \omega_{2,\psi_1} = -c_1 - \delta_1\xi + d_1\xi^2, \quad (4.41)$$

$$\omega_{1,\psi_2} = c_2 - \delta_2\xi - d_2\xi^2, \quad \omega_{2,\psi_2} = -c_2 - \delta_2\xi + d_2\xi^2. \quad (4.42)$$

These solutions give two branches for each wave ψ_1 and ψ_2 . For every wave number ξ , there are two frequencies which correspond to two wave travelling in different direction. Note that for linear CNLSE (4.35)–(4.36) with $c_1 = c_2 = 0$ and $\delta_1 = \delta_2 = 0$, for every wave number ξ , there are two frequencies satisfying $\omega_{1,\psi_1} = -\omega_{2,\psi_1}$ and $\omega_{1,\psi_2} = -\omega_{2,\psi_2}$, which correspond to two equal waves for both ψ_1 and ψ_2 travelling in opposite directions.

It is important to note that while the dispersion relation of the linearized CNLSE (4.35)–(4.36) has two roots (4.38), the dispersion relation of the multisymplectic form (4.1) has four roots (4.41),(4.42).

4.3.1 The Preissman Box Scheme

For the linearized CNLSE (4.35)–(4.36) the numerical dispersion relation (4.10) is given by

$$\begin{aligned} \mathcal{D}_\Delta(\Omega_P, \Xi_P) &= \frac{1}{d_1^2 d_2^2} (c_1^2 - 2c_1 d_1 \Xi_P^2 - \delta_1^2 \Xi_P^2 + d_1^2 \Xi_P^4 - 2\delta_1 \Xi_P \Omega_P - \Omega_P^2) \\ &\quad (c_2^2 - 2c_2 d_2 \Xi_P^2 - \delta_2^2 \Xi_P^2 + d_2^2 \Xi_P^4 - 2\delta_2 \Xi_P \Omega_P - \Omega_P^2) = 0. \end{aligned}$$

where the pseudo wave number and the pseudo frequency for the Preissman scheme are defined as

$$\Xi_P := \frac{2 \tan\left(\frac{\Xi \Delta x}{2}\right)}{\Delta x}, \quad \Omega_P := \frac{2 \tan\left(\frac{\Omega \Delta t}{2}\right)}{\Delta t}.$$

Thus, we get

$$\mathcal{D}_{\Delta,\psi_1}(\Omega_P, \Xi_P) = c_1^2 - 2c_1 d_1 \Xi_P^2 - \delta_1^2 \Xi_P^2 + d_1^2 \Xi_P^4 - 2\delta_1 \Xi_P \Omega_P - \Omega_P^2 = 0, \quad (4.43)$$

$$\mathcal{D}_{\Delta,\psi_2}(\Omega_P, \Xi_P) = c_2^2 - 2c_2 d_2 \Xi_P^2 - \delta_2^2 \Xi_P^2 + d_2^2 \Xi_P^4 - 2\delta_2 \Xi_P \Omega_P - \Omega_P^2 = 0, \quad (4.44)$$

Solving (4.43)-(4.44) for Ω_P we obtain

$$\Omega_{P,\psi_1} = \mp c_1 - \delta_1 \Xi_P \pm d_1 \Xi_P^2, \quad \Omega_{P,\psi_2} = \mp c_2 - \delta_2 \Xi_P \pm d_2 \Xi_P^2. \quad (4.45)$$

These dispersion relations are $2\pi/\Delta x$ periodic in Ξ and $2\pi/\Delta t$ periodic in Ω . With the use of inverse trigonometric function it is possible to solve such equation for Ω , so

that we can exhibit the functional dependence explicitly. But in general, the resulting formulas are less appealing and often harder to work it because the trigonometric functions may not be invertible in the corresponding domain. In our situation we use the invertibility of the $\tan(\theta)$ for $\theta \in [-\pi/2, \pi/2]$ so that (4.45) is equivalent to

$$\Omega_{\psi_1} = \frac{2}{\Delta t} \tan^{-1} \left[\frac{\Delta t}{2} \left(-\delta_1 \frac{2 \tan\left(\frac{\Xi \Delta x}{2}\right)}{\Delta x} \mp d_1 \frac{4 \tan^2\left(\frac{\Xi \Delta x}{2}\right)}{\Delta x^2} \pm c_1 \right) \right] \quad (4.46)$$

$$\Omega_{\psi_2} = \frac{2}{\Delta t} \tan^{-1} \left[\frac{\Delta t}{2} \left(-\delta_2 \frac{2 \tan\left(\frac{\Xi \Delta x}{2}\right)}{\Delta x} \mp d_2 \frac{4 \tan^2\left(\frac{\Xi \Delta x}{2}\right)}{\Delta x^2} \pm c_2 \right) \right] \quad (4.47)$$

where c_1 and c_2 are defined in 4.33. Thus, there are four frequency for every wave number.

4.3.2 Coupled Six-Point Scheme

Applying the coupled six-point scheme (3.59)-(3.60) to the linearized CNLS (4.35)-(4.36) yields

$$i \left[\delta_t^+ \delta_x^2(\psi_1) + \delta_1 \delta_x^+ \delta_t \delta_x(\Psi_1) \right] + d_1 \delta_x^{+2} \delta_t(\psi_1) + c_1 \delta_t \delta_x^2 \psi_1 = 0, \quad (4.48)$$

$$i \left[\delta_t^+ \delta_x^2(\psi_2) + \delta_2 \delta_x^+ \delta_t \delta_x(\Psi_2) \right] + d_2 \delta_x^{+2} \delta_t(\psi_2) + c_2 \delta_t \delta_x^2 \psi_2 = 0, \quad (4.49)$$

Substituting the plane waves

$$\psi_{1m}^n = \hat{\mathbf{u}}_1 e^{i(\Xi x_m + \Omega t_n)}, \quad \psi_{2m}^n = \hat{\mathbf{u}}_2 e^{i(\Xi x_m + \Omega t_n)} \quad (4.50)$$

into (4.48)-(4.49) and cancelling the exponential terms yields two algebraic equations in $\hat{\mathbf{u}}_1$ and $\hat{\mathbf{u}}_2$

$$\begin{aligned} \left[\tan\left(\frac{\Omega \Delta t}{2}\right) + \frac{\delta_1 \Delta t}{\Delta x} \tan\left(\frac{\Xi \Delta x}{2}\right) + \frac{2d_1 \Delta t}{\Delta x^2} \tan^2\left(\frac{\Xi \Delta x}{2}\right) - \frac{\Delta t}{32} c_1 \right] \hat{\mathbf{u}}_1 &= 0, \\ \left[\tan\left(\frac{\Omega \Delta t}{2}\right) + \frac{\delta_2 \Delta t}{\Delta x} \tan\left(\frac{\Xi \Delta x}{2}\right) + \frac{2d_2 \Delta t}{\Delta x^2} \tan^2\left(\frac{\Xi \Delta x}{2}\right) - \frac{\Delta t}{32} c_2 \right] \hat{\mathbf{u}}_2 &= 0, \end{aligned}$$

$$\begin{pmatrix} \mathcal{W}_1(\Xi) & 0 \\ 0 & \mathcal{W}_2(\Xi) \end{pmatrix} \begin{pmatrix} \hat{\mathbf{u}}_1 \\ \hat{\mathbf{u}}_2 \end{pmatrix} = \begin{pmatrix} 0 \\ 0 \end{pmatrix}$$

where

$$\begin{aligned} \mathcal{W}_1(\Xi) &= \tan\left(\frac{\Omega \Delta t}{2}\right) + \frac{\delta_1 \Delta t}{\Delta x} \tan\left(\frac{\Xi \Delta x}{2}\right) + \frac{2d_1 \Delta t}{\Delta x^2} \tan^2\left(\frac{\Xi \Delta x}{2}\right) - \frac{\Delta t}{32} c_1 \\ \mathcal{W}_2(\Xi) &= \tan\left(\frac{\Omega \Delta t}{2}\right) + \frac{\delta_2 \Delta t}{\Delta x} \tan\left(\frac{\Xi \Delta x}{2}\right) + \frac{2d_2 \Delta t}{\Delta x^2} \tan^2\left(\frac{\Xi \Delta x}{2}\right) - \frac{\Delta t}{32} c_2 \end{aligned}$$

To get a nontrivial solution the determinant of the coefficient matrix must be zero.

This gives

$$\Omega_{6,\psi_1} = \frac{2}{\Delta t} \tan^{-1} \left[\frac{\Delta t}{2} \left(-\delta_1 \frac{2 \tan\left(\frac{\Xi \Delta x}{2}\right)}{\Delta x} - d_1 \frac{4 \tan^2\left(\frac{\Xi \Delta x}{2}\right)}{\Delta x^2} + \frac{c_1}{16} \right) \right], \quad (4.51)$$

$$\Omega_{6,\psi_2} = \frac{2}{\Delta t} \tan^{-1} \left[\frac{\Delta t}{2} \left(-\delta_2 \frac{2 \tan\left(\frac{\Xi \Delta x}{2}\right)}{\Delta x} - d_2 \frac{4 \tan^2\left(\frac{\Xi \Delta x}{2}\right)}{\Delta x^2} + \frac{c_2}{16} \right) \right]. \quad (4.52)$$

because $\tan(\theta)$ is invertible for $-\pi/2 \leq \theta \leq \pi/2$. Notice that for every wave number there are two frequencies.

Now we compare the numerical dispersion relations obtained from the multisymplectic schemes with the exact dispersion relation. We see that the dispersion relations for the continuous case (4.41)-(4.42) represent a polynomial relation between the wave number ξ and the frequency ω , while the discrete model obtained using the Preissman scheme (4.46)-(4.47) and using the six point scheme (4.51)-(4.52) amounts to a trigonometric relation between the numerical wave number Ξ and the numerical frequency Ω . We recall that the CNLSE (2.26)-(2.27) is integrable for $d_1 = d_2$ and $a_1 = a_2 = e$ [52], it is non-integrable for other cases [82]. Here we compare the dispersion curves of the integrable and non-integrable cases and also we compare the effect of the linearized term corresponding to the constants c_1 and c_2 .

The dispersion curves for the linearized CNLSE (4.35)-(4.36) with $\delta_1 = \delta_2 = 1, d_1 = d_2 = 1$ and $c_1 = c_2 = 1$ for the step sizes $\Delta x = \Delta t = 0.1$ are displayed in Fig. 4.3. First we note that the exact dispersion relation gives two frequencies for every wave number as expected. The plot shows that the dispersion relation for the Preissman box scheme is close to the exact dispersion relation. For the coupled six point scheme there is only one frequency for every wave number. This behavior of the coupled six point scheme is due to the fact that we eliminate the auxiliary variables in the multisymplectic form. However, the figure shows that the dispersion curve of the coupled six point scheme preserves the one branch of the exact dispersion curve. In Fig. 4.4, we fixed the parameters $\delta_1, \delta_2, d_1, d_2$ and changed c_1 and c_2 as $c_1 = c_2 = 0$ and we observe that the results are almost the same with Fig. 4.3. This shows that the linearized term does not affect the numerical schemes. In Fig. 4.3 and 4.4 we see that there are no temporal or spatial parasitic waves. The accuracy is good for a small wave number which correspond to many grid points in the discretization as in the case of linearized NLSE.

Since c_1 and c_2 are in no way related to Δt and Δx , it is interesting to know how the dispersion relations change as the parameters c_1 and c_2 change. In Fig. 4.5 we plot the exact and numerical dispersion relations of the Preissman box scheme and the coupled six point scheme for $\Delta x = \Delta t = 0.1, \delta_1 = \delta_2 = 1, d_1 = d_2 = 1, c_1 = c_2 = -10$. The figure shows that there are no parasitic waves for both methods. Notice that while the Preissman box scheme is still close to the exact dispersion relation in low frequencies, the coupled six point scheme gives poor approximation. However, if we decrease the step sizes we see that numerical dispersion relations are close to the exact dispersion relation. For $\Delta x = 0.05, \Delta t = 0.02$, in Fig. 4.6, the dispersion relations become more 'flattened' and as a result each plot shows a close correlation between the numerical and exact dispersion relation. In Fig. 4.7 and 4.8 we plot the numerical and exact dispersion relations for $c_1 = 0.01 < \Delta x = \Delta t = 0.1 < c_2 = 1$ and for $c_2 = 0.01 < \Delta x = \Delta t = 0.1 < c_1 = 1$. In both cases we see that the dispersion curves are almost the same with Fig. 4.3 and 4.4 showing that the linearized terms which correspond to the constants c_1 and c_2 does not effect the numerical schemes.

We note that all the above cases were integrable cases ($d_1 = d_2$). Now compare the dispersion curves of the integrable and non-integrable cases of the linearized CNLSE (4.35)-(4.36). Fig. 4.9 and 4.10 shows the numerical and exact dispersion curves for the integrable case $\delta_1 = \delta_2 = 5, d_1 = d_2 = 1/2$ with $c_1 = c_2 = 1$ and $\Delta x = \Delta t = 0.1$ and for the non-integrable case $\delta_1 = \delta_2 = 5, 1/2 = d_1 \neq d_2 = -1/2$ with $c_1 = c_2 = 1$ and $\Delta x = \Delta t = 0.1$ respectively. From the figures we see that the Preissman box scheme exhibit better behavior, qualitatively preserving the exact dispersion relation for small frequencies. Also, the coupled six point scheme preserves the one branch of the exact dispersion relation. In each case the discrete dispersion relation is an accurate approximation when Ξ is small, which correspond to many grid point per wavelength, because the number of points per spatial wavelength for the wave (4.7) is $2\pi/\Xi\Delta x$.

We observe that the multisymplectic Preissman scheme does not have temporal or spatial parasitic waves for any problem based on the relation (4.46)-(4.47) since $\tan(\Omega_{\psi_1}\Delta t/2)$ and $\tan(\Omega_{\psi_2}\Delta t/2)$ are invertible for $-\pi/2 < \Omega_{\psi_1}\Delta t/2 < \pi/2$ and $-\pi/2 < \Omega_{\psi_2}\Delta t/2 < \pi/2$. By the same argument, the coupled six point scheme does not have temporal or spatial parasitic waves for any problem of the form (4.51)-(4.52). Both the exact and the numerical dispersion relations of these schemes are very close

to each other, as a result each plot shows a close correlation between the numerical and the exact dispersion relations.

In fact we observed two main characteristic of a multisymplectic integrator [56]. The first is the absence of numerically induced diffusion which is apparent from the real numerical dispersion relation. The second characteristic of a multisymplectic integrator is the non-existence of computational modes. It is well known that the Preissman scheme is a multisymplectic integrator [21] and the numerical dispersion relation of the Preissman scheme did not produce any computational modes. Also we observed that the coupled six point scheme did not produce any computational modes and for this reason we will consider the coupled six point scheme to be a multisymplectic integrator, which is also apparent from the fact that the coupled six point scheme was obtained from the multisymplectic Preissman scheme.

4.4 Linear Stability Analysis for Six-Point Scheme

In this section we investigate the linear stability of the six-point scheme (3.61)-(3.62). In general, linear stability analysis for nonlinear equation can not be justified. However, it is found to be effective in practice [28]. In [25] the linear stability of a new six-point scheme for the cubic NLSE (2.1) was investigated and it was shown that the scheme was unconditionally linearly stable. Following [25], we consider the linear CNLSE (4.35)-(4.36) and discuss the linear stability of the six-point scheme (3.61)-(3.62).

Applying the six-point scheme (3.61)-(3.62) to the linearized CNLSE (4.35)-(4.36), we obtain

$$\begin{aligned}
& \frac{i}{2\Delta t} \left[(\psi_{1_{m-1/2}}^{n+1} - \psi_{1_{m-1/2}}^n) + (\psi_{1_{m+1/2}}^{n+1} - \psi_{1_{m+1/2}}^n) \right. \\
& \left. + \frac{\delta_1}{2\Delta x} \left((\psi_{1_{m+1/2}}^{n+1} - \psi_{1_{m-1/2}}^{n+1}) + (\psi_{1_{m+1/2}}^n - \psi_{1_{m-1/2}}^n) \right) \right] \\
& + \frac{d_1}{\Delta x^2} \left(\psi_{1_{m-1}}^{n+1/2} - 2\psi_{1_m}^{n+1/2} + \psi_{1_{m+1}}^{n+1/2} \right) \\
& + \frac{c_1}{2} \left(\psi_{1_{m+1/2}}^{n+1/2} + \psi_{1_{m-1/2}}^{n+1/2} \right),
\end{aligned} \tag{4.53}$$

$$\begin{aligned}
& \frac{i}{2\Delta t} \left[(\psi_{2m-1/2}^{n+1} - \psi_{2m-1/2}^n) + (\psi_{2m+1/2}^{n+1} - \psi_{2m+1/2}^n) \right. \\
& \left. + \frac{\delta_2}{2\Delta x} \left((\psi_{2m+1/2}^{n+1} - \psi_{2m-1/2}^{n+1}) + (\psi_{2m+1/2}^n - \psi_{2m-1/2}^n) \right) \right] \\
& + \frac{d_2}{\Delta x^2} \left(\psi_{2m-1}^{n+1/2} - 2\psi_{2m}^{n+1/2} + \psi_{2m+1}^{n+1/2} \right) \\
& + \frac{c_2}{2} \left(\psi_{2m+1/2}^{n+1/2} + \psi_{2m-1/2}^{n+1/2} \right).
\end{aligned} \tag{4.54}$$

Let

$$\psi_{1m}^n = e^{iml\Delta x} \xi_1 \quad \text{and} \quad \psi_{2m}^n = e^{iml\Delta x} \xi_2 \tag{4.55}$$

where l is an arbitrary integer. Substituting (4.55) into (4.53)–(4.54) and rearranging the terms we obtain the amplification matrix

$$G(\xi) = \begin{pmatrix} \xi_1 \\ \xi_2 \end{pmatrix} = - \begin{pmatrix} a_1 + ib & 0 \\ 0 & a_2 + ib \end{pmatrix}^{-1} \begin{pmatrix} a_1 - ib \\ a_2 - ib \end{pmatrix} \tag{4.56}$$

where

$$\begin{aligned}
a_1 &= -\frac{\delta_1 \Delta t}{\Delta x} \sin(l\Delta x) - \frac{2d_1 \Delta t}{\Delta x^2} \sin^2\left(\frac{l\Delta x}{2}\right) + \frac{c_1 \Delta t}{2} \cos^2\left(\frac{l\Delta x}{2}\right), \\
a_2 &= -\frac{\delta_2 \Delta t}{\Delta x} \sin(l\Delta x) - \frac{2d_2 \Delta t}{\Delta x^2} \sin^2\left(\frac{l\Delta x}{2}\right) + \frac{c_2 \Delta t}{2} \cos^2\left(\frac{l\Delta x}{2}\right), \\
b &= 2 \cos^2\left(\frac{l\Delta x}{2}\right).
\end{aligned}$$

The eigenvalues of the amplification matrix G are

$$\lambda_1 = -\left(\frac{a_1^2 - b^2}{a_1^2 + b^2}\right) + \left(\frac{2a_1 b}{a_1^2 + b^2}\right) i, \quad \lambda_2 = -\left(\frac{a_2^2 - b^2}{a_2^2 + b^2}\right) + \left(\frac{2a_2 b}{a_2^2 + b^2}\right) i. \tag{4.57}$$

We notice that $|\lambda_1| = |\lambda_2| = 1$. Since G is Hermitian, the scheme (3.61)–(3.62) is linearly stable (see [79] p.268). Thus we have proven the following:

Theorem 4.2 *The multisymplectic integrator (3.61)–(3.62) is unconditionally linearly stable.*

This means that there is no restriction on time step Δt , but we must choose it by care to obtain accurate results.

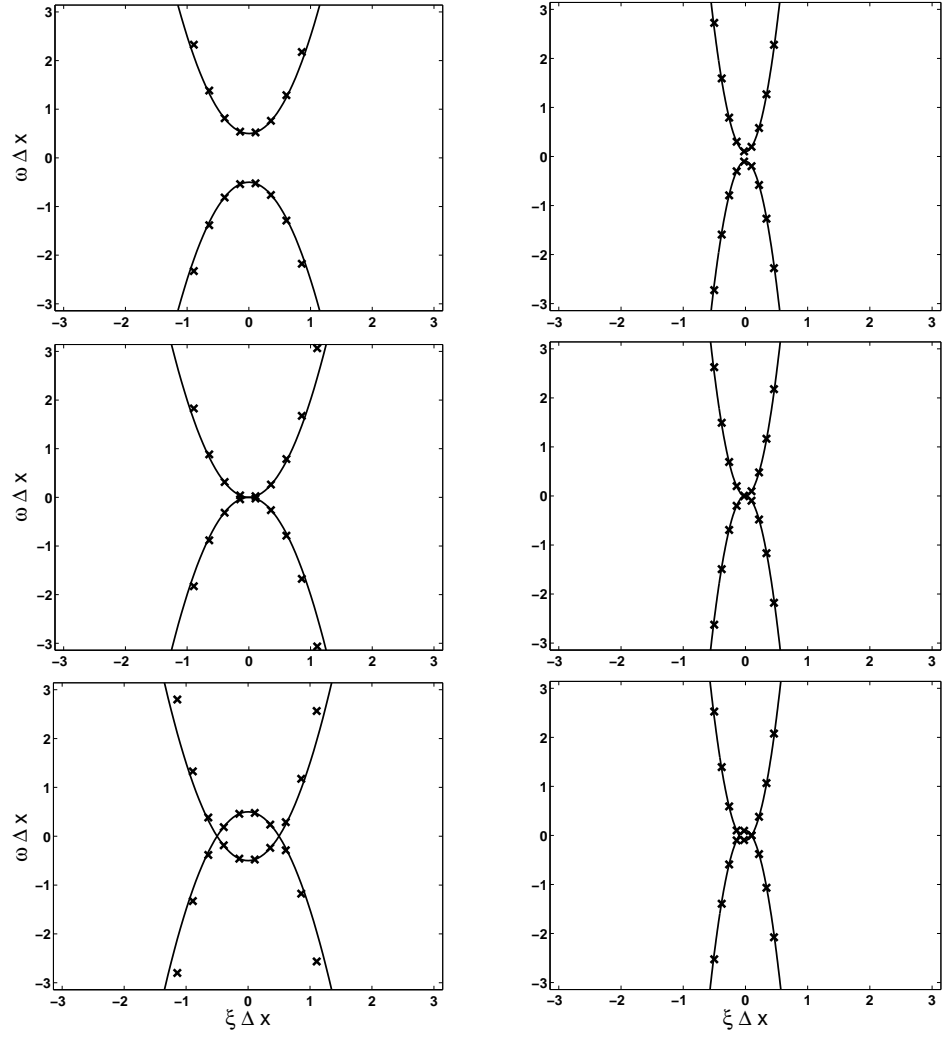


Figure 4.1: The effect of discretization in space ($\Delta t \rightarrow 0$) for linearized NLSE (4.19). Solid line: exact dispersion relation (4.24); crossed: numerical dispersion relation with continuous time (4.28). The left plot: with $\Delta x = 0.5$. The right plot : with $\Delta x = 0.1$. The top plot : $\mathbf{a} = -1 < 0$, The middle plot : $\mathbf{a} = 0$. The bottom plot : $\mathbf{a} = 1 > 0$

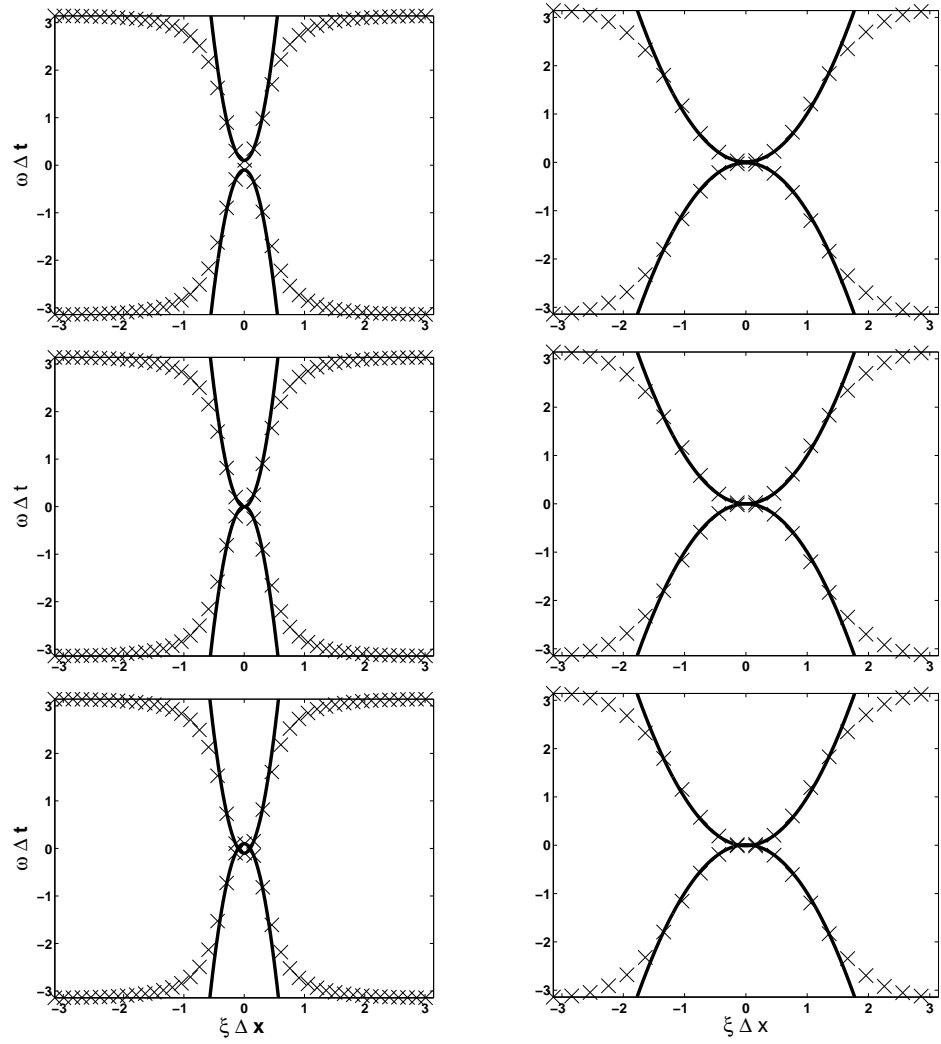


Figure 4.2: The effect of discretization for linearized NLSE (4.19). Solid line: exact dispersion relation (4.24); crossed: numerical dispersion relation (4.27). The left plot: with $\Delta x = 0.1$, $\Delta t = 0.1$. The right plot : with $\Delta x = 0.1$, $\Delta t = 0.01$. The top plot : $\mathbf{a} = -1 < 0$, The middle plot : $\mathbf{a} = 0$. The bottom plot : $\mathbf{a} = 1 > 0$

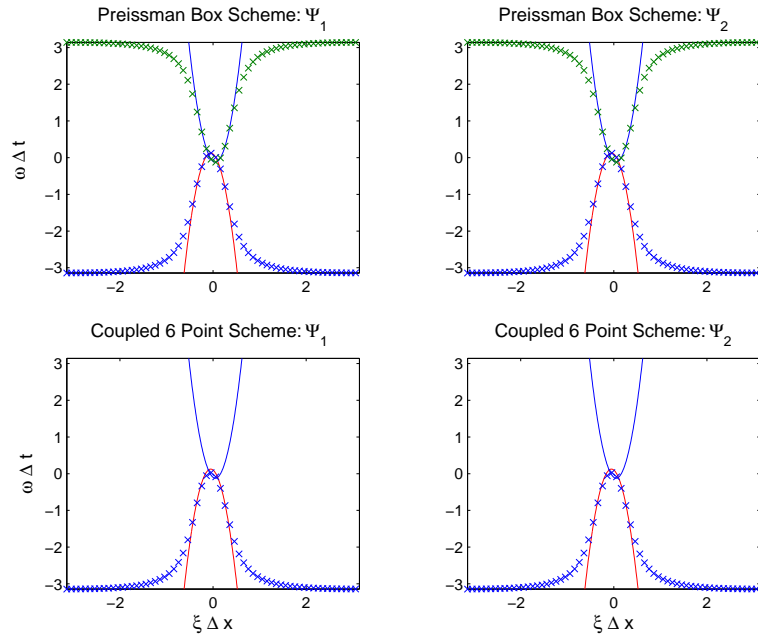


Figure 4.3: For $\Delta x = \Delta t = 0.1$, $\delta_1 = \delta_2 = 1$, $d_1 = d_2 = 1$, $c_1 = c_2 = 1$, exact (solid) and numerical (crossed) dispersion relation for linearized CNLSE (4.35)-(4.36).

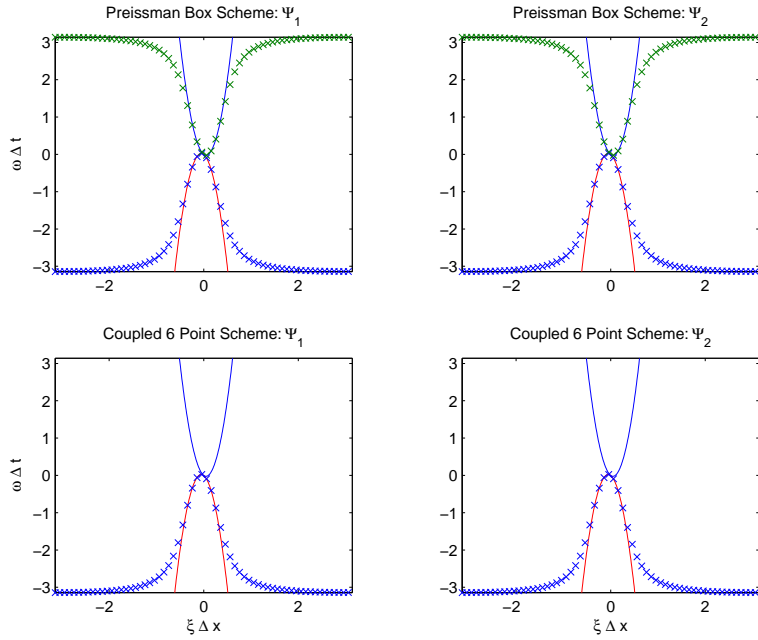


Figure 4.4: For $\Delta x = \Delta t = 0.1$, $\delta_1 = \delta_2 = 1$, $d_1 = d_2 = 1$, $c_1 = c_2 = 0$, exact (solid) and numerical (crossed) dispersion relation for linearized CNLSE (4.35)-(4.36).

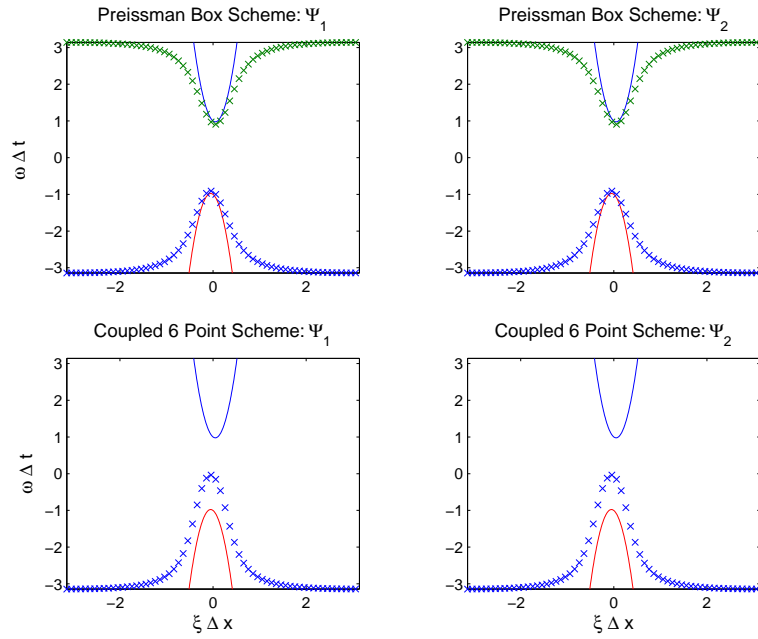


Figure 4.5: For $\Delta x = \Delta t = 0.1, \delta_1 = \delta_2 = 1, d_1 = d_2 = 1, c_1 = c_2 = -10$, exact (solid) and numerical (crossed) dispersion relation for linearized CNLSE (4.35)-(4.36).

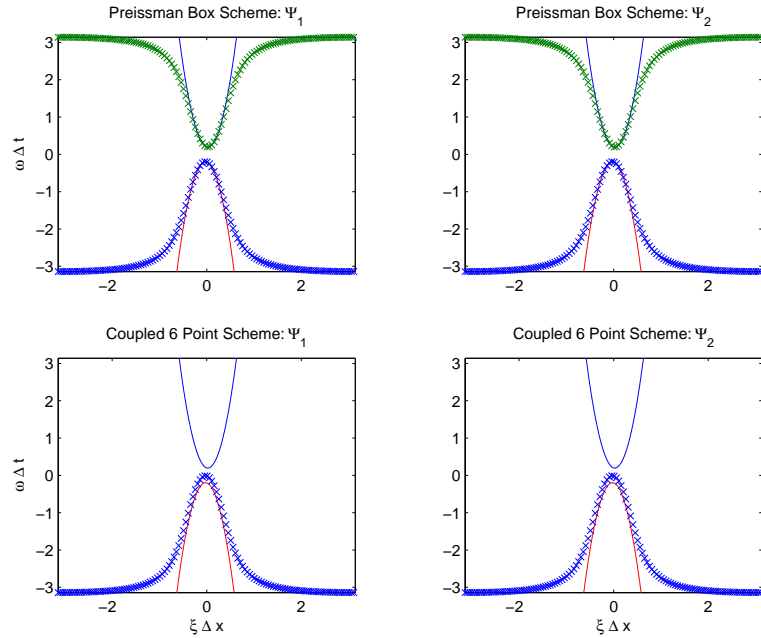


Figure 4.6: For $\Delta x = 0.05, \Delta t = 0.02, \delta_1 = \delta_2 = 1, d_1 = d_2 = 1, c_1 = c_2 = -10$, exact (solid) and numerical (crossed) dispersion relation for linearized CNLSE (4.35)-(4.36).

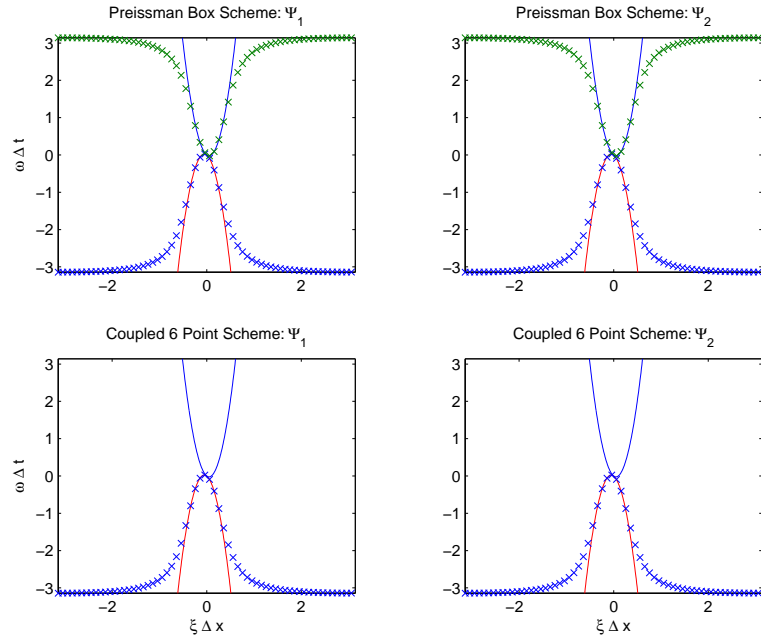


Figure 4.7: For $c_1 = 0.01 < \Delta x = \Delta t = 0.1 < c_2 = 1, \delta_1 = \delta_2 = 1, d_1 = d_2 = 1$, exact (solid) and numerical (crossed) dispersion relation for linearized CNLSE (4.35)-(4.36).

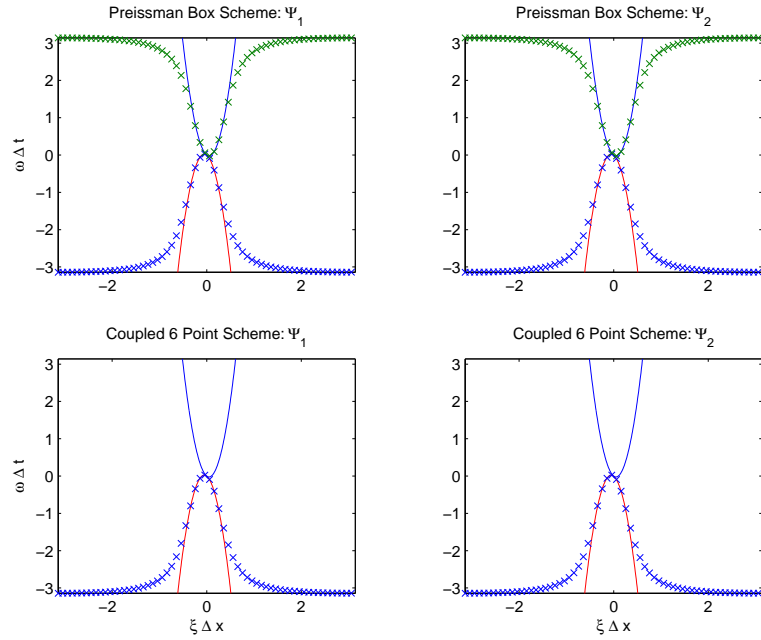


Figure 4.8: For $c_2 = 0.01 < \Delta x = \Delta t = 0.1 < c_1 = 1, \delta_1 = \delta_2 = 1, d_1 = d_2 = 1$, exact (solid) and numerical (crossed) dispersion relation for linearized CNLSE (4.35)-(4.36).

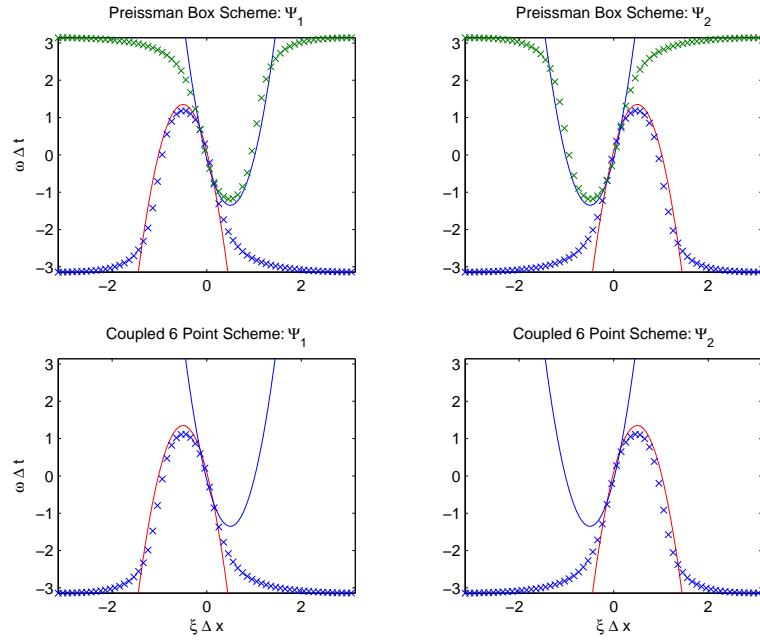


Figure 4.9: Dispersion curves of the integrable case: $\delta_1 = 5, \delta_2 = -5, d_1 = d_2 = 1/2$, with $c_1 = c_2 = 1, \Delta x = \Delta t = 0.1$. Exact (solid) and numerical (crossed) dispersion relation for linearized CNLSE (4.35)-(4.36).

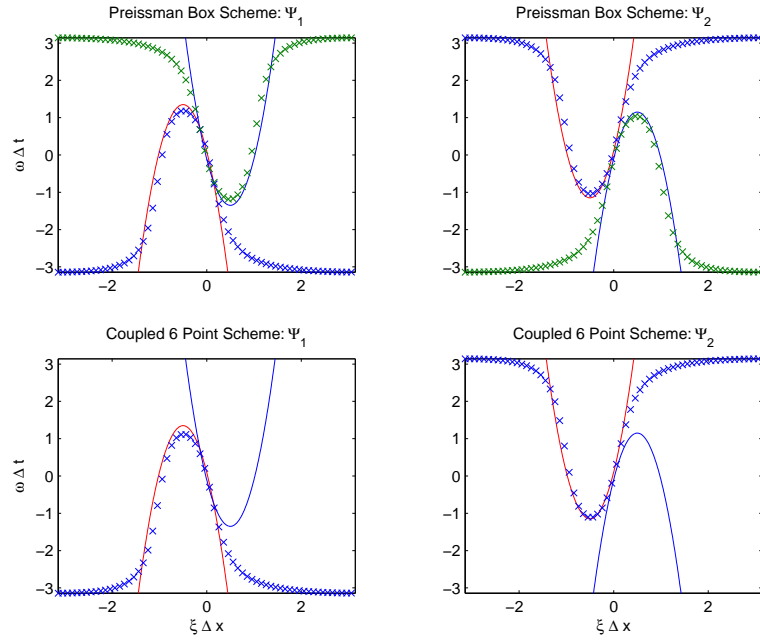


Figure 4.10: Dispersion curves of the non-integrable case: $\delta_1 = \delta_2 = 5, 1/2 = d_1 \neq d_2 = -1/2$, with $c_1 = c_2 = 1, \Delta x = \Delta t = 0.1$. Exact (solid) and numerical (crossed) dispersion relation for linearized CNLSE (4.35)-(4.36).

CHAPTER 5

BACKWARD ERROR ANALYSIS

One of the most efficient ways to analyze the effect of discretization error in a numerical solution is known as backward error analysis (BEA), in which a system of differentials is compared with the modified equations that are satisfied by the numerical solution. A modified equation is a truncated series in powers of step size, that is solved to higher order by a numerical scheme. Such a transformation induces an error which can be made exponentially small, and the results remain valid on exponentially long time intervals [33]. It is very useful when the qualitative behavior of a numerical scheme is of interest, and when statements over long time intervals are needed.

The idea of backward error analysis was first introduced by Wilkinson to understand the propagation of rounding errors in numerical linear algebra. Later, the idea of BEA have been applied to ODE's [30, 31].

Although the expansions used in BEA depend on the numerical scheme, it can be done for any finite difference method (see [33](Chapter 9), [69](Chapter 10)). In particular, if a symplectic integrator is used to discretize a Hamiltonian system of ODE's, the modified equations are also Hamiltonian, and these types of integrators have proved to give accurate and efficient results for long time integration [32, 63]. Recently, the ideas of backward error analysis have been applied to PDE's in multi-symplectic form [55, 56].

In this chapter, we summarize the results about the BEA for ODE's and PDE's given in [55, 56].

Consider the initial value problem

$$y' = f(y(t)), \quad y(0) = y_0. \quad (5.1)$$

Let $\varphi_t(y_0)$ be the exact flow of (5.1) and $\Phi_{\Delta t}(y)$ be a numerical method that approx-

imates the solution of (5.1). A forward error analysis consist in the study of the local error $y_1 - \varphi_{\Delta t}(y_0)$ and the global error $y_n - \varphi_{n\Delta t}(y_0)$ where y_0, y_1, y_2, \dots are approximations produced by the numerical method $\Phi_{\Delta t}(y)$ in the solution space. However, the idea of BEA consists in searching for a modified differential equation $\tilde{y}' = f_{\Delta t}(\tilde{y})$ of the form

$$\tilde{y}' = f(\tilde{y}) + \Delta t f_2(\tilde{y}) + \Delta t^2 f_3(\tilde{y}) + \dots, \quad (5.2)$$

$$\tilde{y}(0) = y_0 \quad (5.3)$$

such that

$$y_n = \tilde{y}(n\Delta t) \quad (5.4)$$

and studying the difference of the vector fields $f(y)$ and $f_{\Delta t}(y)$. We notice in (5.4) that $\tilde{y}(n\Delta t)$ is the exact solution of (5.2), while y_n is the approximate solution obtained from $\Phi_{\Delta t}(y)$. In order to make this point clear, we consider the ODE (5.1) and apply the first order explicit Euler method with step size Δt and get

$$y^{n+1} = y^n + \delta t f(y^n). \quad (5.5)$$

The Taylor series expansion of $y(t_n + \Delta t)$ about t_n gives

$$y(t_{n+1}) = y(t_n) + \Delta t y'(t_n) + \frac{\Delta t^2}{2} y''(t_n) + \mathcal{O}(\Delta t^3) \quad (5.6)$$

and replacing the derivatives from the original equation (5.1), we obtain

$$y(t_{n+1}) = y(t_n) + \Delta t f(y(t_n)) + \frac{\Delta t^2}{2} f_y(y(t_n)) f(y(t_n)) + \mathcal{O}(\Delta t^3) \quad (5.7)$$

where $f_y(y(t_n))$ denotes the Jacobian of f . Ignoring all terms of order Δt^3 and by eliminating the reference to the point $n\Delta t$, the modified PDE associated with the Euler scheme (5.5) can be written as

$$y' = \tilde{f} := f(y) - \frac{\Delta t}{2} f_y(y) f(y). \quad (5.8)$$

Comparing the modified equation (5.8) with (5.1), we see that only one term is added to the original equation (5.1). Therefore, the modified PDE (5.8) is called a first order modification. In [56] it was shown that, the explicit Euler scheme (5.5) solves the modified equation (5.8) to a second order accuracy. If more terms are used in the Taylor series, the numerical scheme solves the modified equation to a higher accuracy (see [56] for details).

Notice that in the preceding analysis we eliminate the higher order derivatives in (5.6) by differentiating the original equation (5.1). Following [56], we call this analysis as BEA1. However, for higher order modification this becomes more complicated. Now we give a revised approach to find the modified equation called BEA2 [56].

Consider the Hamiltonian ODE (1.1). Introducing

$$y^{n+1/2} := \frac{1}{2}(y^{n+1} + y^n)$$

and discretizing (1.1) by the implicit midpoint rule yields

$$J \frac{y^{n+1} + y^n}{\Delta t} = \nabla_y H(y^{n+1/2}). \quad (5.9)$$

Then using Taylor series expansion about $t_{n+1/2}$ we find that

$$\frac{y(t_{n+1}) - y(t_n)}{\Delta t} = y_t(t_{n+1/2}) + \frac{\Delta t^2}{2 \cdot 2!} y_{ttt}(t_{n+1/2}) + \frac{\Delta t^4}{2^4 5!} y_{tttt}(t_{n+1/2}) + \dots$$

and

$$\frac{y(t_{n+1}) + y(t_n)}{\Delta t} = y_t(t_{n+1/2}) + \frac{\Delta t^2}{2 \cdot 2!} y_{tt}(t_{n+1/2}) + \frac{\Delta t^4}{2^4 4!} y_{tttt}(t_{n+1/2}) + \dots$$

Taking the expansion out to $\mathcal{O}(\Delta t^{2\rho})$ we can write

$$\frac{y^{n+1} + y^n}{2} = \sum_{j=0}^{\rho} A_j(\tau) \partial_t^{2j} y \quad (5.10)$$

and

$$\frac{y^{n+1} - y^n}{\Delta t} = \sum_{j=0}^{\rho} B_j(\tau) \partial_t^{2j+1} y \quad (5.11)$$

where $\tau := \Delta t/2$ and

$$A_k(\tau) = \frac{\tau^{2k}}{(2k)!}, \quad B_k(\tau) = \frac{\tau^{2k}}{(2k+1)!}.$$

Substituting the identities (5.10) and (5.11) into (5.9) we obtain the general modified equation

$$J \left(\sum_{j=0}^{\rho} B_j(\tau) \partial_t^{2j+1} y \right) = \nabla_y H \left(\sum_{j=0}^{\rho} A_j(\tau) \partial_t^{2j} y \right) \quad (5.12)$$

which can also be written as a modified Hamiltonian system. A similar approach is carried out for Symplectic Euler method in [33]

Note that the BEA1 and BEA2 can only be applied to a system of ODE's. However, they can be applied to PDE's by considering the system of ODE's that result from the semi-discretization of PDE's. But this partially describes the error induced from

the numerical scheme because in the modified equation only the powers of Δt will appear. On the other hand, the backward error analysis can be applied to PDE's to obtain a modified PDE in which the modification terms contain powers of Δt and Δx . This can be achieved by the revised approach in both time and space which was introduced in [55] and known as BEA3 approach. In order to make this point clear, we consider the multisymplectic PDE (1.43) and the Preissman box discretization (3.22) to find the modified PDE associated with the Preissman box discretization. For this, we introduce

$$\tau = \frac{\Delta t}{2} \quad \text{and} \quad \chi = \frac{\Delta x}{2}$$

and define the notation

$$(\mathcal{Y}(z))_{m+\frac{1}{2}}^{n+\frac{1}{2}} = \mathcal{Y}(z(t_{n+1/2}, x_{m+1/2})). \quad (5.13)$$

Using the Taylor series expansion about $t_{n+1/2}$ we find that

$$\begin{aligned} \delta_t^+ z(t_n) &= \frac{z(t_{n+\frac{1}{2}} + \frac{\Delta t}{2}) - z(t_{n+\frac{1}{2}} - \frac{\Delta t}{2})}{\Delta t} \\ &= \left(z_t + \frac{1}{3!} \left(\frac{\Delta t}{2} \right)^2 z_{ttt} + \frac{1}{5!} \left(\frac{\Delta t}{2} \right)^4 z_{tttt} + \mathcal{O}(\Delta t^6) \right)^{n+\frac{1}{2}}. \end{aligned} \quad (5.14)$$

Using the Taylor series expansion about $x_{m+\frac{1}{2}}$ and performing the similar calculation by changing the role of t and n to x and m , we obtain

$$\begin{aligned} \delta_x^+ z(x_m) &= \frac{z(x_{m+\frac{1}{2}} + \frac{\Delta x}{2}) - z(x_{m+\frac{1}{2}} - \frac{\Delta x}{2})}{\Delta x} \\ &= \left(z_x + \frac{1}{3!} \left(\frac{\Delta x}{2} \right)^2 z_{xxx} + \frac{1}{5!} \left(\frac{\Delta x}{2} \right)^4 z_{xxxx} + \mathcal{O}(\Delta x^6) \right)_{m+\frac{1}{2}}. \end{aligned} \quad (5.15)$$

Substituting (5.14) and (5.15) into the multisymplectic discretization (3.22) yields

$$\begin{aligned} \mathbf{M} \delta_t^+ z_{m+\frac{1}{2}}^n + \mathbf{K} \delta_x^+ z_m^{n+\frac{1}{2}} - \nabla_z S \left(z_{m+\frac{1}{2}}^{n+\frac{1}{2}} \right) &= \\ &= (\mathbf{M} z_t + \mathbf{K} z_x - \nabla_z S(z) + \mathcal{O}(\Delta x^2 + \Delta t^2))_{m+\frac{1}{2}}^{n+\frac{1}{2}} \end{aligned} \quad (5.16)$$

which shows that the Preissman box discretization (3.22) is second order in time and space.

Expansions (5.14) and (5.15) can be rewritten in a more compact way as

$$\delta_t^+ z(t_n) = \sum_{k=0}^{\sigma} \frac{\tau^{2k}}{(2k+1)!} \partial_t^{2k+1} z, \quad \delta_x^+ z(x_m) = \sum_{k=0}^{\sigma} \frac{\chi^{2k}}{(2k+1)!} \partial_x^{2k+1} z \quad (5.17)$$

where we have truncated the terms higher than $\Delta t^{2\sigma}$ and $\Delta x^{2\sigma}$. Substituting these expansions into the multisymplectic Preissman box scheme (3.22) yields the modified

equation

$$\mathbf{M} \left(\sum_{k=0}^{\sigma} \frac{\tau^{2k}}{(2k+1)!} \partial_t^{2k+1} z \right) + \mathbf{K} \left(\sum_{k=0}^{\sigma} \frac{\chi^{2k}}{(2k+1)!} \partial_x^{2k+1} z \right) = \nabla_z S(z) \quad (5.18)$$

which is satisfied by the numerical solution up to $\mathcal{O}(\Delta t^{2\sigma} + \Delta x^{2\sigma})$.

Note that for $\sigma = 0$, the modified equation (5.18) becomes the multisymplectic PDE (1.43). For $\sigma = 1$ modification, (5.18) takes the form

$$\mathbf{M} z_t + \frac{(\Delta t)^2}{24} \mathbf{M} z_{ttt} + \mathbf{K} z_x \frac{(\Delta x)^2}{24} \mathbf{K} z_{xxx} = \nabla_z S(z) \quad (5.19)$$

which can be viewed as a generalized (higher order) multisymplectic PDE and is satisfied by the numerical solution up to $\mathcal{O}(\Delta t^4 + \Delta x^4)$. For example, the modified equation for the discrete NLSE (3.45) with $\sigma = 1$ modification can be written as

$$\begin{aligned} - \left(q_t + \frac{\Delta t^2}{24} q_{ttt} \right) - \left(v_x + \frac{\Delta x^2}{24} v_{xxx} \right) &= a(p^2 + q^2) p \\ \left(p_t + \frac{\Delta t^2}{24} p_{ttt} \right) - \left(\omega_x + \frac{\Delta x^2}{24} \omega_{xxx} \right) &= a(p^2 + q^2) q \\ p_x + \frac{\Delta x^2}{24} p_{xxx} &= v \\ q_x + \frac{\Delta x^2}{24} q_{xxx} &= \omega. \end{aligned} \quad (5.20)$$

The modified equation for the discrete CNLSE (3.50) with $\sigma = 1$ can be written as

$$\begin{aligned} q_{2t} + \frac{\Delta t^2}{24} q_{2ttt} - p_{1x} - \frac{\Delta x^2}{24} p_{1xxx} - z_1 q_1 + \frac{\delta_1}{2d_1} \left(p_2 - \frac{\delta_1}{2} q_1 \right) &= 0 \\ -q_{1t} - \frac{\Delta t^2}{24} q_{1ttt} - p_{2x} - \frac{\Delta x^2}{24} p_{2xxx} - z_1 q_2 - \frac{\delta_1}{2d_1} \left(p_1 + \frac{\delta_1}{2} q_2 \right) &= 0 \\ q_{4t} + \frac{\Delta t^2}{24} q_{4ttt} - p_{3x} - \frac{\Delta x^2}{24} p_{3xxx} - z_2 q_3 + \frac{\delta_2}{2d_2} \left(p_4 - \frac{\delta_2}{2} q_3 \right) &= 0 \\ -q_{3t} - \frac{\Delta t^2}{24} q_{3ttt} - p_{4x} - \frac{\Delta x^2}{24} p_{4xxx} - z_2 q_4 - \frac{\delta_2}{2d_2} \left(p_3 + \frac{\delta_2}{2} q_4 \right) &= 0 \\ q_{1x} + \frac{\Delta x^2}{24} q_{1xxx} - \frac{1}{d_1} \left(p_1 + \frac{\delta_1}{2} q_2 \right) &= 0 \\ q_{2x} + \frac{\Delta x^2}{24} q_{2xxx} - \frac{1}{d_1} \left(p_2 - \frac{\delta_1}{2} q_1 \right) &= 0 \\ q_{3x} + \frac{\Delta x^2}{24} q_{3xxx} - \frac{1}{d_2} \left(p_3 + \frac{\delta_2}{2} q_4 \right) &= 0 \\ q_{4x} + \frac{\Delta x^2}{24} q_{4xxx} - \frac{1}{d_2} \left(p_4 - \frac{\delta_2}{2} q_3 \right) &= 0. \end{aligned} \quad (5.21)$$

Eliminating the variables p_1, \dots, p_4 and using the fact that $\psi_1 = q_1 + iq_2$ and $\psi_2 = q_3 + iq_4$ the modified equation (5.21) can be written as

$$\begin{aligned}
i \left[\psi_{1t} + \frac{\Delta t^2}{24} \psi_{1ttt} + \delta_1 \left(\psi_{1x} + \frac{\Delta x^2}{24} \psi_{1xxx} \right) \right] + d_1 \left(\psi_{1xx} + \frac{\Delta x^2}{12} \psi_{1xxxx} \right) \\
+ d_1 \left(\frac{\Delta x^2}{24} \right)^2 \psi_{1xxxxxx} + (a_1 |\psi_1|^2 + e |\psi_2|^2) \psi_1 = 0, \tag{5.22}
\end{aligned}$$

$$\begin{aligned}
i \left[\psi_{2t} + \frac{\Delta t^2}{24} \psi_{2ttt} + \delta_2 \left(\psi_{2x} + \frac{\Delta x^2}{24} \psi_{2xxx} \right) \right] + d_2 \left(\psi_{2xx} + \frac{\Delta x^2}{12} \psi_{2xxxx} \right) \\
+ d_2 \left(\frac{\Delta x^2}{24} \right)^2 \psi_{2xxxxxx} + (e |\psi_1|^2 + a_2 |\psi_2|^2) \psi_2 = 0. \tag{5.23}
\end{aligned}$$

The modified equation with $\sigma = 1$ modification (5.19) can be rewritten as multisymplectic PDE. To make this more clear, we consider the modified equation with $\sigma = 1$ modification (5.19). Introducing the auxiliary variables

$$p = z_t, \quad q = p_t, \quad r = z_x, \quad s = r_x, \tag{5.24}$$

the modified equation (5.19) can be rewritten as a first-order system of equations

$$\begin{aligned}
\mathbf{M}z_t + \frac{(\Delta t)^2}{24} \mathbf{M}q_t + \mathbf{K}z_x + \frac{(\Delta x)^2}{24} \mathbf{K}s_x &= \nabla_z S(z), \\
-\frac{(\Delta t)^2}{24} \mathbf{M}p_t &= -\frac{(\Delta t)^2}{24} \mathbf{M}q, \\
\frac{(\Delta t)^2}{24} \mathbf{M}z_t &= \frac{(\Delta t)^2}{24} \mathbf{M}p, \\
-\frac{(\Delta x)^2}{24} \mathbf{K}r_x &= -\frac{(\Delta x)^2}{24} \mathbf{K}s, \\
\frac{(\Delta x)^2}{24} \mathbf{K}z_x &= \frac{(\Delta x)^2}{24} \mathbf{K}r
\end{aligned} \tag{5.25}$$

or in multisymplectic form

$$\tilde{\mathbf{M}}\tilde{z}_t + \tilde{\mathbf{K}}\tilde{z}_x = \nabla_{\tilde{z}} \tilde{S}(\tilde{z}) \tag{5.26}$$

where

$$\tilde{\mathbf{M}} = \begin{bmatrix} \mathbf{M} & \mathbf{0} & \frac{(\Delta t)^2}{24} \mathbf{M} & \mathbf{0} & \mathbf{0} \\ \mathbf{0} & -\frac{(\Delta t)^2}{24} \mathbf{M} & \mathbf{0} & \mathbf{0} & \mathbf{0} \\ \frac{(\Delta t)^2}{24} \mathbf{M} & \mathbf{0} & \mathbf{0} & \mathbf{0} & \mathbf{0} \\ \mathbf{0} & \mathbf{0} & \mathbf{0} & \mathbf{0} & \mathbf{0} \\ \mathbf{0} & \mathbf{0} & \mathbf{0} & \mathbf{0} & \mathbf{0} \end{bmatrix},$$

$$\tilde{\mathbf{K}} = \begin{bmatrix} \mathbf{K} & \mathbf{0} & \mathbf{0} & \mathbf{0} & \frac{(\Delta x)^2}{24} \mathbf{K} \\ \mathbf{0} & \mathbf{0} & \mathbf{0} & \mathbf{0} & \mathbf{0} \\ \mathbf{0} & \mathbf{0} & \mathbf{0} & \mathbf{0} & \mathbf{0} \\ \mathbf{0} & \mathbf{0} & \mathbf{0} & -\frac{(\Delta x)^2}{24} \mathbf{K} & \mathbf{0} \\ \frac{(\Delta x)^2}{24} \mathbf{K} & \mathbf{0} & \mathbf{0} & \mathbf{0} & \mathbf{0} \end{bmatrix}$$

and

$$\tilde{S}(\tilde{z}) = S(z) + \frac{\Delta t^2}{24} q^T \mathbf{M} p + \frac{\Delta x^2}{24} r^T \mathbf{K} s.$$

Note that $\tilde{\mathbf{M}}$ and $\tilde{\mathbf{K}}$ are skew-symmetric matrices due to the skew-symmetry of the matrices \mathbf{M} and \mathbf{K} . Associated with the multisymplectic formulation (5.26), one can define the two forms

$$\tilde{\omega} = \langle \tilde{\mathbf{M}}, \tilde{U}, \tilde{V} \rangle, \quad \tilde{\kappa} = \langle \tilde{\mathbf{K}}, \tilde{U}, \tilde{V} \rangle \quad (5.27)$$

where \tilde{U} and \tilde{V} are the solutions of the variational equation corresponding to the modified multisymplectic formulation (5.26). Using the results in Section 1.4 one can derive the modified energy conservation law

$$\partial_t \tilde{E}(\tilde{z}) + \partial_x \tilde{F}(\tilde{z}) = 0, \quad (5.28)$$

and the modified momentum conservation law

$$\partial_t \tilde{I}(\tilde{z}) + \partial_x \tilde{G}(\tilde{z}) = 0, \quad (5.29)$$

where

$$\begin{aligned} \tilde{E}(\tilde{z}) &= \tilde{S}(\tilde{z}) - \frac{1}{2} \tilde{\kappa}(\tilde{z}_x, \tilde{z}), & \tilde{F}(\tilde{z}) &= \frac{1}{2} \tilde{\kappa}(\tilde{z}_t, \tilde{z}), \\ \tilde{G}(\tilde{z}) &= \tilde{S}(\tilde{z}) - \frac{1}{2} \tilde{\omega}(\tilde{z}_t, \tilde{z}), & \tilde{I}(\tilde{z}) &= \frac{1}{2} \tilde{\omega}(\tilde{z}_x, \tilde{z}). \end{aligned} \quad (5.30)$$

By direct computation modified energy conservation (5.28) of the CNLSE (2.26)-(2.27) can be obtained with the energy density

$$\tilde{E}(z) = S(z) - \frac{1}{2} \left(z^T \mathbf{K} z_x - \frac{\Delta x^2}{6} z_x^T \mathbf{K} z_{xx} + \frac{\Delta t^2}{12} z_t^T \mathbf{M} z_{tt} + \frac{\Delta x^2}{24} z^T \mathbf{K} z_{xx} \right) \quad (5.31)$$

and the energy flux

$$\tilde{F}(z) = \frac{1}{2} \left(z^T \mathbf{K} z_t + \frac{\Delta x^2}{24} z^T \mathbf{K} z_{xxt} - \frac{\Delta x^2}{24} z_x^T \mathbf{K} z_{xt} - \frac{\Delta x^2}{24} z_t^T \mathbf{K} z_{xx} \right). \quad (5.32)$$

Similarly, the modified momentum conservation (5.29) of the CNLSE (2.26)-(2.27) can be obtained with the momentum density

$$\tilde{I}(z) = \frac{1}{2} \left(z^T \mathbf{M} z_x + \frac{\Delta t^2}{24} z^T \mathbf{M} z_{xtt} - \frac{\Delta t^2}{24} z_t^T \mathbf{M} z_{xt} - \frac{\Delta t^2}{24} z_x^T \mathbf{M} z_{tt} \right) \quad (5.33)$$

and the modified momentum flux

$$\tilde{G}(z) = S(z) - \frac{1}{2} \left(z^T \mathbf{M} z_t - \frac{\Delta x^2}{12} z_x^T \mathbf{K} z_{xx} + \frac{\Delta t^2}{24} z^T \mathbf{M} z_{tt} \right). \quad (5.34)$$

The modified equation (5.26) can also be derived from a modified Lagrangian density which is also invariant under the transformation (1.59) [57]. Then the corresponding modified conservation law can be found by multiplying the modified equation (5.19) by $(\mathbf{A}z)^T$. Thus we get

$$z^T \mathbf{M} \mathbf{A} z_t + \frac{\Delta t^2}{24} z^T \mathbf{M} \mathbf{A} z_{tt} + z^T \mathbf{K} \mathbf{A} z_x + \frac{\Delta x^2}{24} z^T \mathbf{K} \mathbf{A} z_{xx} = 0, \quad (5.35)$$

where we have used the skew-symmetry of the matrices \mathbf{M} and \mathbf{K} , and the identity (1.60). Using the identities

$$\begin{aligned} z^T \mathbf{M} \mathbf{A} z_t &= \frac{1}{2} \partial_t (z^T \mathbf{M} \mathbf{A} z) \\ z^T \mathbf{M} \mathbf{A} z_{tt} &= \partial_t (z^T \mathbf{M} \mathbf{A} z_{tt}) - \frac{1}{2} \partial_t (z_t^T \mathbf{M} \mathbf{A} z_t) \\ z^T \mathbf{K} \mathbf{A} z_x &= \frac{1}{2} \partial_x (z^T \mathbf{K} \mathbf{A} z) \\ z^T \mathbf{K} \mathbf{A} z_{xx} &= \partial_x (z^T \mathbf{K} \mathbf{A} z_{xx}) - \frac{1}{2} \partial_x (z_x^T \mathbf{K} \mathbf{A} z_x) \end{aligned} \quad (5.36)$$

the equality (5.35) can be written as

$$\begin{aligned} \partial_t \left(z^T \mathbf{M} \mathbf{A} z + \frac{\Delta t^2}{12} z^T \mathbf{M} \mathbf{A} z_{tt} - \frac{\Delta t^2}{24} z_t^T \mathbf{M} \mathbf{A} z_t \right) + \\ \partial_x \left(z^T \mathbf{K} \mathbf{A} z + \frac{\Delta x^2}{12} z^T \mathbf{K} \mathbf{A} z_{xx} - \frac{\Delta x^2}{24} z_x^T \mathbf{K} \mathbf{A} z_x \right) = 0. \end{aligned} \quad (5.37)$$

Thus we obtain the additional modified conservation law which is the modified version of the conservation law (1.61).

Another form of backward analysis can be performed by expanding the Taylor's series about both $t_{n+1/2}$ and $x_{m+1/2}$. In this case we get

$$\begin{aligned} \delta_t^+ z_{m+\frac{1}{2}}^n &= \frac{1}{2\Delta t} (z_{m+1}^{n+1} + z_m^{n+1} - z_{m+1}^n - z_m^n) \\ &= \left(z_t + \frac{\chi^2}{2!} z_{xxt} + \frac{\tau^2}{3!} z_{ttt} + \frac{\chi^2 \tau^2}{2!3!} z_{xxtt} + \frac{\chi^4}{4!} z_{xxxxt} + \mathcal{O}(\chi^6 + \tau^6) \right)_{m+\frac{1}{2}}^{n+\frac{1}{2}} \\ \delta_x^+ z_m^{n+\frac{1}{2}} &= \frac{1}{2\Delta x} (z_{m+1}^{n+1} + z_{m+1}^n - z_m^{n+1} - z_m^n) \\ &= \left(z_x + \frac{\chi^2}{3!} z_{xxx} + \frac{\tau^2}{2!} z_{xtt} + \frac{\chi^2 \tau^2}{2!3!} z_{xxxt} + \frac{\chi^4}{5!} z_{xxxxx} + \mathcal{O}(\chi^6 + \tau^6) \right)_{m+\frac{1}{2}}^{n+\frac{1}{2}} \\ z_{m+\frac{1}{2}}^{n+\frac{1}{2}} &= \frac{1}{4} (z_{m+1}^{n+1} + z_{m+1}^n + z_m^{n+1} + z_m^n) \\ &= \left(z + \frac{\chi^2}{2!} z_{xx} + \frac{\tau^2}{2!} z_{tt} + \frac{\chi^2 \tau^2}{2!2!} z_{xxtt} + \frac{\chi^4}{4!} z_{xxxx} + \mathcal{O}(\chi^6 + \tau^6) \right)_{m+\frac{1}{2}}^{n+\frac{1}{2}}. \end{aligned}$$

Substituting these into the Preissman box scheme (3.22), we get

$$\mathbf{M}\delta_t^+ z_{m+\frac{1}{2}}^n + \mathbf{K}\delta_x^+ z_m^{n+\frac{1}{2}} - \nabla_z S(z_{m+\frac{1}{2}}^{n+\frac{1}{2}}) = \mathbf{M}z_t + \mathbf{K}z_x - \nabla_z S(z) + \mathcal{O}(\Delta x^2 + \Delta t^2) \quad (5.38)$$

which again shows that the Preissman box discretization is second order both in space and time. We can write these expansions in compact form as

$$z_{m+\frac{1}{2}}^{n+\frac{1}{2}} = \sum_{k=0}^{\sigma} \sum_{l=0}^{\sigma} X_k(\chi) X_l(\tau) \partial_x^{2k} \partial_t^{2l} z \quad (5.39)$$

$$\delta_x^+ z_m^{n+\frac{1}{2}} = \sum_{k=0}^{\sigma} \sum_{l=0}^{\sigma} X_k(\tau) T_l(\chi) \partial_x^{2l+1} \partial_t^{2k} z \quad (5.40)$$

$$\delta_t^+ z_{m+\frac{1}{2}}^n = \sum_{k=0}^{\sigma} \sum_{l=0}^{\sigma} X_k(\chi) T_l(\tau) \partial_x^{2k} \partial_t^{2l+1} z. \quad (5.41)$$

After substituting these expansions into (3.22) we get the general modified PDE

$$\mathbf{M} \left(\sum_{k=0}^{\sigma} \sum_{l=0}^{\sigma} X_k(\chi) T_l(\tau) \partial_x^{2k} \partial_t^{2l+1} z \right) + \mathbf{K} \left(\sum_{k=0}^{\sigma} \sum_{l=0}^{\sigma} X_k(\tau) T_l(\chi) \partial_x^{2l+1} \partial_t^{2k} z \right) \quad (5.42)$$

$$= \nabla_z S \left(\sum_{k=0}^{\sigma} \sum_{l=0}^{\sigma} X_k(\chi) X_l(\tau) \partial_x^{2k} \partial_t^{2l} z \right) \quad (5.43)$$

It is important to note that the case $\sigma = 0$ corresponds to no modification and the equation (5.42) becomes the standard first-order multisymplectic PDE (1.43). However, for higher modification, for example $\sigma = 1$ modification the modified equation (5.42) becomes

$$\begin{aligned} \mathbf{M} \left(z_t + \frac{\chi^2}{2} z_{xxt} + \frac{\tau^2}{6} z_{ttt} + \frac{\chi^2 \tau^2}{12} z_{xxttt} \right) + \mathbf{K} \left(z_x + \frac{\chi^2}{6} z_{xxx} + \frac{\tau^2}{2} z_{xtt} + \frac{\chi^2 \tau^2}{12} z_{xxxtt} \right) \\ = \nabla_z S \left(z + \frac{\chi^2}{2} z_{xx} + \frac{\tau^2}{2} z_{tt} + \frac{\chi^2 \tau^2}{4} z_{xxtt} \right) \end{aligned} \quad (5.44)$$

which can be considered as a generalized (higher-order) multisymplectic PDE and is satisfied by the numerical solution up to $\mathcal{O}(\Delta x^4 + \Delta t^4)$. This modified equation can be written in the form of the multisymplectic PDE (1.43). To do this, we introduce

$$\begin{aligned} \tilde{z} &= z + \frac{\chi^2}{2} z_{xx} + \frac{\tau^2}{2} z_{tt} + \frac{\chi^2 \tau^2}{4} z_{xxtt} \\ &= z + \frac{\Delta x^2}{8} z_{xx} + \frac{\Delta t^2}{8} z_{tt} + \frac{\Delta x^2 \Delta t^2}{64} z_{xxtt} \end{aligned} \quad (5.45)$$

where we have used the definitions (5). Then

$$z_t + \frac{\chi^2}{2} z_{xxt} + \frac{\tau^2}{6} z_{ttt} + \frac{\chi^2 \tau^2}{12} z_{xxttt} = \tilde{z}_t - \frac{\Delta t^2}{12} \tilde{z}_{ttt} + \mathcal{O}(\Delta t^4) \quad (5.46)$$

and

$$z_x + \frac{\chi^2}{6} z_{xxx} + \frac{\tau^2}{2} z_{xtt} + \frac{\chi^2 \tau^2}{12} z_{xxxtt} = \tilde{z}_x - \frac{\Delta x^2}{12} \tilde{z}_{xxx} + \mathcal{O}(\Delta x^4). \quad (5.47)$$

Substituting (5.45),(5.46) and (5.47) into (5.44) yields

$$\mathbf{M} \left(\tilde{z}_t - \frac{\Delta t^2}{12} \tilde{z}_{ttt} \right) + \mathbf{K} \left(\tilde{z}_x - \frac{\Delta x^2}{12} \tilde{z}_{xxx} \right) = \nabla_{\tilde{z}} S(\tilde{z}) \quad (5.48)$$

where we ignored all terms containing $\mathcal{O}(\Delta x^4 + \Delta t^4)$. In order to write (5.48) as a first-order multisymplectic PDE, we introduce

$$a = \tilde{z}_t, \quad b = a_t, \quad v = \tilde{z}_x, \quad w = v_x, \quad (5.49)$$

and rewrite (5.48) as

$$\begin{aligned} \mathbf{M} \tilde{z}_t - \frac{(\Delta t)^2}{12} \mathbf{M} b_t + \mathbf{K} \tilde{z}_x - \frac{(\Delta x)^2}{12} \mathbf{K} w_x &= \nabla_{\tilde{z}} S(\tilde{z}) \\ \frac{(\Delta t)^2}{12} \mathbf{M} a_t &= \frac{(\Delta t)^2}{12} \mathbf{M} b \\ -\frac{(\Delta t)^2}{12} \mathbf{M} \tilde{z}_t &= -\frac{(\Delta t)^2}{12} \mathbf{M} a \\ \frac{(\Delta x)^2}{12} \mathbf{K} v_x &= \frac{(\Delta x)^2}{12} \mathbf{K} w \\ -\frac{(\Delta x)^2}{12} \mathbf{K} \tilde{z}_x &= -\frac{(\Delta x)^2}{12} \mathbf{K} v \end{aligned} \quad (5.50)$$

or in multisymplectic form

$$\hat{\mathbf{M}} \hat{z}_t + \hat{\mathbf{K}} \hat{z}_x = \nabla_{\hat{z}} \hat{S}(\hat{z}) \quad (5.51)$$

where $\hat{z} = (\tilde{z}, a, b, v, w)^T$, $\nabla_{\hat{z}} \hat{S}(\hat{z}) = S(\tilde{z}) + \frac{\Delta t^2}{12} a^T \mathbf{M} b + \frac{\Delta x^2}{12} v^T \mathbf{K} w$ and

$$\hat{\mathbf{M}} = \begin{bmatrix} \mathbf{M} & \mathbf{0} & -\frac{(\Delta t)^2}{12} \mathbf{M} & \mathbf{0} & \mathbf{0} \\ \mathbf{0} & \frac{(\Delta t)^2}{12} \mathbf{M} & \mathbf{0} & \mathbf{0} & \mathbf{0} \\ -\frac{(\Delta t)^2}{12} \mathbf{M} & \mathbf{0} & \mathbf{0} & \mathbf{0} & \mathbf{0} \\ \mathbf{0} & \mathbf{0} & \mathbf{0} & \mathbf{0} & \mathbf{0} \\ \mathbf{0} & \mathbf{0} & \mathbf{0} & \mathbf{0} & \mathbf{0} \end{bmatrix}$$

$$\hat{\mathbf{K}} = \begin{bmatrix} \mathbf{K} & \mathbf{0} & \mathbf{0} & \mathbf{0} & -\frac{(\Delta x)^2}{12} \mathbf{K} \\ \mathbf{0} & \mathbf{0} & \mathbf{0} & \mathbf{0} & \mathbf{0} \\ \mathbf{0} & \mathbf{0} & \mathbf{0} & \mathbf{0} & \mathbf{0} \\ \mathbf{0} & \mathbf{0} & \mathbf{0} & \frac{(\Delta x)^2}{12} \mathbf{K} & \mathbf{0} \\ -\frac{(\Delta x)^2}{12} \mathbf{K} & \mathbf{0} & \mathbf{0} & \mathbf{0} & \mathbf{0} \end{bmatrix}.$$

CHAPTER 6

NUMERICAL RESULTS

In this chapter we examine the performance of the multisymplectic integrators; Preissman box scheme (MS), the six-point scheme (MS6) and the semi-explicit symplectic (SE) scheme. We use uniformly distributed mesh points in space and constant time steps for all schemes. The numerical schemes are compared for two problem classes: plane waves and soliton solutions with periodic boundary conditions.

Because the multisymplectic integrators MS and MS6 are implicit, to advance the solution in time, we have used Newton iteration. As stopping criteria for the Newton iteration we have used the error tolerance 10^{-10} between two successive iterates. At each Newton step, system of dimension $8N \times 8N$ for MS and $4N \times 4N$ for MS and SE schemes has been solved by LU decomposition. All programs have been written and run in Matlab 6.5.

As mentioned in the preceding chapters, the preservation of the conserved quantities like energy, momentum and additional conservation property by the multisymplectic integrators in long term computation plays an important role and they can be used to monitor the accuracy and qualitative behavior of the solutions. We have computed the residuals of the local conserved quantities for multisymplectic Preissman and six-point schemes as the local energy conservation

$$LE(n) = \Delta x(E_{m+1/2}^{n+1} - E_{m+1/2}^n) + \Delta t(F_{m+1}^{n+1/2} - F_m^{n+1/2}), \quad (6.1)$$

the local momentum conservation

$$LM(n) = \Delta x(I_{m+1/2}^{n+1} - I_{m+1/2}^n) + \Delta t(G_{m+1}^{n+1/2} - G_m^{n+1/2}) \quad (6.2)$$

and the local additional conservation law

$$LA(n) = \Delta x(T_{m+1/2}^{n+1} - T_{m+1/2}^n) + \Delta t(V_{m+1}^{n+1/2} - V_m^{n+1/2}). \quad (6.3)$$

The residuals of the local conserved quantities for the semi-explicit symplectic scheme have been computed as the local energy conservation

$$LE(n) = \Delta x(E_m^{n+1} - E_m^n) + (\Delta t/2)(F_{m+1}^{n+1/2} - F_{m-1}^{n+1/2}), \quad (6.4)$$

the local momentum conservation

$$LM(n) = \Delta x(I_m^{n+1} - I_m^n) + (\Delta t/2)(G_{m+1}^{n+1/2} - G_{m-1}^{n+1/2}) \quad (6.5)$$

and the local additional conservation law

$$LA(n) = \Delta x(T_m^{n+1} - T_m^n) + (\Delta t/2)(V_{m+1}^{n+1/2} - V_{m-1}^{n+1/2}). \quad (6.6)$$

Once the local conserved quantities are evaluated the global invariants $\mathcal{E}(t)$ in (1.64), $\mathcal{I}(t)$ in (1.65) and $\mathcal{T}(t)$ in (1.66) can be computed over the space domain. The errors in the global invariants are then given as

$$GE(n) = \sum_{m=1}^M \Delta x(E_m^n - E_m^0), \quad (6.7)$$

$$GM(n) = \sum_{m=1}^M \Delta x(I_m^n - I_m^0), \quad (6.8)$$

$$GA(n) = \sum_{m=1}^M \Delta x(T_m^n - T_m^0). \quad (6.9)$$

Here E^0 , I^0 and T^0 are the initial values, and E^n , I^n and T^n are the values at time $t = n\Delta t$ of the conserved quantities.

The outline of this chapter is as follows: In Sec. 6.1 we present the numerical results for CNLSE with plane wave solutions. The numerical results obtained by the multisymplectic integrators and semi-explicit symplectic integrator are compared with those existing in the literature for different parameter values of the CNLSE and the initial conditions. In Sec 6.2 CNLSE with soliton solutions is considered. Single soliton, elastic (corresponds to the integrable case of CNLSE) and inelastic soliton collisions are computed using the Preissman and six-point schemes and the numerical results are compared with those in the literature.

6.1 The plane wave solutions of CNLSE

Waves represented by function of one variable of the form

$$\omega(x, t) = f(x - ct)$$

with a nonzero constant c are called travelling waves. The constant $|c|$ denotes the speed of the wave. If $c < 0$, then the profile of the wave at a later time t is a translation of the initial profile $\omega(x, 0) = f(x)$ by an amount ct in the negative x -direction with constant speed $|c|$. If $c > 0$, then the profile of the wave represents a wave moving in positive x -direction with speed c . Plane waves of PDE's which retain their shapes for a long period of time are known as solitary waves or solitons. Many analytical and numerical studies were carried out for solitary wave solutions of CNLSE (see [42, 41, 74, 76, 82, 86] and reference therein). This will be the subject of the next section. Less attention is paid for the study of periodic plane wave solutions of the CNLSE. In [74] the stability of the periodic solution of the form

$$\begin{aligned}\psi_1 &= a_1 \exp(i(\xi_1 - \omega_1)), \\ \psi_2 &= a_2 \exp(i(\xi_2 - \omega_2)),\end{aligned}\tag{6.10}$$

have been studied analytically and criteria for the stability have been obtained.

In this Section we consider the CNLSE system (2.26)-(2.27) with $\delta_1 = \delta_2 = 0$, $d_1 = d_2 = 1$, $a_1 = a_2$, i.e.,

$$\begin{aligned}i \frac{\partial \psi_1}{\partial t} + \frac{\partial^2 \psi_1}{\partial x^2} + (|\psi_1|^2 + e |\psi_2|^2) \psi_1 &= 0, \\ i \frac{\partial \psi_2}{\partial t} + \frac{\partial^2 \psi_2}{\partial x^2} + (e |\psi_1|^2 + |\psi_2|^2) \psi_2 &= 0\end{aligned}\tag{6.11}$$

with periodic plane wave solution.

Analytical solutions of the CNLSE can be obtained only for a few parameter values where the self-modulation coefficients $a_1 = a_2$ and the cross-phase modulation term e are equal, which corresponds to the integrable case studied by Manakov in [48] (see Sec. 2.2). For all other cases, where the coefficients are different, numerical studies are necessary. Recently several methods have been developed in order to understand the dynamics of plane wave solutions of the CNLSE for various combination of parameters (see [75, 81] and reference therein). Among them we mention two numerical approaches which lead to better understanding of the dynamics of the CNLSE. The first one is the Hopscotch method used in [81]. The Hopscotch method uses both an explicit and an implicit scheme in time as follows: If m and n are the spatial and temporal location in the discrete equation, then if $(m + n)$ is odd, the explicit scheme should be used; if $(m + n)$ is even, the implicit scheme should be used. The other approach is based on a combination of discretizing the CNLSE in space by

using a pseudospectral method with the fourth-order Runge-Kutta integrator in time [75]. In these papers the accuracy of the solutions were checked only using the norm conservation of each compound of the CNLSE

$$C_1(\psi_1) = \int_{-L/2}^{L/2} |\psi_1|^2 dx, \quad \text{and} \quad C_2(\psi_2) = \int_{-L/2}^{L/2} |\psi_2|^2 dx \quad (6.12)$$

where L denotes the spatial period of the solution.

In the following we will compare our numerical results obtained by the multisymplectic Preissman, six-point and the semi-explicit symplectic scheme for different cases studied in [75, 81]. For multisymplectic integrators we have plotted the local conservation of energy, momentum and additional conserved quantity in order to show how their preservation affects the accuracy of the numerical results for the periodic waves in long term. Because the additional conserved quantity is quadratic, it is preserved by the Preissman scheme up to the rounding error. The preservation of the energy and momentum over time with the error of order $\mathcal{O}(\Delta x)^4$ and $\mathcal{O}(\Delta t)^4$ can be explained using the backward error analysis in Chapter 5. The semi-explicit symplectic integrator does not preserve the conserved quantities locally, but the growth in the residual of these quantities over time is not much, so that the results obtained are comparable with those in the literature. Another useful numerical aspect of multisymplectic schemes over the non-symplectic schemes can be seen by the numerical results with initial phase shifts. Due to the excellent preservation of the dispersion relations proved in Chapter 4 the multisymplectic scheme preserve the shape of the waves overtime very well in case of initial phase shifts.

To solve the CNLSE system (6.11) numerically, we use the following initial conditions [81]:

$$\psi_1(x, 0) = a_0(1 - \varepsilon \cos \xi x), \quad \psi_2(x, 0) = b_0(1 - \varepsilon \cos \xi(x + \theta)), \quad (6.13)$$

where a_0 and b_0 are the initial amplitudes of the unperturbed periodic waves, $\varepsilon \ll 1$ is a small parameter which represents the strength of perturbation, ξ is the wave number of the perturbation, and θ is the initial phase difference between the two perturbations. In the numerical experiments we choose $\xi = 0.5$ and $\varepsilon = 0.1$. Three sets of parameters are used for the initial condition (6.13) which are listed in Table 6.1.

Table 6.1: Values of parameter for the initial condition (6.13) of the CNLS equation (6.11).

	a_0	b_0	θ
Case 1) $e = 1$ (Elliptic Polarization)			
(1a)	0.5	0.5	0
(1b)	0.5	0.5	$3\pi/2$
(1c)	0.68	0.2	$3\pi/2$
Case 2) $e = 2/3$ (Linear Polarization)			
(2a)	0.5	0.5	0
(2b)	0.5	0.5	$3\pi/2$
(2c)	0.63	0.2	0
Case 3) $e = 2$ (Circular Polarization)			
(3a)	0.5	0.5	0
(3b)	0.5	0.5	$3\pi/2$
(3c)	0.78	0.2	0

6.1.1 Numerical Simulation I: Elliptical Polarization ($e = 1$)

We consider the CNLS equation (6.11) with $e = 1$. This is the integrable case that Manakov [48] studied. The numerical solutions were computed using the perturbed initial condition (6.13). From the linear stability analysis [75], the plane wave solution (6.10) is linearly stable if the perturbation wave number ξ is greater than the critical value $\xi_c = \sqrt{2(a_0^2 + b_0^2)}$. Otherwise, it is unstable. For case (1a) (see Table 6.1) $\xi_c = 1$. The present choice of $\xi = 1/2$ implies that the plane wave is unstable. For this problem, the exact values of the conserved quantities (6.12) are $C_1(\psi_1) = 3.1573$ and $C_2(\psi_2) = 3.1573$.

Figure 6.1 provides the results for CNLS equation (6.11) with initial condition (6.13) (see Table 6.1 1a), obtained by the schemes MS, MS6 and SE for (a-d) $N = 256, \Delta t = 0.1$ and for (e-f) $N = 256, \Delta t = 0.01$. In this problem the spatial period is $2\pi/\xi$ or 4π for $\xi = 1/2$. From the Fig. 6.1 we see that, within that length there is only one single peak which we call one-hump state. The figure shows that the amplitude of ψ_1 and ψ_2 undergoes oscillations between the near-uniform state and the one-hump state as in the Hopscotch method (see [81]). This is basically a Fermi-Pasta-Ulam (FPU) recurrence phenomenon which is defined as an event from the past appears to be happening again as clearly as the first time you experienced it [11]. Fig. 6.2 shows the errors in local energy (3.51)-(3.52) and the local momentum (3.53)-(3.54) conservation law. We see that the MS scheme preserves the local energy and

momentum very well. However, the local errors for MS6 scheme is greater than the MS scheme; this is because we eliminate the auxiliary variables $p_i, i = 1, \dots, 4$ in the MS integrator. But for the local conservation (3.51)–(3.54) we need the eliminated variables $p_i, i = 1, \dots, 4$ which are approximated by first-order forward difference approximation which increases the local conservation errors. In SE scheme the local energy and momentum errors are increasing because SE is not a multisymplectic integrator. It should be pointed out that the errors are concentrated in the regions of the solutions where there are two peaks.

Fig. 6.3 shows the results for errors in additional conservation law (3.55). We notice that the multisymplectic schemes MS and MS6 shows a bounded oscillating behavior, whereas the error in SE scheme is increasing.

The errors in global energy (6.7) and global momentum (6.8) conservations are displayed in Fig. 6.4. It is worth noting that both MS and MS6 schemes preserves the global momentum very well (up to the error criterion of 10^{-9}) because it is quadratic invariant. Although the SE scheme is not a multisymplectic integrator, it preserves the global momentum very well too.

Fig. 6.5 shows that the multisymplectic six-point integrator MS6 preserves the conserved quantities (3.71) and (3.73).

Plots in Fig. 6.6 show the surfaces $|\psi_1(x, t)|$ and $|\psi_2(x, t)|$ of the waveform obtained using MS6 (3.61)–(3.62) and SE (3.99) schemes for initial data (6.13) (see Table 6.1(1b)) with a) MS6 using $N = 256, \Delta t = 0.1$ and b) SE using $N = 256, \Delta t = 0.01$, both for $T = 100$. The surface of the wave form obtained using MS integrator (3.50) is similar to the surface of MS6 (see Fig. 6.6(a)). In [81] the authors have shown that within the introduction of the phase difference $\theta = 3\pi/2$ between the initial conditions (6.13) (see Table 6.1(2a)) the evolution of ψ_1 ceases to become periodic after a few cycles in Hopscotch method. However, Fig. 6.6 shows that the periodicity of the solution is not destroyed for MS6 and SE integrators. On the other hand, the SE scheme shows small vibration with time. Thus, a phase difference may have dramatic effect on the long time integration for SE scheme. We notice that although there is no phase difference for ψ_1 , initially introducing a phase difference on ψ_2 affects the evolution of ψ_1 .

Fig. 6.7 show the results for the CNLS equation (6.11) using the initial data (6.13) for a) MS6 using $N = 256, \Delta t = 0.1$, b) SE using $N = 256, \Delta t = 0.01$. The values

Table 6.2: Elliptic polarization ($e = 1$): The absolute maximum error in the local and global conservation laws for the CNLS equation (6.11).

		LE	LM	LACL	GE	GM	GACL
MS		1.2E-05	3.7E-04	1.9E-14	5.2E-06	1.0E-08	1.9E-13
MS6	1a	3.1E-03	8.6E-03	1.6E-03	4.5E-03	2.6E-10	1.6E-12
SE		7.4E-01	1.7E-01	9.5E-01	1.3E-02	2.5E-05	1.3E-02
MS		2.3E-05	6.3E-04	2.3E-14	9.9E-06	1.4E-06	2.5E-13
MS6	1b	5.5E-03	1.3E-02	2.6E-03	8.4E-03	6.4E-07	2.1E-12
SE		5.5E-01	7.1E-01	8.8E-01	3.9E-02	1.4E-04	5.7E-02
MS		1.4E-05	3.8E-04	1.9E-14	6.1E-06	1.4E-04	2.0E-13
MS6	1c	3.0E-03	8.6E-03	1.6E-03	4.5E-03	3.6E-05	1.1E-12
SE		5.8E-01	3.2E-01	7.9E-01	2.1E-01	1.0E-02	1.7E-02

of the parameters in the initial condition (6.13) is listed in Table 6.1(1c). Here we notice that a_0 and b_0 are varied such that ξ_c is kept constant, and a phase difference $\theta = 3\pi/2$ is introduced initially. For this case, the periodic oscillation between the one-hump state and the near uniform state was again destroyed using Hopscotch method (see [81]). However, Fig.6.7 shows that in the multisymplectic integrator MS6 and in the semi-explicit integrator SE the periodicity is not destroyed. The result of MS integrator (3.50) is exactly same with MS6 (see Fig. 6.7-a).

Table 6.2 shows the absolute maximum error in the local energy (LE), momentum (LM) and additional conservation (LACL) and global energy (GE), momentum (GM) and additional conservation (GACL) for the CNLS equation (6.11) with initial data (6.13) using the MS integrator (3.50), MS6 integrator (3.61)-(3.61) and SE integrator (3.99). From the table we see that the multisymplectic schemes MS and MS6 preserves the quadratic invariants such as GM and ACL.

Table 6.3 shows the values of the conserved quantities (6.12) obtained using MS, MS6 and SE integrators for various time. The integrals (6.12) are approximated by Simpson's rule. The almost constant values of both $C_1(\psi_1)$ and $C_2(\psi_2)$ show that the schemes are working well.

6.1.2 Numerical Simulation II: Linear Polarization ($e = 2/3$)

We consider the CNLS equation (6.11) with $e = 2/3$. This is a non-integrable case. The numerical solutions were computed using the perturbed initial condition (6.13). From the linear stability analysis [75], the plane wave solution is linearly stable if the

Table 6.3: Elliptic polarization ($e = 1$): Exact and approximate values of the conserved quantities (6.12) for various time for the CNLS equation (6.11).

		(1a)		(1b)		(1c)	
		$C_1(\psi_1)$	$C_2(\psi_2)$	$C_1(\psi_1)$	$C_2(\psi_2)$	$C_1(\psi_1)$	$C_2(\psi_2)$
	Exact Values	3.1573	3.1573	3.1573	3.1573	5.8397	0.5052
	Time						
MS	25	3.1574	3.1574	3.1578	3.1578	5.8390	0.5050
	50	3.1574	3.1574	3.1574	3.1574	5.8390	0.5050
	75	3.1576	3.1576	3.1574	3.1574	5.8390	0.5050
	100	3.1588	3.1588	3.1578	3.1578	5.8390	0.5050
MS6	25	3.1574	3.1574	3.1578	3.1578	5.8390	0.5050
	50	3.1574	3.1574	3.1573	3.1573	5.8390	0.5050
	75	3.1577	3.1577	3.1575	3.1575	5.8390	0.5050
	100	3.1597	3.1597	3.1576	3.1576	5.8390	0.5050
SE	25	3.1527	3.1527	3.1574	3.1574	5.8390	0.5050
	50	3.1521	3.1521	3.1575	3.1575	5.8390	0.5050
	75	3.1524	3.1524	3.1577	3.1577	5.8390	0.5050
	100	3.1545	3.1545	3.1572	3.1572	5.8390	0.5050

perturbation wave number ξ is greater than the the critical value

$$\xi_c = \sqrt{a_0^2 + b_0^2 + \sqrt{(a_0^2 + b_0^2) - \frac{20}{9}a_0^2b_0^2}}.$$

Otherwise, it is unstable.

For $a_0 = b_0 = 0.5$ (see Table 6.1 2(a-b)), $\xi_c = 0.91$. For this choice, $\xi = 0.5$ implies that that the plane wave is unstable. The exact vales of the conserved quantities (6.12) are $C_1(\psi_1) = 3.1573$ and $C_2(\psi_2) = 3.1573$.

Fig. 6.8 shows the surfaces $|\psi_1(x, t)|$ and $|\psi_2(x, t)|$, and local energy conservation errors for CNLS equation (6.11) with initial data (6.13) (see Table 6.1 2a) obtained using a) MS6 integrator (3.61)-(3.62) for $N = 256$, $\Delta t = 0.1$ b) SE integrator (3.99) for $N = 256$, $\Delta t = 0.01$. The surface $|\psi_1(x, t)|$ of the waveform obtained using MS integrator (3.50) is same as the surface obtained using MS6 integrator (see Fig. 6.8(a)). Fig. 6.8 shows that the solution again evolves between the near-uniform state and the one-hump state as in the Hopscotch method [81]. However, comparing with the Hopscotch method, the results obtained using the MS and SE integrators shows that the number of oscillation increases. Fig. 6.8(c) shows the local energy errors. From the figure we see that although the error in MS6 scheme remains bounded, the error in SE scheme increases in time. Also we notice that errors are concentrated in the

region where there are two peaks as in the elliptic polarization case.

Fig. 6.9(a-b) shows that the initial phase difference in $\psi_2(x, 0)$ effects the evolution of $\psi_1(x, t)$ as in the case of elliptic polarization. From the figure we see that, the spatial location of peaks in $|\psi_1(x, t)|$ is affected by those in $|\psi_2(x, t)|$. We also notice that, within the introduction of a phase difference between the initial conditions, the period of oscillation decreases. To see this effect one can compare Fig. 6.8 and Fig. 6.9. On the other hand, in Hopscotch method [81], a phase difference between the perturbations has no effect on the spatial locations of peaks of ψ_1 and on the periodicity of the evolution of ψ_1 . Fig. 6.9(c) shows the local energy errors. From the figure we see the error in MS6 scheme remains bounded and the error in SE scheme increases in time again. The errors are concentrated in the region where there are two peaks as in the previous cases.

For $a_0 = 0.63$, $b_0 = 0.2$, ξ_c remains at 0.91. A change in the ratio of a_0/b_0 , or a change of the initial amplitude changes the period of oscillation again as in the Hopscotch method [81]. The larger amplitude difference between the perturbations, the shorter period of oscillation between the near-uniform state and the one-hump state will become. However, in the large scale dynamics, namely oscillation between a near-uniform state and a one-hump state, remains unchanged (see Fig. 6.10). The bottom plots in Fig. 6.10 shows the local energy errors for MS6 and SE schemes. We notice that while the local energy errors remains bounded in MS6 integrator, it grows in time in SE integrator.

Table 6.4 shows the errors in local and global conservation in linear polarization case. From the table we see that MS integrator preserves the conserved quantities better than MS6 and SE schemes.

6.1.3 Numerical Simulation III: Circular polarization ($e = 2$)

We consider the CNLS equation (6.11) with $e = 2$. In nonlinear optics, this is the circular polarization mode case. This case is also non-integrable. The interaction between perturbed periodic waves is very strong since the eave-wave interaction coefficient e is two times the dispersion coefficients $d_1 = d_2 = 1$. The numerical solutions were computed using the perturbed initial condition (6.13). From the linear stability

Table 6.4: Linear polarization ($e = 2/3$): The absolute maximum error in the local and global conservation laws for the CNLS equation (6.11)

		LE	LM	LACL	GE	GM	GACL
MS		6.0E-06	1.7E-04	1.3E-14	1.1E-06	1.3E-14	1.3E-13
MS6	2a	1.8E-03	5.6E-03	1.2E-03	2.5E-03	1.5E-14	4.1E-13
SE		1.9E-01	2.7E-02	3.1E-01	1.2E-03	4.7E-11	1.3E-03
MS		5.7E-06	1.6E-04	1.3E-14	2.2E-06	1.3E-14	1.2E-13
MS6	2b	1.6E-03	5.2E-03	1.1E-03	2.3E-03	9.5E-14	4.1E-13
SE		4.7E-01	4.4E-01	1.1E-00	1.8E-02	7.3E-11	4.0E-02
MS		5.8E-06	1.6E-04	1.2E-14	6.5E-06	3.8E-16	1.3E-13
MS6	2b	1.7E-03	5.1E-03	1.1E-03	2.3E-03	4.6E-16	3.3E-13
SE		5.4E-02	6.4E-03	8.2E-02	3.1E-04	1.2E-15	2.0E-04

analysis [75], the critical perturbation wave number is

$$\xi_c = \sqrt{a_0^2 + b_0^2} + \sqrt{(a_0^2 + b_0^2)^2 + 12a_0^2b_0^2}$$

above which the plane wave solution (6.10) is stable; otherwise, it is unstable.

For $a_0 = b_0 = 0.5$ (see Table 6.1 3(a-b)), $\xi_c = 1.23$. The present choice of $\xi = 0.5$ implies that the plane wave is unstable. For this case the exact vales of the conserved quantities (6.12) are $C_1(\psi_1) = 3.1573$ and $C_2(\psi_2) = 3.1573$.

When the initial amplitudes are equal $a_0 = b_0 = 0.5$ and there is no phase difference initially, the evolution is more complex than the elliptic and linear polarization cases. Fig. 6.11 shows the evolution of $|\psi_1(x, t)|$ of the waveform for CNLS equation (6.11) with initial data (6.13) (see Table 6.1 3a) obtained using a) MS integrator (3.50) for $N = 256$, $\Delta t = 0.1$ b) MS6 integrator (3.61)-(3.62) for $N = 256$, $\Delta t = 0.1$ c) SE integrator (3.99) for $N = 256$, $\Delta t = 0.01$. Exactly the same results are obtained for the surface $|\psi_2(x, t)|$ which are not shown here. The results obtained using MS and MS6 integrators show that one peak splits into two peaks and two peaks remerge again. This phenomena repeats itself throughout the evolution (see Fig. 6.11 a,b). The same results were obtained in the Hopscotch method. However in Fig. 6.11(c), the results obtained using SE integrator show that after a period of time the separated peaks coupled together, remain stationary and oscillating in their strength. Fig. 6.12 shows the local errors in energy conservation. From the figure we see that the errors in multisymplectic integrators MS and MS6 remains bounded and do not grow in time. However the local energy error in SE scheme increases in time and shows a chaotic behavior in long time dynamics. Also the errors are concentrated on the region where

there are peaks.

When we introduce a phase angle between the perturbations, the evolution pattern changes. There are two oscillating pulses excited from a single pulse. Initially, one pulse propagates toward the left, another propagates toward the right. After a period of time, they merge again. This pattern repeats itself with different periods (see Fig. 6.13). The results obtained using MS integrator show that they move away in opposite directions (Fig. 6.13 a). The same results were obtained in the Hopscotch method. From Fig. 6.13 we see that the local errors are concentrated throughout the propagation of the wave.

When the initial amplitudes are different and there is no initial phase difference, the dynamic changes again. Fig. 6.14 shows the results for different initial amplitudes ($a_0 = 0.78, b_0 = 0.2$) and zero phase difference. For this case the solitary wave-like pulses were observed: two pulses are coupled together and form a new bound state, remaining stationary and oscillating in their strength. Similar results were obtained for the Hopscotch method.

6.2 Soliton Solutions of CNLSE

As mentioned in the preceding section, there exist only few integrable cases of CNLSE for which analytical solutions by the inverse scattering transform exist. For all other cases extensive numerical computations are needed in order to understand the complicated wave phenomenon in the CNLSE. As the fiber technology advanced, the interest in optical solitons grows rapidly. Various soliton collision scenarios such as transmission, reflection and creation of a new soliton have been reported. If a system is integrable, solitary waves collide elastically, that is they preserve their shape after collision. However if the system is non-integrable the collision may be highly non-trivial and the collision may inelastic, that is the shapes of the solitons are changed after collision. In general the speed and height of the solitary waves are not preserved in the collision. In a non-integrable system, for some parameter values, the solitary waves reflect one another while, for different parameter values, the wave pass through each other but emerge with different speeds and amplitude. Additionally, the soliton interactions can lead to large and rapidly decaying oscillating radiative tails. Because the CNLSE is non-integrable in general, the solitary waves of an integrable and non-

integrable CNLSE are of interest by many authors (see [3, 42, 41, 71, 86, 89, 87] and reference therein).

In [42] the CNLSE (2.26)-(2.27) with $\delta_1 = -\delta_2$, $d_1 = d_2 = 1/2$, $a_1 = a_2$ and a homogenous Neumann type boundary condition was considered. Solitary wave solutions were studied numerically by introducing a finite difference method which is second order in space and time and conserves the energy of the system exactly. In [41] the CNLSE (2.26)-(2.27) with $\delta_1 = \delta_2 = 0$, $d_1 = d_2 = 1/2$, $a_1 = a_2 = 1$ was solved numerically by a finite difference method which is fourth-order in space and second order in time. It was shown that the finite difference scheme preserves the conserved quantities (2.59)-(2.60) under homogenous boundary conditions. In [3] the Ablowitz-Ladik (AL) type integrable discretization (see Sec 3.1) was applied to the CNLSE (2.26)-(2.27) with $\delta_1 = \delta_2 = 0$, $d_1 = d_2 = -1$, $a_1 = a_2 = 2$. It was notice that although the Ablowitz-Ladik discrete NLSE (3.9) is integrable, the integrability of the the AL type of the CNLSE depends on the cross-modulation term e . Further it was shown that the AL type discretization of the CNLSE results in a non-canonical Hamiltonian or Poisson structure which can be solved only by a nonlinear transformation of the variables into canonical Hamiltonian form.

However in all these works, the symplectic and multisymplectic structures of the CNLSE were not carried. Recently some authors applied symplectic and multisymplectic methods to NLSE in [72, 71]. In [71] the symplectic structure of the CNLSE (2.26)-(2.27) with $\delta_1 = \delta_2 = 0$, $d_1 = d_2 = -1$, $a_1 = a_2 = 1$ was considered with homogenous boundary conditions. Further, a symplectic six-point scheme based on the symplectic structure of the CNLSE was derived to study the collision behavior of the soliton waves of the CNLSE. We notice that the symplectic six-point scheme found in [71] is different from the six-point scheme that we have derived using the multisymplectic structure of the CNLSE. But the numerical results show that the symplectic six-point scheme is not very usefull in the solitary wave simulation of the CNLSE because local errors of the conserved quantities are averaged over the space and therefore do not reflect the local multisymplectic structure of the system in space and time. Further in [71] it was shown that the symplectic six-point scheme preserves the discrete average norm conservation (3.71) and (3.73), which are used to show the accuracy of the symplectic scheme. The solitary wave solutions of the CNLSE (2.26)-(2.27), as a multisymplectic structure, with $\delta_1 = \delta_2 = 0$, $d_1 = d_2 = 1$, $a_1 = a_2 = 1$

under periodic boundary conditions was studied numerically in [72]. The same six-point scheme was used as in [71] and it was shown that it preserves the average norms. The numerical results were reported for the collisions of the soliton with the mesh size $\Delta x = 0.2$ and the time step $\Delta t = 0.02$. Additionally, trapping, reflection, transaction, fusion of two solitons and creation of a new soliton were observed numerically. The accuracy of the multisymplectic six-point scheme was checked by monitoring only the global energy error.

We notice that in all these numerical simulations, the local energy, momentum and additional conservation properties of the CNLSE were neglected. They lacked also a backward error analysis and dispersion analysis of the multisymplectic scheme. In this work we have shown that the multisymplectic integrators based on the multisymplectic conservative PDE's give highly accurate energy and momentum conservation on the solitary wave solutions of the CNLSE. Although in [72] and [71] the mesh size and time step were chosen as $\Delta x = 0.2$ and $\Delta t = 0.02$, we have shown that the multisymplectic integrators like Preissman and six-point schemes well simulate the solitary wave solutions of the CNLSE with $\Delta x = 0.1$ and $\Delta t = 0.1$ which decreases the computation time.

In this section we investigate the performance of the proposed schemes MS and MS6 for the evolution of a single soliton. We consider the CNLS equation (2.26)-(2.27) with $\delta_1 = -\delta_2 = \delta, d_1 = d = 1/2, a_1 = a_2 = 1$, [42]; that is

$$\begin{aligned} i \left(\frac{\partial \psi_1}{\partial t} + \delta \frac{\partial \psi_1}{\partial x} \right) + \frac{1}{2} \frac{\partial^2 \psi_1}{\partial x^2} + (|\psi_1|^2 + e |\psi_2|^2) \psi_1 &= 0, \\ i \left(\frac{\partial \psi_2}{\partial t} - \delta \frac{\partial \psi_2}{\partial x} \right) + \frac{1}{2} \frac{\partial^2 \psi_2}{\partial x^2} + (e |\psi_1|^2 + |\psi_2|^2) \psi_2 &= 0. \end{aligned} \tag{6.14}$$

In general the equation (6.14) is nonintegrable [82]. However for $e = 1$, (6.14) reduces to the Manakov equation which is shown to be integrable [48]. The exact solution of (6.14) is given by [42]

$$\begin{aligned} \psi_1(x, t) &= \sqrt{\frac{2\alpha}{1+e}} \operatorname{sech}(\sqrt{2\alpha}(x-vt)) \exp i((v-\delta)x - \zeta t), \\ \psi_2(x, t) &= \pm \sqrt{\frac{2\alpha}{1+e}} \operatorname{sech}(\sqrt{2\alpha}(x-vt)) \exp i((v+\delta)x - \zeta t) \end{aligned} \tag{6.15}$$

where α and v are real constants and $\zeta = (v^2 - \delta^2)/2 - \alpha$.

Table 6.5: Various values for the conserved quantities (6.12) for the CNLS equation (6.14) with initial data (6.16) with $\alpha = 0.5, v = 1.0, e = 2/3, \delta = 0.5$ over the spatial interval $[-40, 40]$ and time interval $[0, 40]$ using MS and MS6 integrators with $N = 400, \Delta t = 0.1$.

	MS		MS6	
Time	$C_1(\psi_1)$	$C_2(\psi_2)$	$C_1(\psi_1)$	$C_2(\psi_2)$
10	1.6957	1.6936	1.6954	1.6932
20	1.6962	1.6949	1.6961	1.6945
30	1.6958	1.6940	1.6954	1.6939
40	1.6962	1.6944	1.6959	1.6939
Exact	1.6971	1.6971	1.6971	1.6971

6.2.1 Numerical Simulation I: Evolution of Single Soliton

We solve the CNLS equation (6.14) with the initial condition [42]

$$\begin{aligned}\psi_1(x, 0) &= \sqrt{\frac{2\alpha}{1+e}} \operatorname{sech}(\sqrt{2\alpha}x) \exp i((v-\delta)x), \\ \psi_2(x, 0) &= \sqrt{\frac{2\alpha}{1+e}} \operatorname{sech}(\sqrt{2\alpha}x) \exp i((v+\delta)x).\end{aligned}\tag{6.16}$$

In our experiment we choose $e = 2/3$ which is a nonintegrable case. We present here the result of an integration with

$$\alpha = 0.5, v = 1.0, \delta = 0.5, -40 \leq x \leq 40, 0 \leq t \leq 40.$$

We divide the spatial length into $N = 400$ subintervals. We choose the temporal step size as $\Delta t = 0.1$. The spatial domain have been chosen large enough so that the boundaries do not affect the solitary wave propagation. For these parameters, the exact values of the conserved quantities (6.12) are $C_1 = 1.6971$ and $C_2 = 1.6971$. Simpson's rule is used for the integrals (6.12) in the numerical integrations and the results are shown in Table. 6.5. The nearly constant values shows that the integrals in (6.12) are conserved through the integration. This shows that the schemes are working well. We also study the accuracy of the schemes MS, MS6 and SE by calculating the infinity norm

$$L_\infty = \max_{1 < m < N} \{ | \|\psi_1^e(x_m, t_n)\| - \|\psi_1^a(x_m, t_n)\| | \}\tag{6.17}$$

where $\psi_1^e(x_m, t_n)$ is the exact value obtained from (6.15) and $\psi_1^a(x_m, t_n)$ is the approximate values obtained from difference schemes MS at the point (x_m, t_n) . Table 6.6 shows the accuracy of the MS integrator using L_∞ error norm (6.17) for the CNLS

Table 6.6: Accuracy of the MS integrator using L_∞ error norm 6.17 for the CNLS equation (6.14) with initial data (6.16) with $\alpha = 0.5, v = 1.0, e = 2/3, \delta = 0.5$ over the spatial interval $[-40, 40]$ and time interval $[0, 40]$ using MS integrator with $N = 400, \Delta t = 0.1$.

Time	L_∞
10	0.2033
20	0.3929
25	0.4669
30	0.5396
35	0.6132
40	0.6832

equation (6.14) with initial data (6.16) with $\alpha = 0.5, v = 1.0, e = 2/3, \delta = 0.5$ over the spatial interval $[-40, 40]$ and time interval $[0, 40]$ using MS integrator with $N = 400, \Delta t = 0.1$.

Fig. 6.15 shows the wave forms for CNLS equation (6.14) with initial condition (6.16) obtained using (a) MS integrator (b) MS6 integrator with $N = 400, \Delta t = 0.1$. From the figure, we can see that the evolution of the soliton is well simulated by MS and MS6 integrators. Fig. 6.15 shows solitary wave has quasiperiodic structure. Fig. 6.16 provides the results obtained using MS6 integrator. From the figure we see that the single soliton is moving to the right with velocity $v = 1$ at $t = 0, 10, 15, \dots, 40$. The same result is reported in [42].

Fig. 6.17 shows the local and global conservations of the energy and momentum for MS and MS6 integrators. We notice that the schemes MS and MS6 well preserve the local and global conservations. In local conservations we note that the error occur mainly when the soliton travels into the spatial domain $[-40, 40]$.

6.2.2 Numerical Simulation II : Evolution of Colliding Soliton

In this section, we solve the CNLS equation (6.14) with the initial condition [42]

$$\begin{aligned}\psi_1(x, 0) &= \sum_{j=1}^2 \sqrt{\frac{2\alpha_j}{1+e}} \operatorname{sech}(\sqrt{2\alpha_j}x_j) \exp i((v_j - \delta)x_j) \\ \psi_2(x, 0) &= \sum_{j=1}^2 \sqrt{\frac{2\alpha_j}{1+e}} \operatorname{sech}(\sqrt{2\alpha_j}x_j) \exp i((v_j + \delta)x_j),\end{aligned}\tag{6.18}$$

where

$$\alpha_1 = 1, \alpha_2 = 0.5, v_1 = 1.0, v_2 = 0.1, x_1 = x + 20, x_2 = x - 5.$$

Table 6.7: Various values for the conserved quantities (6.12) for the CNLS equation (6.14) with initial data (6.18) with $e = 2/3$ over the spatial interval $[-40, 40]$ and time interval $[0, 40]$ using MS and MS6 integrators with $N = 400$, $\Delta t = 0.1$.

Time	MS		MS6	
	$C_1(\psi_1)$	$C_2(\psi_2)$	$C_1(\psi_1)$	$C_2(\psi_2)$
10	2.8956	2.8933	2.8952	2.8930
20	2.8965	2.8947	2.8962	2.8942
30	2.8978	2.8947	2.8998	2.8867
40	2.8996	2.8956	2.8995	2.8824
Exact	2.8971	2.8971	2.8971	2.8971

These equations corresponds to two solitary waves, one initially located at $x = -20$ and moving to the right with velocity v_1 , and the second initially located at $x = 5$ moving to the right with velocity v_2 [42]. We solve the problem using the proposed schemes MS and MS6 for the spatial interval $-40 \leq x \leq 40$ using $N = 400$ spatial mesh points for times up to $t = 40$ using the time step $\Delta t = 0.1$.

In our first experiment we choose $e = 1$ which is an integrable case.

Fig. 6.18 shows the wave forms obtained using the MS and MS6 integrators. From the figure we can see that the schemes well simulates the evolution of the waves. Fig. 6.19 shows the evolution of the waves $\psi_1(x, t)$ and $\psi_2(x, t)$ at time $t = 0, 10, 15, \dots, 40$. From the figure we notice that the taller (faster) wave catches up and with the shorter (slower) wave, then it collides with the shorter wave and leaves it behind. From the figure we notice that the interaction is elastic that the two solitons left the interaction region without any disturbances in their identities. Two waves emerge without any changes in their shapes and they conserve the energy almost exactly. This phenomenon shows that there is no energy exchange during the collusion. Fig. 6.20 represents the local and global energy and momentum conservation. In the local conservations of energy and momentum, we note that the error mainly occur through the faster soliton evolution. From both local and global conservation, we can see that the error increases when the interaction takes place. Fig.6.21 shows the contour plots of the waves $\psi_1(x, t)$ and $\psi_2(x, t)$. From these figures, we can see that after the collision there is a small changes in the direction; that is collision causes a small phase shift in solitons.

In our second experiment we choose $e = 2/3$ which is a non-integrable case.

Fig. 6.22 shows the wave forms obtained using the MS and MS6 integrators. From

the figure we can see that the schemes simulate the evolution of the waves as good as the integrable case $e = 1$. Fig. 6.23 shows the evolution of the waves $\psi_1(x, t)$ and $\psi_2(x, t)$ at time $t = 0, 10, 15, \dots, 40$. From the figure we notice that the taller (faster) wave catches up and with the shorter (slower) wave, then it collides with the shorter wave and leaves it behind. From the figure we notice that the colliding waves undergo an inelastic collision in case $e = 1$, that is, the two waves change their original shapes after collision. The taller one becomes more taller and the shorter one becomes more shorter. This phenomenon shows that there is an energy exchange during the collision. Fig. 6.24 represents the local and global energy and additional conservation. From the figure we notice that the error occurs mainly through the faster soliton evolution again. From both local and global conservation, we can see that the error increases when the interaction takes place. Fig.6.25 shows the contour plots of the waves $\psi_1(x, t)$ and $\psi_2(x, t)$. From these figures, we can see that after the collision there is a small changes in the direction; that is, the collision causes a small phase shift in solitons.

6.3 CONCLUSION and FUTURE WORK

The coupled nonlinear Schrödinger equation CNLSE plays an important role in nonlinear optics, in transmission of information over long distances, in geophysics and so on. Because of its technical importance and symplectic nature it has attracted the interest of many researchers in the last thirty years. There exists only for few parameter integrable cases of the CNLSE for which analytical solutions are available. For a wide range of physically interesting cases one has to find accurate numerical solutions in order to understand the dynamics of the underlying nonlinear wave phenomena. Several discretization schemes have been applied for solving the CNLSE; like as a discrete integrable system, semi-discretized Hamiltonian ODE's obtained either by finite difference or pseudospectral approximations.

Throughout this thesis we have applied, using the multisymplectic structure of the CNLSE, the multisymplectic integrators Preissman and six-point schemes. In particular we have considered several local conservation laws such as energy, momentum, additional conserved quantity due to the symmetry and averaged norm associated with the multisymplectic structure of the CNLSE and analyzed the behavior of the

multisymplectic integrators with respect to these conservation laws. It was shown that the Preissman and six-point schemes preserve the discrete multisymplectic quadratic conservation laws like momentum and averaged norm exactly. Higher order polynomial conserved quantities like energy are preserved in long term integration with a small error. Because both schemes are fully implicit and expensive, a new semi-explicit method was derived based on symplectic discretization in space, combined with linear-nonlinear, even-odd splitting in time using the Hamiltonian formulation of CNLSE.

For linearized CNLSE, numerical dispersion relations were derived. The non-dissipative character of multisymplectic schemes makes them very attractive for preservation of the shape of the periodic waves and soliton of solution of the CNLSE during the computation. Also, the six-point scheme for the linearized CNLSE was shown to be unconditionally linearly stable. Because the discrete form of the conserved quantities are preserved exactly by the multisymplectic schemes only for linear systems, we have shown the almost preservation of the conserved quantities for the CNLSE using the concept of the backward stability analysis. The backward stability analysis of the multisymplectic schemes are done by deriving the modified equations simultaneously in space and time variables for the discretized equations and conservation laws. It turned out that the modified equations are correct to higher order in space and time variables than the original ones.

All three numerical methods are applied to the CNLSE with plane wave and soliton solutions for various combinations of parameters under periodic boundary conditions. In the current literature mostly the preservation of the norms of each of the solution components are given as a measure of the accuracy of the solutions. Numerical results show that for certain parameter ranges the Fermi-Pasta-Ulam recurrence occurs for the unperturbed destabilized periodic solutions of the CNLSE as for the single NLSE. This suggests that the CNLSE has a kind of solutions that the waves ψ_1 and ψ_2 are in proportion while for other ranges of parameters, solitary wave-like pulses are excited. We have examined the effect of the initial phase differences on the long-time evolution of the underlying physical systems. We have focused on the context of wave propagation along a birefringent optical fiber. In the case of elliptical and linear polarization, a phase difference does not have a significant influence on the long-time evolution. On the other hand, in the circular polarized mode, a phase difference results

in complex dynamics.

The numerical results obtained show that the distribution of the errors in the local conserved quantities over the space and time domains is in a very good agreement with the behavior of the wave solutions. They confirm the theoretical results predicted by the backward error and linear dispersion analysis. The Preissman and the six-point schemes preserve the shape of the waves and solitons and the results are superior to those in the literature obtained by non-symplectic methods by using larger mesh sizes in space and time steps. The semi-explicit method gives good results for a small time step for the plane wave solutions but it fails in case of soliton collisions. However a modified soliton can be obtained to represent a better numerical solution in both space and time.

It turns out that the multisymplectic integrators like Preissman and six-point schemes are very robust methods for the integration of the CNLSE and can be used further to investigate the complicated nonlinear phenomena like collisions of waves, solitons etc. in the CNLSE for different values of parameters.

Although there are lots of numerical studies for single PDE's, there is few structure preserving numerical studies for coupled PDE's. The work done here can be applied to other coupled PDE's like the N-coupled NLSE.

VITA

Ayhan Aydın was born in Ankara, on March 20, 1972. He was graduated from Ankara Atatürk Lisesi in 1989 and received his B.S. degree in Faculty of Arts and Sciences, Department of Mathematics from Middle East Technical University (METU), in 1995. He received his M.Sc. degree in the same department, with a thesis entitled "Poisson Integrators for Completely Integrable Hamiltonian Systems" in 1998. He worked at the Department of Mathematics, Faculty of Arts and Sciences, Kırıkkale University as an instructor between 1996 and 2001. He has been an instructor at the Department of Mathematics, Faculty of Arts and Sciences, Atılım University since 2001. His main areas of interest are structure preserving numerical methods for differential equations. He has an oral presentation and accepted paper at XVI. National Mathematics Congress entitled with "Multisymplectic Structure of coupled nonlinear Schrödinger equation and Preissman scheme".

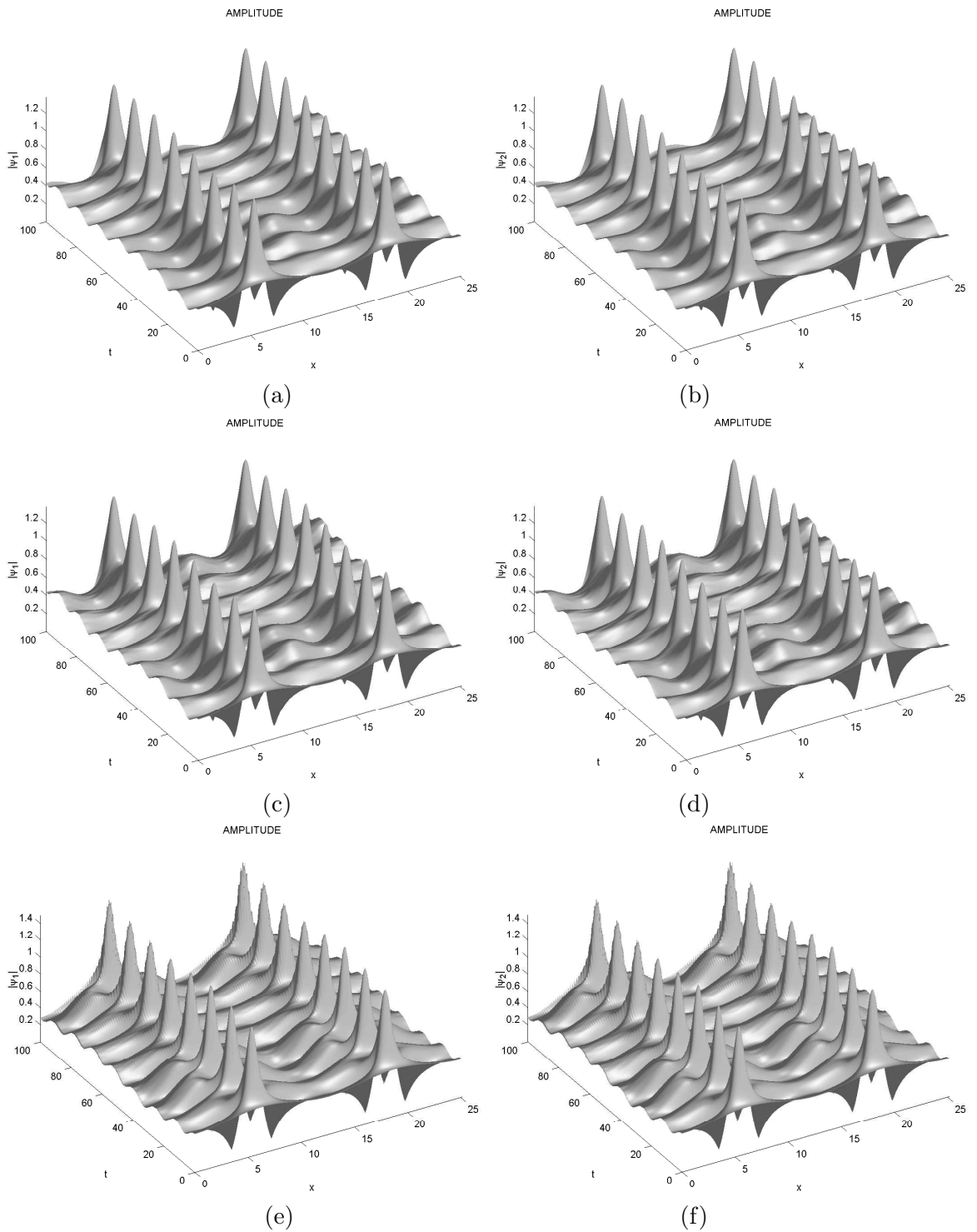


Figure 6.1: Long-time evolution of the destabilized wave solutions for CNLSE with $e = 1$, $a_0 = 0.5$, $b_0 = 0.5$, $\varepsilon = 0.1$, $\theta = 0$, $N = 256$, $T = 100$. Left plots : surface of $|\psi_1|$. Right plots : surface of $|\psi_2|$. (a-b) The multisymplectic scheme MS (c-d) the multisymplectic six point scheme MS6 (e-f) the semi-explicit scheme SE

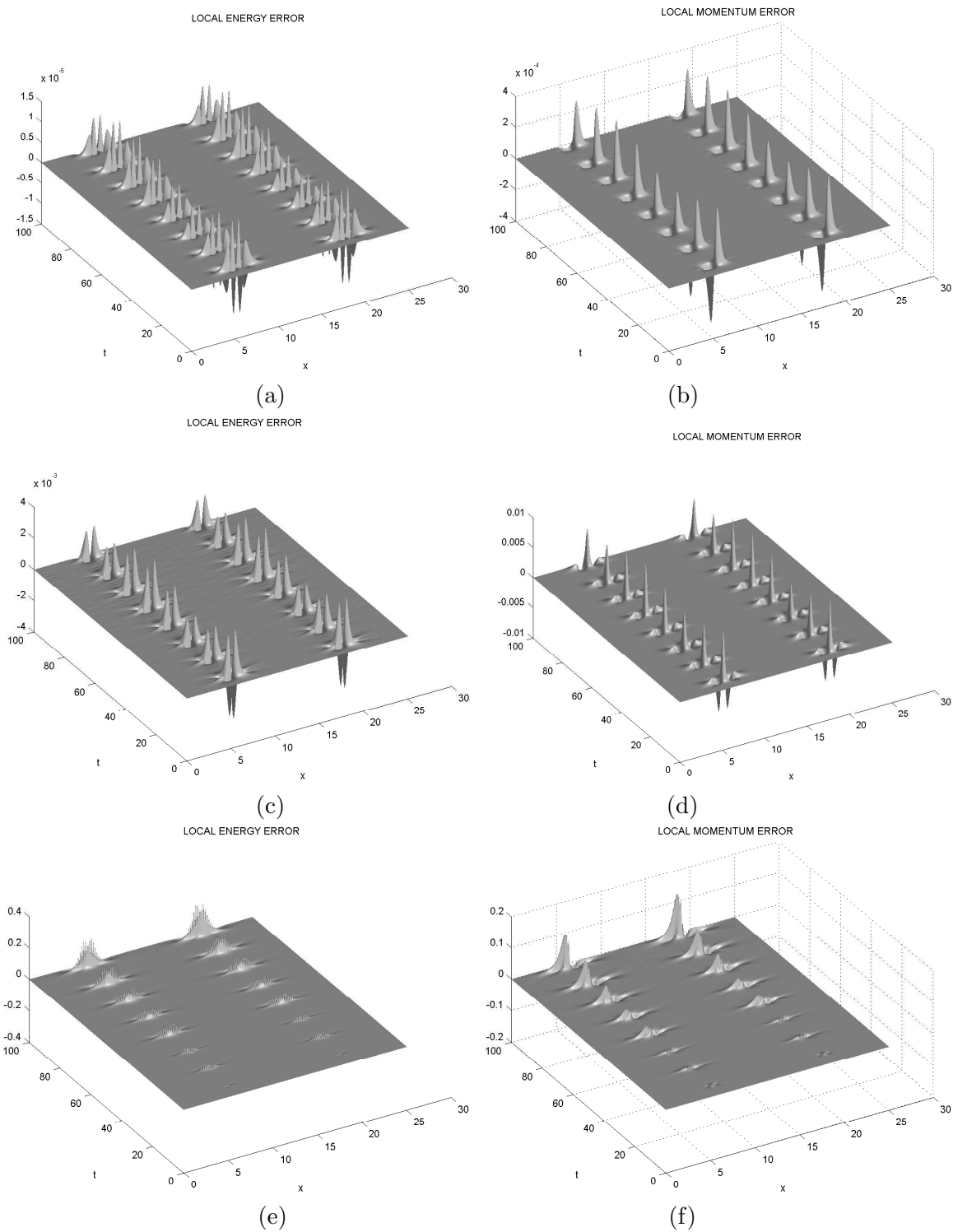
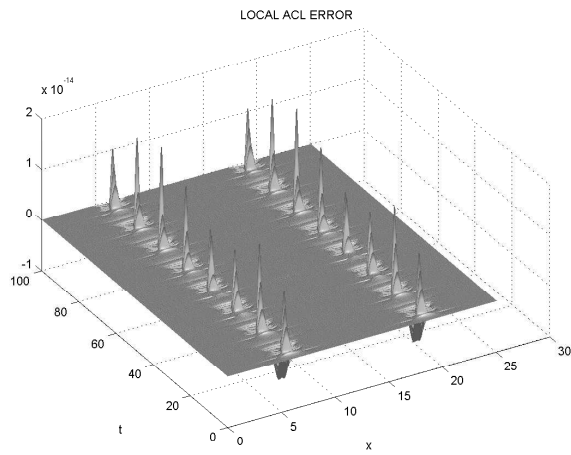
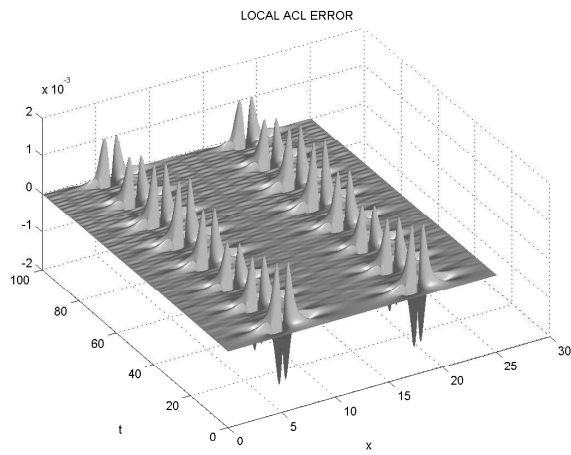


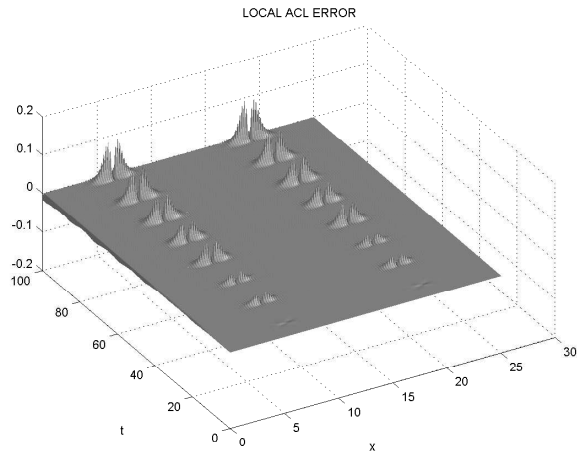
Figure 6.2: Errors in local energy and momentum conservation laws of the destabilized wave solutions for CNLSE with $e = 1$, $a_0 = 0.5$, $b_0 = 0.5$, $\varepsilon = 0.1$, $\theta = 0$, $N = 256$, $T = 100$. Left plots : error in local energy. Right plots : error in local momentum. (a-b) The multisymplectic scheme MS (c-d) the multisymplectic six point scheme MS6 (e-f) the semi-explicit scheme SE



(a)



(b)



(c)

Figure 6.3: Errors in local additional conservation laws of the destabilized wave solutions for CNLSE with $e = 1$, $a_0 = 0.5$, $b_0 = 0.5$, $\varepsilon = 0.1$, $\theta = 0$, $N = 256$, $T = 100$. Left plots : error in local energy. Right plots : error in local momentum. (a-b) The multisymplectic scheme MS (c-d) the multisymplectic six point scheme MS6 (e-f) the semi-explicit scheme SE

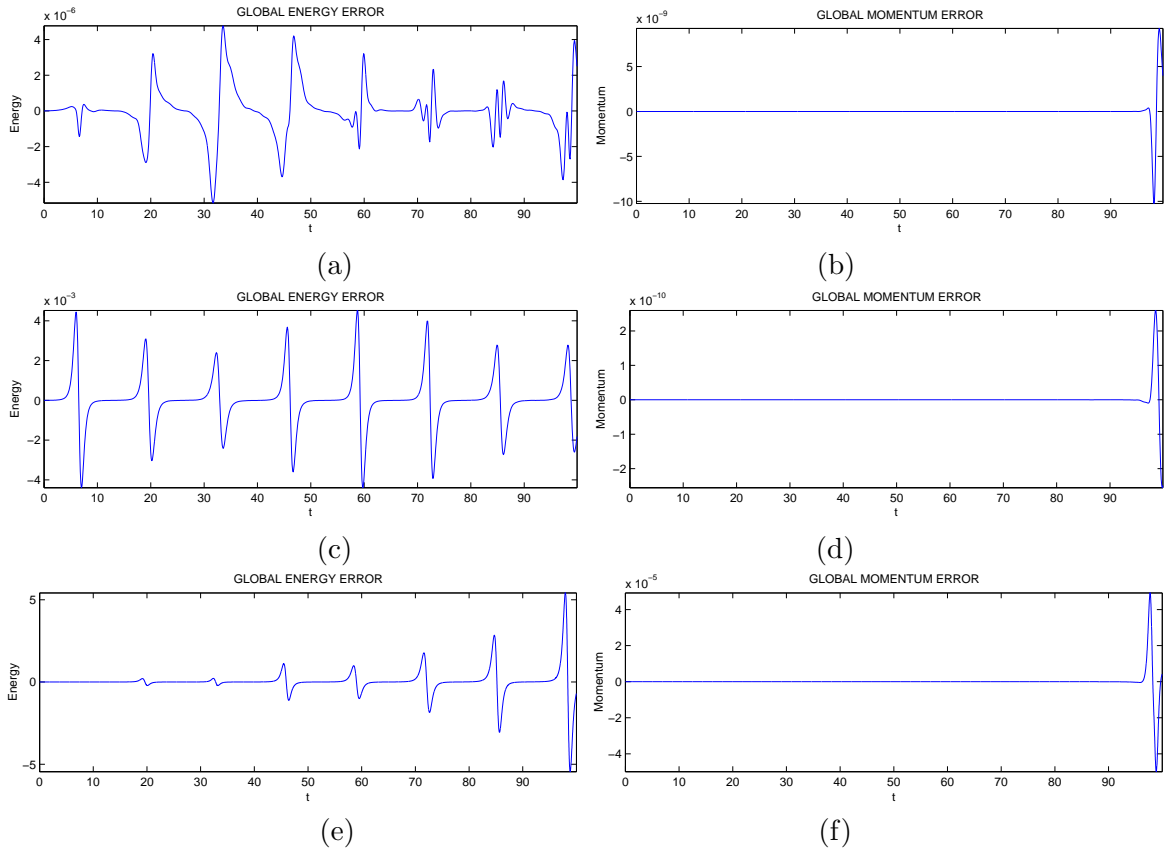
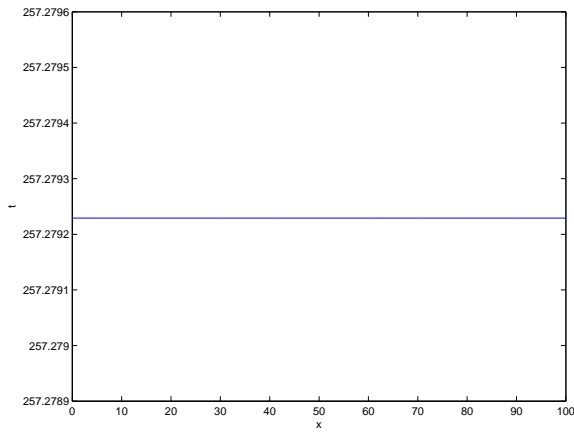
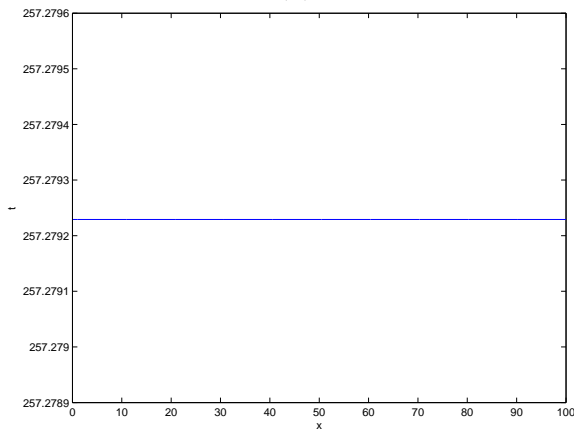


Figure 6.4: Errors in global energy and momentum conservation laws of the destabilized wave solutions for CNLSE with $e = 1$, $a_0 = 0.5$, $b_0 = 0.5$, $\varepsilon = 0.1$, $\theta = 0$, $N = 256$, $T = 100$. Left plots : error in local energy. Right plots: error in local momentum. (a-b) The multisymplectic scheme MS (c-d) the multisymplectic six point scheme MS6 (e-f) the semi-explicit scheme SE



(a)



(b)

Figure 6.5: Conservation property of the MS6 scheme for the destabilized wave solutions of the CNLSE with $e = 1$, $a_0 = 0.5$, $b_0 = 0.5$, $\varepsilon = 0.1$, $\theta = 0$, $N = 256$, $T = 100$. (a) The conserved quantity (3.71) (b) The conserved quantity (3.73)

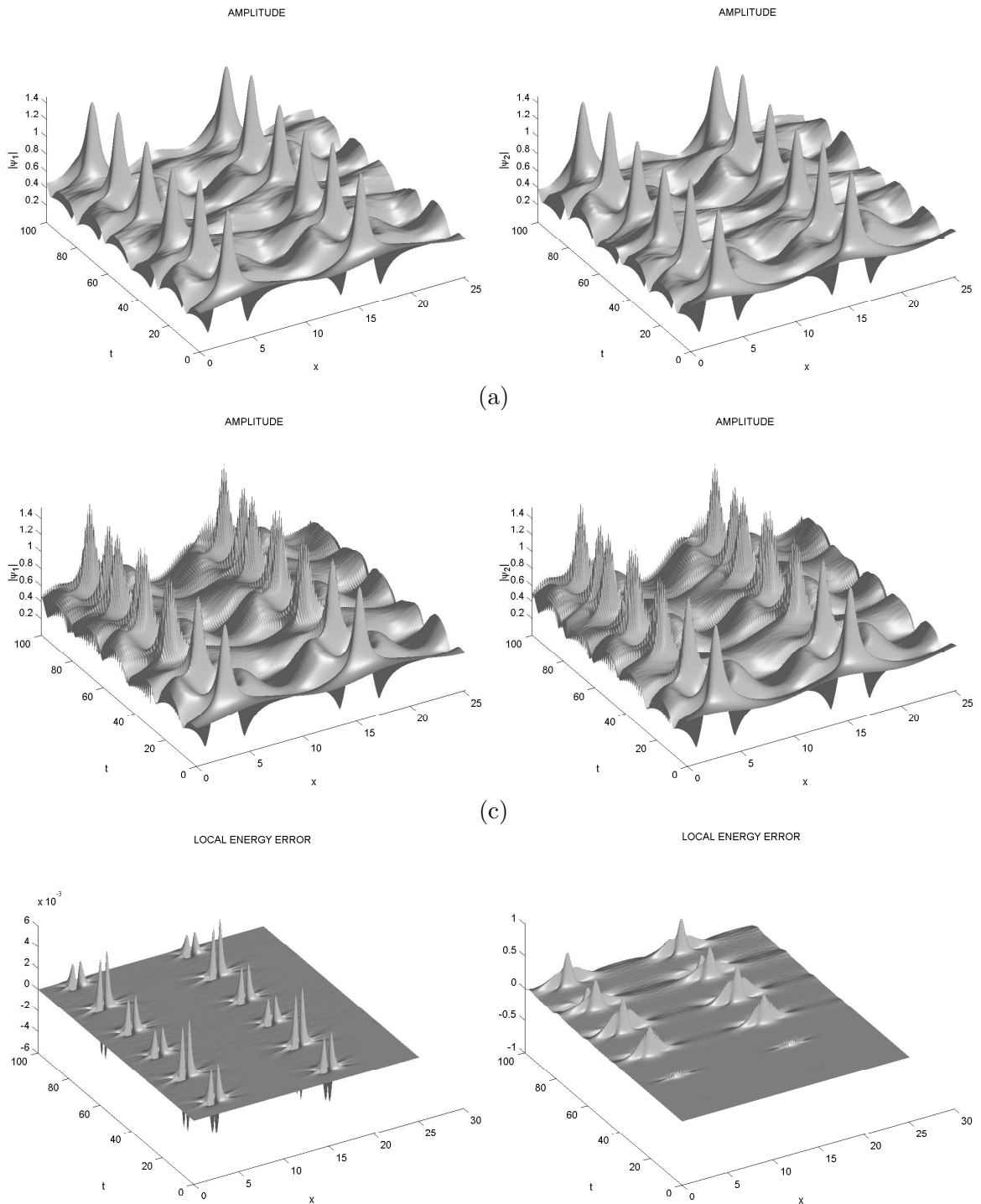


Figure 6.6: Long-time evolution of the destabilized wave solutions for CNLSE with $e = 1$, $a_0 = 0.5$, $b_0 = 0.5$, $\varepsilon = 0.1$, $\theta = 3\pi/2$, $N = 256$, $T = 100$. Surfaces of $|\psi_1|$ and $|\psi_2|$. (a) The multisymplectic scheme MS6 (b) the semi-explicit scheme SE (c) Local energy errors; left plot: MS6, right plot: SE

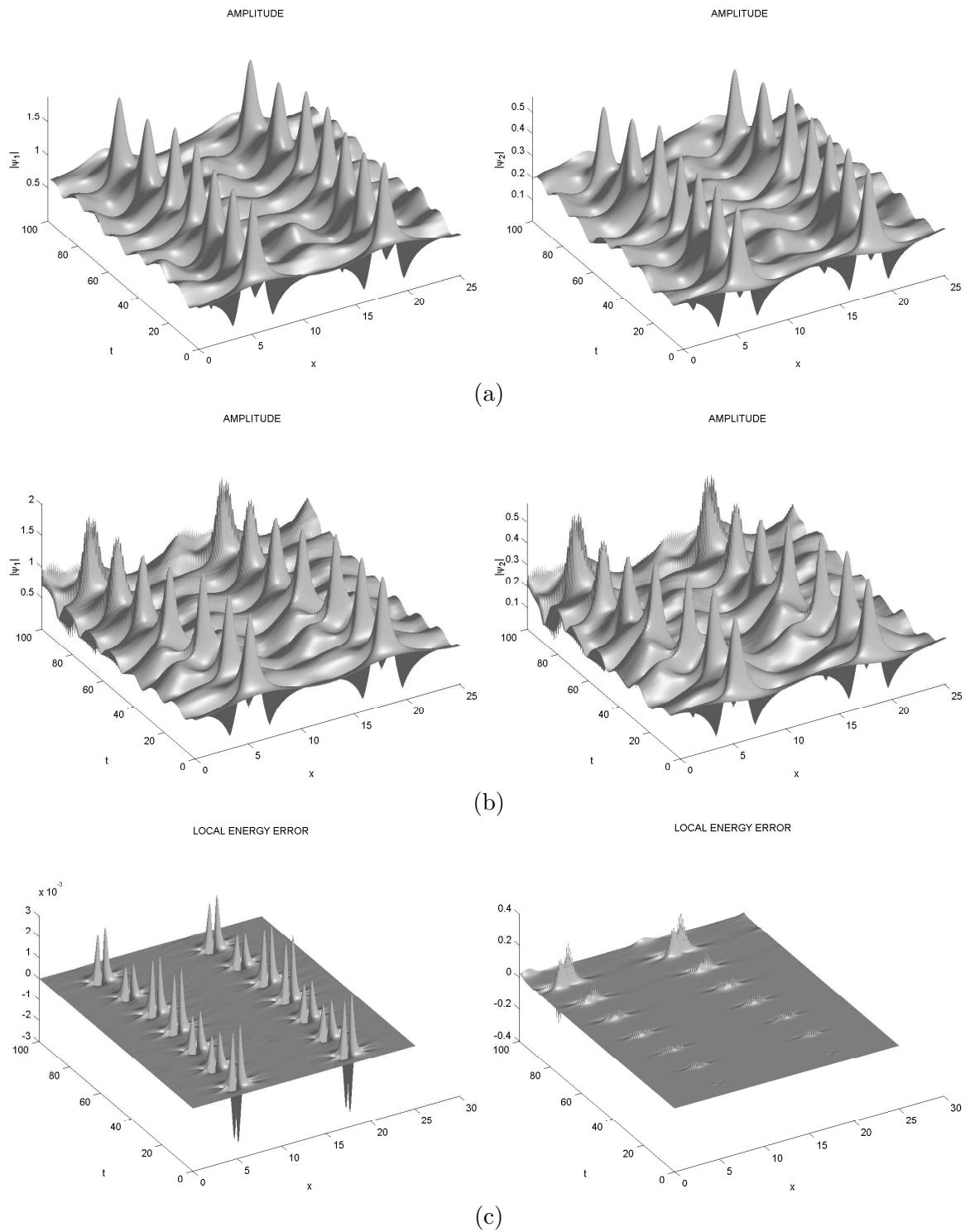


Figure 6.7: Long-time evolution of the destabilized wave solutions for CNLSE with $e = 1$, $a_0 = 0.68$, $b_0 = 0.2$, $\varepsilon = 0.1$, $\theta = 3\pi/2$, $N = 256$, $T = 100$. Surfaces of $|\psi_1|$ and $|\psi_2|$. (a) The multisymplectic scheme MS6 (b) the semi-explicit scheme SE (c) Local energy errors; left plot: MS6, right plot: SE

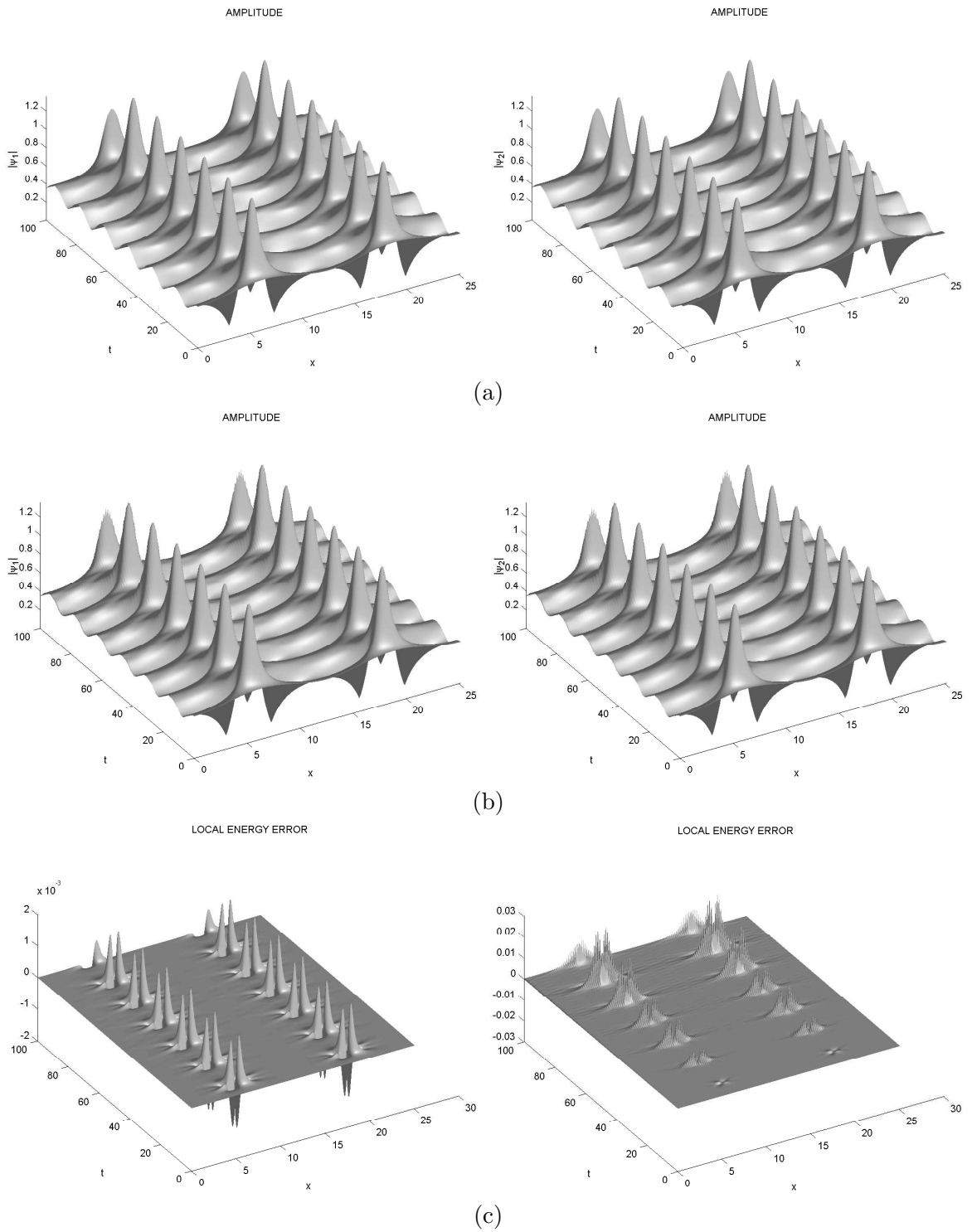


Figure 6.8: Long-time evolution of the destabilized wave solutions for CNLSE with $e = 2/3$, $a_0 = 0.5$, $b_0 = 0.5$, $\varepsilon = 0.1$, $\theta = 0$, $N = 256$, $T = 100$. Surfaces of $|\psi_1|$ and $|\psi_2|$: (a) The multisymplectic scheme MS6 (b) the semi-explicit scheme SE (c) Local energy errors; left plot: MS6; right plot :SE

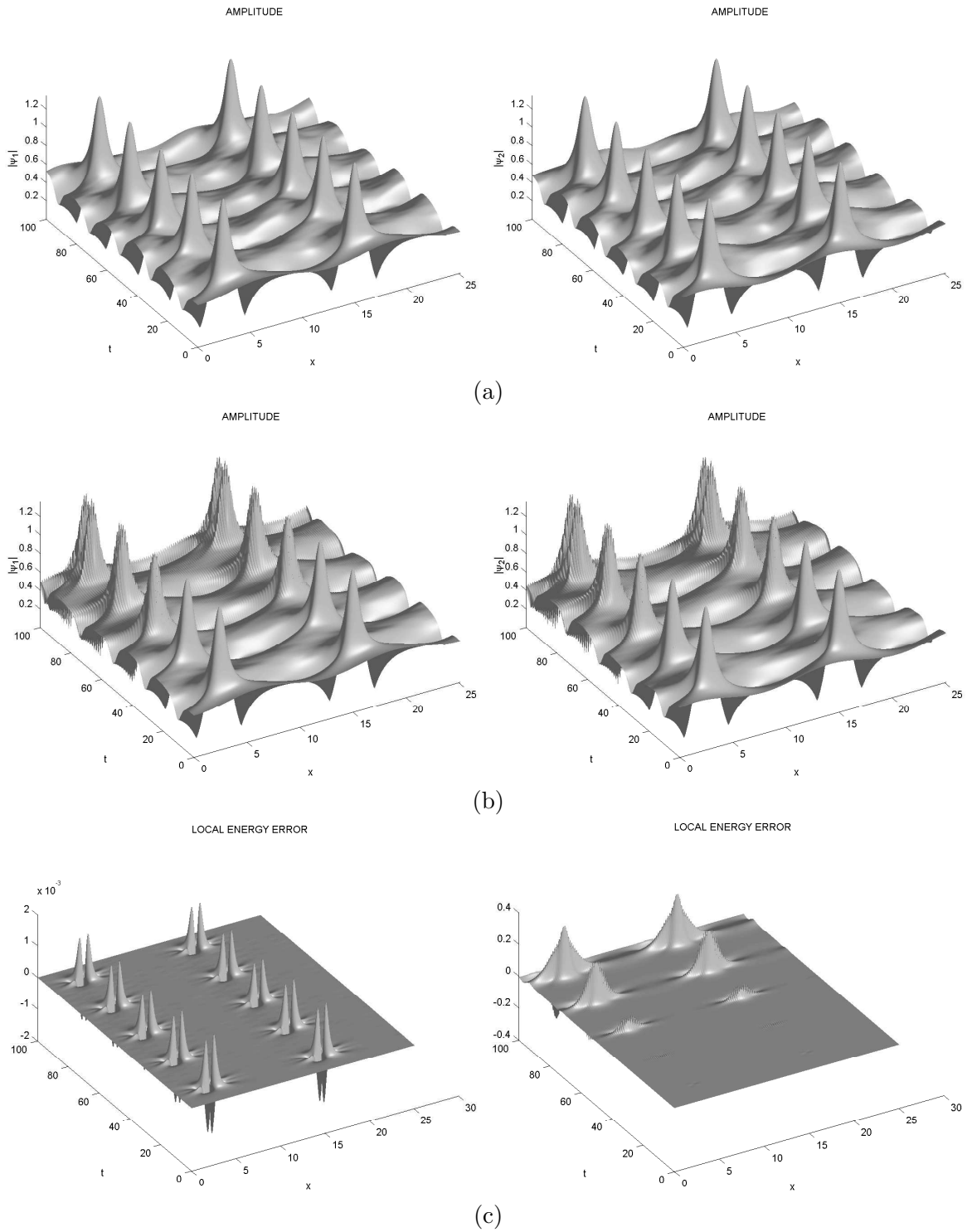


Figure 6.9: Long-time evolution of the destabilized wave solutions for CNLSE with $e = 2/3$, $a_0 = 0.5$, $b_0 = 0.5$, $\varepsilon = 0.1$, $\theta = 3\pi/2$, $N = 256$, $T = 100$. Surfaces of $|\psi_1|$ and $|\psi_2|$: (a) The multisymplectic scheme MS6 (b) the semi-explicit scheme SE (c) Local energy errors; left plot: MS6; right plot :SE

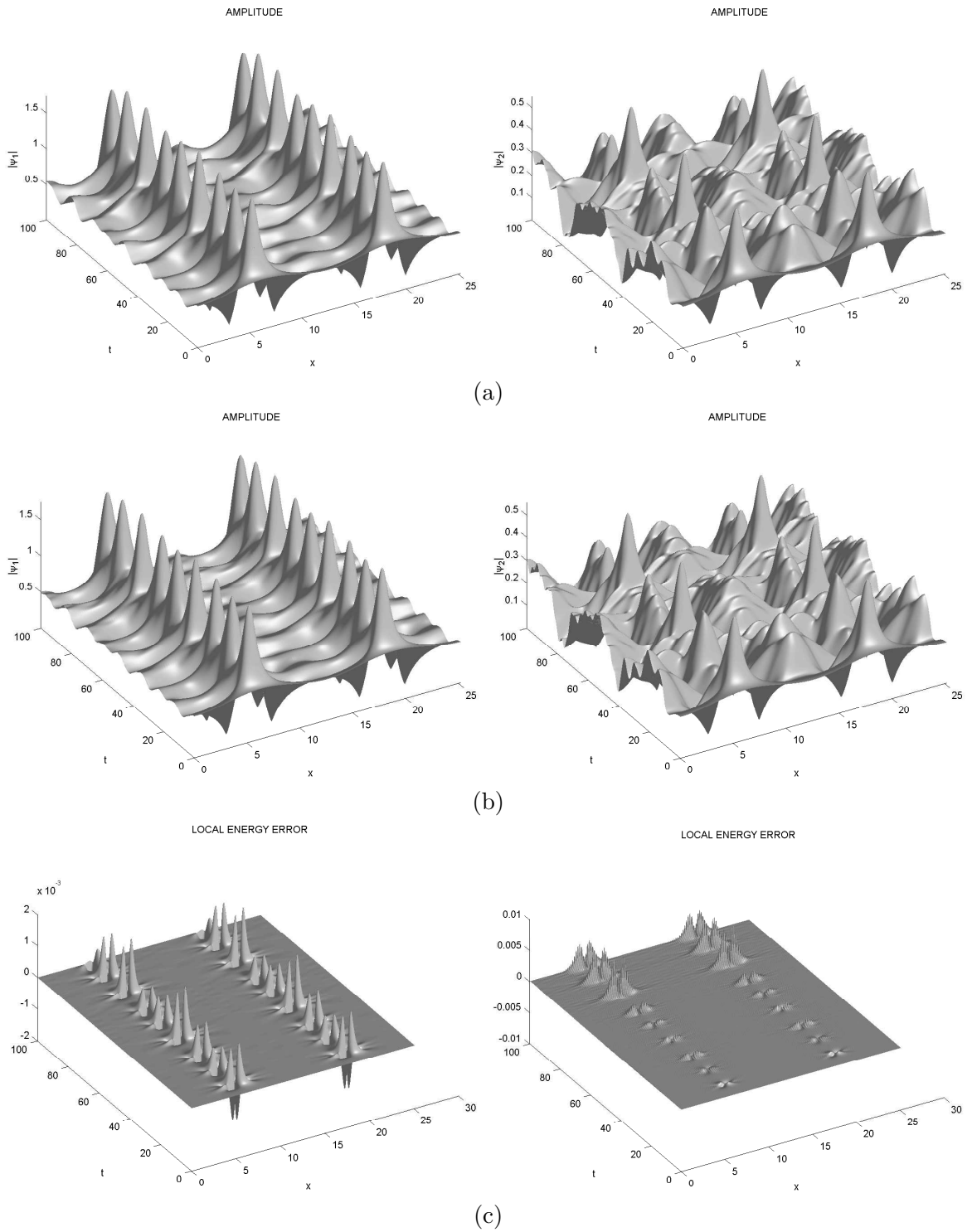


Figure 6.10: Long-time evolution of the destabilized wave solutions for CNLSE with $e = 2/3$, $a_0 = 0.63$, $b_0 = 0.2$, $\varepsilon = 0.1$, $\theta = 0$, $N = 256$, $T = 100$. Surfaces of $|\psi_1|$ and $|\psi_2|$: (a) The multisymplectic scheme MS6 (b) the semi-explicit scheme SE (c) Local energy errors; left plot: MS6; right plot :SE

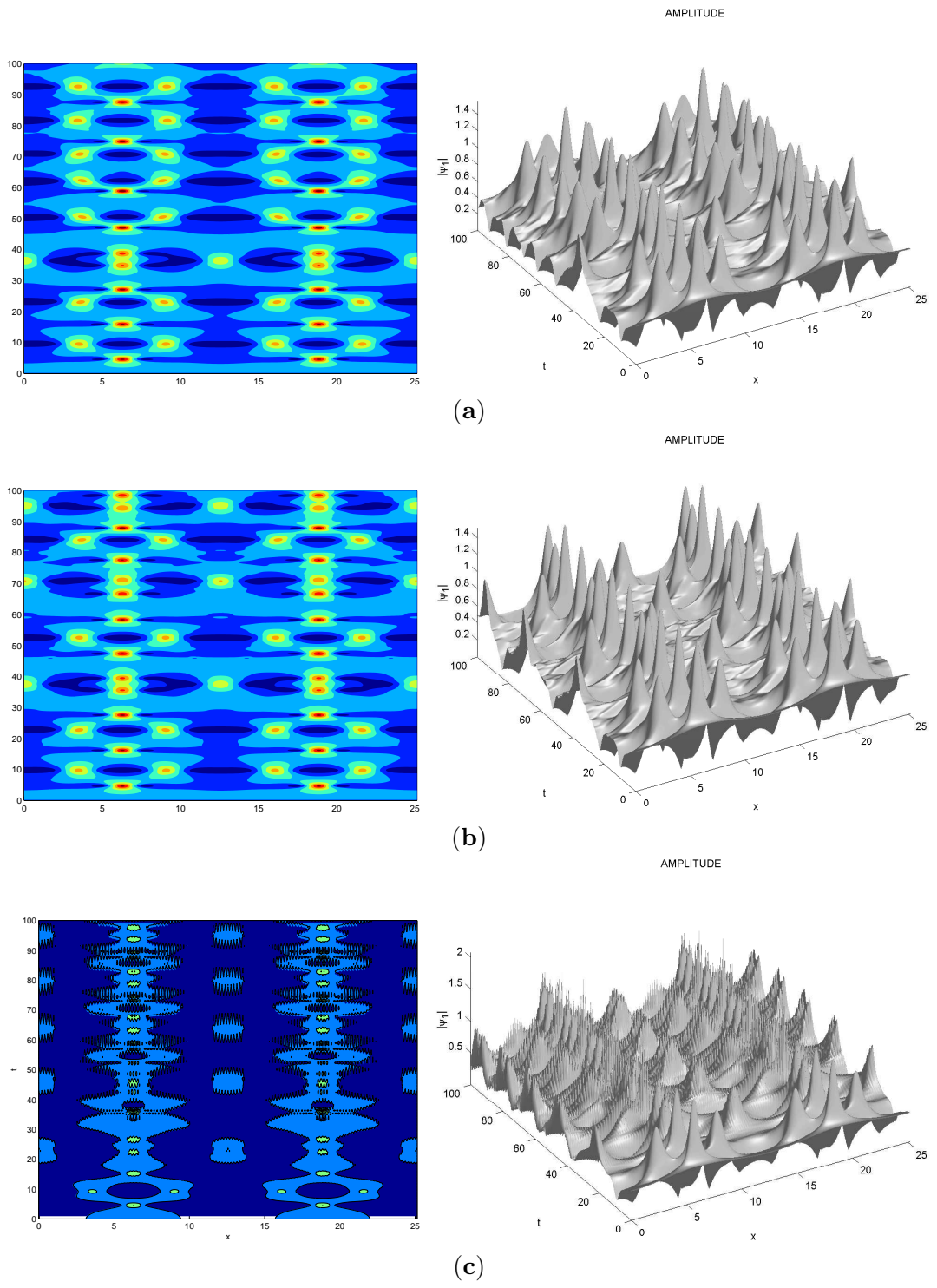
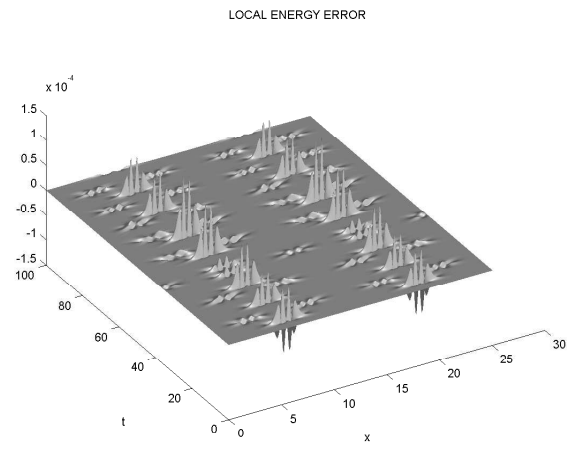
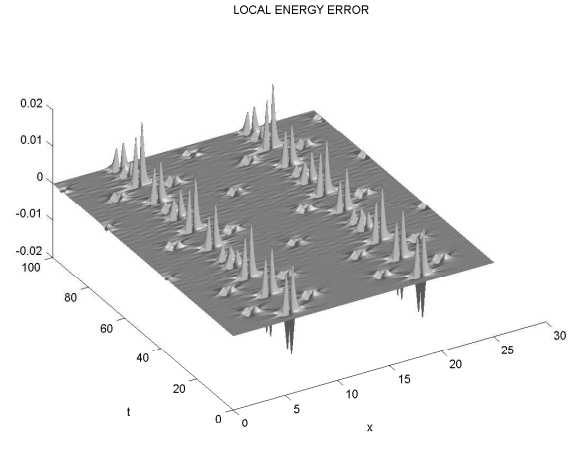


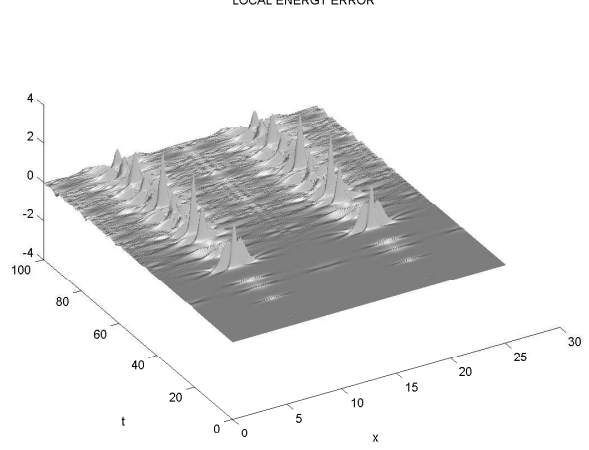
Figure 6.11: Long-time evolution of the destabilized wave solutions for CNLSE with $e = 2$, $a_0 = 0.5$, $b_0 = 0.5$, $\varepsilon = 0.1$, $\theta = 0$, $N = 256$, $T = 100$. Left plots : Contour plot of $|\psi_1|$. Right plots : surface of $|\psi_1|$. (a) The multisymplectic scheme MS (b) the multisymplectic six point scheme MS6 (c) the semi-explicit scheme SE



(a)



(b)



(c)

Figure 6.12: Errors in local energy conservation laws of the destabilized wave solutions for CNLSE with $e = 2$, $a_0 = 0.5$, $b_0 = 0.5$, $\varepsilon = 0.1$, $\theta = 0$, $N = 256$, $T = 100$. (a) The multisymplectic scheme MS (b) the multisymplectic six point scheme MS6 (c) the semi-explicit scheme SE

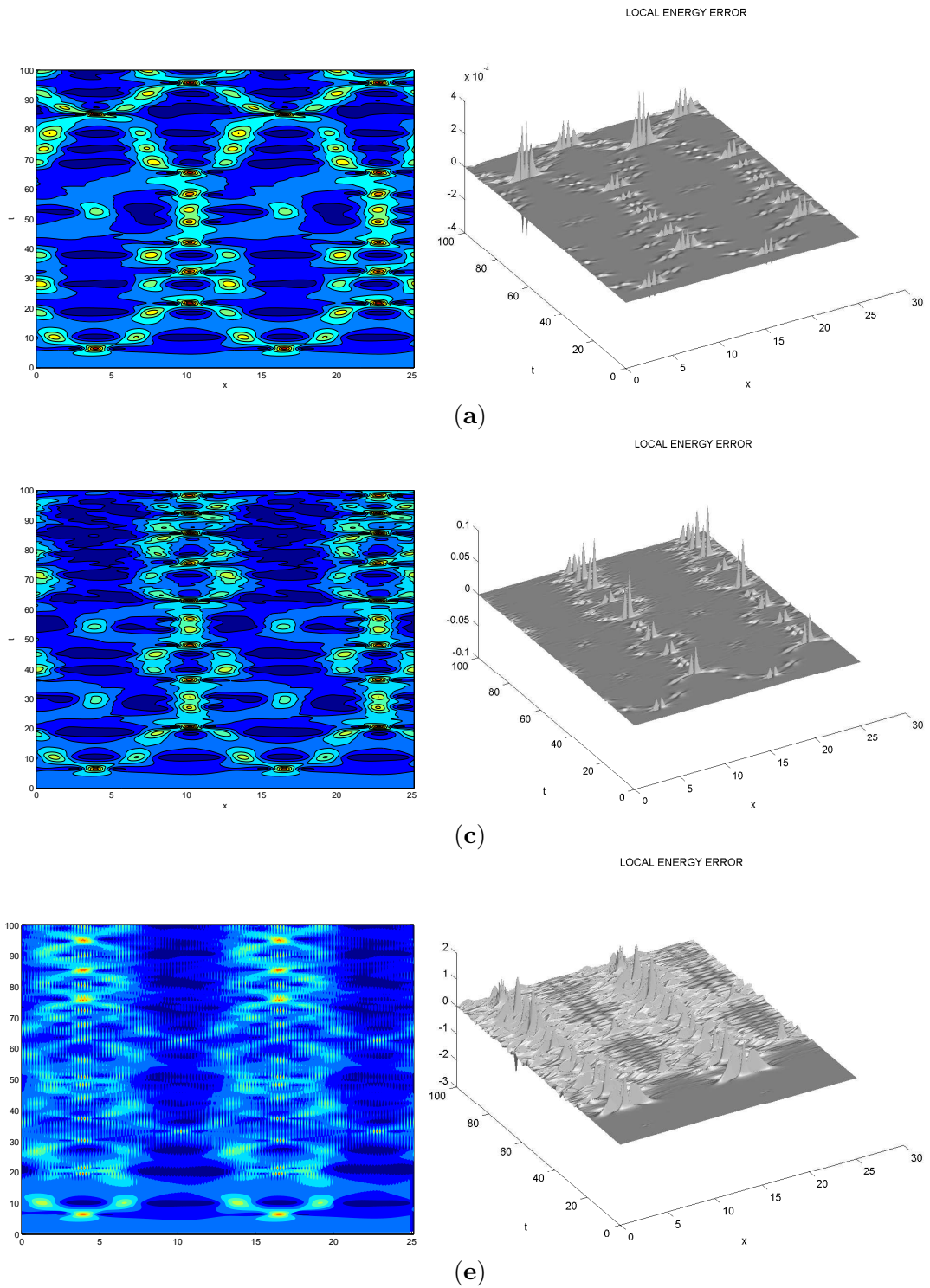


Figure 6.13: Long-time evolution of the destabilized wave solutions for CNLSE with $e = 2$, $a_0 = 0.5$, $b_0 = 0.5$, $\varepsilon = 0.1$, $\theta = 3\pi/2$, $N = 256$, $T = 100$. Left plots: Contour plots of $|\psi_1|$. Right plots: Local energy error. (a) The multi-symplectic scheme MS (b) the multi-symplectic six point scheme MS6 (c) the semi-explicit scheme SE

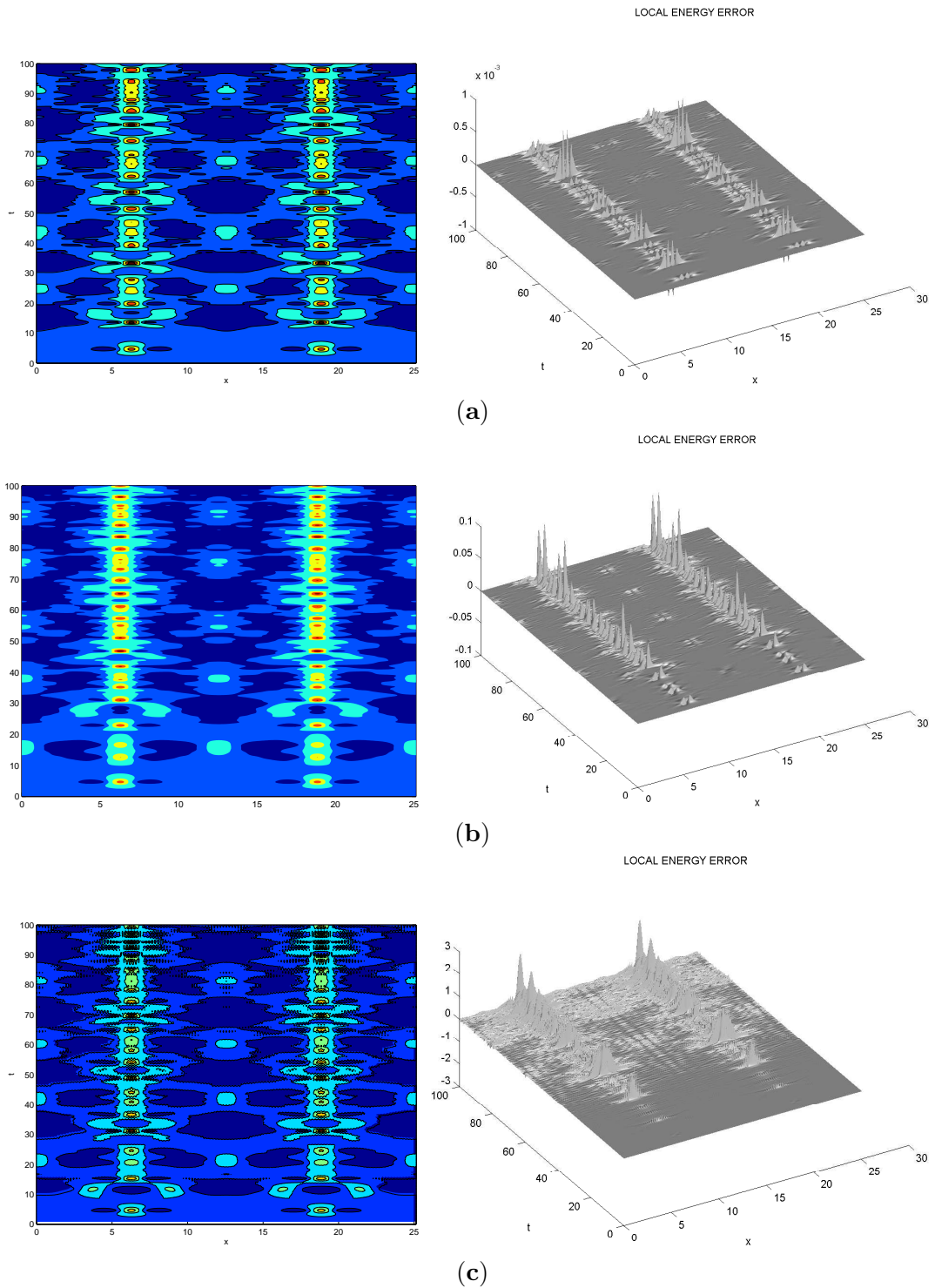


Figure 6.14: Long-time evolution of the destabilized wave solutions for CNLSE with $e = 2$, $a_0 = 0.78$, $b_0 = 0.2$, $\varepsilon = 0.1$, $\theta = 0$, $N = 256$, $T = 100$. Left plots : Contour plots of $|\psi_1|$. Right plots: Local energy error (a) The multi-symplectic scheme MS (b) the multi-symplectic six point scheme MS6 (c) the semi-explicit scheme SE

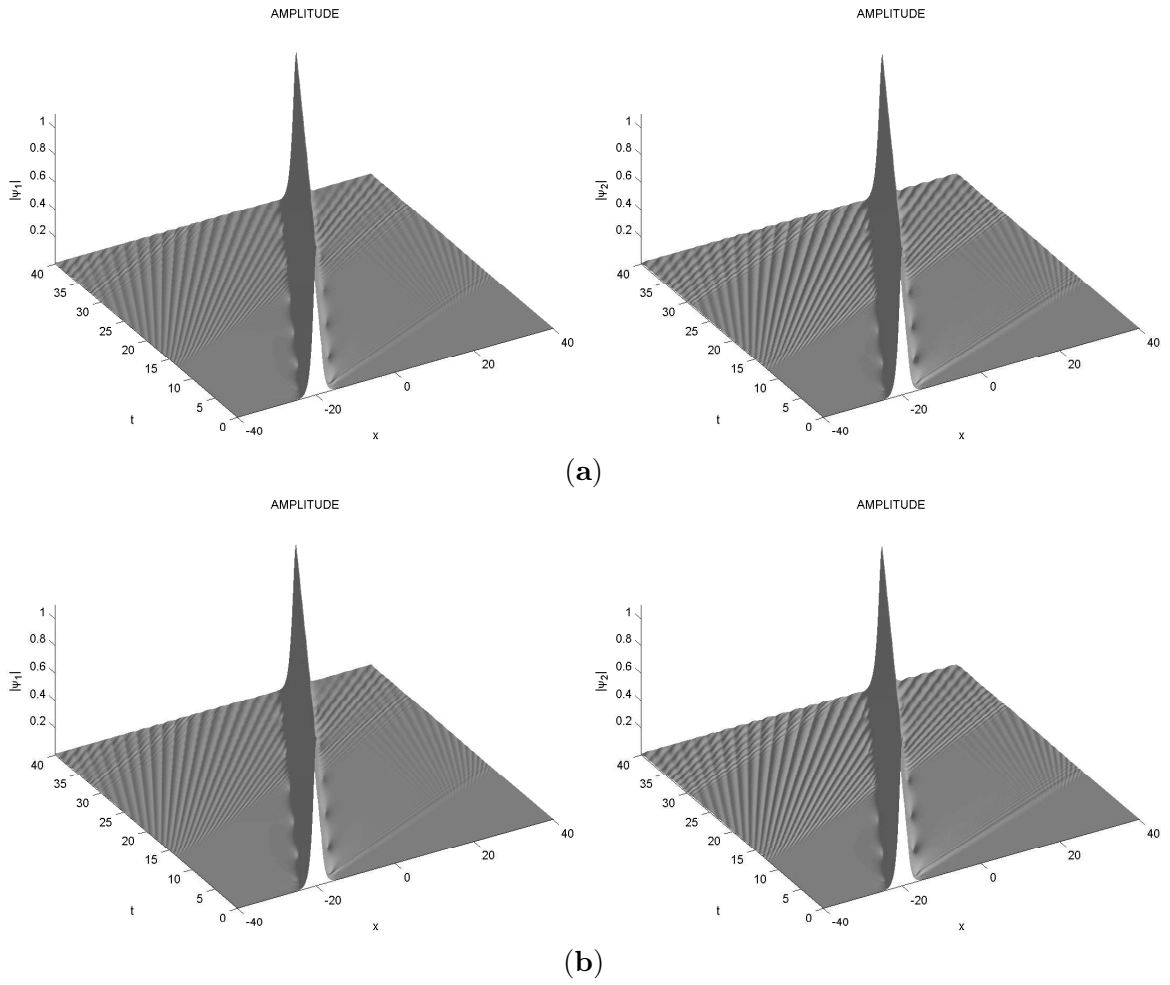


Figure 6.15: Wave forms : One soliton solution of CNLSE with $e = 2/3$ (a) MS integrator, (b) MS6 integrator

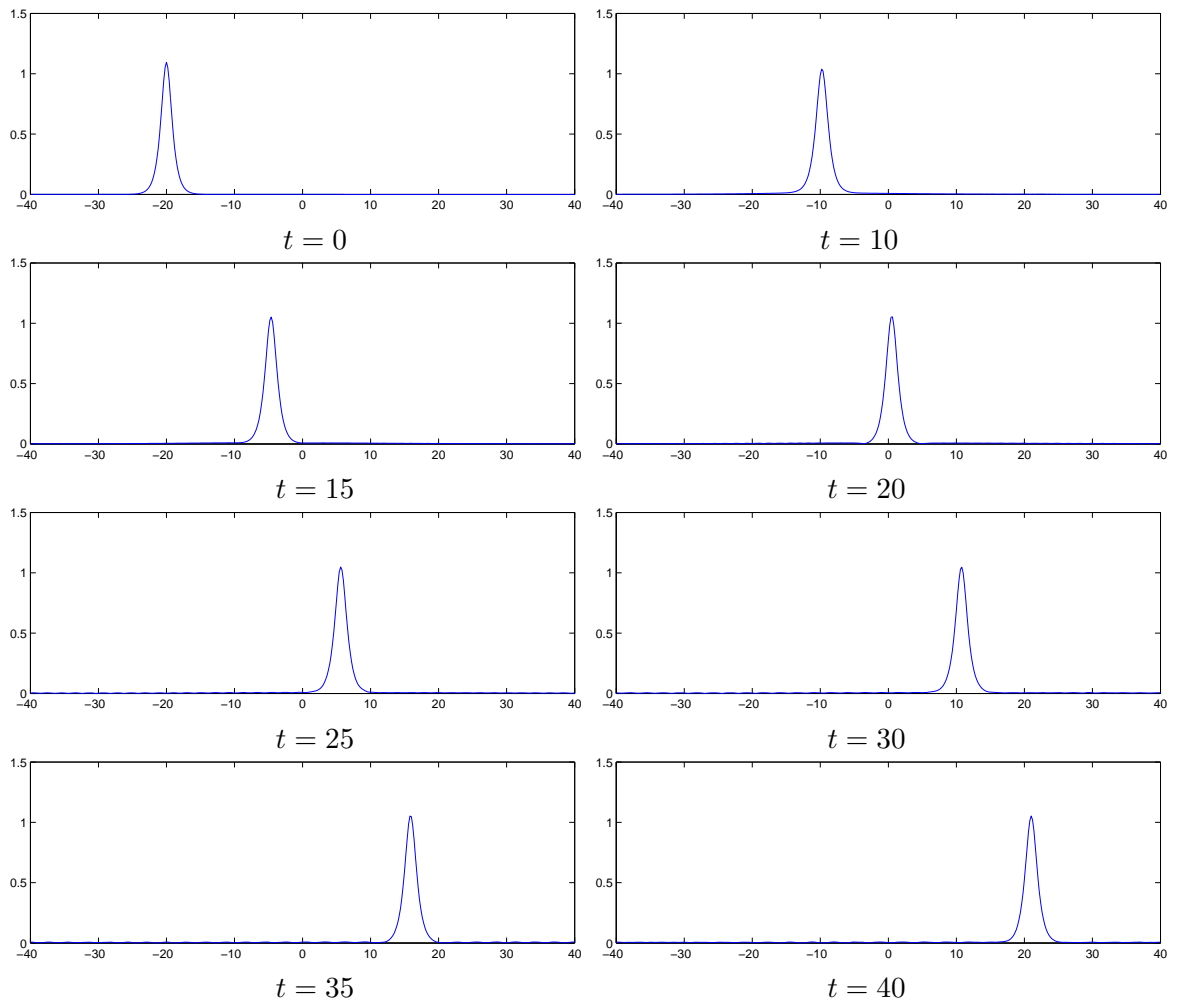


Figure 6.16: Evolution of the wave $|\psi_1|$: One soliton solution of CNLSE with $e = 2/3$ obtained using MS6 integrator

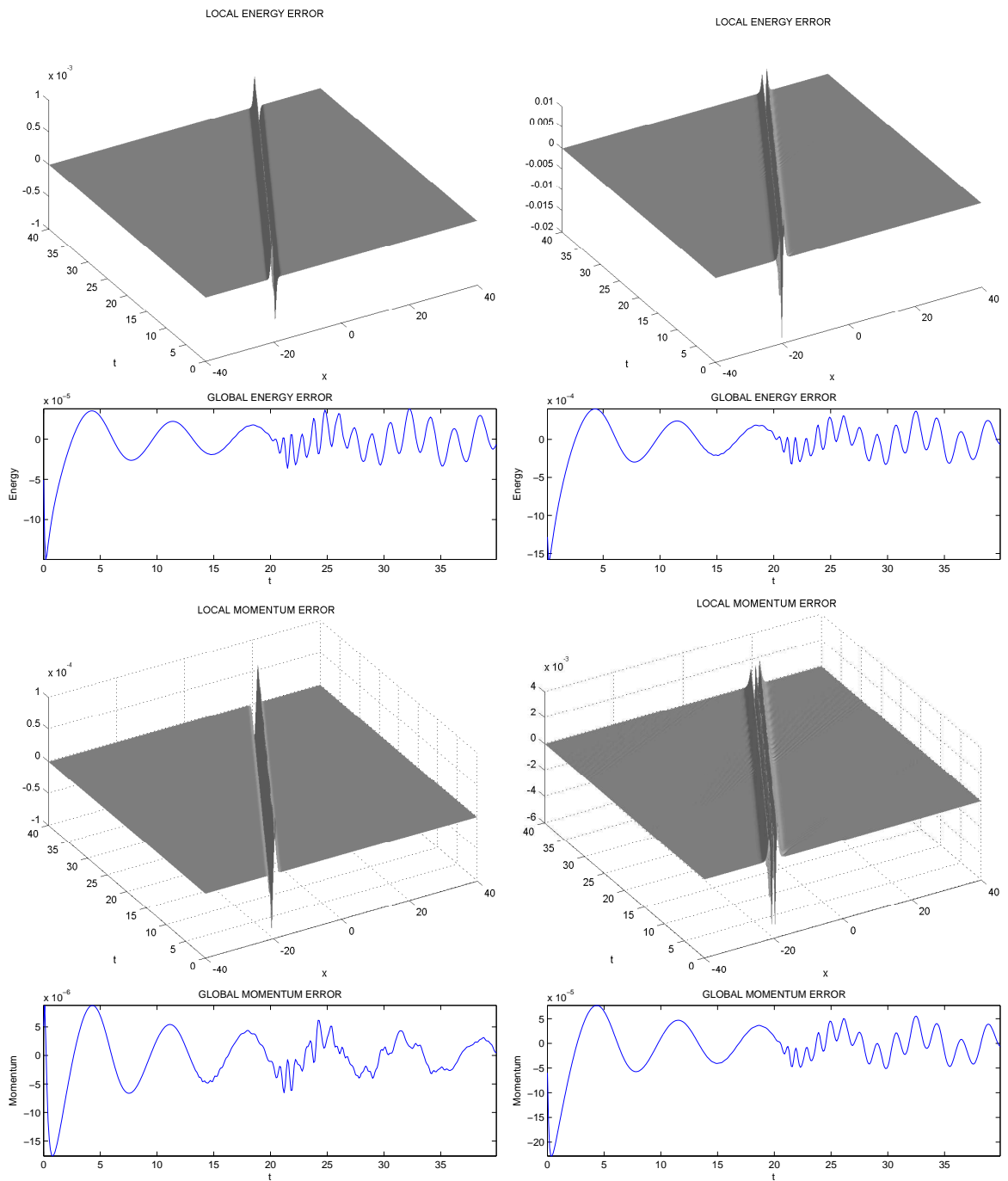


Figure 6.17: Local and global conservation of energy : One soliton solution of CNLSE with $e = 2/3$ Left plots: MS integrator; right plots: MS6 integrator

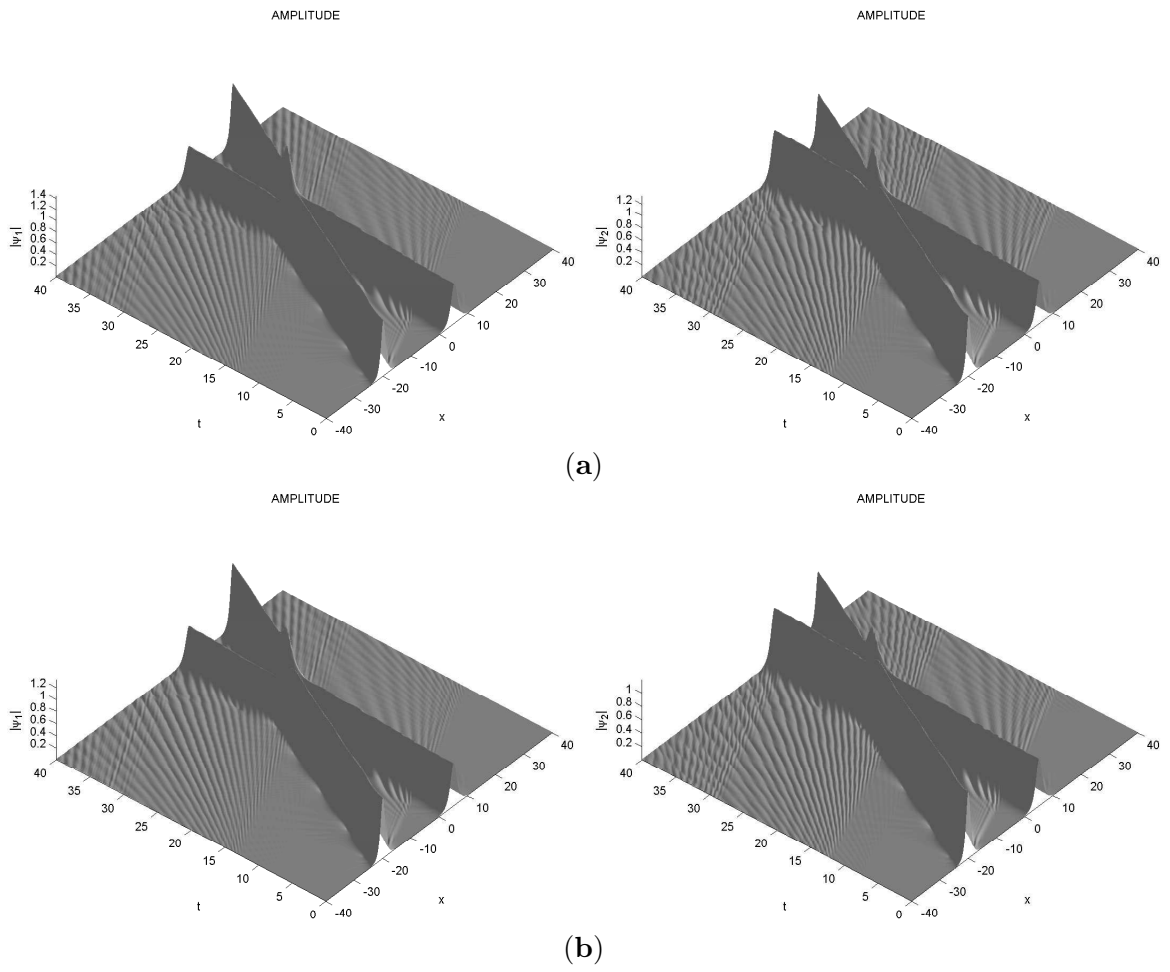


Figure 6.18: Wave forms : Elastic collision of two solitons with $e = 1$ obtained using (a) MS integrator (b) MS6 integrator

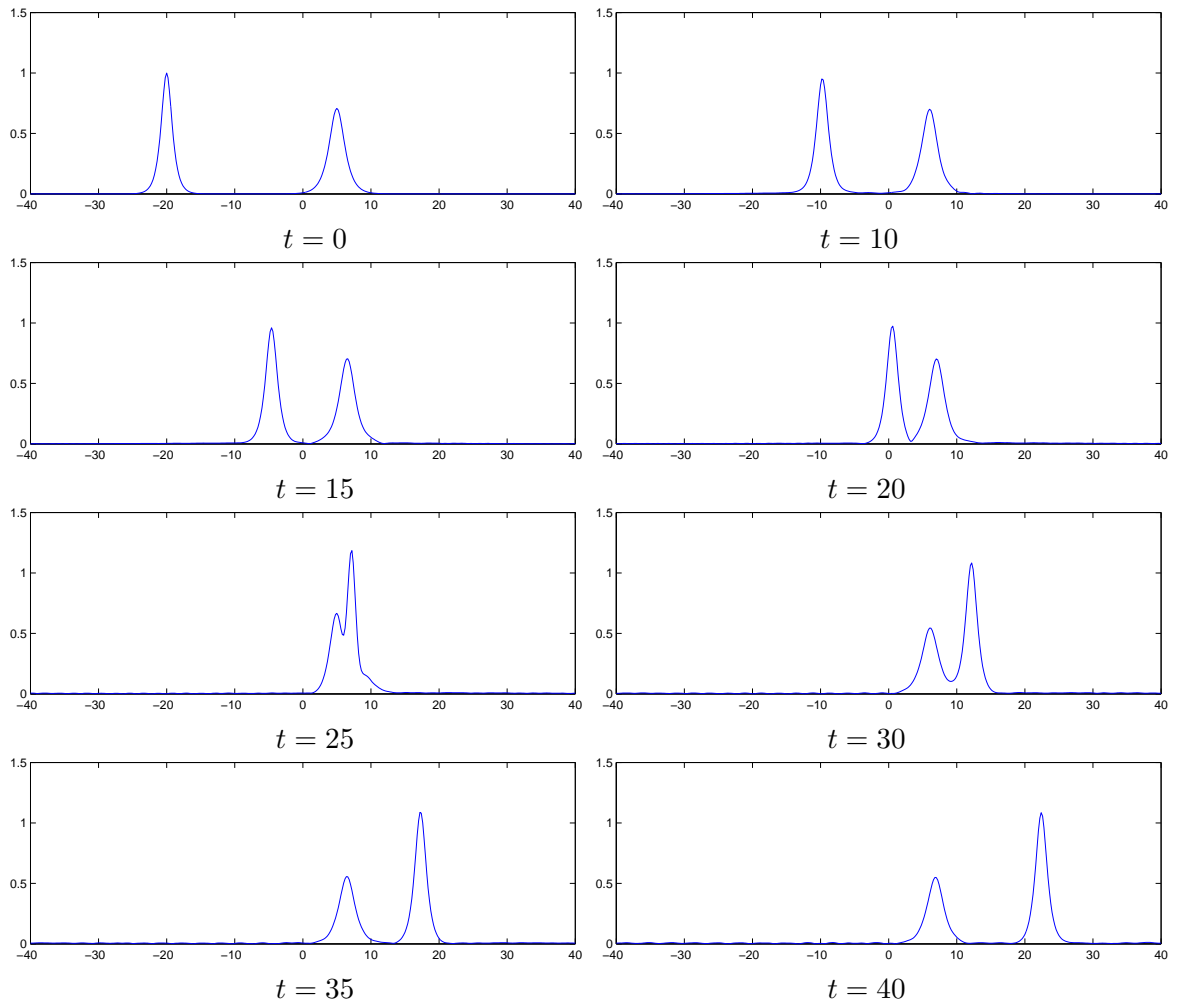


Figure 6.19: Evolution of the wave $|\psi_1|$: Two soliton solution of CNLSE with $e = 1$ obtained using MS integrator.

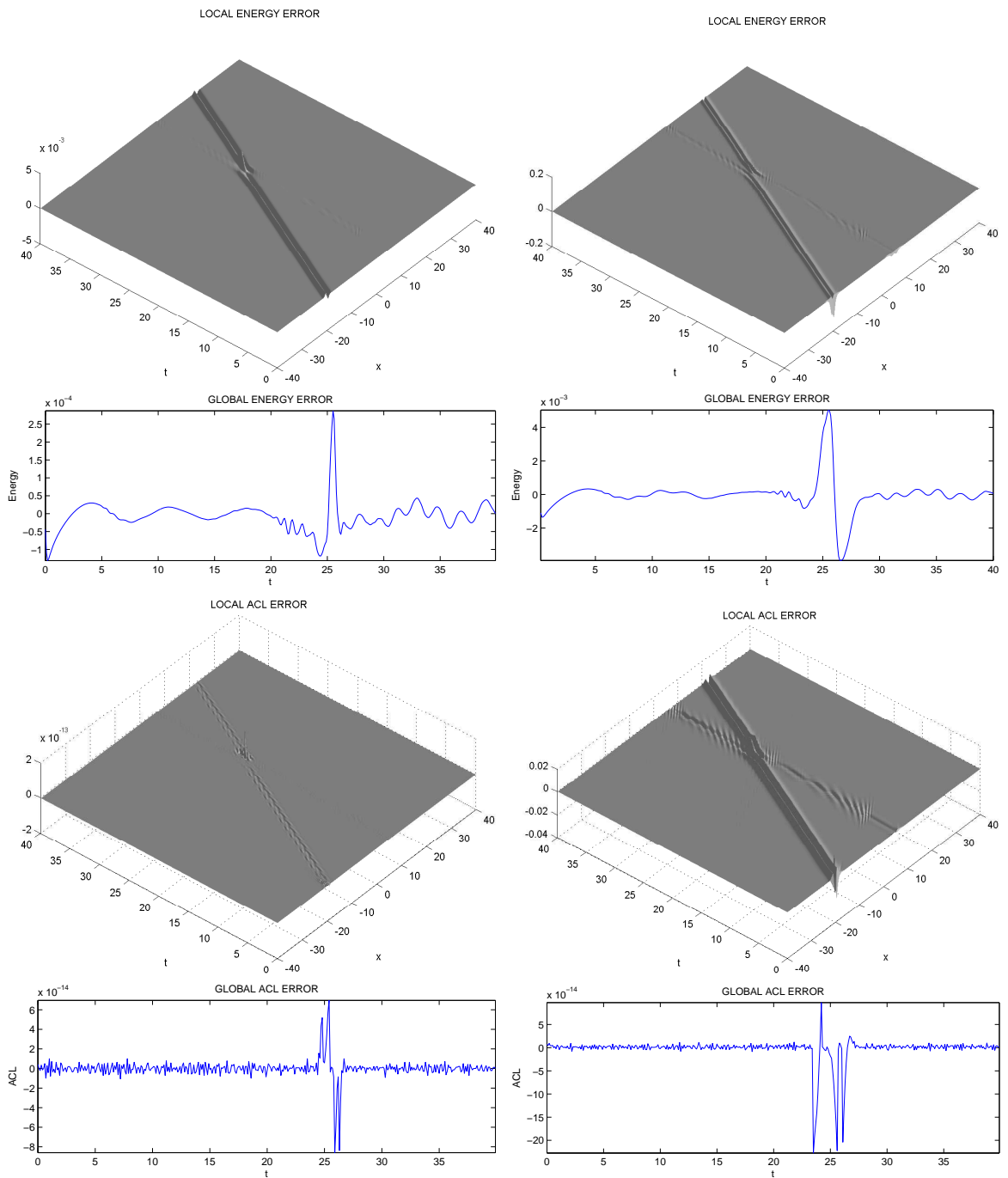


Figure 6.20: Local and global conservation of energy and momentum : Two soliton solution of CNLSE with $e = 1$. Left plots: MS integrator; right plots: MS6 integrator.

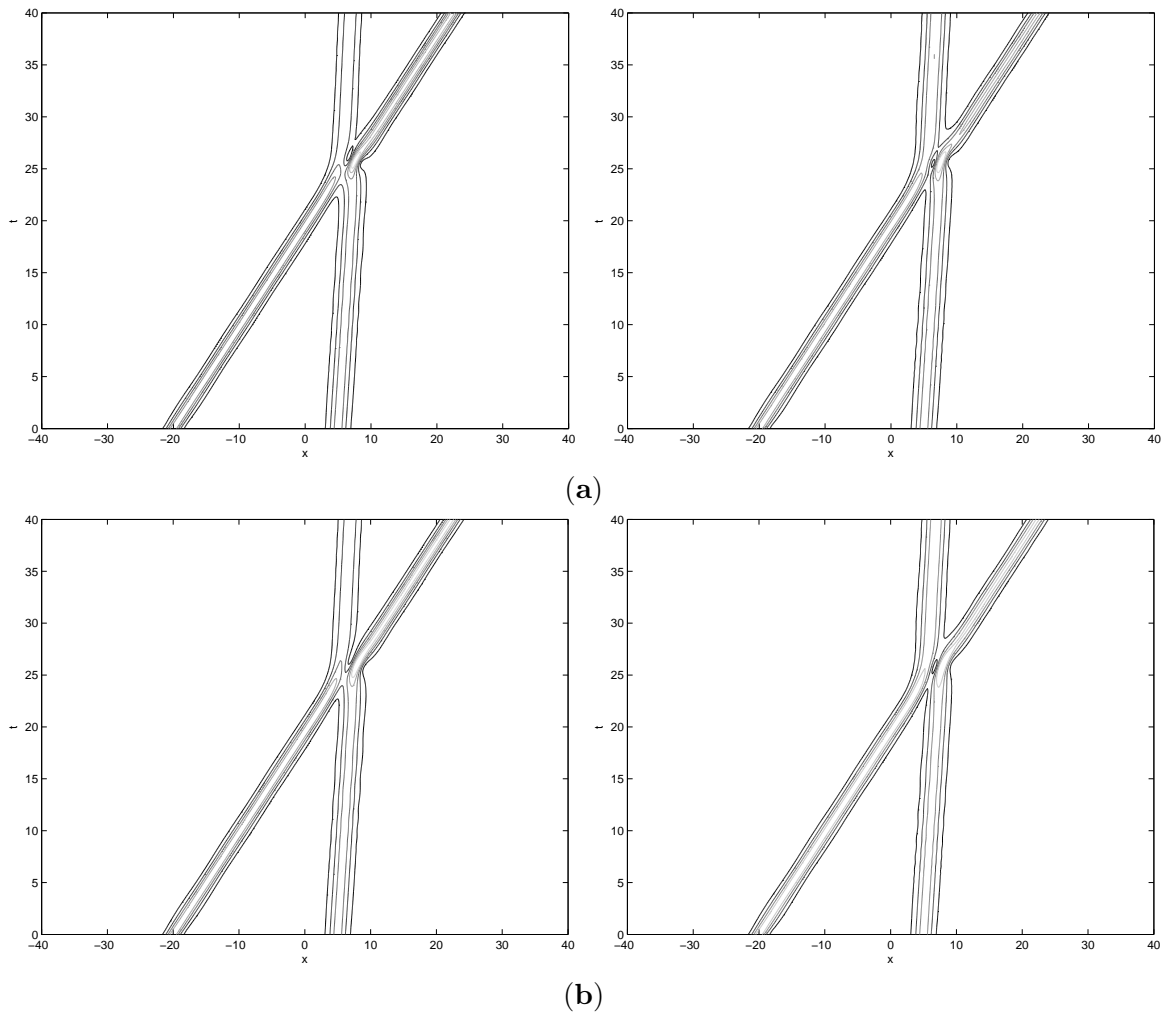


Figure 6.21: Contour plots: Two soliton solution of CNLSE with $e = 1$ obtained using (a) MS integrator (b) MS6 integrator.

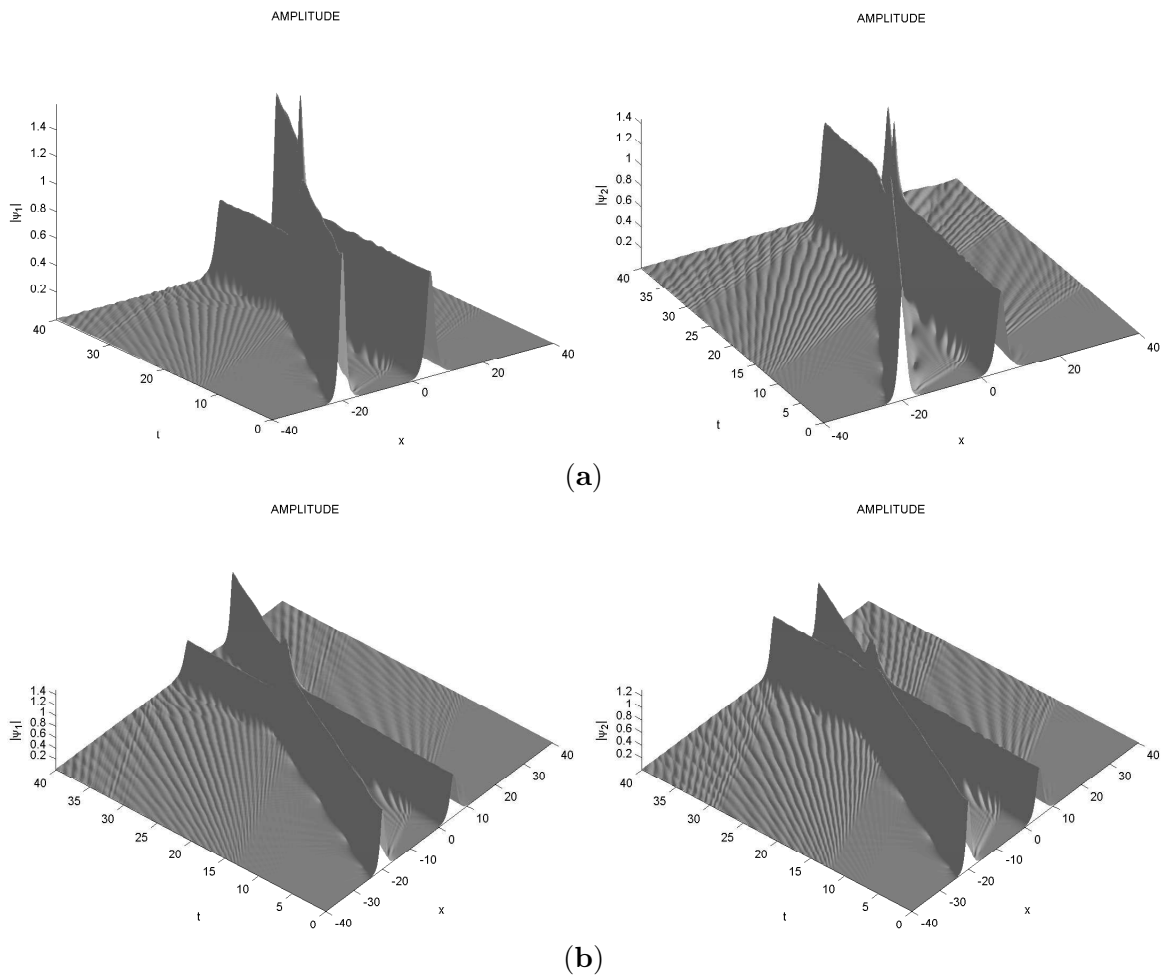


Figure 6.22: Inelastic collision of two solitons with $e = 2/3$ obtained using (a) MS integrator (b) MS6 integrator.

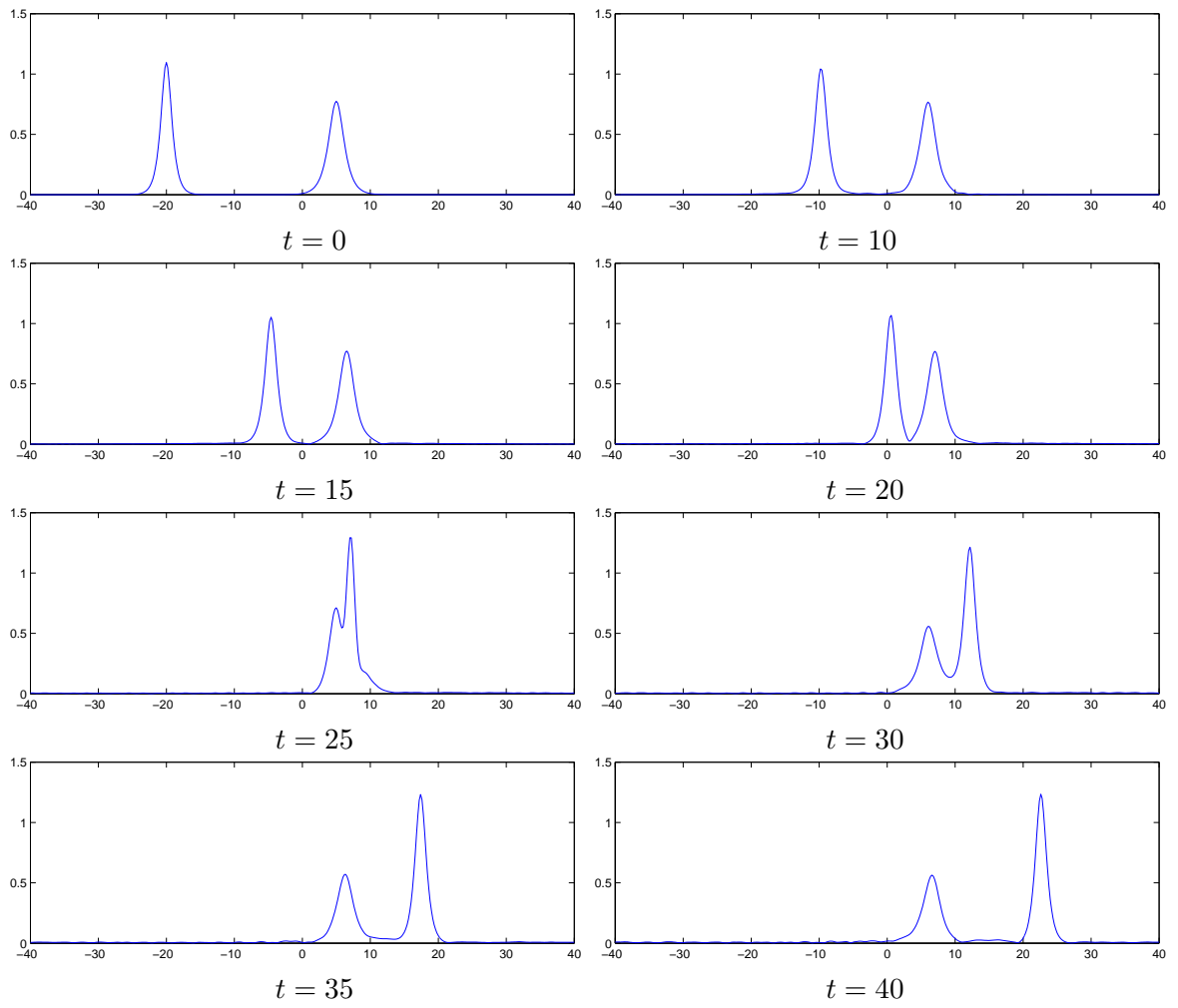


Figure 6.23: Evolution of the wave $|\psi_1|$: Two soliton solution of CNLSE with $e = 2/3$, $\delta_1 = \delta_2 = 0.5$, obtained using MS integrator

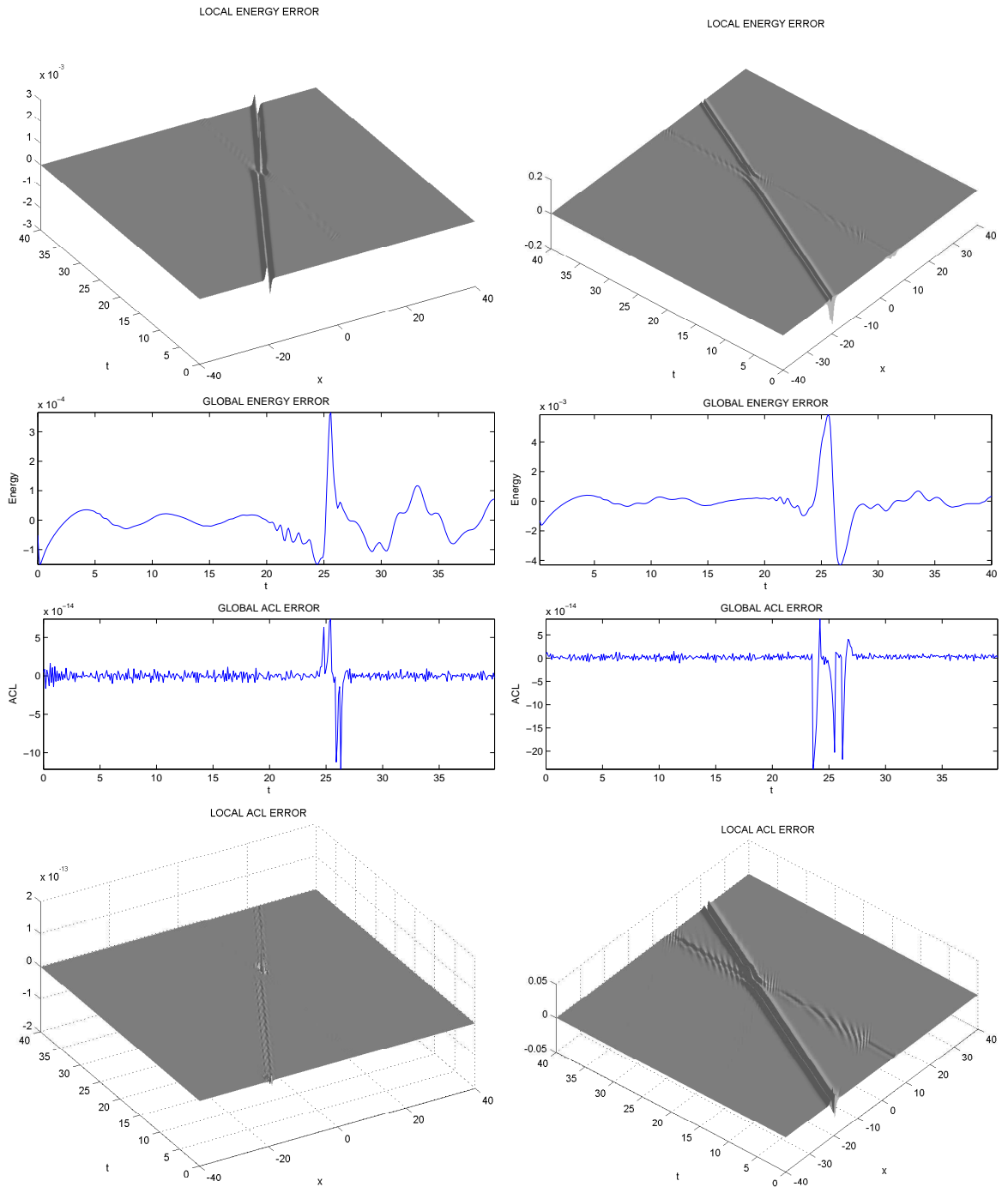


Figure 6.24: Local and global conservation of energy and additional conservation : Two soliton solution of CNLSE with $e = 2/3, \delta_1 = \delta_2 = 0.5$. Left plots: MS integrator; right plots: MS6 integrator.

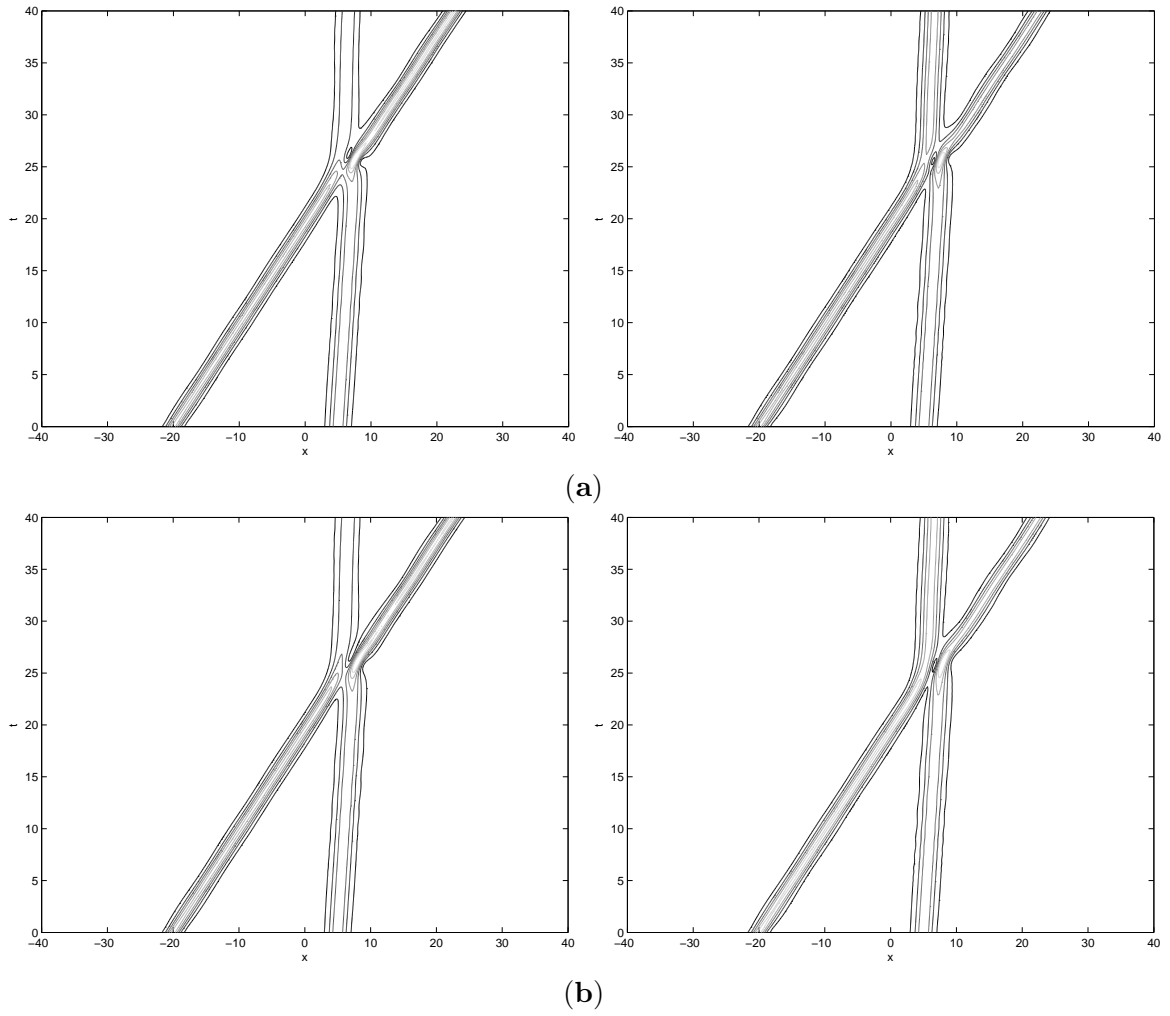


Figure 6.25: Contour plots: Two soliton solution of CNLSE with $e = 2/3, \delta_1 = \delta_2 = 0.5$, obtained using (a) MS integrator (b) MS6 integrator.

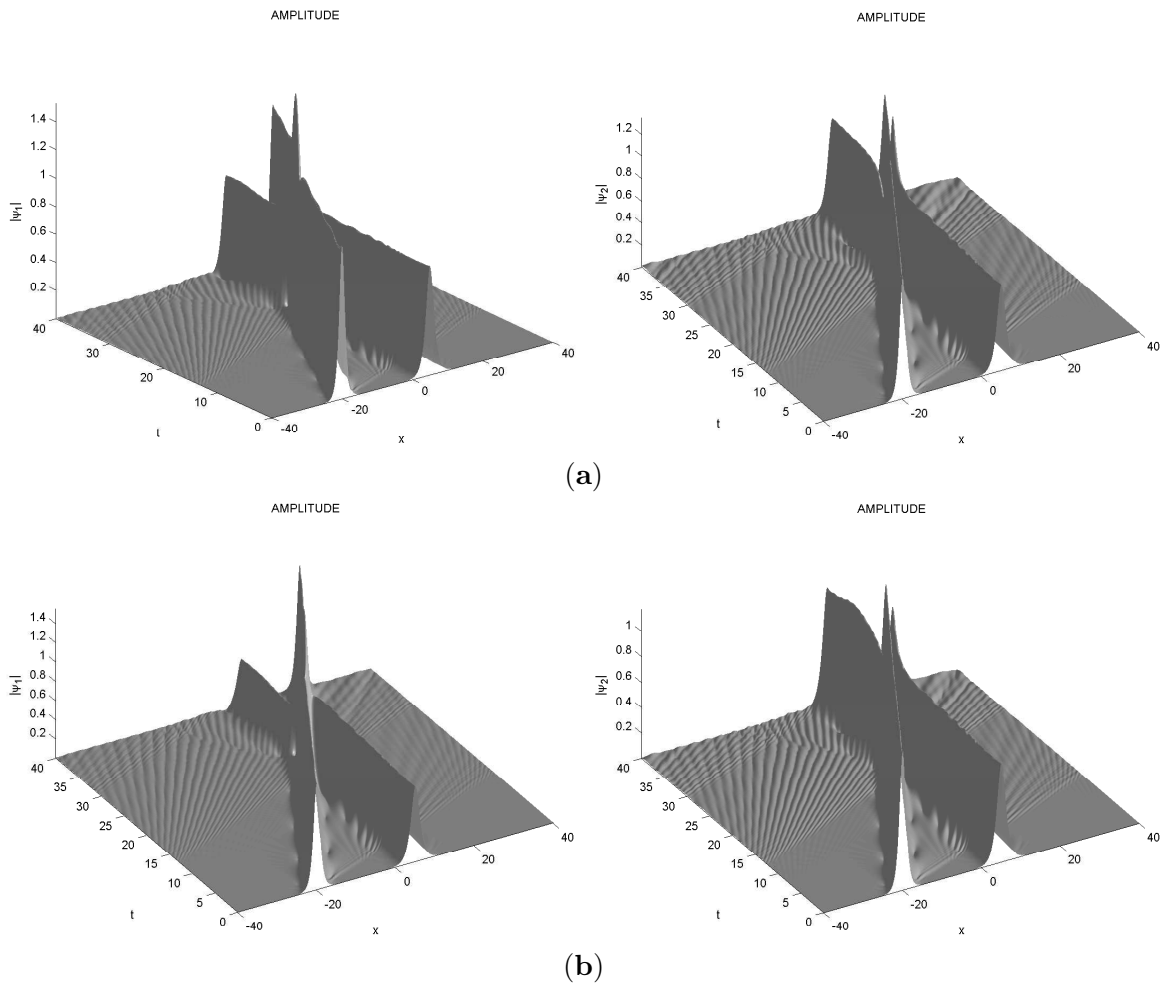


Figure 6.26: Inelastic collision of two solitons of CNLSE with $e = 2/3$, $\delta_1 = \delta_2 = 0.2$, obtained using (a) MS integrator (b) MS6 integrator.

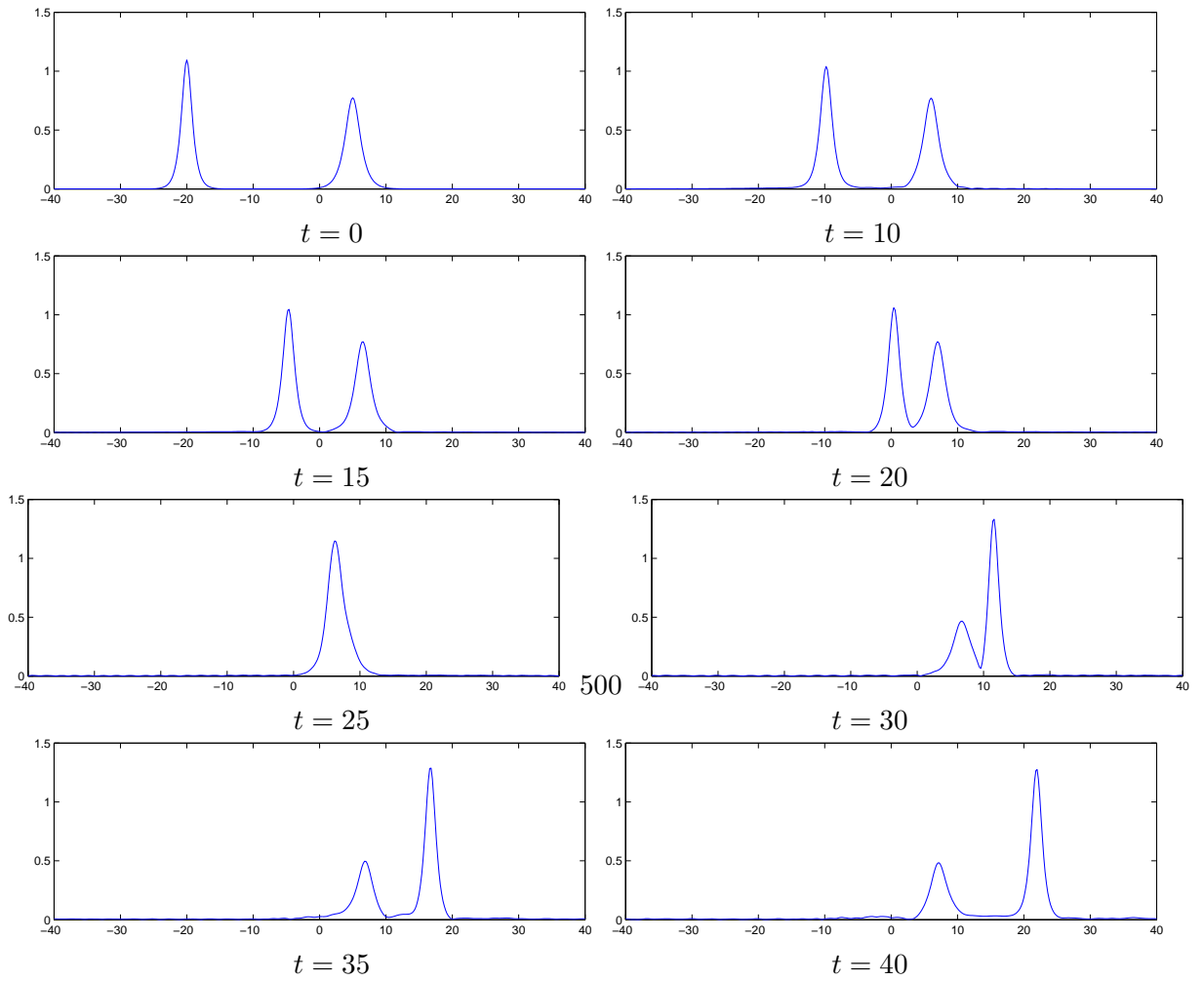


Figure 6.27: Evolution of the wave $|\psi_1|$: Two soliton solution of CNLSE with $e = 2/3$, $\delta_1 = \delta_2 = 0.2$, obtained using MS6 integrator.

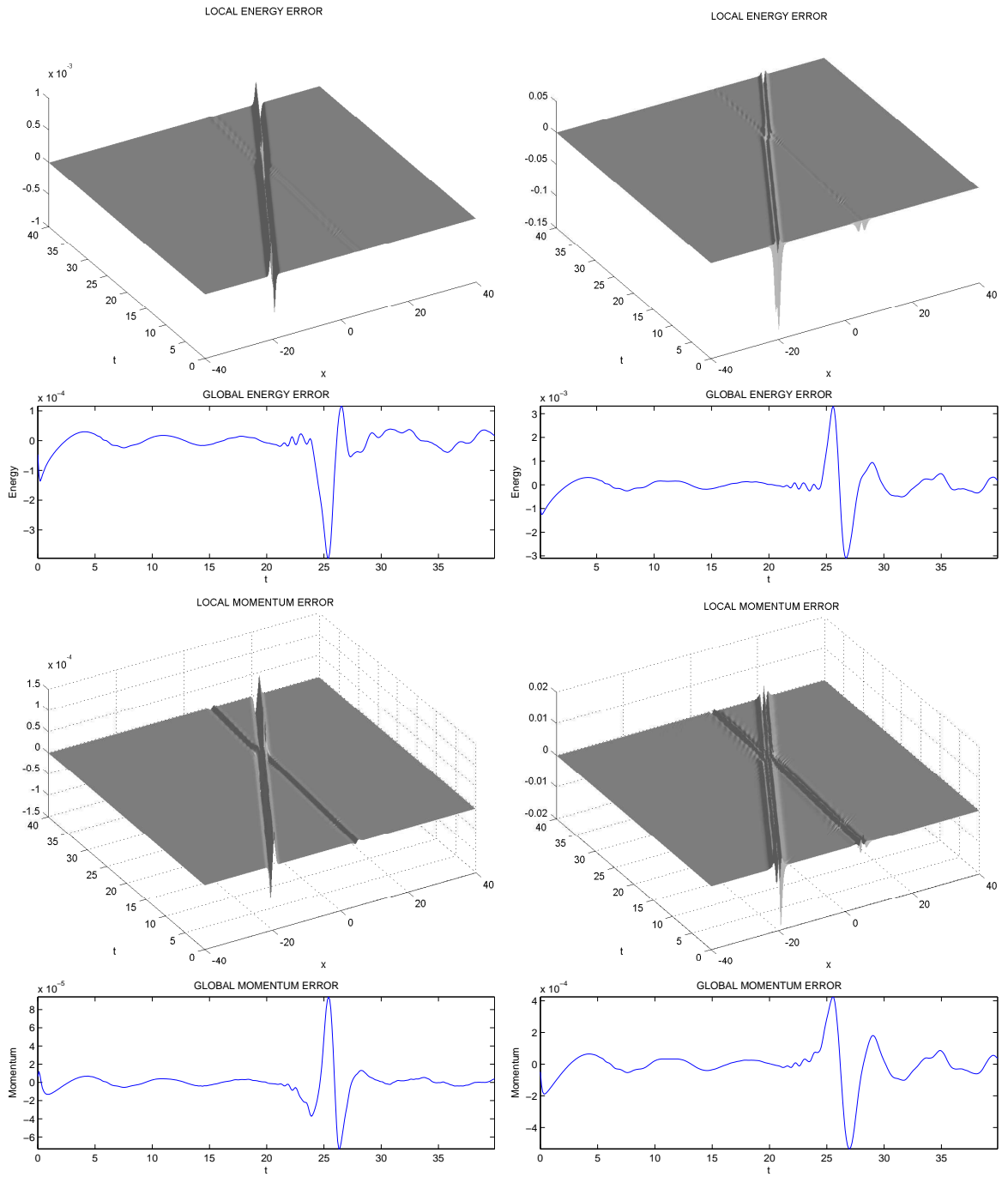


Figure 6.28: Local and global conservation of energy and momentum conservation : Two soliton solution of CNLSE with $e = 2/3, \delta_1 = \delta_2 = 0.2$. Left plots: MS integrator; right plots: MS6 integrator.

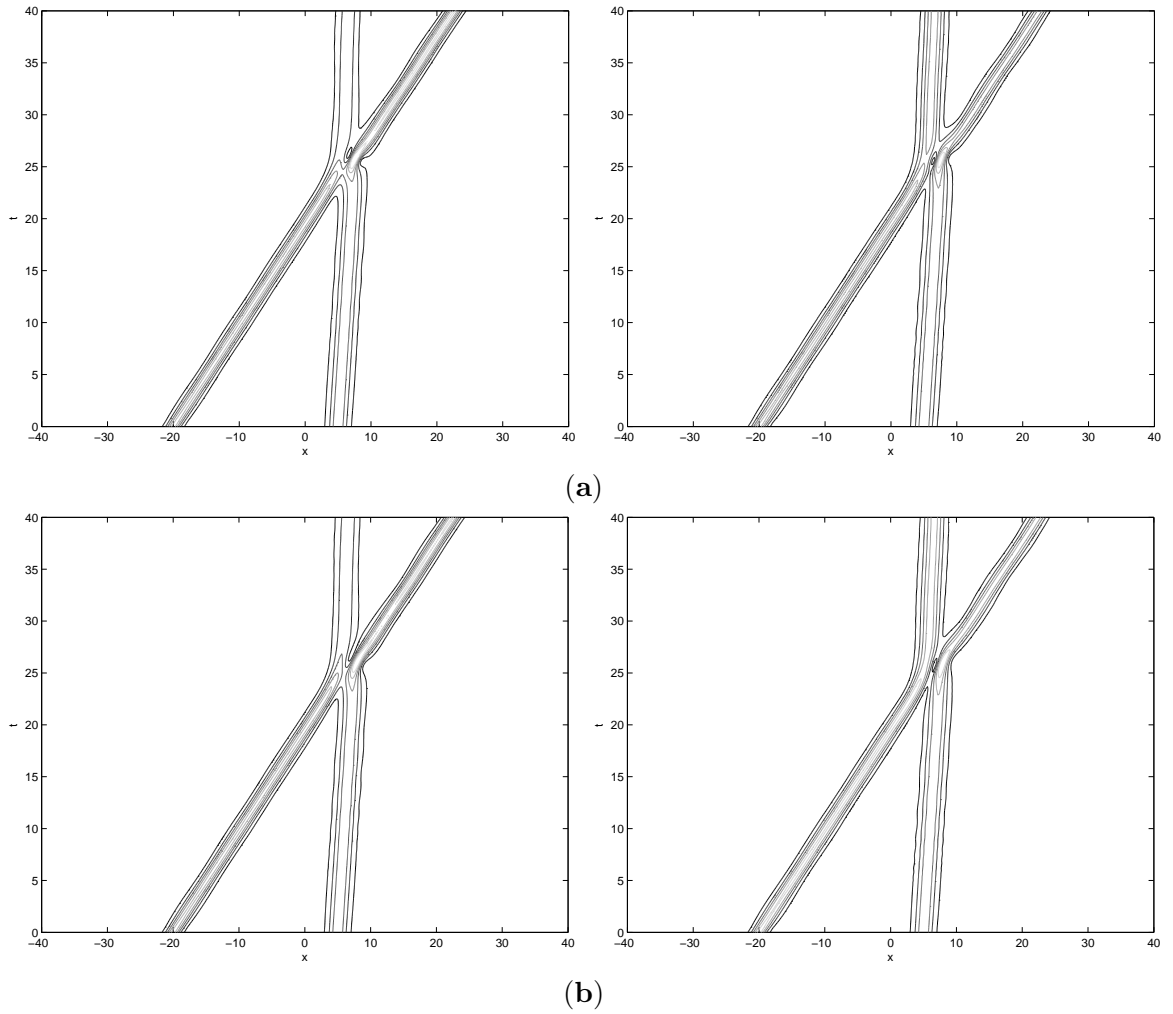


Figure 6.29: Contour plots: Two soliton solution of CNLSE with $e = 2/3$, $\delta_1 = \delta_2 = 0.2$, $d_1 = d_2 = 0.5$, $a_1 = a_2 = 1$, $N = 400$, $\Delta t = 0.1$ obtained using (a) MS integrator (b) MS6 integrator.

REFERENCES

- [1] M.J. Ablowitz, B.M. Herbst, and C.M. Schober, *On the numerical solution of the Sine–Gordon equation. I. Integrable discretization and homoclinic manifolds*, Computational Physics **126** (1996), 299–314.
- [2] M.J. Ablowitz and J.F. Ladik, *A nonlinear difference scheme and inverse scattering*, Studies in Applied Mathematics **55** (1976), 213–229.
- [3] M.J. Ablowitz, Y. Ohta, and A.D. Trubatch, *On discretizations of the vector nonlinear Schrödinger equation*, Physics Letters A **253** (1999), 287–304.
- [4] M.J. Ablowitz and C.M. Schober, *Hamiltonian integrators for the nonlinear Schrödinger equation*, International, Modern Physics C **5** (1994), 397–401.
- [5] M.J. Ablowitz, C.M. Schober, and B.M. Herbst, *Discretizations, integrable systems and computations*, Phys. A: Math.Gen. **34** (2001), 10671–10693.
- [6] M.J. Ablowitz and H. Segur, *Solitons and the inverse scattering transform*, SIAM, Philadelphia (1981).
- [7] R.E. Abraham and J.E. Marsden, *Foundations in mechanics*, MA, 1978, Readings.
- [8] G.P. Agrawal, *Nonlinear fiber optics*, second edition ed., Academic Press, New York, 1995.
- [9] N. Akhmediev and A. Ankiewicz, *First-order exact solutions of the nonlinear Schrödinger equation in the normal–dispersion regime*, Phys. Rev. A **47** (1993), 3213–3221.
- [10] N. Akhmediev and A. Ankiewicz, *Solitons: Nonlinear pulses and beams*, Chapman and Hall, London, 1997.
- [11] N.N. Akhmediev, *Nonlinear physics—déjà vu in optics*, Nature **413** (2001), 267–268.
- [12] V.I. Arnold, *Mathematical methods of classical mechanics*, Springer, New York, 1978.
- [13] U. Ascher and R. McLachlan, *Multisymplectic box schemes and the Korteweg–de Vries equation*, Applied Numerical Mathematics **48** (2004), 255–269.
- [14] D.J. Benney and A.C. Newell, *The propagation of nonlinear wave envelopes*, J. Math. and Phys. **46** (1967), 133.
- [15] R.N. Bracewell, *The Fourier Transform and its Applications*, McGraw Hill, London, 2000.

- [16] T.J. Bridges, *Hamiltonian bifurcations of the spatial structure for coupled nonlinear Schrödinger equations*, *Physica D* **57** (1992), 375–394.
- [17] T.J. Bridges, *Multisymplectic structures, boussinesq equations and periodic travelling waves*, IUTAM Symposium on Nonlinear Waves in Fluids (Singapore) (A. Mielke and K. Kirchgassnes, eds.), World Scientific, 1995.
- [18] T.J. Bridges, *Multi-symplectic structures and wave propagation*, *Mathematical Proceedings Cambridge Philosophical Society* **121** (1997), 147–190.
- [19] T.J. Bridges and G. Derks, *The symplectic Evans matrix, and the instability of solitary waves and fronts with symmetry*, *Archiv für Rational Mechanik Analysis* **156** (2001), 1–87.
- [20] T.J. Bridges and T.J. Laine-Pearson, *Multisymplectic relative equilibria, multi-phase wavetrains, and coupled NLS equations*, *Studies Applied Mathematics* **107** (2001), 137–155.
- [21] T.J. Bridges and S. Reich, *Multi-symplectic integrators: numerical schemes for Hamiltonian PDEs that conserve symplecticity*, *Physics Letters A* **284** (2001), 184–193.
- [22] T.J. Bridges and S. Reich, *Multi-symplectic spectral discretizations for the Zakharov–Kuznetsov and shallow water equations*, *Physica D* **152–153** (2001), 491–504.
- [23] J.B. Chen and M.Z. Qin, *Multi-Symplectic Fourier Pseudospectral Method for the Nonlinear Schrödinger Equation*, *Elect. Trans. on Numer. Anal.* **12** (2001), 193–204.
- [24] J.B. Chen and M.Z. Qin, *A multisymplectic variational integrator for the nonlinear Schrödinger equation*, *Numer. Methods PDEs* **18** (2002), 523–536.
- [25] J.B. Chen, M.Z. Qin, and Y.F. Tang, *Symplectic and multisymplectic methods for the nonlinear Schrödinger equation*, *Comput. Math. Appl.* **43** (2002), 1095–1106.
- [26] K.W. Chow and D.W.C. Lai, *Periodic solutions for systems of coupled nonlinear Schrödinger equations with five and six components*, *Phys. Rev. E* **65** (2002), 26613–26622.
- [27] K.W. Chow and D.W.C. Lai, *Periodic solutions for systems of coupled nonlinear Schrödinger equations with three and four components*, *Phys. Rev. E* **68** (2003), 17601–17604.
- [28] B.F. Feng and T. Mitsui, *A finite difference method for the Korteweg–de Vries and the Kadomtsev–Petviashvili equations*, *J. Computational Applied Mathematics* **90** (1998), 95–116.
- [29] M.G. Forest, D.W. McLaughlin, D.J. Muraki, and O.C. Wright, *Nonfocusing instabilities in coupled, integrable nonlinear Schrödinger pdes*, *Nonlinear Sciences* **10** (2000), 291–331.
- [30] D.F. Griffiths and J.M. Sanz-Serna, *On the scope of the method of modified equations*, *SIAM J. Sci. Comput.* **7** (1986), 994–1008.

- [31] E. Hairer, *Backward analysis of numerical integrators and symplectic methods*, Annals of Num. Math. **1** (1994), 107–132.
- [32] E. Hairer and C. Lubich, *The Life-span of backward error analysis for numerical integrators*, Num. Math. **76** (1997), 441–462.
- [33] E. Hairer, C. Lubich, and G. Wanner, *Geometric numerical integration structure-preserving algorithms for ordinary differential equations*, 31, Springer, New York, 2002.
- [34] A. Hasegawa, *Optical solitons in fibers*, Springer-Verlag, Berlin, 1989.
- [35] B.M. Herbst, F. Varadi, and M.J. Ablowitz, *Symplectic methods for the nonlinear Schrödinger equation*, Mathematical Computation and Simulation **37** (1994), 353–369.
- [36] F.T. Hioe, *N coupled nonlinear Schrödinger equations: Special set and applications to $N=3$* , J. Math. Phys. **43** (2002), 6325–6338.
- [37] J. Hong and M.Z. Qin, *Multisymplecticity of the Centered Box Discretization for Hamiltonian PDEs with $m \geq 2$ Space Dimensions*, Appl. Math. Lett. **15** (2002), 1005–1011.
- [38] A. Iserles, *A First Course in the Numerical Analysis of Differential Equations*, Cambridge University Press, Cambridge, 1996.
- [39] A.L. Islas, D.A. Karpeev, and C.M. Schober, *Geometric integrators for the nonlinear Schrödinger equation*, Computational Physics **173** (2001), 116–148.
- [40] A.L. Islas and C.M. Schober, *On the preservation of phase structure under multisymplectic discretization*, Computational Physics **197** (2004), 585–609.
- [41] M.S. Ismail and S.Z. Alamri, *Highly accurate finite difference method for coupled nonlinear Schrödinger equation.*, Computational Mathematics **81** (2004), 333–351.
- [42] M.S. Ismail and T.R. Taha, *Numerical simulation of coupled nonlinear Schrödinger equation*, Math. Comput. Sim. **56** (2001), 547–562.
- [43] T. Kanna and M. Lakshmanan, *Exact Soliton Solutions, Shape Changing Collisions, and Partially Poherent Solitons in Coupled Nonlinear Schrödinger Equations*.
- [44] B. Karasözen, *Poisson Integrators*, to appear in Mathematics and Computational Modelling (2004).
- [45] D.A. Karpeev and C.M. Schober, *Symplectic integrators for discrete nonlinear Schrödinger systems*, Mathematical Computation and Simulation **56** (2001), 145–156.
- [46] G.L. Lamb, *Elements of solitons*, John Wiley and Sons, New York, 1980.
- [47] T. Liu and M.Z. Qin, *Multisymplectic geometry and multisymplectic preissman scheme for the KP equation*, J. Math. Phys. **43** (2002), 4060–4077.

- [48] S.V. Manakov, *On the theory of two-dimensional stationary self-focusing of electromagnetic waves*, Sov. Phys. JETP **38** (1974), 248–253.
- [49] J.E. Marsden, G.W. Patrick, and S. Shkoller, *Multisymplectic geometry, variational integrators, and nonlinear PDEs*, Communication Mathematical Physics **199** (1998), 351–395.
- [50] J.E. Marsden and T.S. Ratiu, *Introduction to mechanics and symmetry*, second ed., 17, Springer, New York, 1999.
- [51] R.I. McLachlan and G.R.W. Quispel, *Splitting methods*, Acta Numerica (2002), 341–434.
- [52] C.R. Menyuk, *Nonlinear Pulse Propagation in Birefringent Optical Fibers*, IEEE J. Quantum Electronics **23** (1987), 174–176.
- [53] C.R. Menyuk, *Stability of solitons in birefringent optical fibers*, Journal of Optics Society American B **5** (1988), 392–402.
- [54] C.R. Menyuk, *Pulse Propagation in an Elliptically Birefringent Kerr Medium*, IEEE J. Quantum Electronics **25** (1989), 2674–2682.
- [55] B. Moore and S. Reich, *Backward error analysis for multi-symplectic integration methods*, Num. Math. **95** (2003), 625–652.
- [56] B.E. Moore, *A Modified Equations Approches for Multi-Symplectic Integration Methods*, Ph.D. thesis, Department of Mathematics and Statistics School of Electronics and Physical Sciences, University of Surrey, 2003.
- [57] E.B. Moore and S. Reich, *Multi-symplectic integration methods for hamiltonian PDEs*, Future Generation Computer Systems **19** (2003), 395–402.
- [58] K.W. Morton and D.F. Mayers, *Numerical Solution of Partial Differential Equations*, Cambridge University Press, Cambridge, 1994.
- [59] A.C. Newell, *Solitons in mathematics and physics*, CBMS–NFS Regional Conference in Applied Mathematics (Philadelphia,PA), vol. 48, SIAM, 1985.
- [60] P.J. Olver, *Applications of lie groups to differential equations*, second ed., 107, Springer–Verlag, New York, 1993.
- [61] A. Preissman, *Propogation des intumescences dan les canaux et rivières*, First Congress French Association for Computation., 1961.
- [62] R. Radhakrishnan, M. Lashmanan, and J. Hietarinta, *Inelastic collision and switching of coupled bright solitons in optical fibers*, Phys. Rev. E **56** (1997), 2213–2216.
- [63] S. Reich, *Backward error analysis for numerical integrators*, SIAM, Numerical Analalys **36** (1999), 1549–1570.
- [64] S. Reich, *Finite volume methods for multi-symplectic PDEs*, BIT **40** (2000), 559–582.
- [65] S. Reich, *Multi-symplectic Runge–Kutta collocation methods for Hamiltonian wave equations*, Computational Physics **157** (2000), 473–499.

- [66] M.P. Robinson, *The solution of nonlinear Schrödinger equations using orthogonal spline collocation*, Computers Mathematics and Application **33** (1997), 39–57.
- [67] A. Rouhi and J. Wright, *A new operator splitting method for the numerical solution of partial differential equations*, Comput. Phys. Comm. **85** (1995), 18–28.
- [68] J.M. Sanz-Serna, *Methods for the numerical solution of the nonlinear Schrödinger equation*, Mathematical Computation **43** (1984), 21–27.
- [69] J.M. Sanz-Serna and M.P. Calvo, *Numerical Hamiltonian Problems*, Chapman and Hall, London, 1994.
- [70] W.A. Strauss, *The Schrödinger equation*, North-Holland Mathematics Studies, vol. 730, pp. 452–465, North-Holland, New-York, 1978.
- [71] J.Q. Sun and X.Y. Gu Z.Q. Ma, *Numerical study of the soliton waves of the coupled nonlinear Schrödinger system*, Physica D **196** (2004), 311–328.
- [72] J.Q. Sun and M.Z. Qin, *Multi-Symplectic methods for the coupled 1D nonlinear Schrödinger system.*, Comp. Phys. Comm. **155** (2003), 221–235.
- [73] M. Suzuki, *Convergence of general decompositions of exponential operators*, Communication in Mathematical Physics **163** (1994), 491–508.
- [74] B. Tan and J.P. Boyd, *Coupled-mode solitary wave in a pair of cubic Schrödinger equations with cross modulations: Analytical solution and collisions.*, Chaos, Solitons & Fractals **11** (2000), 1113–1129.
- [75] B. Tan and J.P. Boyd, *Stability and long time evolution the periodic solutions of the two coupled nonlinear Schrödinger equations*, Chaos Solitons and Fractals **12** (2001), 721–734.
- [76] Y. Tan and J. Yang, *Resonance-and phase-induced window sequences in vector-soliton collision*, Phy. Let. A **288** (2001), 309–315.
- [77] Y.F. Tang, V.M. Perez-Garcia, and L. Vazquez, *Symplectic Methods for Ablowitz-Ladik model*, Appl. Math. and Comp. **82** (1997), 17–38.
- [78] Y.F. Tang, L. Vazquez, F. Zhang, and V.M. Perez Garcia, *Symplectic methods for the nonlinear schrödinger equation*, Comput. Math. Applic **32** (1996), 73–83.
- [79] J.W. Thomas, *Numerical partial differential equations: Finite difference methods*, Springer, 1995.
- [80] L.N. Trefethen, *Finite differences and spectral methods for ordinary and partial differential equations*, unpublished text, 1996, available at <http://web.comlab.ox.ac.uk/oucl/work/nick.trefethen/pdetext.html>.
- [81] S.C. Tsang and K.W. Chow, *The evolution of periodic waves of the coupled nonlinear Schrödinger equations.*, Math & Compt. Simul. **66** (2004), 551–564.
- [82] M. Wadati, T. Iizuka, and M. Hisakado, *A coupled nonlinear Schrödinger equation and optical solitons*, J. Phys. Soc. Japan **61** (1992), 2241–2245.
- [83] Y.S. Wang and M.Z. Qin, *Multisymplectic Schemes for the Nonlinear Klein-Gordon Equation.*, Math. Comp. Model. **36** (2002), 963–977.

- [84] M.I. Weinstein, *Solitary waves of nonlinear dispersive evolution equations with critical power nonlinearities*, J. Diff. Eq. **69** (1987), 192–203.
- [85] G.B. Whitham, *Linear and Nonlinear Waves*, Wiley–Interscience, New York, 1974.
- [86] J. Yang, *Classifications of the solitary waves in coupled nonlinear Schrödinger equations.*, Physica D **108** (1997), 92–112.
- [87] J. Yang, *Interactions of vector solitons*, Phys. Rev. E **64** (2001), 1–16.
- [88] J. Yang and D.J. Benney, *Some properties of nonlinear wave systems*, Stud. Appl. Math. **96** (1996), 111–139.
- [89] J. Yang and Y. Tan, *Fractal structure in the collision of vector solitons*, Phys. Rev. Lett. **85** (2000), 3624–3627.
- [90] H. Yoshida, *Construction of higher order Symplectic Integrators*, Physics Letters A **150** (1990), 262–268.
- [91] V.E. Zakharov and E.L. Schulman, *To the integrability of the system of two coupled nonlinear Schrödinger equations.*, Physica D **4** (1982), 270–274.
- [92] V.E. Zakharov and A.B. Shabat, *Exact theory of two–dimensional self–focusing and one–dimensional self–modulation of waves in nonlinear media*, Sov. Phys. JETP **34** (1972), 62–69.
- [93] P.F. Zhao and M.Z. Qin, *Multisymplectic geometry and multisymplectic preissman scheme for the KdV equation*, J. of Phys. A: Math. and General **33** (2000), 3613–3626.